# NON-INVASIVE DETERMINATION OF ARTERIAL WALL STIFFNESS FOR CARDIOVASCULAR RISK ASSESSMENT IN HORSES

Lisse Vera

Dissertation submitted in fulfillment of the requirements for the degree of Doctor in Veterinary Science (PhD)

Equine Cardioteam Ghent University

Department of Large Animal Internal Medicine

Faculty of Veterinary Medicine

Ghent University

August 2020

**Promotors**

Prof. Dr. Gunther van Loon

Prof. Dr. Koen Chiers

*“ As the arteries grow hard, the heart grows soft ”*

*H.L Mencken*

**Lisse Vera (2020)**

Non-invasive determination of arterial wall stiffness for cardiovascular risk assessment in horses

This research was funded by the Research Foundation Flanders (1134917N).

**Promotors**

Prof. Dr. Gunther van Loon

Faculty of Veterinary Medicine, Ghent University

Prof. Dr. Koen Chiers

Faculty of Veterinary Medicine, Ghent University

**Members of the Examination Committee**

Prof. Dr. Jeroen Dewulf

Chairman

Faculty of Veterinary Medicine, Ghent University

Dr. Stijn Schauvliege

Secretary

Faculty of Veterinary Medicine, Ghent University

Prof. Dr. John Keen

The Royal (Dick) School of Veterinary Studies, University of Edinburgh

Prof. Dr. Patrick Segers

Faculty of Engineering and Architecture, Ghent University

Prof. Dr. Pascale Smets

Faculty of Veterinary Medicine, Ghent University

## Table of content

## List of Abbreviations

| | |
|---|---|
| 1D | One-dimensional |
| Ad | Diastolic lumen area |
| Ao | Aorta |
| As | Systolic lumen area |
| AGE | Advanced glycation end products |
| BC | Backward compression |
| BE | Backward expansion |
| CaCCA | Caudal common carotid artery |
| $CC_A$ | Arterial compliance coefficient calculated from lumen area measurement |
| CCA | Common carotid artery |
| $CC_D$ | Arterial distensibility coefficient calculated from lumen area measurement |
| CO | Cardiac output |
| CrCCA | Cranial common carotid artery |
| CV | Coefficient of variation |
| DAP | Diastolic arterial pressure |
| $DC_A$ | Arterial distensibility coefficient calculated from lumen area measurement |
| $DC_D$ | Arterial distensibility coefficient calculated from diameter measurement |
| Dd | Diastolic diameter |
| DistAo | Distal aorta |
| Ds | Systolic diameter |
| ECG | Electrocardiogram |
| EIA | External iliac artery |
| FA | Femoral artery |
| FC | Forward compression |
| FE | Forward expansion |
| HR | Heart rate |
| IMT | Intima media thickness |
| LV | Left ventricle |
| MA | Median Artery |
| MAP | Mean arterial pressure |
| NA | Not applicable |
| PP | Pulse pressure |
| ProxAo | Proximal aorta |
| PWV | Pulse wave velocity |
| $PWV_{a\text{-}e}$ | Aorta to external iliac artery pulse wave velocity |

| | |
|---|---|
| $PWV_{c-c}$ | Caudal carotid to cranial carotid pulse wave velocity |
| $PWV_{c-e}$ | Carotid to external iliac artery pulse wave velocity |
| $S_A$ | Arterial lumen area strain |
| SAP | Systolic arterial pressure |
| $S_D$ | Arterial diameter strain |
| SI | Stiffness index |
| SV | Stroke volume |
| SVR | systemic vascular resistance |
| WPA | Wave power analysis |
| ΔA | Arterial lumen area change |
| ΔD | Arterial diameter change |
| ΔP | Pulse pressure |

# PREFACE

Very little is known about the arterial pathophysiology in horses. Nevertheless, vascular disorders leading to changes in arterial physiology may be associated with acute fatalities in horses. Arterial rupture associated with exercise, parturition or breeding, and aorto-cardiac or aorto-pulmonary fistulation are of great concern as these are often fatal events. All those arterial pathologies might result from altered vascular wall properties associated with age, sex or breed.

As the most important function of the arterial wall is buffering the differences in blood pressure by elastic expansion during systole and passive recoil during diastole, the functionality of the arterial wall can be expressed by measuring arterial elasticity. In human medicine arterial elasticity is evaluated by means of arterial wall stiffness. Local as well as regional wall stiffness can be assessed. In horses, assessment of arterial wall properties has been poorly explored and little information is available regarding possible effects of age, sex or breed on the arterial wall.

In the introduction of this thesis, a brief overview is given of the composition and function of the arterial wall, followed by an exposition of the normal arterial wall function. In this part the pathophysiology of blood pressure and different methodologies of measuring blood pressure are described, together with a short review of the biomechanical properties of the arterial wall and mathematical models, used to understand and study arterial physiology. The next part of the introduction focusses on the measurement of arterial wall stiffness and influencing factors such as age, sex and breed. Finally, an overview is given of common, possibly fatal, vascular disorders in horses.

The first part of the research section of this PhD aims at explaining and understanding the normal equine arterial physiology. In a second part, a method to noninvasively measure arterial wall stiffness in horses is developed. The third part describes the effect of age and breed on the properties of the arterial wall. The effect of age is not only assessed *in vivo*, but also *ex vivo* by biomechanical testing and histological assessment.

# CHAPTER 1:

# INTRODUCTION

In human medicine, measurement of arterial wall stiffness is routinely used to asses vascular health and is proven to be independently linked with mortality. In horses, no methods to measure arterial wall stiffness *in vivo* and as such, assess vascular health, have been described. Nevertheless, several clinical findings suggest that arterial wall stiffness plays an important role in the pathophysiology of arterial rupture in horses. Although the condition is rare, it is often fatal and therefore affects not only horse welfare but also rider safety. Arterial rupture in horses has been associated with age, breed (e.g. aortic rupture in Friesian horses), exercise, copulation and treatment with α1-agonists. In human medicine, increasing age has been described as one of the most important factors contributing to increased arterial wall stiffness, and a similar pathophysiology is likely to exist in horses.

In order to unravel the pathophysiology of arterial rupture in horses and develop strategies to reduce the risk for arterial rupture, better knowledge of the characteristics of the equine arterial wall and the effect of blood pressure is necessary. A method to assess the arterial wall characteristics *in vivo* must be developed. Such a method would allow to screen horses and identify risk factors for arterial rupture. The *in vivo* measurement technique of arterial wall stiffness should be validated by histology and *ex vivo* biomechanical testing.

## 1. Normal structure of the arterial wall

The arterial wall is composed of three different layers: the tunica intima, tunica media and tunica adventitia (Fig. 1).

The tunica intima in the innermost layer of the arterial wall and consists of a single layer endothelial cells, and a small layer of collagen, the lamina basalis[1]. The most important function of this layer is to prevent the blood from clotting, provide nutrient transport from and to the blood stream[1] and regulate vasodilation or vasoconstriction in muscular arteries.

The tunica media is the middle layer of the arterial wall and consists of an internal elastic lamina, containing mostly elastin, followed by a thick layer of concentric patterns of elastic fibers and smooth muscle cells intertwined with small bundles of collagen fibers and an external elastic lamina, again containing mostly elastin. The ratio between elastin, collagen and smooth muscle cells varies along the arterial tree. From central arteries (elastic arteries) towards more peripheral arteries (muscular arteries) the tunica media becomes increasingly muscular, with a reduced amount of elastic fibers and more smooth muscle cells[1]. The main function of the tunica media is to stretch and recoil with changing arterial pressures[2].

The tunica adventitia is the outermost layer of the arterial wall, consisting of  of longitudinally orientated collagen fibers in combination with fibroblasts, elastic fibers, nerves and vasa vasorum, providing blood supply to the arterial wall itself. From the elastic (central) to the

muscular (peripheral) arteries, this layer becomes thicker. The collagen fibers of tunica adventitia prevent the artery from overstretching and rupturing under normal physiological circumstances[1].

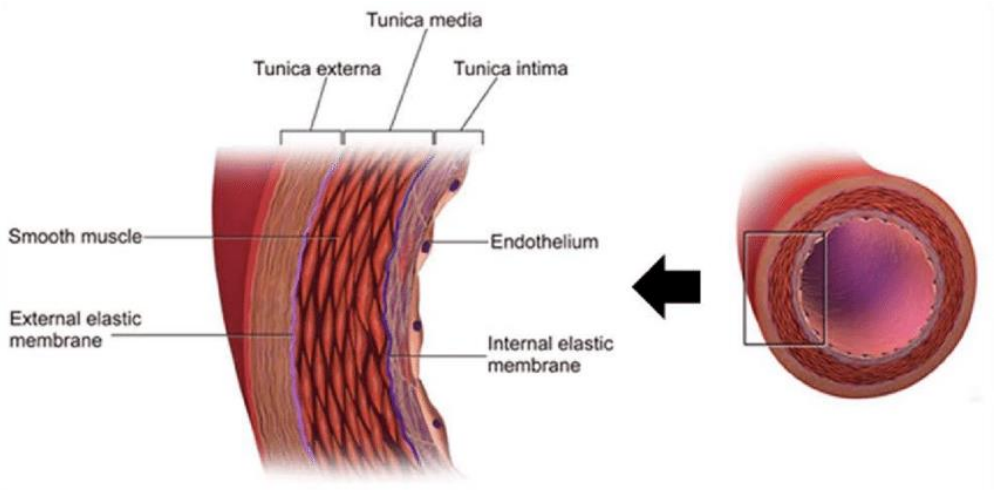


*Figure 1: Schematic representation of the different layers in the arterial wall (adapted from Wikipedia)*

## *1.1. Major components of the arterial wall*

### *1.1.1. Elastic fibers*

Elastic fibers are an essential part of the arterial wall, responsible for elasticity and resilience of major arteries[3; 4]. Due to physiological forces, elastic fibers deform by storing energy, in order to release the stored energy afterwards by passive recoil. Elastic fibers are composed of elastin, an insoluble, stable polymer formed by extensively crosslinked tropoelastin[4]. A schematic overview of elastin synthesis can be found in Fig. 2. In nearly all species tropoelastin is encoded by one single gene[5; 6] and is expressed by various cell types during neonatal stage of development[6]. Immediately after translation, to prevent premature aggregation, the tropoelastin molecule is bounded to its molecular chaperone in the rough endoplasmatic reticulum. This chaperone-tropoelastin complex persists in the Golgi apparatus, until excretion. After excretion the complex will be localized on the cell surface, where the tropoelastin will be separated from its chaperone. The chaperone is recycled, while the tropoelastin molecule itself is aligned and modified to be incorporated in an elastic network by irreversible polymerization[6; 7]. An elastin core, an insoluble polymer, consisting of several cross-linked tropoelastin molecules[6], is formed. This elastin core is extremely stable, and in combination with a very slow turnover, mature elastin is said to lasts for the entire life[6]. However, in humans, the elastin half-life time has been suggested to be around 70 years, which means that, due to the long life-expectancy, degradation and modification of elastic fibers within the arterial wall might contribute to the pathogenesis of arterial aging. Some authors even report an elastin half-life time of only 40-50 years, which would even more explain the age-related

stiffening of large elastic arteries [8; 9]. Those crosslinked elastin cores, in combination with an outer layer of microfibrils form the elastic fibers[10]. Those microfibrils consists mostly of fibrillin, combined with several fibrillin-binding proteins[11] (Fig. 3). In humans, three fibrillin isoforms have been described, nevertheless fibrillin-1 is by far the most abundant in mature tissue. Multiple heritable connective tissue disorders, including the well-known Marfan syndrome, highlight the importance of fibrillin-1 in elastic tissue[11; 12].

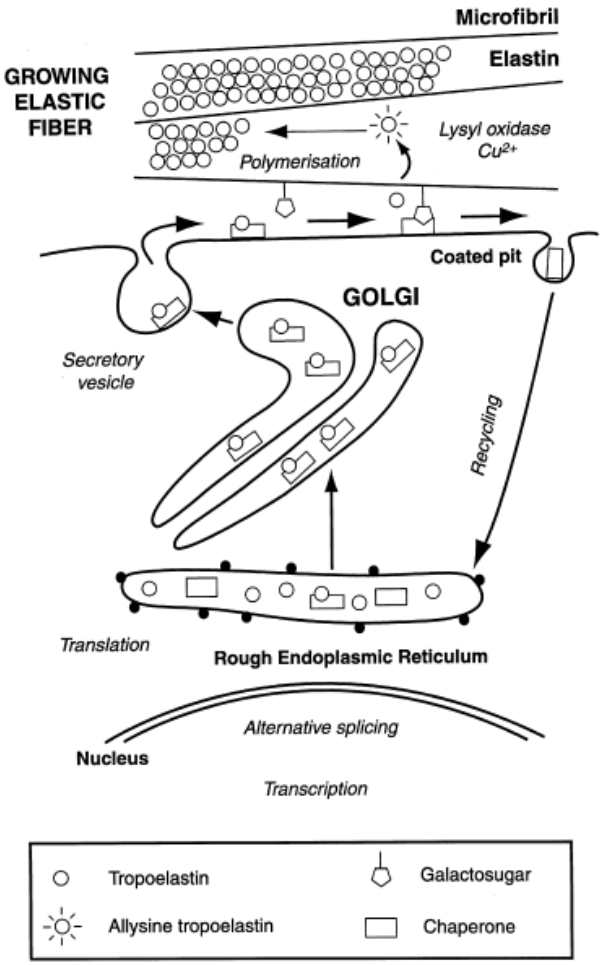


*Figure 2: Schematic representation of the elastin synthesis[6].*

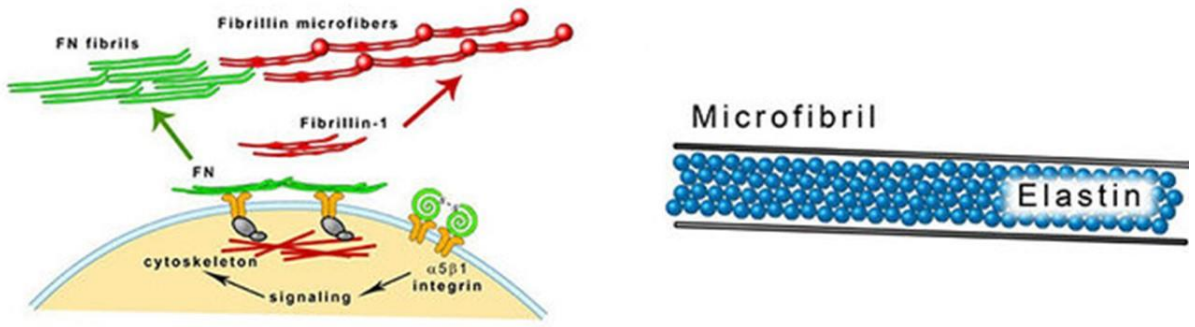


*Figure 3: Schematic representation of microfibril assemblage and elastic fiber formation[13]*

### *1.1.2. Smooth muscle cells*

Smooth muscle cells are the stromal cells of the arterial wall[14] and the major cell type of the tunica media[15]. Their contractile function enables them to participate in the blood pressure regulation[14], while their synthetic function enables them to construct and maintain or repair several components of the arterial wall[14; 16]. This phenotypic diversity is the result of genetic programming in combination with environmental signals, including biomechanical factors, extra cellular matrix components and stretch and shear stress[16]. The two ends of the phenotypic spectrum of smooth muscle cells are the contractile and synthetic vascular smooth muscle cells, with many intermediate phenotypes in between. Synthetic and contractile smooth muscle cells have a completely different microscopic appearance. Contractile cells are elongated, spindle-shaped cells, in contrary to synthetic cells, which are less elongated and have a cobblestone morphology. Also the inside of the cells is completely different. Synthetic cells contain lots of organelles, necessary for the protein synthesis, whereas in contractile cells those organelles are replaced by contractile filaments. Another important difference is that synthetic cells have higher growth potential, and a higher migratory capacity in comparison with contractile cells[16]. This migration and proliferation forms the basis of intimal thickening during hypertension and formation of atherosclerotic plaques[17]. The contractile cells, as the name suggests, are responsible for the regulation of the vascular tone via vessel constriction[18], while the synthetic cells are able to produce extra cellular matrix proteins[19; 20] and collagen[21]. Overall, the tunica media consists mostly of contractile smooth muscle cells, fulfilling the contractile function of the arterial wall, while the synthetic cell type, present in a smaller amount, is necessary for the maintenance and physiological remodelling of the arterial wall[16].

### *1.1.3. Collagen*

Collagen is a protein, which is mostly produced by fibroblasts, but can also be produced by other cell types like epithelial cells and smooth muscle cells[21; 22]. It is made of amino acids and provides the structural support of connective tissue. Collagen is responsible for the rigidity and resistance to tension in multiple tissues including bone, tendons, skin, ligaments and arteries[23]. The synthesis of collagen is a complex interaction of intracellular and extracellular events[24]. Intracellularly the corresponding collagen chain genes are transcribed to mRNA in the nucleus, afterwards the mRNA moves into the cytoplasm and interacts with ribosomes to be translated to pre-pro-polypeptide chains. These chains travel to the endoplasmic reticulum, where they are modified multiple times to become pro-collagen. Still in the endoplasmic reticulum three pro-collagen chains form a triple helix. Now the pro-collagen is ready to be transported to the Golgi apparatus, where the final modifications are made, before being assembled in secretory vesicles for transport to the extracellular space. Extracellularly, the

enzyme collagen peptidase removes the ends of the pro-collagen chains in order to become tropocollagen. Afterwards the enzyme lysyl oxidase enables the formation of collagen fibrils by modulating bounding between multiple tropocollagen chains[23]. A schematic overview of the collagen synthesis can be found in Fig. 4. At least 16 types of collagen exist, nevertheless 80 to 90 % of the total collagen in the body consists of collagen type I, II and III, which are long, thin fibrils. Type IV collagen in contrary forms a two-dimensional reticulum[22]. Collagen type I and III are the two most prominent types of collagen in the arterial wall, they are both present in the tunica intima, media and adventitia. Type IV collagen is only present in the endothelial basement membrane and the basement membranes of the smooth muscle cells[25].

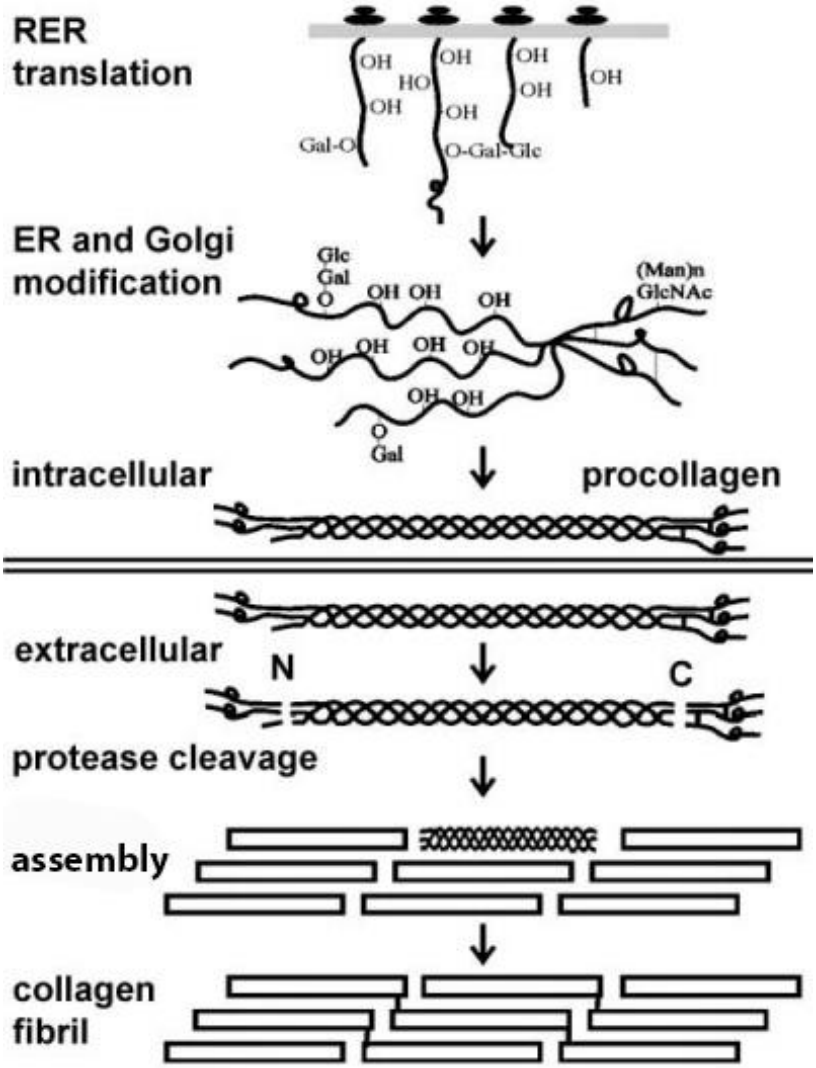


*Figure 4: Schematic representation of the collagen synthesis (adapted from http://flipper.diff.org/app/items/Collagen).*

### *1.1.4. Proteoglycans*

Although proteoglycans are a minor component of the arterial wall, they are essential for viscoelasticity of the arterial wall, lipid metabolism, haemostasis and thrombosis[20]. Proteoglycans are produced by smooth muscle cells and endothelial cells, and play an important role in cellular adhesion, migration and proliferation, important processes in the development of arteries, but also in the development of vascular lesions such as lipid retention, calcification and retention of macrophages[26]. The two most important proteoglycans associated with vascular disease are hyaluronan and versican[26].

## 2. Physiological function of arteries

Arteries carry blood that is ejected by the heart during systole, away from the heart, over the whole body. There are two different arterial circuits, the systemic circuit and the pulmonary circuit. The pulmonary circuit transports blood from the right ventricle, low in oxygen, to the lungs, where it can be oxygenated before it is returned to the left atrium via the pulmonary veins. The systemic circuit transports oxygen rich blood to the rest of the body. The function of the systemic arterial tree is dual: conducting blood towards the downstream circulation in the first place, but also buffer the enormous pulsatile difference between systolic and diastolic pressure, in order to guarantee a continuous blood flow towards the organs. This conversion, from pulsatile pressure to continuous pressure is performed by the proximal, elastic arteries. During systole, when blood is pumped away from the heart, a part of the ejected blood and energy is retained due to the elasticity of the arterial wall. During diastole, this part of the ejected blood and energy is released again, thanks to passive recoil of the arterial wall and thereby buffering the pulse pressure, which is the difference between diastolic and systolic arterial pressure, guaranteeing a continuous blood flow at the level of the arterioles[27].

### *2.1. Blood pressure*

Pressure depends on dynamic influences, for example acceleration and friction in a moving fluid, and on static influences, for example gravitational forces[28]. Arterial blood pressure is referred to as systolic, diastolic and mean arterial blood pressure. While blood volume is proportional to body mass and heart rate varies enormously in mammals, in combination with a cardiac output which also scales to body mass, systolic and diastolic arterial pressure are independent of body mass. The major reason for the constant blood pressure across mammalian species is the lower mass-specific metabolism in larger species, which can be sustained by a lower capillary density, resulting in less resistance arteries per mass. Therefore peripheral vascular resistance increases proportionally to the increase in cardiac output[29]. Also heart rate scaling in between species plays an important role in maintaining constant blood pressure: total peripheral resistance multiplied with total compliance, divided by the

cardiac period is constant across species[30]. Whether mean aortic pressure is influenced by body mass remains unclear and some authors suggest that mean aortic pressure is the same across species[29], while other authors do describe an effect of body mass[31; 32]. Mean aortic blood pressure differing among species seems logical, as the distance between the heart and the brain gets longer and mean arterial pressure at brain-level needs to be constant. For example, giraffes need a higher mean aortic pressure in order to guarantee sufficient blood supply to the brain[29].

### *2.1.1. Blood pressure regulation*

Blood pressure (BP) is the result of cardiac output (CO) and total peripheral resistance (TPR), BP= CO * TPR, which means blood pressure can be highly regulated by physiological adaptations. The blood pressure in a mammalian body is measured by baroreceptors, which are located in the aortic arch and carotid sinus. Blood pressure-induced mechanical deformations evoke afferent nerve signals, resulting in efferent sympathetic traffic, leading to adaptations in heart rate and peripheral vascular resistance[33]. On the other hand, the renin-angiotensin system also regulates arterial blood pressure. This system works through interactions between kidney, cardiovascular system and central nervous system[34]. When blood pressure becomes too low, renal hypoperfusion will result in renin production by the kidney. Renin is an enzyme that converts the plasma protein angiotensinogen, produced by the liver, to angiotensin 1. In the lungs and the kidneys angiotensin 1 is converted to angiotensin 2 by the angiotensin-converting enzyme. This angiotensin 2 has multiple functions, all resulting in an elevated blood pressure. Angiotensin 2 stimulates vasoconstriction of the peripheral arteries and also stimulates the pituitary gland to produce anti-diuretic hormone in order to stimulate water retention by the kidneys. Lastly, it stimulates the adrenal gland to produce aldosterone, which in turn stimulates sodium reabsorption and as such, has an anti-diuretic effect, increasing blood volume and blood pressure[34; 35]. A schematic review of the renin-angiotensin system can be found in Fig. 5.

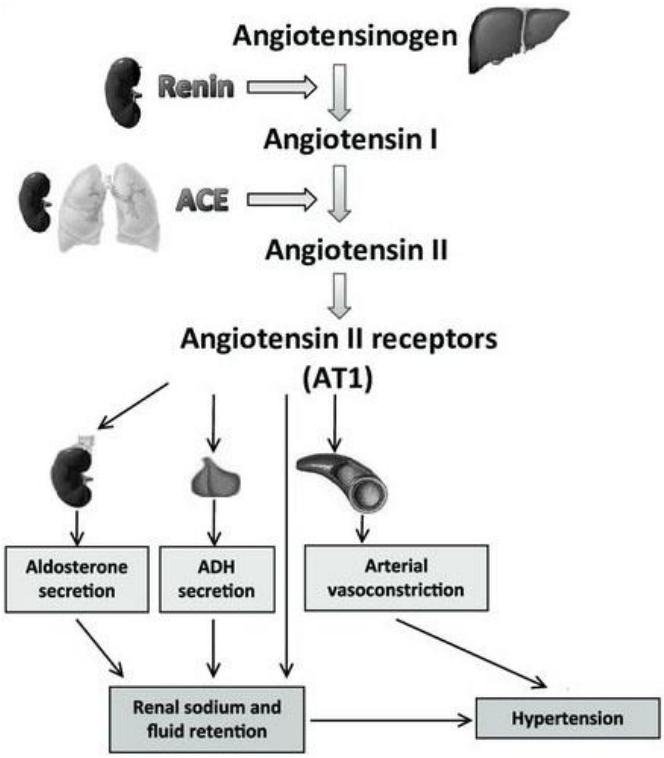


*Figure 5:: Schematic representation of the renin-angiotensin system to control blood pressure[36]. ACE: angiotensin-converting enzyme; ADH: anti-diuretic hormone*

### *Peripheral vascular resistance*

Peripheral vascular resistance plays an important role in regulating blood pressure, as blood pressure is the result of cardiac output and systemic vascular resistance[37]. When blood vessels constrict (vasoconstriction) systemic vascular resistance increases, while dilation of blood vessels (vasodilation) leads to a decrease in systemic vascular resistance. Vascular resistance is not only important for the regulation of systemic blood pressure, but especially for maintaining organ perfusion, preventing abnormal blood pressure at organ level which would cause tissue damage. To prevent organ damage, there is a large drop in pressure at the level of the arterioles, which are the main regulators of peripheral vascular resistance. The basis for this mechanism is given by the Hagen-Poiseuille equation: $R= 8Ln/(\pi*r^4)$, where R is the resistance of blood flow, L is the length of the vessel, n is the blood viscosity and r is the radius of the blood vessel. As such, modifying the radius of the vessel has an important effect on blood flow resistance [37].

Peripheral vascular resistance is regulated by neuro-hormonal response and by locally produced metabolites. Norepinephrine, released into the bloodstream during an adrenergic response, binds to the α1-receptor of the vascular smooth muscle cells. This leads to an intracellular increase in guanosinetriphosphate (GTP), which activates phospholipase C and starts the inositol triphosphate (IP3) pathway. Intracellularly stored calcium is released and results in vascular smooth muscle cell contraction[37; 38]. Other molecules that cause

vasoconstriction include thromboxane, endothelin, angiotensin II, vasopressin and dopamine[37; 39]. Epinephrine on the other hand binds to the β2-receptors of the vascular smooth muscle cells, increasing cyclic adenosine monophosphate (cAMP), leading to an increased activity of protein kinase A. Protein kinase A phosphorylates myosin-light-chain kinase (MLCK), decreasing its activity and as such leading to vasodilation[37]. Other molecules that cause vasodilation include nitric oxide, histamine, prostacyclin, prostaglandin D2 and E2, adenosine, bradykinin, carbon dioxide, and vasoactive intestinal peptide[37; 40]. Also the endothelium itself can modulate blood pressure (endothelium derived vasodilation or vasoconstriction), by releasing nitric oxide (NO) or endothelin, respectively[37].

### *2.1.2. Blood pressure measurement*

Arterial pressure is influenced by four major mechanisms: 1) the cardiac output and peripheral resistance, determining the mean value of the blood pressure; 2) the flow amplitude and characteristic arterial resistance, determining the pressure amplitude; 3) the orthostatic pressure and 4) the local flow velocity, of which the influence is rather small [28]. Arterial blood pressure can be measured invasively and non-invasively.

#### *2.1.2.1. Invasive blood pressure measurement*

Invasive blood pressure measurement means that the blood pressure is directly measured in the corresponding artery. To measure blood pressure, a catheter or needle is inserted in a superficial artery, which will be connected to a pressure transducer using a fluid-filled line. The pressure transducer will translate the pulsatile pressure in an electronical signal, which can be displayed continuously on a screen. The pressure transducer needs to be situated at the level of the heart, in order to correct for gravitational forces. In humans and small animals this technique is frequently used in intensive care for monitoring critically ill patients. It is also frequently used during surgical interventions and experimental conditions, in both small and large animals. Those fluid-filled systems are relatively inexpensive, but measurement errors up to 20 mmHg are reported. Those measurement errors might be due to damping, mostly due to air bubbles or small blood clots. Another possible cause of measurement error is systolic overshooting. All pressure waves have a natural resonant frequency. If the fluid filled hydraulic system vibrates at the same frequency, the peak of tracing will be much higher than the actual pressure inside the artery, leading to systolic overshooting. Pressure tip catheters, where the pressure sensor is placed directly on the tip of the catheter, are more precise, but also more expensive. They are nowadays routinely used to monitor intra-cardiac pressure during cardiac surgeries in humans where precise blood pressure monitoring is necessary[41].

### *2.1.2.2. Noninvasive blood pressure measurement*

The noninvasive techniques of blood pressure measurement can be divided into three categories: the auscultatory method, the oscillometric technique and the Doppler technique.

***The auscultatory blood pressure measurement***

The auscultatory method can be used in humans, but is not used in small animal or equine medicine. For this method, a sphygmomanometer cuff is placed around the arm. The pressure in the cuff is inflated above systolic pressure. A stethoscope is placed at the corresponding artery distal from the cuff. As the cuff is inflated above systolic pressure, there is no blood flow in the corresponding artery and nothing can be heard through the stethoscope. When the cuff is slowly deflated, the pressure at which the first sound can be heard through the stethoscope can be defined as the systolic arterial pressure. Thereafter the cuff is further deflated until no sound can be heard at all, this pressure can be noted as the diastolic pressure[42]. A schematic representation of the auscultatory method is represented in Fig. 6.

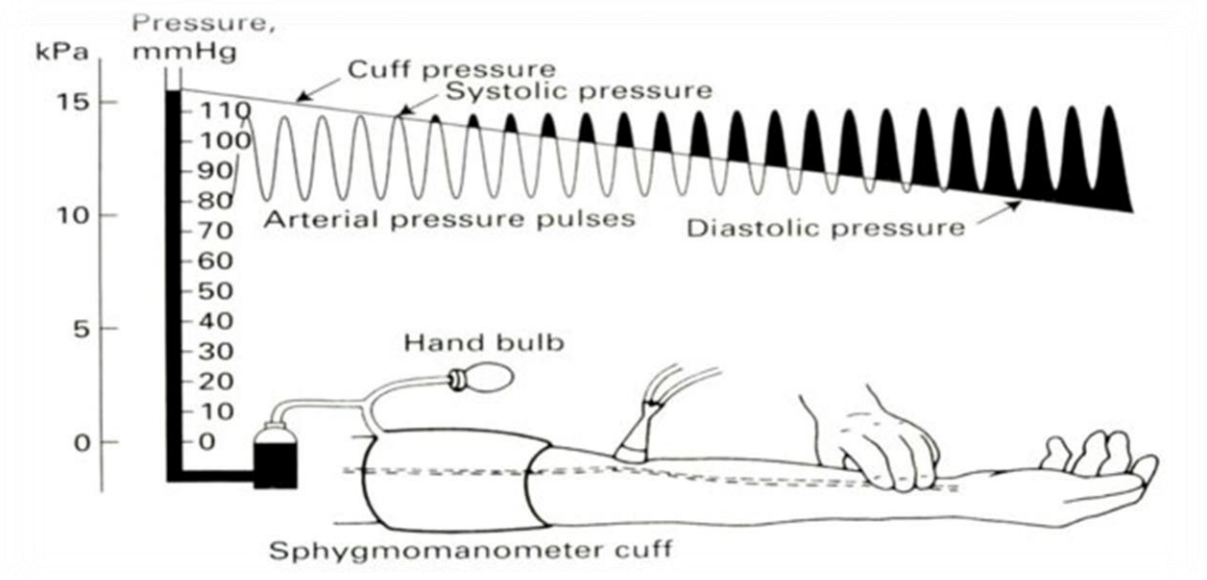


*Figure 6: Auscultatory blood pressure measurement[42].*

***The oscillometric blood pressure measurement***

Similar as for the auscultatory technique, for the oscillometric technique a cuff is placed over a superficial artery, and inflated above systolic pressure. During gradual deflation of the cuff, the reducing pressure exerted on the artery allows blood to flow through, which sets up detectable vibrations of the arterial wall[43]. Those vibrations, also called oscillations are recorded. The oscillations start at systolic pressure and continue below diastolic pressure. The point of maximal oscillations is registered as the mean arterial blood pressure, while diastolic blood pressure cannot be measured and will be estimated using algorithms[44]. The oscillometric technique can be used in humans and small animals, but also in horses, where it

is the most commonly used technique. In human patients the cuff is placed around the arm, while in horses and small animals the cuff is placed around the leg (in anesthetized horses), or around the base of the tail over the coccygeal artery. A schematic representation of the oscillometric measurement is displayed in Fig. 7.

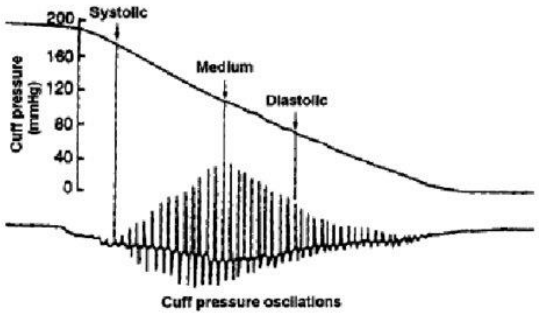


*Figure 7: Schematic representation of oscillometric blood pressure measurement[45]*

***The Doppler ultrasound blood pressure measurement technique***

This technique is based on an ultrasound transmitter and receiver placed over the corresponding superficial artery, in combination with a sphygmomanometer cuff. This technique is the most used technique in small animals, but can also be used in horses. The principle is basically the same as the other techniques: the cuff is first inflated above systolic pressure and afterwards slowly deflated. At systolic pressure, the red blood cells and consequently the arterial wall starts to move, which causes a Doppler phase shift in the reflected ultrasound. The point where diminution of arterial movement occurs is recorded as diastolic pressure[44], which is not reliable in small animals. A schematic overview of the ultrasonic blood pressure measurement can be found in Fig 8.

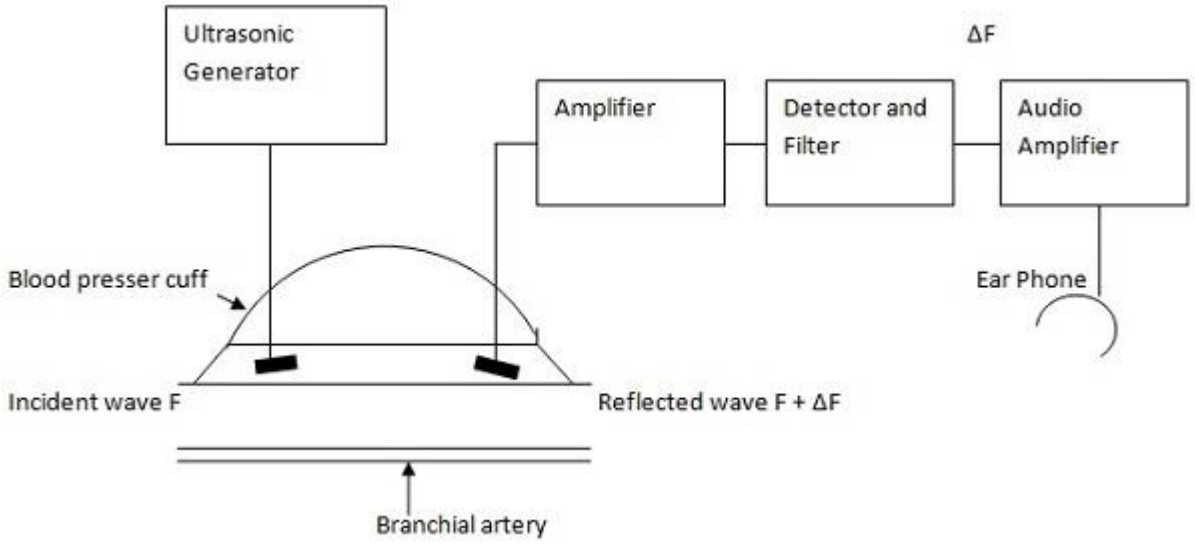


*Figure 8: Schematic representation of the ultrasonographic blood pressure measurement[46].*

### *2.1.3. Normal blood pressure in horses*

Blood pressure measurement in horses can be performed both invasively and noninvasively. Invasive blood pressure measurement requires cannulation of an artery, which is labor intensive and time consuming and in some cases even dangerous or impossible in the standing awake horse[47]. Therefore, in horses, invasive techniques are usually only applied in experimental settings or under general anesthesia, as hypotension increases anesthesia-related morbidity and mortality[48-50]. The noninvasive oscillometric method, using a cuff placed around the base of the tail, is by far the most used method in the standing, non-sedated horse[47]. To correct the reading at the level of the coccygeal artery to the level of the heart base, for each centimeter in difference between the right atrium and the tail cuff, a correction factor should be applied to correct for hydrostatic pressure[47]. In literature, a range of correction factors is used. Tearney et al.[50] for example used a correction factor of 0.735 mmHg for every centimeter difference between the measurement site and the sternum, while Hatz et al.[51] and Tunsmeyer et al.[52] used a correction factor of 0.74 mmHg. Dryan et al. [53] on the other hand used a correction factor of 0.75 mmHg for every centimeter in difference as he states that one cm fluid height of $H_2O$ is equal to 0.75 mmHg, while, Olsen et al.[54] and Heliczer et al.[47] used a correction factor of 0.76 and 0.77 mmHg, respectively. The hydrostatic pressure of 1 cm of water is 0.74 mmHg. Nevertheless blood has a higher density compared to water. Therefore the correct correction factor is 0.77 mmHg for every cm difference in height, as $\Delta bp = d_v . \frac{sg_b}{sg_m}$, where $\Delta bp$ represents the difference in blood pressure, $d_v$ the vertical distance from the measurement point to the heart in mm, $sg_b$ the specific gravity of blood (1.05)[55] and $sg_m$ the specific gravity of Hg (13.6)[56].

Noninvasive blood pressure measurement in standing, non-sedated horses is useful to monitor progression of cardiac and renal disease, evaluate chronic or severe pain and monitor fluid resuscitation[47; 54]. Multiple studies compared the agreement between invasively and noninvasively measured blood pressure in awake and anesthetized horses. Heliczer et al.[47] investigated the agreement between noninvasive and invasive blood pressure measurements at different blood pressure ranges in standing horses and compared them with horses under general anesthesia. For noninvasive measurements, oscillometry was used at the level of the tail, while invasive measurements were performed simultaneously at the level of the transverse facial artery. Measurements were performed in normal pressure ranges, in induced hypertension (using phenylephrine IV) and in induced hypotension (using acepromazine IV). A group of 8 standing horses and 8 anesthetized horses was used. They concluded that both in the standing and anesthetized group, the noninvasively measured blood pressure was strongly correlated with the invasive one and was able to reliably differentiate increases and decreases in blood pressure. Nevertheless the accuracy and precision of the noninvasively

measured blood pressure was limited in the standing horses, in comparison with the anesthetized horses[47]. Another study of Olsen et al. in seven standing conscious trotter horses showed that the oscillometric mean arterial blood pressure, which is the most important value to assess cardiovascular status, could be measured with a high overall accuracy, in combination with a high overall precision. The lowest measurement error was found during normo- and hypertension. In this study hypertension was induced using IV dobutamine in combination with atropine, while hypotension was induced using IV acepromazine[54].

Another important consideration when blood pressure is measured noninvasively is an appropriate cuff bladder width-to-tail circumference ratio. A too small cuff will overestimate arterial blood pressure, while a too large cuff will underestimate arterial blood pressure. Hatz et al.[51] and Heliczer et al.[47] used a cuff to tail circumference ratio of 0.4, while Tunsmeyer et al.[52] and Olsen et al.[54] used a ratio between 0.4-0.6. In contrast with these authors and with manufacturer descriptions, Tearney et al.[50] found a cuff widt-to-tail circumference ratio of 0.25 the best cuff width for equivalence between invasive and oscillometric mean arterial blood pressure, measured in anesthetized horses in lateral recumbency.

Parry et al.[57] published normal limits (within the 2.5$^{th}$ and 97.5$^{th}$ percentiles) for corrected noninvasive coccygeal measured arterial blood pressure in 296 clinically normal horses, including 97 thoroughbreds, 97 standardbreds and 102 Hacks. Published normal limits were 68-159 mmHg for systolic arterial blood pressure and 45-97 mmHg for diastolic arterial blood pressure. Other values for standing, conscious, healthy horses that can be found in literature are for example the normotensive values reported by Heliczer et al.[47] (142±20 mmHg systolic, 100±18 mmHg diastolic and 116±20 mmHg mean arterial blood pressure), measured in 7 horses, or the ones reported by Nostell et al.[58] (113±11 mmHg systolic, 69±12 mmHg diastolic and 87±16 mmHg mean arterial blood pressure), measured in 13 horses, 11 standardbreds and 2 warmblood horses.

### 3. Biomechanical characteristics of the arterial wall

It is obvious that the arterial wall is not homogeneous, also called *inhomogeneity*. As mentioned previously the arterial wall consists of three different layers: the tunica intima, media and adventitia, with each layer containing its own specific amount of elastin, collagen, smooth muscle cells and proteoglycans. It is therefore clear that the arterial wall can be considered as multi-phase material, meaning a material that is composed of multiple materials, all with their own, largely different characteristics[59]. Another important characteristic of the arterial wall is its *anisotropy*, which means that the elastic properties differ between the longitudinal and circumferential direction[60], an important property to keep in mind when uni-axial tensile tests are performed[59]. Next to this inhomogeneity and anisotropy, *non-linearity* is another

important characteristic which means that the stress-strain relationship curve is non-linear (Fig. 9), because arterial tissue becomes stiffer the more it is deformed[59; 60]. Stress represents the ratio of the load or force to the cross-sectional area of the material to which the load is applied, while the strain is a measure of the deformation of the material as a result of the force applied. There is an important difference between engineering stress and strain and true stress and strain, due to the original shrinking of the tissue and the development of elongation during stress tests. True stress is always larger than the engineering stress, while true strain in always lower. Engineering stress can be defined as ratio of the load (force) to the original cross sectional area, while true stress represents the ratio of load (force) to the actual cross sectional area. Similarly, engineering strain represents the ratio of the amount of deformation to the original length, while true strain can be defined as the natural logarithm of the ratio of current length to original length. Finally, the arterial wall shows *visco-elasticity*, which is shown by the fact that the arterial wall exhibits stress-relaxation. When an artery is deformed and kept at this deformation for a while, it is observed that the stress, needed to maintain this deformation will decrease to a new steady state[59].

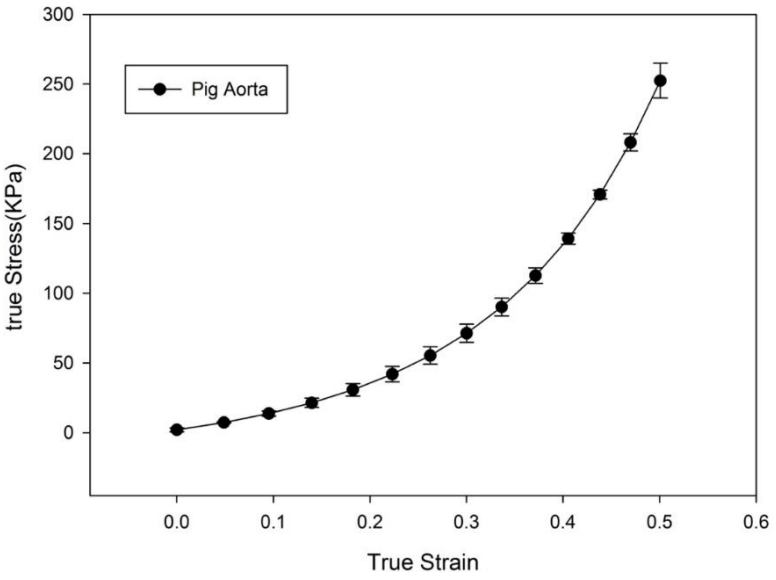


*Figure 9: Stress-strain curve from a pig aorta, indicating the non-linearity of the arterial wall*

Due to the inhomogeneity, anisotropy and visco-elasticity of the arterial wall, characterizing the biomechanical properties of the arterial wall is challenging. Wall tissue can be investigated using tensile tests, whereby the arterial wall is stretched in a controlled way from a zero-stress state until rupture occurs. Using this technique force-extension data can be converted into stress-strain relations, describing the biomechanical properties of the arterial wall[61; 62].

### *3.1. Uniaxial tensile test*

Uniaxial tensile tests are the simplest and most widely used method in order to characterize the biomechanical properties of the arterial wall *ex vivo*. Samples need to be collected in circumferential and longitudinal direction and need to be dogbone-shaped (Fig. 10). The tissue sample is clamped into manual or pneumatic grips, taking care not to damage the tissue. During a tensile test the force necessary for displacement is recorded. Force-extension data are collected and converted into stress-strain curves[62].

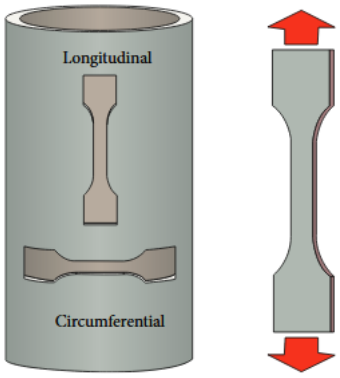


*Figure 10: Dogbone-shaped sample collection for uni-axial tensile tests [62].*

### *3.2. Biaxial tensile test*

Biaxial tensile tests better simulate the real, *in vivo* behavior of the arterial wall. As the longitudinal and circumferential direction can be tested at once, differences in tissue properties between the two directions can be assessed. A square piece of arterial wall needs to be collected for a biaxial test. The tissue sample is anchored using hooks and as such connected to the stretcher arms. Starting from stretch free state, stress-strain curves are recorded (Fig. 11). This method is less suitable for stretching until rupture, due to the attachment technique and the square-shaped samples[62].

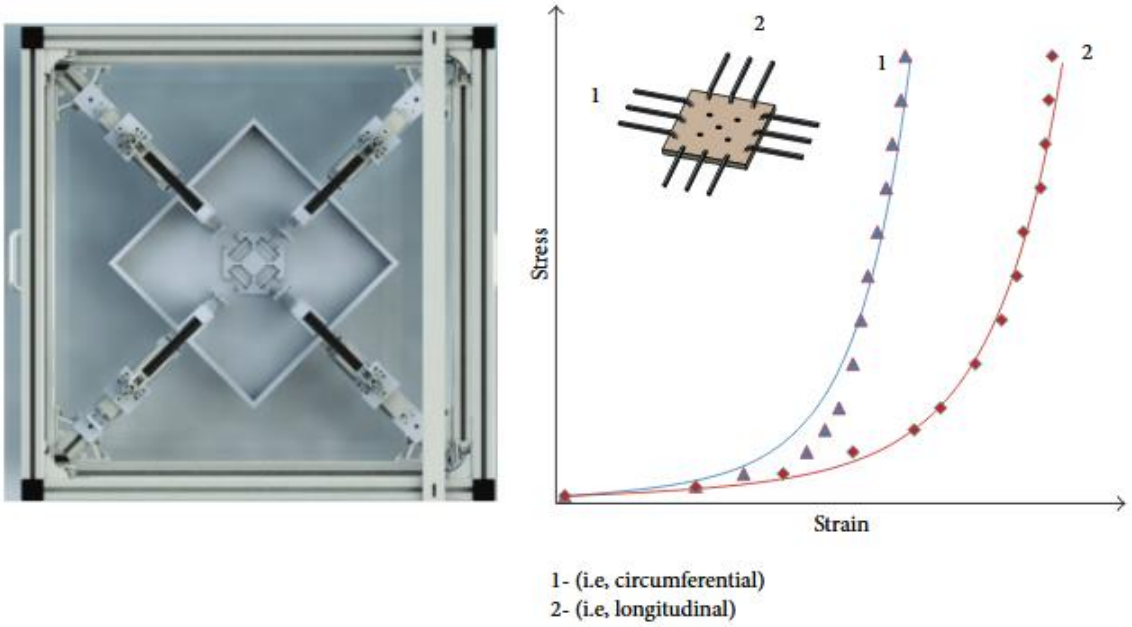


*Figure 11: Biaxial tensile test and derived stress-strain curve for the longitudinal and circumferential direction[62].*

### *3.3. Inflation-extension test*

Another way of testing the biomechanical properties of the arterial wall is the inflation-extension test. This test mimics best the *in vivo* situation as the whole cylindrical segment is pressurized and is preferred over a biaxial test which does not take into account sample curvature[62]. Tissue deformation can be monitored using video-based tracking techniques or ultrasound analysis[62; 63]. For video tracking, multiple markers are embedded in or affixed to the specimen. With traditional video tracking, a blood vessel is commonly assumed to be a perfect cylindrical tube and only the outer diameter is assessed. Recently, advanced three-dimensional tracking systems have been applied to measure non-uniform deformation of arterial tissue, by monitoring circumferential changes. Ultrasound can be used to monitor circumferential changes. However, cross-sectional image quality is not always optimal at 4 and 8 o'clock position, which makes manual tracking of the arterial wall more difficult. Ultrasonographic diameter measurements on the other hand reveal good reproducibility independent of imaging plane and load applied to the arterial wall. As such, a reliable estimation of the arterial stiffness can be obtained for a physiologic pressure range[63].

## 4. Mathematical models of the arterial tree

Models of the arterial tree can be used to study blood flow, blood pressure and flow waveforms. Models are always a simplistic version of the reality, but are very helpful to understand the function and physiology of biological systems[64].

### *4.1. Zero-dimensional (Windkessel) model*

The Windkessel model is used to understand variations in pressure during the cardiac cycle and over the arterial tree due to the elasticity of the major arteries. The model was named after the Windkessel present in fire engines, because this Windkessel can be compared to the volume elasticity of large arteries (Fig. 12)[65]. This Windkessel model is also called the lumped model, as it studies the pressure-flow relation of the whole arterial system by two parameters: the compliance and the resistance. This Windkessel model belongs to the zero-dimensional models, as it is composed of an in-series combination of resistive and compliant elements of the arterial tree and variables are only a function of time, not space. The advantage of this model is that only a few parameters are necessary to study the arterial network. However, this model cannot be used to study wave travel and wave reflections over the arterial tree[64; 65].

The compliance (C) can be defined as the ratio of volume change (ΔV) to pressure change (ΔP; C=ΔV/ΔP) and represents the sum of the compliances of all major arteries over the arterial tree. A high compliance means that a small increase in pressure induces a large increase in volume and vice versa. Resistance can be defined as the degree to which a substance prevents flow through it. In zero-dimensional models, the resistance of the arterial tree can be considered as the sum of all individual resistances of the arterial microcirculation, because the resistance in the small arteries and arterioles contributes the most to the arterial resistance. As the law of Poiseuille states: the resistance is related to the length of the vessel and inversely proportional to the blood vessel radius to the fourth power[65].

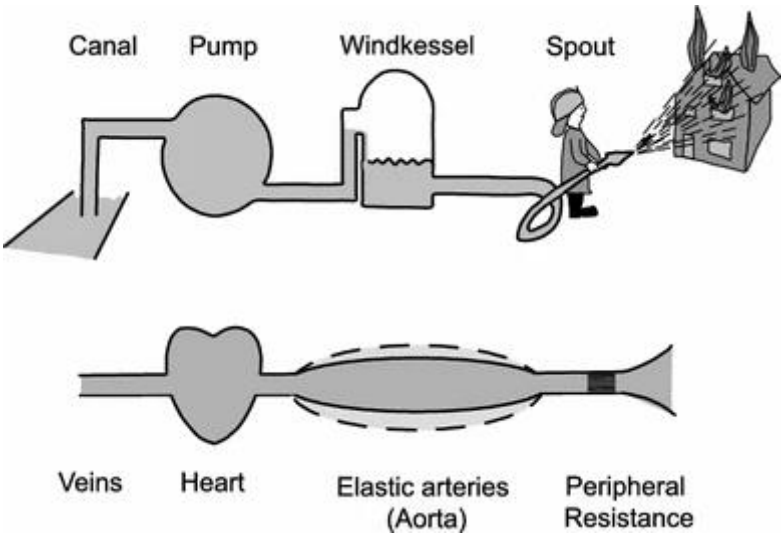


*Figure 12: Schematic representation of the Windkessel model, in the fire engine and in the arterial tree[65]. The so called two-element Windkessel model consists of a resistance and a compliance element.*

### *4.2. One-dimensional models*

The so-called one-dimensional (1D) models are based on the Navier-Strokes equation, describing the flow of incompressible fluids. In those 1D models the main arteries of the arterial tree are divided into small interconnected straight arterial segments. In each of these segments, the Navier-Strokes equation can be solved. Appropriate 1D models can be used to easily and precisely model the forward and reflected waves in the arterial tree, making those models ideal to study pressure and flow wave propagation along the arterial tree[64]. An example of a 1D model of the systemic arterial circulation in mice is represented in Fig. 13.

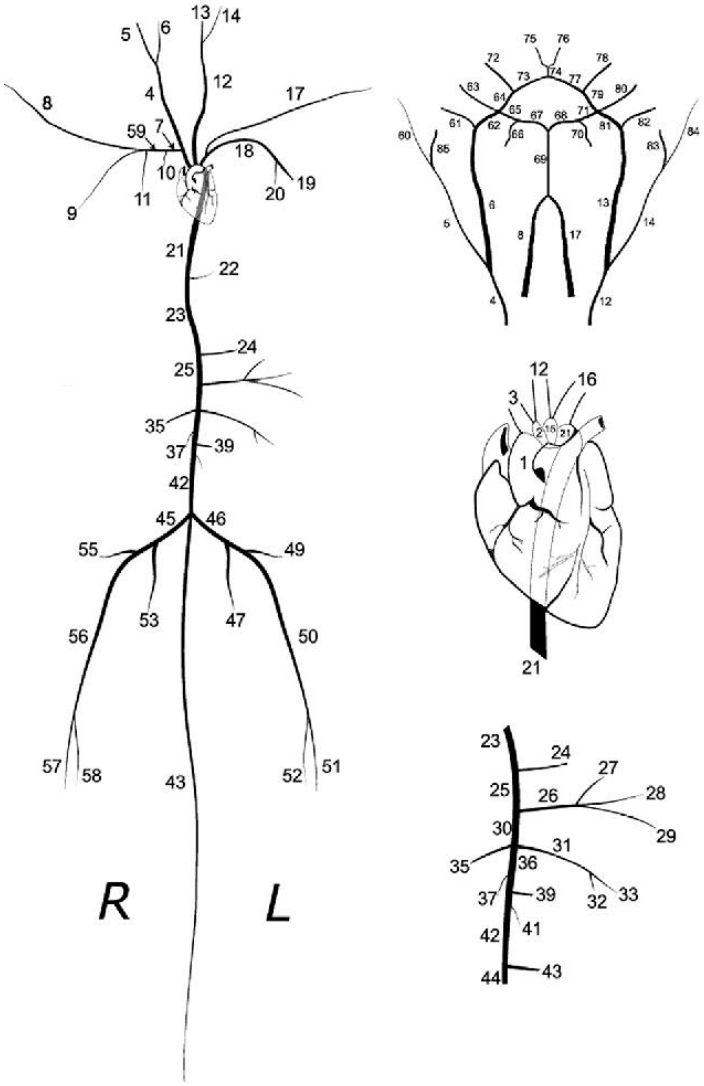


*Figure 13: Schematic representation of a 1D model describing the systemic arterial circulation in mice.*

In human medicine, a wide range of 1D models is available, allowing researchers to study the normal and abnormal physiology of the arterial system, without the need of *in vivo* measurements[66-68]. A large number of arterial segments can be included which allows specific information about blood flow or pressure wave characteristics at the level of individual branches and even in patient-specific situations to be obtained[69; 70].

## 5. Measurement of arterial wall stiffness

In 2006 an expert consensus on the methodological issues and clinical applications of arterial wall stiffness in human patients has been published[71]. Local and regional arterial stiffness can be measured directly and noninvasively at various sites along the arterial tree. Local and regional stiffness measurements are based on measurement of parameters which are directly linked to arterial wall stiffness at a specific site or over a part of the arterial tree, respectively[71].

### *5.1. Regional measurement of arterial wall stiffness*

Because the aorta contributes most to the arterial buffering capacity, the aorta is the most important vessel when assessing arterial wall stiffness[72]. Moreover, the regional stiffness of the aorta has been proven to be an independent predictor of cardiovascular outcome[71-74].

*The carotid to femoral pulse wave velocity*, generally accepted as the most simple and robust way to measure regional arterial wall stiffness, is considered as the gold standard method to assess arterial stiffness in humans[71; 75; 76]. In many epidemiological studies, pulse wave velocity has been shown to be of highly predictive value for cardiovascular events[71-74]. The pulse wave velocity can also be measured more towards the periphery, for example at the upper or lower limb, but these values do not have a proven predictive value[71]. A higher pulse wave velocity indicates stiffer arteries, while a lower pulse wave velocity indicates more compliant arteries. The pulse wave velocity is usually measured using pulsed wave Doppler ultrasound or tonometry to capture the pulse wave noninvasively at two different arterial sites, for example the common carotid artery and the femoral artery in case of carotid to femoral pulse wave velocity[71; 77; 78]. Tonometry uses noninvasive pressure sensors applied transcutaneously over the carotid and femoral artery, while for the Doppler ultrasound method, Doppler velocity signals of the carotid and femoral artery are used. In both cases, the pulse transit time is calculated from the foot (onset) of one pressure wave to the foot of the other pressure wave, called the foot-to-foot method (Fig. 14). The pressure wave is usually captured simultaneously at both places. Another option is to use the electrocardiogram (ECG) as a timing reference. Hereby, the time interval between the R wave of the synchronized ECG and the onset of the waveform is measured. The shortest time interval, at the level of the carotid artery, is subtracted from the longest time interval, at the level of the femoral artery, in order to calculate the pulse transit time. To calculate the pulse wave velocity (m/s) the traveled distance between the two measuring places (m) is divided by the pulse transit time (s)[71; 77]. The traveled distance between the two measuring places is usually estimated from body surface measurements. Some authors use the direct surface measurement between the carotid and the femoral artery[79], while others subtract the distance from the sternal notch to the carotid

artery from the distance between the carotid and femoral artery[80] or from the distance between the sternal notch and femoral artery[81; 82]. Also multiplying the surface distance between the carotid and the femoral artery with a correction factor has been described[83]. Huybrechts et al.[84] compared the true traveled distance, obtained by MRI measurements to several body surface measurements. They concluded that the surface measurement between carotid end femoral artery, multiplied with a correction factor of 0.8 corresponds the best with the real traveled distance[84].

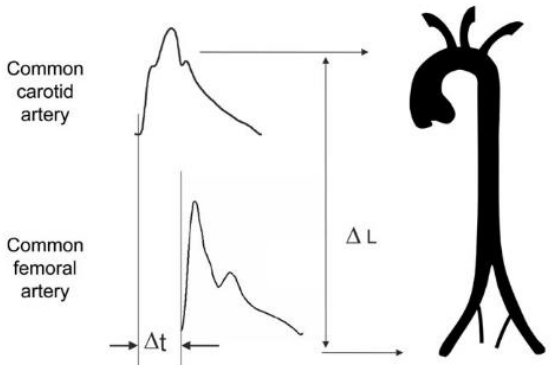


*Figure 14: Measurement of carotid to femoral artery pulse wave velocity using the foot to foot method[71].*

### *5.2. Local measurement of arterial wall stiffness*

Ultrasound devices can be used to assess local arterial stiffness of reachable arteries. Local stiffness parameters are based on the change in volume, driven by pressure changes. All types of classical vascular ultrasound can be used to determine those changes in diameter during the cardiac cycle, but manual measurements are limited in precision. Therefore echotracking devices were developed to measure diameter changes with very high precision[71]. Multiple local stiffness parameters are described in literature, such as:

-*The stroke change in diameter or lumen area* (ΔD;ΔA) is the systolic (Ds;As) minus the diastolic diameter or lumen area (Dd;Ad)[71].

$\Delta D=Ds-Dd$

$\Delta A=As-Ad$

-*The arterial diameter or lumen area strain* ($S_D$; $S_A$) represents the relative change in diameter or lumen area during the cardiac cycle, and is thus defined as the stroke change in diameter or lumen area (ΔD;ΔA) divided by the diastolic diameter or lumen area (Dd;Ad)[85].

$S_D$ (%) $=\Delta D/Dd$

$S_A$ (%) $=\Delta A/Ad$

-*The arterial compliance coefficient* ($CC_D$;$CC_A$) represents the absolute diameter or lumen area change that occurs between systole and diastole, i.e. the pulse pressure. This means that the arterial compliance coefficient is equal to the stroke change diameter or in lumen area (ΔD;ΔA) divided by the pulse pressure (ΔP)[86].

$CC_D=\Delta D/\Delta P$

$CC_A=\Delta A/\Delta P$

-*The arterial distensibility coefficient* ($DC_D$;$DC_A$) represents the relative diameter or lumen area change that occurs between systole and diastole, i.e. the pulse pressure. This means that the distensibility coefficient is equal to the stroke change in diameter or area (ΔD;ΔA) to the diastolic diameter or area (Dd;Ad), divided by the pulse pressure (ΔP)[86].

$DC_D=(\Delta D/Dd)/\Delta P$

$DC_A=(\Delta A/Ad)/\Delta P$

-*The stiffness index* (SI) represents the ratio of the natural logarithm of systolic (SAP) to diastolic arterial pressure (DAP) divided by the relative diameter change[87].

$SI=\ln(SAP/DAP)/(\Delta D/Dd)$

## 6. Physiological and pathological changes of the arterial wall

The arterial wall is a dynamic structure, which is able to adapt to different physiological and pathological circumstances. Multiple studies show that long-term changes in arterial blood flow and/or blood pressure can lead to blood vessel diameter increase and thickening of the arterial wall[88-90]. Arterial blood flow generates arterial wall shear stress, frictional stress on the vascular lumen surface, while arterial blood pressure creates arterial wall hoop stress, a tensile stress on the arterial wall in the circumferential direction[89]. The effect of arterial blood flow was, among others, studied by Kamiya and Togawa in 1980[88]. They created an arteriovenous shunt between the common carotid artery and the external jugular vein in 12 dogs. After a long-term follow-up period of 6 to 8 months, the arterial radius and the arterial wall shear stress was defined. Results showed that the arterial diameter increased with the flow rate and that eventually the shear stress had recovered to almost normal values. Wolinsky[90] on the other hand, studied the effect of hypertension on the arterial wall in rats. Ten weeks of hypertension revealed an increased diameter and an increased arterial wall thickness, as result of an increased thickness of the tunica media. In addition, the total amount of collagen in the arterial wall was increased in hypertensive rats.

### *6.1. The effect of aging on the arterial wall*

The organ systems of mammals, and other vertebrates are designed to work efficiently up to reproductive age, not beyond. Thus as mammals become older, degenerative processes start to occur[91]. Vascular aging is associated with changes in structural and mechanical arterial wall properties, leading to a loss of elasticity and arterial compliance. As mammals age, there will be an increase in collagen, cross-linking of collagen, elastin fracture, calcification and a decrease in the amount of elastin[92]. Other characteristics of vascular aging are endothelial dysfunction, resulting in a reduced bioavailability of the endothelium-synthesized nitric oxide, leading to decreased endothelium depended dilation[93] and increased arterial wall thickness of medium and large sized arteries due to smooth muscle cell phenotype switch and migration[94; 95].

The mechanisms of aging and the effect on life and health span, among which cardiovascular health, have been well studied in several animal species, for example in mice, rats, primates, fish, birds and even dogs. All those species are studied as models for human aging. Normal aged mice show very low prevalence of cardiovascular disease, in contrary to the naked mole rat, which has a way longer life span[96]. Aged dogs (>7 years) are known to reveal a dilated and stiffer aorta in comparison with young dogs (1-2 years). Moreover decreased aortic strain was shown to be significantly related with the amount of collagen in the aortic wall[97]. In horses, up to now, only little is known about the functional changes of the arterial wall due to aging. Concerning the histological age-related changes, one study, performed by Endoh et al.[98] showed that from the first year to the mature stage of life, the amount of elastin in the aortic wall decreased, while the amount of collagen increased. Ueno et al.[99] showed changes of the uterine artery wall, like smooth muscle cell atrophy, fibrosis and intima thickening in older mares, compared to younger mares.

### *6.1.1. Functional changes of the human arterial wall due to aging*

In humans, age-related loss of compliance, leading to an increase in systolic and a decrease in diastolic arterial pressure is a well-known phenomenon[92]. As mentioned previously, in order to guarantee a continuous flow towards the peripheral tissues, the arterial tree is designed to buffer cardiac pulsations. During systole young, compliant, elastic vessels show a large increase in diameter, retaining a large volume of blood, which results in a relatively small increase in systolic pressure. During diastole, the arterial wall releases the retained blood volume, by passive recoil. Therefore young, healthy individuals with compliant arteries show a relatively small arterial pulse pressure, which is the pressure difference between systolic and diastolic arterial blood pressure. In older individuals with stiffer elastic vessels, during systole only a small fraction of the blood volume is retained, as the arterial wall is not compliant enough, and therefore the systolic pressure will increase. During diastole, only a small volume of retained blood will be released, resulting in a low diastolic pressure, and thus a high pulse

pressure (Fig. 15)[27]. The elevated systolic pressure will induce increased left ventricular afterload and left ventricular hypertrophy. The increased ventricular afterload will increase myocardial oxygen demand but due to the lower diastolic blood pressure, coronary circulation is reduced and thus myocardial blood supply is decreased instead of increased, explaining the increased incidence of myocardial infarctions, chronic ischemic heart disease and sudden cardiac death due to arrhythmias in the elderly[100].

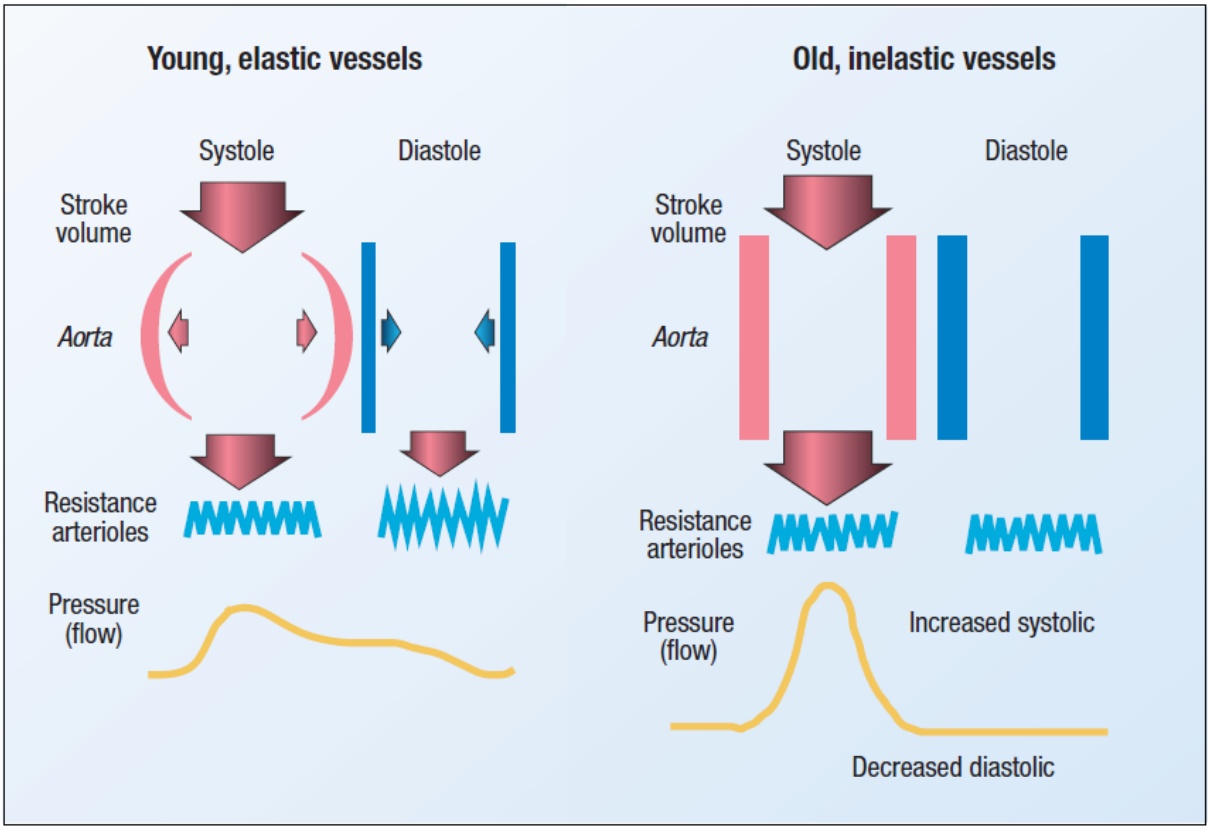


*Figure 15: Effect of the age and elasticity of the arterial wall on the arterial blood pressure[27].*

As large arteries stiffen, the velocity of the pulse wave, an important parameter for arterial wall stiffness, will increase. Increased pulse wave velocity, due to aging, will also contribute to an increased systolic blood pressure, by earlier return of the reflected waves.

### *6.1.2. Structural changes of the human arterial wall due to aging*

As described above, in human medicine, the arterial wall is known to stiffen with age. This stiffening is caused by an increased loss of vascular smooth muscle cells, endothelial disruption, fibrosis, elastin fragmentation, calcification and amyloidosis[101]. Aged vessels show an increase in reactive oxygen species, resulting in endothelial dysfunction. Vascular smooth muscle cells will start to migrate towards the intima, where they proliferate and start producing collagen and proteoglycans, being responsible for the increased arterial wall thickness. In contrast, due to apoptosis, the amount of smooth muscle cells decreases in the

tunica media and the elastin in the media will be fragmented and replaced by collagen and calcification, which is the major cause of increased stiffness in aged arteries[102].

Various pathways contribute to these structural changes including inflammatory cytokines and matrix metalloproteinases[102]. An increase in inflammatory mediators enables white blood cells to infiltrate into the arterial wall. Macrophages are activated and release additional inflammatory cytokines, after which they die by necrosis, thereby releasing their cytokines, leading to the degradation of elastin. Matrix metalloproteinases on their turn, mediate elastin degradation and also have a collagenolytic activity, causing uncoiled, stiffer collagen, contributing to the increased arterial stiffness[103].

### *6.2. Gender differences in arterial wall stiffness*

Multiple studies were carried out in order to assess the influence of gender on the human arterial wall[104; 105]. A multicenter cross-sectional study performed by Kim et al.[104] showed that women had a significantly higher augmentation index compared to men, however pulse wave velocity was higher in men than in women. Recent publications also indicate that women show a higher arterial stiffness compared to men when aging[105], especially after the onset of the menopause[106]. On the other hand, the Asklepios study, including 2026 apparently healthy, middle aged subjects (35-55 years old) found no difference in pulse wave velocity between men and women[107].

Testosterone, the male sex hormone, belongs to the family of androgens and binds to the androgen receptor to induce physiological actions. Testosterone seems to have a protective role in arterial stiffening. Low serum levels of testosterone impair endothelial function and are proven to correlate with increased arterial stiffness. Indeed, in testosterone deficient patients replacement of testosterone leads to decreased arterial stiffness and blockage of testosterone production leads to increased arterial stiffness[105].

Estrogen, the female sex hormone, binds to estrogen receptors (α and β) and also seems to play a protective role in arterial wall stiffening[106]. Before puberty, females have less compliant arteries than males of the same age, while after puberty the arterial stiffness decreases in females and starts to increase in males. From puberty on until the menopause, women seem to be protected against cardiovascular disease compared to age-matched men, while postmenopausal loss of estrogen induces accelerated stiffening of arteries and increased incidence of cardiovascular disease[106]. Next to this, estrogen deficiency has also been shown to promote collagen synthesis, which is associated with arterial stiffening[105].

Very little is known about gender differences in arterial wall stiffness in our domestic animals. In dogs Nogueria et al.[108] found no difference in the arterial wall stiffness by measuring

carotid to femoral pulse wave velocity, between healthy male and female dogs. In horses, no information was found regarding the influence of gender on the arterial wall.

### *6.3. Effect of training on arterial wall stiffness*

Several studies show that regular exercise training reduces arterial stiffness in humans[109; 110]. An inverse relationship between training level and arterial stiffness, including pulse wave velocity, augmentation index, stiffness index and arterial strain has been found[110-113]. Arterial compliance decreases with age, but the magnitude of the reduction in arterial compliance will be attenuated when aerobic exercise is performed. Recent studies even show that a relatively brief (13 to 14 weeks) period of regular aerobic exercise can restore some of the losses of arterial compliance in normally non-active old and middle-aged men. Moreover the increase in arterial compliance seen in this situation is independent from changes in body weight, arterial blood pressure or metabolic risk factors[113].

On the other side, resistance training, which is a popular mode of exercises nowadays, seems to have a negative effect on arterial wall stiffness. Kawano et al.[114] studied carotid artery stiffness in a group of 12 middle-aged men, who were performing resistance training for >10 years and compared it with a control group of 17 age-match men, who had not participated in a regular exercise program over the last 2 years. They found that the stiffness index and the systolic and mean arterial blood pressure were significantly higher in the resistance trained group. Cortez-Cooper et al.[115] showed that, also in women, 11 weeks of high-intensity strength and power training increases arterial stiffness, as the carotid augmentation index and the carotid to femoral pulse wave velocity were elevated.

In our domestic animals, nothing was found about the influence of training on the arterial wall stiffness.

### *6.4. Racial differences in arterial wall stiffness*

Elderly black people are known to have a higher risk of developing hypertension and increased vascular stiffness. Indeed, black people were found to have a lower aortic distensibility, but without any difference in arterial wall thickness, which suggests that hypertension itself possibly accounted for the stiffer arteries[116]. Other studies concluded that the elevated blood pressure was not the sole cause of the increased arterial stiffness, as even after correction for blood pressure, aortic stiffness was increased in African people, compared to Europeans. Therefore, Chaturverdi et al.[117] suggested that the increased vascular stiffness is due to ethnic differences in vascular remodeling. Goel et al.[118] showed that black people and Hispanics had higher aortic stiffness compared to white people, with the highest values in black

people. Asians on their turn show a higher pulse wave velocity thus stiffer arteries in comparison with African people, even after correction for age and blood pressure[119].

Not only during adulthood or with aging racial differences are found. African-American children have significantly higher pulse wave velocity and thus a higher arterial stiffness compared to white children. After correction for height there appeared to be no difference in blood pressure and arterial wall thickness between those African-American children and white children, but the difference in arterial wall stiffness remained significant[120].

Again, in our domestic animals, studies investigating differences in arterial wall stiffness between different breeds have not been found.

## 7. Arterial disorders in horses

Arterial wall stiffness is well-studied in human medicine, but as described in the previous paragraphs, very poorly in horses. Nevertheless, vascular disorders such as exercise-induced arterial rupture, parturition or breeding-associated arterial rupture, aortic rupture and aorto-cardiac or aorto-pulmonary fistula formation are of great concern in equine medicine as they are mostly fatal and affect horse welfare and rider safety. All those arterial pathologies might be linked to altered arterial wall properties due to aging, gender differences, racial differences or even differences in training level, but in depth pathophysiological research is still lacking. The most common arterial disorders in horses, together with their prevalence and possible pathophysiological background are described beneath.

### *7.1. Exercise-induced arterial rupture*

Arterial rupture is one of the most important causes of sudden death in horses next to arrhythmias, intestinal lesions and spinal cord injury[121-126]. Looking at cardiovascular causes of sudden death in specific, most deaths occur during exercise or racing, mostly, but not always during the fastest work, while other horses collapse within one hour after the effort[122; 127]. Aortic rupture itself is well known as a fatal condition in sport horses, mostly occurring during exercise. Over the last years some famous horses died in front of a big public in different sport disciplines, for example the Olympic jumping horse Hickstead during the famous jumping of Verona, Admir Ratki a seven year old racing horse, who collapsed and died just after crossing the finish line of the Melbourne cup and Filur, the 23 year old warmblood, who died during the four-in-hand FEI world cup qualification in Stockholm, gaining massive media and public attention for aortic rupture in (sport)horses.

Besides the aorta, also other (major) abdominal or thoracic arteries tend to rupture during exercise. Lyle et al.[124] found that 56% of the 143 investigated sudden deaths in Thoroughbred horses, suffered exercises associated sudden-death due to cardiac or

pulmonary failure. Of those horses 20% died due to pulmonary hemorrhage, while another 27% of the examined horses died due to a hemorrhagic shock. Gelberg et al.[125] reviewed 25 post mortem examinations of racing or training Thoroughbreds. In only eight cases the cause of death could be identified. Six of those eight cases showed massive thoracic or abdominal bleeding, but the site of the vascular rupture could not be identified. Another important finding of Gelberg et al.[125] is that nearly all examined horses had pulmonary congestion and/or pulmonary hemorrhage. DeLay[126] reported 963 post mortem examinations of sudden deaths and euthanasia's associated with exercise. That review included Thoroughbreds, Standardbreds and Quarter horses. In 157 out of the 963 horses sudden death occurred and was causally associated with racing or training activities. Those 157 horses died during or immediately after the activity. Thirty-four horses (22%) died due to cardiovascular reasons, of which 15 showed hemopericardium with 13 cases surely defined as aortic rupture. Eight % of the horses (13/157) died due to hemothorax, hemoabdomen, mediastinal or pulmonary hemorrhage.

### *7.2. Aorta-cardiac fistula*

Aortic rupture is not always immediately fatal. In those cases, rupture occurs most often at the level of the right aortic sinus with formation of an aorto-cardiac fistula ending up in the right ventricle, right atrium or left ventricle[128; 129]. Typical signs of an aorto-cardiac fistulation include colic, acute distress, exercise intolerance, monomorphic ventricular tachycardia, the presence of a right-sided continuous murmur and bounding arterial pulses[128; 129]. It has been described at different ages and breeds, including Thoroughbred horses, Quarter horses, Standardbreds, Arabian horses and cross-breeds. Aorto-cardia fistula have been described in both females and males, but stallions seem to be predisposed, especially during coitus[129]. Rooney et al.[130] described eight cases in stallions, with a mean age of 15 year, indicating a higher incidence in older stallions.

Whether or not histological changes are present in cases developing an aorta-cardiac fistula is not clear. Marr et al.[129] described no histological changes in four horses died from aorto-cardiac fistula, while Sleeper et al.[131] reported disorganization of fibrous tissue in the area of the fistula in a chronic case and Briceno et al.[132] reported clear degenerative changes within the aortic wall, with loss of continuity and disorganization of elastic fibers (Fig. 16).

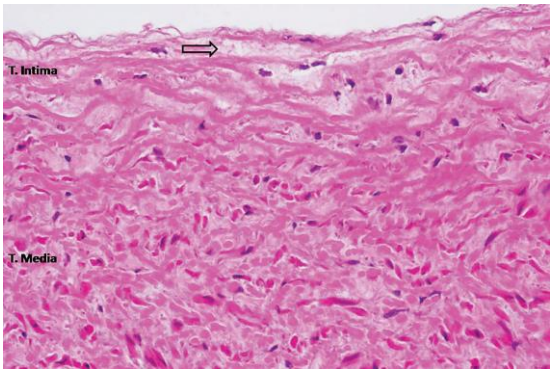


*Figure 16: Histological section of a ruptured aorta in horse, evidencing degenerative changes with loss of continuity of elastic fibers[132]; haematoxylin and eosin staining.*

### *7.3. Aortopulmonary fistula in Friesian horses*

It is widely known that Friesians or more prone to aortic rupture, compared to other breeds[133; 134], without any sex or age predilection[135]. In contrast with other breeds where aortic rupture almost always occurs at the aortic root, in Friesian horses the aorta ruptures close to the ligamentum arteriosum, with formation of an aortopulmonary fistula (Fig. 17)[134]. In those cases, an aortic pseudoaneurysm is found, starting from a transverse rupture of the aorta, near the ligamentum arteriosum. This pseudoaneurysm is a blood-filled cavity surrounded by granulation tissue, ending up in the pulmonary artery via a transverse rupture. Horses suffering from aortic rupture usually show subacute or chronic signs for weeks to months before death. The most important clinical signs are colic, resting tachycardia, peripheral oedema, coughing, jugular pulsation and a strong bounding pulsation in the carotid artery[134]. Aortic rupture in combination with aortopulmonary fistulation can occur at any age, although most of the cases reported are rather young[134]. Antemortem diagnosis of this pathology is very important in order to differentiate from ‘normal colic’ and prevent cases of sudden death during riding or handling the horse, involving rider and handler safety. Indicative clinical signs need to be combined with advanced ultrasound imaging in order to correctly diagnose the presence of an aortopulmonary fistula. On standard echocardiographic images, an enlarged pulmonary artery and subsequently dilation of the right ventricle and atrium can be visible. The pulmonary artery might be displaced to the left and most of the times, already on the normal right-sided images the pseudoaneurysm is visible between the aorta and the pulmonary artery. Next to these findings, the diastolic diameter of the aorta might be small, due to the large left-to-right-shunt. Non-classic ultrasound views are necessary to visualize the fistula itself, but might be challenging due to the heavy musculature of Friesian horses, in combination with the location of the fistula, being often obscured by the air filled lungs.

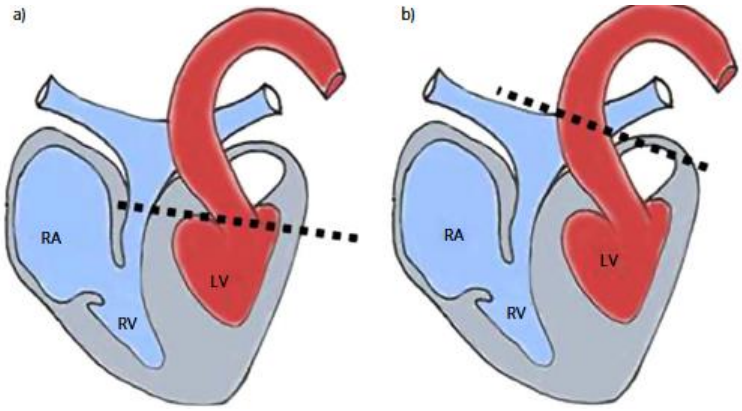


*Figure 17: Aortic rupture (indicated by the dashed line) in most breeds is typically located at the base of the heart (a), while in Friesians ruptures occurs near the ligamentum arteriosum (b)[134].*

The reason why Friesian horses are more prone to aortic rupture remains unclear. Embryological malformation could be a cause, but affected animals are normal at birth and no other cardiac developmental abnormalities are described in Friesians with aortic rupture, making this hypothesis less likely[134]. In addition, we have recently found the first case of a 10 year old asymptomatic Friesian stallion with an aortic rupture in combination with a pseudoaneurysm, which did not connect to the pulmonary artery[136]. These observations favor a progressive condition starting from an aortic rupture. Medial necrosis has been described in affected Friesians (Fig.18) [137] and can be caused by ischemia[138], connective tissue disorders[139], increased blood pressure[140] or inflammation[141]. Whether or not these are also causable factors in Friesian horses is not clear. A difference in connective tissue metabolism and homeostasis between Warmblood and Friesian horses is suspected[142]. Ploeg et al.[142] found an increase in lysylpyridinoline cross-links, elastin cross-linking and matrix metalloproteinases in aortic tissue of affected Friesians. Also in tissue of flexor tendons differences were found in collagen lysine hydroxylation and pyrrole cross-links. Moreover Saey et al.[143] recently found a higher rate of collagen degeneration in Friesian horses compared to Warmblood horses in urinary samples. Another study by Saey et al.[144] found significant structural differences between unaffected Friesian and Warmblood horses, with an increased thickness of the tunica media and an increased area % of collagen type I in Friesian horses compared to age-matched Warmblood horses. Affected Friesians showed a decreased amount of elastin in combination with smooth muscle cell hypertrophy, compared to Warmbloods and non-affected Friesians, which suggests not only collagen disorders, but also some degree of elastin deficiency. On the other hand, no biochemical evidence for the predisposition of Friesian horses to aortic rupture could be found[61].

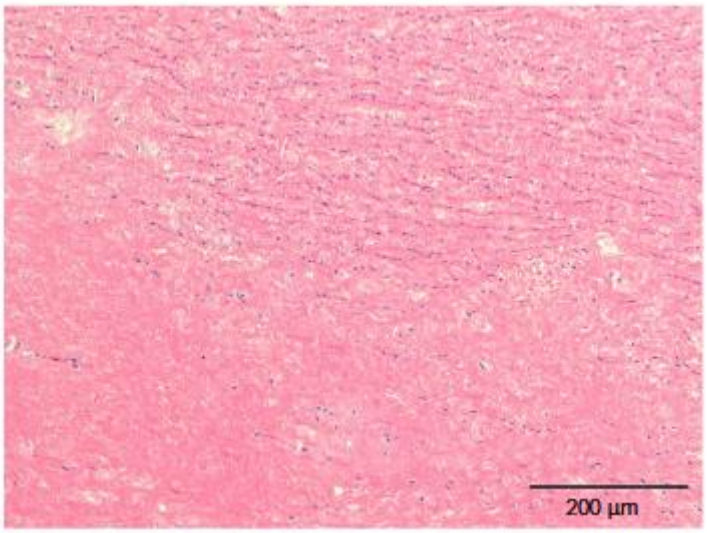


*Figure 18: Medial necrosis (lower part) in the aortic wall of an affected Friesian, characterised by smooth muscle cells with loss of nuclei[134]; haematoxylin and eosin staining*

### *7.4. Parturition-associated arterial rupture*

Arterial rupture is a well-recognized cause of pregnancy associated fatality in mares. Nevertheless arterial rupture is not always fatal. Blood might accumulate in the broad ligaments with formation of a hematoma, which might over time organize and resorb, leading to the survival of the mare. Mares suffering from arterial rupture usually show clinical signs of colic in combination with pale mucous membranes. Williams et al. [145] reported 513 cases of pregnancy-associated arterial rupture, collected over 15 years at the University of Kentucky. They found that rupture can occur during (59%), before (30%, half of these being more than a month before due date) or shortly after (11%) parturition and concluded that arterial rupture occurs mostly in older mares, as 78% of the investigated mares were aged over 15 years, with a mean age of 17 years. Most of the mares were also multiparous, the mean was the 7$^{th}$ parturition and 52% of the mares had produced eight or more foals. Eight mares did only have one foal before and 7 mares had only two, indicating that arterial rupture not only affects multiparous mares. It was mostly, but not always, the uterine artery, in the first 20 cm from the origin, that ruptured. Other arteries were also described to rupture, leading to hemo-abdomen or hemothorax: the left uterine artery (47% of the cases), the right uterine artery (30%), the iliac artery (10%), uterine wall arteries (6%), the aorta (4%), the ovarian artery (3%) and the mesenteric artery (1%). It is believed that those arteries rupture due to chronic intramural degenerative changes and weakening, but during parturition also foaling-associated trauma can play a role. Ueno et al. described the pathological findings of 31 Thoroughbred mares who died from peripartum broad ligament hematomas. Five young, multiparous control horses were also included in the study. Similar to what is described by Williams et al., Ueno et al. described that arterial rupture most often occurred in the proximal part of the uterine artery, followed by

the distal part and the middle part, while the internal iliac artery, caudal mesenteric artery and internal pudendal artery were found to rupture in a minority of the cases (Fig. 19). Histologically the tunica media in close proximity with the site of arterial rupture showed smooth muscle cell atrophy and fibrosis. Also a thickened arterial wall was found, due to disruption and calcification of the internal elastic lamina. These findings were most prominent in the aged multiparous mares, and were not present in young control mares, indicating age and parity associated changes in the arterial wall (Fig. 20 and 21).

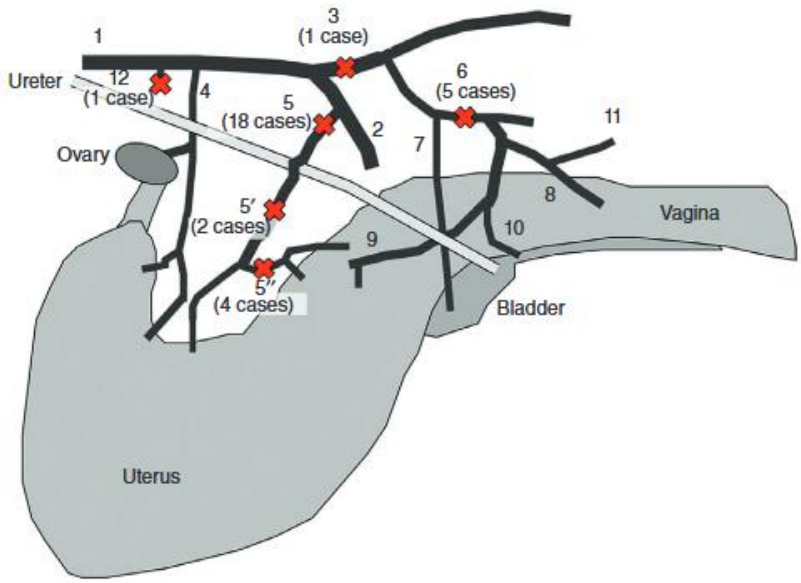


*Figure 19: Most frequently found locations of arterial rupture in pregnant mares described by Ueno. et al. 1: abdominal aorta, 2: external iliac artery, 3: internal iliac artery, 4: ovarian artery, 5: proximal part of the uterine artery, 5': middle part of the uterine artery, 5'': distal part of the uterine artery, 6: internal pudendal artery, 7: umbilical artery, 8: vaginal artery, 9: uterine branch of the vaginal artery; 10: caudal visceral artery, 11: middle rectal artery, 12: caudal mesenteric artery[99].*

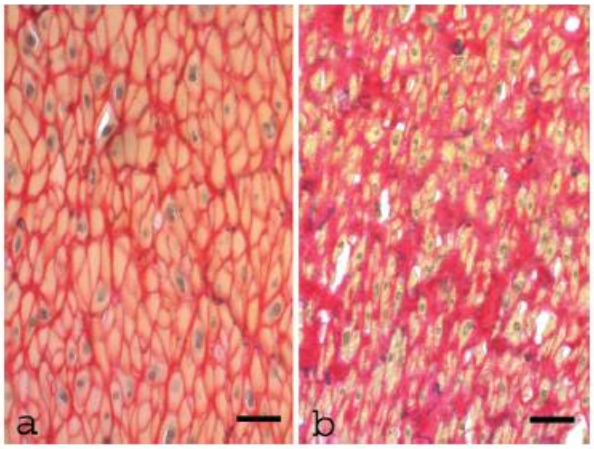


*Figure 20: Histological section of the uterine artery of a young control mare (a) and an old mare (b). The atrophy of smooth muscle cells in combination with fibrosis is clearly visible in the old mare. Elastica von Gieson stain, magnification x20, bar = 120 µm[99].*

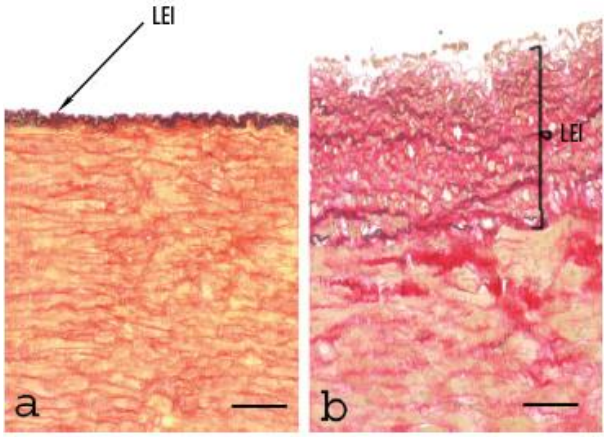


*Figure 21: Histological section of the uterine artery of a young, control mare (a) and an old mare (b). The thickened lamina elastic interna (LEI) is clearly visible in the aged mare. Elastica van Gieson stain, magnification x5, bar = 50 µm[99].*

### *7.5. Phenylephrine associated arterial rupture*

Phenylephrine, an alpha1-agonist, is often used as part of the treatment of nephrosplenic entrapment of the large colon in horses. Nephrosplenic entrapment of the large colon is a common diagnosis in horses showing colic signs[146]. The prognosis is typically good, with successful resolution of the entrapment reported in up to 92% of the cases[147]. Phenylephrine works on the alfa$_1$-adrenergic receptors, which cause splenic contraction and systemic vasoconstriction, leading to increased blood pressure. Severe (fatal) bleeding is a well-known side effect of the therapeutic use of phenylephrine, probably due to the induced hypertension. Fréderick et al.[148] reported that all horses showing severe hemorrhage after phenylephrine administration were older than 15 years. Therefore they concluded that aged horses have a higher risk on developing (fatal) bleeding after phenylephrine administration, which could be linked to altered arterial wall properties.

## Conclusion

Literature shows that arterial wall stiffness has been well-studied in humans, as it is proven to be of highly predictive value for the risk of cardiovascular death. Multiple techniques to reliably measure arterial wall stiffness have been validated. Until now, in horses, no standard technique to measure arterial wall stiffness is available and the relation between arterial wall changes and arterial disorders remains largely unknown.

## References

[1] Labrosse, M.R. (2007) Structure and mechanics of the artery. Vascular mechanics and pathology. In: *Vascular mechanics and pathology* Springer.
[2] Wolinsky, H. and Glagov, S. (1967) A Lamellar Unit of Aortic Medial Structure and Function in Mammals. *Circ Res* **20**, 99-&.
[3] Mithieux, S.M. and Weiss, A.S. (2005) Elastin. *Adv Protein Chem* **70**, 437-461.

[4] Vindin, H., Mithieux, S.M. and Weiss, A.S. (2019) Elastin architecture. *Matrix Biol* **84**, 4-16.
[5] Chung, M.I.S., Miao, M., Stahl, R.J., Chan, E., Parkinson, J. and Keeley, F.W. (2006) Sequences and domain structures of mammalian, avian, amphibian and teleost tropoelastins: Clues to the evolutionary history of elastins. *Matrix Biology* **25**, 492-504.
[6] Debelle, L. and Tamburro, A.M. (1999) Elastin: molecular description and function. *Int J Biochem Cell B* **31**, 261-272.
[7] Sandberg, L.B., Gray, R.W. and Franzblau, C. (1977) *Elastin and elastic tissue* Springer
[8] Arribas, S.M., Hinek, A. and Gonzalez, M.C. (2006) Elastic fibres and vascular structure in hypertension. *Pharmacol Ther* **111**, 771-791.
[9] Segers, P., Rietzschel, E.R. and Chirinos, J.A. (2020) How to Measure Arterial Stiffness in Humans. *Arterioscl Throm Vas* **40**, 1034-1043.
[10] Kielty, C.M., Sherratt, M.J. and Shuttleworth, C.A. (2002) Elastic fibres. *J Cell Sci* **115**, 2817-2828.
[11] Thomson, J., Singh, M., Eckersley, A., Cain, S.A., Sherratt, M.J. and Baldock, C. (2019) Fibrillin microfibrils and elastic fibre proteins: Functional interactions and extracellular regulation of growth factors. *Semin Cell Dev Biol* **89**, 109-117.
[12] Robinson, P.N., Arteaga-Solis, E., Baldock, C., Collod-Beroud, G., Booms, P., De Paepe, A., Dietz, H.C., Guo, G., Handford, P.A., Judge, D.P., Kielty, C.M., Loeys, B., Milewicz, D.M., Ney, A., Ramirez, F., Reinhardt, D.P., Tiedemann, K., Whiteman, P. and Godfrey, M. (2006) The molecular genetics of Marfan syndrome and related disorders. *J Med Genet* **43**, 769-787.
[13] Kanta, J. (2016) Elastin in the Liver. *Front Physiol* **7**, 491.
[14] Lacolley, P., Regnault, V., Nicoletti, A., Li, Z.L. and Michel, J.B. (2012) The vascular smooth muscle cell in arterial pathology: a cell that can take on multiple roles. *Cardiovasc Res* **95**, 194-204.
[15] Tang, Y.F., Yang, X.H., Friesel, R.E., Vary, C.P.H. and Liaw, L. (2011) Mechanisms of TGF-beta-Induced Differentiation in Human Vascular Smooth Muscle Cells. *J Vasc Res* **48**, 485-494.
[16] Rensen, S.S.M., Doevendans, P.A.F.M. and van Eys, G.J.J.M. (2007) Regulation and characteristics of vascular smooth muscle cell phenotypic diversity. *Neth Heart J* **15**, 100-108.
[17] Schwartz, S.M., Campbell, G.R. and Campbell, J.H. (1986) Replication of Smooth-Muscle Cells in Vascular-Disease. *Circ Res* **58**, 427-444.
[18] Kovalev, I.V., Baskakov, M.B., Kapilevich, L.V., Panov, A.A., Popov, A.G., Borodin, Y.L., Anfinogenova, Y., Minochenko, I.L., Kilin, A. and Medvedev, M.A. (2003) Electrical and contractile function of vascular smooth muscle cells: Regulation by cGMP-dependent mechanisms. *J Hypertens* **21**, S101-S101.
[19] Violaris, A.G., deJong, M., MacLeod, D.C., Umans, V.A., Verdouw, P.D. and Serruys, P.W. (1996) Increased extracellular matrix synthesis by smooth-muscle cells obtained from in vivo restenotic lesions by directional coronary atherectomy. *Am Heart J* **131**, 613-615.
[20] Wight, T.N. (1989) Cell biology of arterial proteoglycans. *Arteriosclerosis* **9**, 1-20.
[21] Sumpio, B.E., Banes, A.J., Link, W.G. and Johnson, G. (1988) Enhanced Collagen Production by Smooth-Muscle Cells during Repetitive Mechanical Stretching. *Arch Surg-Chicago* **123**, 1233-1236.
[22] Lodish, H., Berk, A. and Zipursky, S.L. (2000) Collagen: the fibrous proteins of the matrix In: *Molecular cell biology*.
[23] Wu, M. and Crane, J.S. (2020) Biochemistry, Collagen Synthesis. In: *StatPearls*, Treasure Island (FL).
[24] Pinnell, S.R. (1982) Regulation of Collagen-Synthesis. *J Invest Dermatol* **79**, S73-S76.
[25] Shekhonin, B.V., Domogatsky, S.P., Muzykantov, V.R., Idelson, G.L. and Rukosuev, V.S. (1985) Distribution of type I, III, IV and V collagen in normal and atherosclerotic human arterial wall: immunomorphological characteristics. *Coll Relat Res* **5**, 355-368.

[26] Wight, T.N. (2008) Arterial remodeling in vascular disease: a key role for hyaluronan and versican. *Front Biosci* **13**, 4933-4937.
[27] Izzo, J.L., Jr. and Shykoff, B.E. (2001) Arterial stiffness: clinical relevance, measurement, and treatment. *Rev Cardiovasc Med* **2**, 29-34, 37-40.
[28] Kenner, T. (1988) Arterial blood pressure and its measurement. *Basic Res Cardiol* **83**, 107-121.
[29] Poulsen, C.B., Wang, T., Assersen, K., Iversen, N.K. and Damkjaer, M. (2018) Does mean arterial blood pressure scale with body mass in mammals? Effects of measurement of blood pressure. *Acta Physiol* **222**.
[30] Westerof, N., Stergiopulos, N., Noble, M.I.M. and Westerhof, B.E. (2019) Comparative physiology. In: *Snapshot of Hemodynamics* Ed: Springer.
[31] Seymour, R.S. and Blaylock, A.J. (2000) The principle of laplace and scaling of ventricular wall stress and blood pressure in mammals and birds. *Physiol Biochem Zool* **73**, 389-405.
[32] Packard, G.C. (2015) Allometric scaling of mammalian blood pressure: A comment on White and Seymour (2014). *Evolution* **69**, 3217-3220.
[33] Joyner, M.J. and Limberg, J.K. (2014) Blood pressure regulation: every adaptation is an integration? *Eur J Appl Physiol* **114**, 445-450.
[34] Sparks, M.A., Crowley, S.D., Gurley, S.B., Mirotsou, M. and Coffman, T.M. (2014) Classical Renin-Angiotensin System in Kidney Physiology. *Compr Physiol* **4**, 1201-1228.
[35] Weir, M.R. and Dzau, V.J. (1999) The renin-angiotensin-aldosterone system: a specific target for hypertension management. *Am J Hypertens* **12**, 205S-213S.
[36] Santos, P.C., Krieger, J.E. and Pereira, A.C. (2012) Renin-angiotensin system, hypertension, and chronic kidney disease: pharmacogenetic implications. *J Pharmacol Sci* **120**, 77-88.
[37] Delong, C. and Sharma, S. (2020) Physiology, Peripheral Vascular Resistance. In: *StatPearls*, Treasure Island (FL).
[38] Thatcher, J.D. (2010) The inositol trisphosphate (IP3) signal transduction pathway. *Sci Signal* **3**, tr3.
[39] Brozovich, F.V., Nicholson, C.J., Degen, C.V., Gao, Y.Z., Aggarwal, M. and Morgan, K.G. (2016) Mechanisms of Vascular Smooth Muscle Contraction and the Basis for Pharmacologic Treatment of Smooth Muscle Disorders. *Pharmacol Rev* **68**, 476-532.
[40] Bagher, P. and Segal, S.S. (2011) Regulation of blood flow in the microcirculation: role of conducted vasodilation. *Acta Physiol (Oxf)* **202**, 271-284.
[41] Gray, R.G., Cabreriza, S.E., Quinn, T.A., Weinberg, A.D. and Spotnitz, H.M. (2010) Feasibility of In Vivo Pressure Measurement Using a Pressure-Tip Catheter via Transventricular Puncture. *Asaio J* **56**, 194-199.
[42] Vlachopoulos, C., O'Roucke, M. and Nichols, W.W. (1998) *McDonald's blood flow in arteries*, 4 edn. p 768.
[43] Berger, A. (2001) How does it work? Oscillatory blood pressure monitoring devices. *Brit Med J* **323**, 919-919.
[44] Ogedegbe, G. and Pickering, T. (2010) Principles and Techniques of Blood Pressure Measurement. *Cardiol Clin* **28**, 571-+.
[45] Nara, A., Burns, M.P. and Downs, W.G. (1996) Automated noninvasive measurement In: *Blood pressure*, Ed: M. electronics. pp 37-40.
[46] Hrishikesan, L. (2018) Electronics and communication: ultrasound blood pressure measurement
[47] Heliczer, N., Lorello, O., Casoni, D. and Navas de Solis, C. (2016) Accuracy and Precision of Noninvasive Blood Pressure in Normo-, Hyper-, and Hypotensive Standing and Anesthetized Adult Horses. *J Vet Intern Med* **30**, 866-872.
[48] Grandy, J.L., Steffey, E.P., Hodgson, D.S. and Woliner, M.J. (1987) Arterial hypotension and the development of postanesthetic myopathy in halothane-anesthetized horses. *Am J Vet Res* **48**, 192-197.

[49] Duke, T., Filzek, U., Read, M.R., Read, E.K. and Ferguson, J.G. (2006) Clinical observations surrounding an increased incidence of postanesthetic myopathy in halothane-anesthetized horses. *Vet Anaesth Analg* **33**, 122-127.
[50] Tearney, C.C., Guedes, A.G.P. and Brosnan, R.J. (2016) Equivalence between invasive and oscillometric blood pressures at different anatomic locations in healthy normotensive anaesthetised horses. *Equine Veterinary Journal* **48**, 357-361.
[51] Hatz, L.A., Hartnack, S., Kummerle, J., Hassig, M. and Bettschart-Wolfensberger, R. (2015) A study of measurement of noninvasive blood pressure with the oscillometric device, Sentinel, in isoflurane-anaesthetized horses. *Vet Anaesth Analg* **42**, 369-376.
[52] Tunsmeyer, J., Hopster, K., Feige, K. and Kastner, S.B.R. (2015) Agreement of high definition oscillometry with direct arterial blood pressure measurement at different blood pressure ranges in horses under general anaesthesia. *Veterinary Anaesthesia and Analgesia* **42**, 286-291.
[53] Drynan, E.A., Schier, M. and Raisis, A.L. (2016) Comparison of invasive and noninvasive blood pressure measurements in anaesthetized horses using the Surgivet V9203. *Veterinary Anaesthesia and Analgesia* **43**, 301-308.
[54] Olsen, E., Pedersen, T.L., Robinson, R. and Haubro Andersen, P. (2016) Accuracy and precision of oscillometric blood pressure in standing conscious horses. *J Vet Emerg Crit Care (San Antonio)* **26**, 85-92.
[55] Trudnowski, R.J. and Rico, R.C. (1974) Specific gravity of blood and plasma at 4 and 37 degrees C. *Clin Chem* **20**, 615-616.
[56] Byrd, J.B. and Brook, R.D. (2014) Arm position during ambulatory blood pressure monitoring: a review of the evidence and clinical guidelines. *J Clin Hypertens (Greenwich)* **16**, 225-230.
[57] Parry, B.W., McCarthy, M.A. and Anderson, G.A. (1984) Survey of resting blood pressure values in clinically normal horses. *Equine Vet J* **16**, 53-58.
[58] Nostell, K.E., Lindase, S.S. and Brojer, J.T. (2016) Blood pressure in Warmblood horses before and during a euglycemic-hyperinsulinemic clamp. *Acta Vet Scand* **58**, 65.
[59] Langewouters, G.J. (1982) *Visco-elasticity of the human aorta in vitro in relation to pressure and age*
[60] Zhou, J. and Fung, Y.C. (1997) The degree of nonlinearity and anisotropy of blood vessel elasticity. *Proc Natl Acad Sci U S A* **94**, 14255-14260.
[61] Saey, V., Famaey, N., Smoljkic, M., Claeys, E., van Loon, G., Ducatelle, R., Ploeg, M., Delesalle, C., Grone, A., Duchateau, L. and Chiers, K. (2015) Biomechanical and biochemical properties of the thoracic aorta in warmblood horses, Friesian horses, and Friesians with aortic rupture. *Bmc Vet Res* **11**.
[62] Avanzini, A., Battini, D., Bagozzi, L. and Bisleri, G. (2014) Biomechanical evaluation of ascending aortic aneurysms. *Biomed Res Int* **2014**, 820385.
[63] Mascarenhas, E.J.S., Peters, M.F.J., Nijs, J., Rutten, M.C.M., van de Vosse, F.N. and Lopata, R.G.P. (2016) Assessment of mechanical properties of porcine aortas under physiological loading conditions using vascular elastography. *J Mech Behav Biomed* **59**, 185-196.
[64] Reymond, P., Vardoulis, O. and Stergiopulos, N. (2012) Generic and patient-specific models of the arterial tree. *J Clin Monit Comput* **26**, 375-382.
[65] Westerhof, N., Lankhaar, J.W. and Westerhof, B.E. (2009) The arterial Windkessel. *Med Biol Eng Comput* **47**, 131-141.
[66] Mynard, J.P. and Smolich, J.J. (2015) One-Dimensional Haemodynamic Modeling and Wave Dynamics in the Entire Adult Circulation. *Annals of Biomedical Engineering* **43**, 1443-1460.
[67] Bessems, D., Rutten, M. and Van De Vosse, F. (2007) A wave propagation model of blood flow in large vessels using an approximate velocity profile function. *Journal of Fluid Mechanics* **580**, 145-168.

[68] Stergiopulos, N., Young, D.F. and Rogge, T.R. (1992) Computer-Simulation of Arterial Flow with Applications to Arterial and Aortic Stenoses. *Journal of Biomechanics* **25**, 1477-1488.

[69] Epstein, S., Willemet, M., Chowienczyk, P.J. and Alastruey, J. (2015) Reducing the number of parameters in 1D arterial blood flow modeling: less is more for patient-specific simulations. *Am J Physiol-Heart C* **309**, H222-H234.

[70] Dobroserdova, T., Simakov, S., Gamilov, T., Pryamonosov, R. and Sakharova, E. (2016) Patient-specific blood flow modelling for medical applications. *20th International Conference on Circuits, Systems, Communications and Computers (Cscc 2016)* **76**.

[71] Laurent, S., Cockcroft, J., Van Bortel, L., Boutouyrie, P., Giannattasio, C., Hayoz, D., Pannier, B., Vlachopoulos, C., Wilkinson, I., Struijker-Boudier, H. and European Network for Non-invasive Investigation of Large, A. (2006) Expert consensus document on arterial stiffness: methodological issues and clinical applications. *Eur Heart J* **27**, 2588-2605.

[72] Lyle, A.N. and Raaz, U. (2017) Killing Me Unsoftly Causes and Mechanisms of Arterial Stiffness. *Arterioscl Throm Vas* **37**, E1-E11.

[73] Vlachopoulos, C., Aznaouridis, K. and Stefanadis, C. (2010) Prediction of cardiovascular events and all-cause mortality with arterial stiffness: a systematic review and meta-analysis. *J Am Coll Cardiol* **55**, 1318-1327.

[74] Vishram-Nielsen, J.K.K., Laurent, S., Nilsson, P.M., Linneberg, A., Sehested, T.S.G., Greve, S.V., Pareek, M., Palmieri, L., Giampaoli, S., Donfrancesco, C., Kee, F., Mancia, G., Cesana, G., Veronesi, G., Kuulasmaa, K., Salomaa, V., Kontto, J., Palosaari, T., Sans, S., Ferrieres, J., Dallongeville, J., Soderberg, S., Moitry, M., Drygas, W., Tamosiunas, A., Peters, A., Brenner, H., Njolstad, I., Olsen, M.H. and Project, M. (2020) Does Estimated Pulse Wave Velocity Add Prognostic Information? MORGAM Prospective Cohort Project. *Hypertension* **75**, 1420-1428.

[75] Philips, N., Faught, B., Hay, J., Cairney, J. and O'Leary, D. (2014) Comparison of two techniques for measuring pulse wave velocity in children. *Faseb J* **28**.

[76] Van Bortel, L.M., Laurent, S., Boutouyrie, P., Chowienczyk, P., Cruickshank, J.K., De Backer, T., Filipovsky, J., Huybrechts, S., Mattace-Raso, F.U., Protogerou, A.D., Schillaci, G., Segers, P., Vermeersch, S., Weber, T., Artery, S., European Society of Hypertension Working Group on Vascular, S., Function and European Network for Noninvasive Investigation of Large, A. (2012) Expert consensus document on the measurement of aortic stiffness in daily practice using carotid-femoral pulse wave velocity. *J Hypertens* **30**, 445-448.

[77] Jiang, B., Liu, B., McNeill, K.L. and Chowienczyk, P.J. (2008) Measurement of pulse wave velocity using pulse wave Doppler ultrasound: Comparison with arterial tonometry. *Ultrasound Med Biol* **34**, 509-512.

[78] Calabia, J., Torguet, P., Garcia, M., Garcia, I., Martin, N., Guasch, B., Faur, D. and Valles, M. (2011) Doppler ultrasound in the measurement of pulse wave velocity: agreement with the Complior method. *Cardiovasc Ultrasoun* **9**.

[79] Asmar, R., Benetos, A., Topouchian, J., Laurent, P., Pannier, B., Brisac, A.M., Target, R. and Levy, B.I. (1995) Assessment of arterial distensibility by automatic pulse wave velocity measurement. Validation and clinical application studies. *Hypertension* **26**, 485-490.

[80] Blacher, J., Guerin, A.P., Pannier, B., Marchais, S.J., Safar, M.E. and London, G.M. (1999) Impact of aortic stiffness on survival in end-stage renal disease. *Circulation* **99**, 2434-2439.

[81] Weber, T., Ammer, M., Rammer, M., Adji, A., O'Rourke, M.F., Wassertheurer, S., Rosenkranz, S. and Eber, B. (2009) Noninvasive determination of carotid-femoral pulse wave velocity depends critically on assessment of travel distance: a comparison with invasive measurement. *J Hypertens* **27**, 1624-1630.

[82] Deiseroth, A., Streese, L., Kochli, S., Wust, R.S., Infanger, D., Schmidt-Trucksass, A. and Hanssen, H. (2019) Exercise and Arterial Stiffness in the Elderly: A Combined Cross-Sectional and Randomized Controlled Trial (EXAMIN AGE). *Front Physiol* **10**.

[83] Mattace-Raso, F.U.S., Hofman, A., Verwoert, G.C., Witteman, J.C.M., Wilkinson, I., Cockcroft, J., McEniery, C., Yasmin, Laurent, S., Boutouyrie, P., Bozec, E., Hansen, T.W., Torp-Pedersen, C., Ibsen, H., Jeppesen, J., Vermeersch, S.J., Rietzschel, E., De Buyzere, M., Gillebert, T.C., Van Bortel, L., Segers, P., Vlachopoulos, C., Aznaouridis, C., Stefanadis, C., Benetos, A., Labat, C., Lacolley, P., Stehouwer, C.D.A., Nijpels, G., Dekker, J.M., Ferreira, I., Twisk, J.W.R., Czernichow, S., Galan, P., Hercberg, S., Pannier, B., Guerin, A., London, G., Cruickshank, J.K., Anderson, S.G., Paini, A., Rosei, E.A., Muiesan, M.L., Salvetti, M., Filipovsky, J., Seidlerova, J., Dolejsova, M. and Stiffnes, R.V.A. (2010) Determinants of pulse wave velocity in healthy people and in the presence of cardiovascular risk factors: 'establishing normal and reference values'. *European Heart Journal* **31**, 2338-2350.

[84] Huybrechts, S.A., Devos, D.G., Vermeersch, S.J., Mahieu, D., Achten, E., de Backer, T.L., Segers, P. and van Bortel, L.M. (2011) Carotid to femoral pulse wave velocity: a comparison of real travelled aortic path lengths determined by MRI and superficial measurements. *J Hypertens* **29**, 1577-1582.

[85] Ohyama, Y., Redheuil, A., Kachenoura, N., Venkatesh, B.A. and Lima, J.A.C. (2018) Imaging Insights on the Aorta in Aging. *Circulation-Cardiovascular Imaging* **11**.

[86] Messas, E., Pernot, M. and Couade, M. (2013) Arterial wall elasticity: state of the art and future prospects. *Diagn Interv Imaging* **94**, 561-569.

[87] O'Rourke, M.F., Staessen, J.A., Vlachopoulos, C., Duprez, D. and Plante, G.E. (2002) Clinical applications of arterial stiffness; definitions and reference values. *Am J Hypertens* **15**, 426-444.

[88] Kamiya, A. and Togawa, T. (1980) Adaptive Regulation of Wall Shear-Stress to Flow Change in the Canine Carotid-Artery. *Am J Physiol* **239**, H14-H21.

[89] Hayashi, K., Makino, A. and Kakoi, D. (2018) Remodeling of arterial wall: Response to changes in both blood flow and blood pressure. *J Mech Behav Biomed* **77**, 475-484.

[90] Wolinsky, H. (1971) Effects of hypertension and its reversal on the thoracic aorta of male and female rats. Morphological and chemical studies. *Circ Res* **28**, 622-637.

[91] Atkinson, J. (2014) Elastin, Calcium and age-related stiffening of the arterial wall In: *Blood pressure and arterial wall mechanics in cardiovascular diseases*, Ed: Springer.

[92] Jani, B. and Rajkumar, C. (2006) Ageing and vascular ageing. *Postgrad Med J* **82**, 357-362.

[93] Seals, D.R., Jablonski, K.L. and Donato, A.J. (2011) Aging and vascular endothelial function in humans. *Clin Sci (Lond)* **120**, 357-375.

[94] Dinenno, F.A., Jones, P.P., Seals, D.R. and Tanaka, H. (2000) Age-associated arterial wall thickening is related to elevations in sympathetic activity in healthy humans. *Am J Physiol-Heart C* **278**, H1205-H1210.

[95] Lacolley, P., Regnault, V. and Avolio, A.P. (2018) Smooth muscle cell and arterial aging: basic and clinical aspects. *Cardiovasc Res* **114**, 513-528.

[96] Mitchell, S.J., Scheibye-Knudsen, M., Longo, D.L. and de Cabo, R. (2015) Animal models of aging research: implications for human aging and age-related diseases. *Annu Rev Anim Biosci* **3**, 283-303.

[97] Kim, S.A., Lee, K.H., Won, H.Y., Park, S., Chung, J.H., Jang, Y. and Ha, J.W. (2013) Quantitative Assessment of Aortic Elasticity With Aging Using Velocity-Vector Imaging and Its Histologic Correlation. *Arterioscl Throm Vas* **33**, 1306-1312.

[98] Endoh, C., Matsuda, K., Okamoto, M., Tsunoda, N. and Taniyama, H. (2017) Morphometric changes in the aortic arch with advancing age in fetal to mature thoroughbred horses. *J Vet Med Sci* **79**, 661-669.

[99] Ueno, T., Nambo, Y., Tajima, Y. and Umemura, T. (2010) Pathology of lethal peripartum broad ligament haematoma in 31 Thoroughbred mares. *Equine Vet J* **42**, 529-533.

[100] Mattace-Raso, F.U.S., van der Cammen, T.J.M., Hofman, A., van Popele, N.M., Bos, M.L., Schalekamp, M.A.D.H., Asmar, R., Reneman, R.S., Hoeks, A.P.G., Breteler, M.M.B. and Witteman, J.C.M. (2006) Arterial stiffness and risk of coronary heart disease and stroke - The Rotterdam Study. *Circulation* **113**, 657-663.

[101] Wang, M., Monticone, R.E. and Lakatta, E.G. (2016) The aging arterial wall In: *Handbook of the biology of aging*
[102] Lee, S.J. and Park, S.H. (2013) Arterial Ageing. *Korean Circ J* **43**, 73-79.
[103] Mozos, I., Malainer, C., Horbanczuk, J., Gug, C., Stoian, D., Luca, C.T. and Atanasov, A.G. (2017) Inflammatory Markers for Arterial Stiffness in Cardiovascular Diseases. *Front Immunol* **8**, 1058.
[104] Kim, J.Y., Park, J.B., Kim, D.S., Kim, K.S., Jeong, J.W., Park, J.C., Oh, B.H., Chung, N. and investigators, K. (2014) Gender Difference in Arterial Stiffness in a Multicenter Cross-Sectional Study: The Korean Arterial Aging Study (KAAS). *Pulse (Basel)* **2**, 11-17.
[105] Ogola, B.O., Zimmerman, M.A., Clark, G.L., Abshire, C.M., Gentry, K.M., Miller, K.S. and Lindsey, S.H. (2018) New insights into arterial stiffening: does sex matter? *Am J Physiol-Heart C* **315**, H1073-H1087.
[106] DuPont, J.J., Kenney, R.M., Patel, A.R. and Jaffe, I.Z. (2019) Sex differences in mechanisms of arterial stiffness. *Br J Pharmacol* **176**, 4208-4225.
[107] Segers, P., Rietzschel, E.R., De Buyzere, M.L., Vermeersch, S.J., De Bacquer, D., Van Bortel, L.M., De Backer, G., Gillebert, T.C., Verdonck, P.R. and Invest, A. (2007) Noninvasive (input) impedance, pulse wave velocity, and wave reflection in healthy middle-aged men and women. *Hypertension* **49**, 1248-1255.
[108] Nogueira, R.B., Pereira, L.A., Basso, A.F., da Fonseca, I.S. and Alves, L.A. (2017) Arterial pulse wave propagation velocity in healthy dogs by pulse wave Doppler ultrasound. *Vet Res Commun* **41**, 33-40.
[109] Pugh, C.J.A., Stone, K.J., Stohr, E.J., McDonnell, B.J., Thompson, J.E.S., Talbot, J.S., Wakeham, D.J., Cockcroft, J.R. and Shave, R. (2018) Carotid artery wall mechanics in young males with high cardiorespiratory fitness. *Exp Physiol* **103**, 1277-1286.
[110] Ashor, A.W., Lara, J., Siervo, M., Celis-Morales, C. and Mathers, J.C. (2014) Effects of exercise modalities on arterial stiffness and wave reflection: a systematic review and meta-analysis of randomized controlled trials. *PLoS One* **9**, e110034.
[111] Tanaka, H., DeSouza, C.A. and Seals, D.R. (1998) Absence of age-related increase in central arterial stiffness in physically active women. *Arterioscler Thromb Vasc Biol* **18**, 127-132.
[112] Binder, J., Bailey, K.R., Seward, J.B., Squires, R.W., Kunihiro, T., Hensrud, D.D. and Kullo, I.J. (2006) Aortic augmentation index is inversely associated with cardiorespiratory fitness in men without known coronary heart disease. *American Journal of Hypertension* **19**, 1019-1024.
[113] Tanaka, H., Dinenno, F.A., Monahan, K.D., Clevenger, C.M., DeSouza, C.A. and Seals, D.R. (2000) Aging, habitual exercise, and dynamic arterial compliance. *Circulation* **102**, 1270-1275.
[114] Kawano, H., Tanimoto, M., Yamamoto, K., Sanada, K., Gando, Y., Tabata, I., Higuchi, M. and Miyachi, M. (2008) Resistance training in men is associated with increased arterial stiffness and blood pressure but does not adversely affect endothelial function as measured by arterial reactivity to the cold pressor test. *Exp Physiol* **93**, 296-302.
[115] Cortez-Cooper, M.Y., DeVan, A.E., Anton, M.M., Farrar, R.P., Beckwith, K.A., Todd, J.S. and Tanaka, H. (2005) Effects of high intensity resistance training on arterial stiffness and wave reflection in women. *Am J Hypertens* **18**, 930-934.
[116] Baldo, M.P., Cunha, R.S., Ribeiro, A.L.P., Lotufo, P.A., Chor, D., Barreto, S.M., Bensenor, I.M., Pereira, A.C. and Mill, J.G. (2017) Racial Differences in Arterial Stiffness are Mainly Determined by Blood Pressure Levels: Results From the ELSA-Brasil Study. *J Am Heart Assoc* **6**.
[117] Chaturvedi, N., Bulpitt, C.J., Leggetter, S., Schiff, R., Nihoyannopoulos, P., Strain, W.D., Shore, A.C. and Rajkumar, C. (2004) Ethnic differences in vascular stiffness and relations to hypertensive target organ damage. *J Hypertens* **22**, 1731-1737.
[118] Goel, A., Maroules, C.D., Mitchell, G.F., Peshock, R., Ayers, C., McColl, R., Vongpatanasin, W. and King, K.S. (2017) Ethnic Difference in Proximal Aortic Stiffness An Observation From the Dallas Heart Study. *Jacc-Cardiovasc Imag* **10**, 54-61.

[119] Diemer, F.S., Baldew, S.M., Haan, Y.C., Karamat, F.A., Oehlers, G.P., van Montfrans, G.A., van den Born, B.H., Peters, R.J.G., Nahar-Van Venrooij, L.M.W. and Brewster, L.M. (2020) Aortic pulse wave velocity in individuals of Asian and African ancestry: the HELISUR study. *J Hum Hypertens* **34**, 108-116.

[120] Lefferts, W.K., Augustine, J.A., Spartano, N.L., Atallah-Yunes, N.H., Heffernan, K.S. and Gump, B.B. (2017) Racial Differences in Aortic Stiffness in Children. *J Pediatr* **180**, 62-67.

[121] Brown, C.M., Kaneene, J.B. and Taylor, R.F. (1988) Sudden and unexpected death in horses and ponies: an analysis of 200 cases. *Equine Vet J* **20**, 99-103.

[122] Platt, H. (1982) Sudden and unexpected deaths in horses: a review of 69 cases. *Br Vet J* **138**, 417-429.

[123] Sanders, D.E. (1986) Sudden-Death in Racehorses. *J Am Vet Med Assoc* **188**, 912-912.

[124] Lyle, C.H., Uzal, F.A., McGorum, B.C., Aida, H., Blissitt, K.J., Case, J.T., Charles, J.T., Gardner, I., Horadagoda, N., Kusano, K., Lam, K., Pack, J.D., Parkin, T.D., Slocombe, R.F., Stewart, B.D. and Boden, L.A. (2011) Sudden death in racing Thoroughbred horses: an international multicentre study of post mortem findings. *Equine Vet J* **43**, 324-331.

[125] Gelberg, H.B., Zachary, J.F., Everitt, J.I., Jensen, R.C. and Smetzer, D.L. (1985) Sudden death in training and racing Thoroughbred horses. *J Am Vet Med Assoc* **187**, 1354-1356.

[126] DeLay, J. (2017) Postmortem findings in Ontario racehorses, 2003-2015. *J Vet Diagn Invest* **29**, 457-464.

[127] Diab, S.S., Poppenga, R. and Uzal, F.A. (2017) Sudden death in racehorses: postmortem examination protocol. *J Vet Diagn Invest* **29**, 442-449.

[128] Sleeper, M.M., Durando, M.M., Miller, M., Habecker, P.L. and Reef, V.B. (2001) Aortic root disease in four horses. *J Am Vet Med Assoc* **219**, 491-496, 459.

[129] Marr, C.M., Reef, V.B., Brazil, T.J., Thomas, W.P., Knottenbelt, D.C., Kelly, D.F., Baker, J.R., Reimer, J.M., Maxson, A.D. and Crowhurst, J.S. (1998) Aorto-cardiac fistulas in seven horses. *Vet Radiol Ultrasound* **39**, 22-31.

[130] Rooney, J.R., Prickett, M.E. and Crowe, M.W. (1967) Aortic ring rupture in stallions. *Pathol Vet* **4**, 268-274.

[131] Sleeper, M.M., Durando, M.M., Miller, M., Habecker, P.L. and Reef, V.B. (2001) Aortic root disease in four horses. *J Am Vet Med Assoc* **219**, 491-496.

[132] Briceno, A.M., Mendez, A., Brewer, K., Hughes, C. and Tobin, T. (2015) Sudden death, aortic rupture in horses, literature review, case studies reported and risk factors. *Braz J Vet Res Anim Sci* **52**, 298-309.

[133] Ploeg, M., Saey, V., de Bruijn, C.M., Grone, A., Chiers, K., van Loon, G., Ducatelle, R., van Weeren, P.R., Back, W. and Delesalle, C. (2013) Aortic rupture and aorto-pulmonary fistulation in the Friesian horse: characterisation of the clinical and gross post mortem findings in 24 cases. *Equine Vet J* **45**, 101-106.

[134] Ploeg, M., Saey, V., van Loon, G. and Delesalle, C. (2017) Thoracic aortic rupture in horses. *Equine Vet J* **49**, 269-274.

[135] Ploeg, M., Saey, V., Delesalle, C., Grone, A., Ducatelle, R., de Bruijn, M., Back, W., van Weeren, P.R., van Loon, G. and Chiers, K. (2015) Thoracic Aortic Rupture and Aortopulmonary Fistulation in the Friesian Horse: Histomorphologic Characterization. *Veterinary Pathology* **52**, 152-159.

[136] De Lange, L., De Clercq, D., Vera, L., Van Steenkiste, G., ter Woort, F. and van Loon, G. (2019) Rupture partielle de la paroi de l'aorte avec dissection et formation d'un pseudo-anévrisme chez un étalon Frison de 10 ans sans symptômes cliniques. In: *teliers et journées annuelles AVEF*, Tours, France p159.

[137] Ploeg, M., Saey, V., Delesalle, C., Grone, A., Ducatelle, R., de Bruijn, M., Back, W., van Weeren, P.R., van Loon, G. and Chiers, K. (2015) Thoracic aortic rupture and aortopulmonary fistulation in the Friesian horse: histomorphologic characterization. *Vet Pathol* **52**, 152-159.

[138] van der Linde-Sipman, J.S., Kroneman, J., Meulenaar, H. and Vos, J.H. (1985) Necrosis and rupture of the aorta and pulmonary trunk in four horses. *Vet Pathol* **22**, 51-53.
[139] Yuan, S.M. and Jing, H. (2011) Cystic medial necrosis: pathological findings and clinical implications. *Rev Bras Cir Cardiovasc* **26**, 107-115.
[140] Schlatmann, T.J. and Becker, A.E. (1977) Histologic changes in the normal aging aorta: implications for dissecting aortic aneurysm. *Am J Cardiol* **39**, 13-20.
[141] Vine, N. and Powell, J.T. (1991) Metalloproteinases in degenerative aortic disease. *Clin Sci (Lond)* **81**, 233-239.
[142] Ploeg, M., Grone, A., van de Lest, C.H.A., Saey, V., Duchateau, L., Wolsein, P., Chiers, K., Ducatelle, R., van Weeren, P.R., de Bruijn, M. and Delesalle, C. (2017) Differences in extracellular matrix proteins between Friesian horses with aortic rupture, unaffected Friesians and Warmblood horses. *Equine Vet J* **49**, 609-613.
[143] Saey, V., Tang, J., Ducatelle, R., Croubels, S., De Baere, S., Schauvliege, S., van Loon, G. and Chiers, K. (2018) Elevated urinary excretion of free pyridinoline in Friesian horses suggests a breed-specific increase in collagen degradation. *Bmc Vet Res* **14**, 139.
[144] Saey, V., Ploeg, M., Delesalle, C., van Loon, G., Grone, A., Ducatelle, R., Duchateau, L. and Chiers, K. (2016) Morphometric Properties of the Thoracic Aorta of Warmblood and Friesian Horses with and without Aortic Rupture. *J Comp Pathol* **154**, 225-230.
[145] Williams, N.M. and Bryant, U.K. (2012) Periparturient Arterial Rupture in Mares: A Postmortem Study. *Journal of Equine Veterinary Science* **32**, 281-284.
[146] van der Linden, M.A., Laffont, C.M. and Sloet van Oldruitenborgh-Oosterbaan, M.M. (2003) Prognosis in equine medical and surgical colic. *J Vet Intern Med* **17**, 343-348.
[147] Hardy, J., Minton, M., Robertson, J.T., Beard, W.L. and Beard, L.A. (2000) Nephrosplenic entrapment in the horse: a retrospective study of 174 cases. *Equine Vet J Suppl*, 95-97.
[148] Frederick, J., Giguere, S., Butterworth, K., Pellegrini-Masini, A., Casas-Dolz, R. and Turpin, M.M. (2010) Severe phenylephrine-associated hemorrhage in five aged horses. *J Am Vet Med Assoc* **237**, 830-834.

# CHAPTER 2:

# SCIENTIFIC AIMS

Arterial disorders may be associated with (acute) fatalities in horses. Although predisposing factors and histological vascular changes have been suggested, the underlying vascular pathophysiology is largely unknown. Therefore the overall objective of this thesis was to investigate the normal arterial hemodynamics and structural and biomechanical characteristics of the equine arterial wall, as well as exploring the effect of specific risk factors.

Very little is known about the characteristics of normal arterial flow and pressure waves in horses, which in part depend on the size and branching pattern of the arterial tree. Therefore, **the first aim was to map the majority of the equine arterial tree and use these data to predict flow profiles and pressures in healthy horses (Chapter 3)**. For this purpose, the whole arterial tree was dissected and measured in detail on necropsy. With these results, a one-dimensional *in silico* model was created in order to simulate and explain normal (ultrasound) flow and pressure waves over the arterial tree in horses.

So far, no techniques have been described for measurement of arterial wall stiffness in horses, which is essential to study vascular properties. **The second aim was to develop a method to reliably measure local** (diameter/area change, compliance, distensibility, strain, stiffness index) **and regional** (pulse wave velocity) **arterial wall stiffness in horses (Chapter 4)**.

In humans, race seems to be associated with differences in arterial wall stiffness and in horses, also breed differences have been suggested. **A third aim was to investigate the effect of breed on the arterial wall stiffness (Chapter 5).** Friesian horses are predisposed to aortic rupture which could indicate an underlying primary vascular disorder. Therefore, the above mentioned techniques were used to compare the arterial wall stiffness between Friesian horses and Warmblood horses.

In human patients, the arterial wall is known to stiffen with age and several clinical findings make it highly probable that this is also the case in horses. Uterine artery rupture for example, occurs more often in older mares compared to young ones, aortic rupture occurs more often in older stallions and the risk for phenylephrine-associated fatal hemorrhage is higher in older horses. **Therefore, the last aim was to investigate the effect of aging on the arterial wall (Chapter 6 and 7)**. In a first study, the arterial wall-stiffness of young and old horses was compared *in vivo* based on the previously developed techniques (Chapter 6). Next, we examined age-related arterial structural changes by histology, while biomechanical properties were tested using an *ex vivo* inflation-extension test (Chapter 7).

# CHAPTER 3:

# A 1D COMPUTER MODEL OF THE ARTERIAL CIRCULATION IN HORSES: AN IMPORTANT RESOURCE FOR STUDYING GLOBAL INTERACTIONS BETWEEN HEART AND VESSELS UNDER NORMAL AND PATHOLOGICAL CONDITIONS

# A 1D computer model of the arterial circulation in horses: an important resource for studying global interactions between heart and vessels under normal and pathological conditions

L. Vera[1¶], D. Campos Arias[2,3¶], S. Muylle[4], N. Stergiopulos[5], P. Segers[2] and G. van Loon[1]

[1] Equine Cardioteam Ghent University, Dept. of Large Animal Internal Medicine, Faculty of Veterinary Medicine, Ghent University, Ghent, Belgium.

[2] IBiTech-bioMMeda, Ghent University, Ghent, Belgium.

[3] Biomechanics and Biomaterials Research Group, CUJAE, Havana, Cuba.

[4] Dept. of Morphology, Faculty of Veterinary Medicine, Ghent University, Ghent, Belgium.

[5] Laboratory of Hemodynamics and Cardiovascular Technology, EPFL, Lausanne, Switzerland.

¶These authors contributed equally to this work.

Adapted from:

**Lisse Vera**, Daimé Campos Arias, Sofie Muylle, Nikos Stergiopulos , Patrick Segers, and Gunther van Loon. 2019. “A 1D Computer Model of the Arterial Circulation in Horses : An Important Resource for Studying Global Interactions between Heart and Vessels under Normal and Pathological Conditions.” *PLOS ONE* 14 (8)

## Abstract

Arterial rupture in horses has been observed during exercise, after phenylephrine administration or during parturition (uterine artery). In human pathophysiological research, the use of computer models for studying arterial hemodynamics and understanding normal and abnormal characteristics of arterial pressure and flow waveforms is very common. The objective of this research was to develop a computer model of the equine arterial circulation, in order to study local intra-arterial pressures and flow dynamics in horses. Morphologically, large differences exist between human and equine aortic arch and arterial branching patterns. Development of the present model was based on post-mortem obtained anatomical data of the arterial tree (arterial lengths, diameters and branching angles); *in vivo* collected ultrasonographic flow profiles from the common carotid artery, external iliac artery, median artery and aorta; and invasively collected pressure curves from carotid artery and aorta. These data were used as input for a previously validated (in humans) 1D arterial network model. Data on terminal resistance and arterial compliance parameters were tuned to equine physiology. Given the large arterial diameters, Womersley theory was used to compute friction coefficients, and the input into the arterial system was provided via a scaled time-varying elastance model of the left heart. Outcomes showed plausible predictions of pressure and flow waveforms throughout the considered arterial tree. Simulated flow waveform morphology was in line with measured flow profiles. Consideration of gravity further improved model based predicted waveforms. Derived flow waveform patterns could be explained using wave power analysis. The model offers possibilities as a research tool to predict changes in flow profiles and local pressures as a result of strenuous exercise or altered arterial wall properties related to age, breed or gender.

## Introduction

A wide range of one dimensional (1D) computer models of the human arterial circulation is available. Such models allow the computation of pressure and flow waveforms throughout the whole arterial network, and hence allow researchers to study the normal and abnormal physiology of the cardiovascular system, without the need of *in vivo* measurements[1-7]. 1D models are well-balanced between complexity and computation costs, making them relevant for many (bio)medical applications. Due to their capability of involving extensive arterial segments, 1D models can provide useful information about characteristics of blood flow at the level of individual branches or even in patient-specific situations[8, 9]. These models can also be used as a non-invasive diagnostic tool, helping physicians to understand observed changes in routine clinical blood pressure measurements and their possible physiological origin and to predict surgical operation results[9-11].

Due to technical limitations, difficult arterial accessibility, and ethical concerns, in-depth pathophysiological research of the equine arterial tree remains challenging and could be facilitated by the application of a model. Because of large differences between human and equine arteries regarding dimensions and branching patterns, especially of the aortic arch, a horse specific 1D model of the arterial circulation is needed.

The aim of this study was therefore to develop a 1D computer model of the equine arterial circulation. Providing reference data on equine arterial hemodynamics and physiology, this model might contribute to a better understanding of some clinical findings, such as the origin of the more oscillatory flow patterns in horses, the higher prevalence of aortic rupture in Friesians compared to Warmblood horses[12, 13], the occurrence of sudden death during exercise due to arterial rupture[14-17], the higher chance of uterine artery rupture in older mares[18, 19], or the higher chance of arterial rupture after phenylephrine administration in older horses[20]. In order to develop a reliable model, several anatomical data of the main equine arterial tree were collected *ex vivo* and combined both with *in vivo* invasive blood pressure measurements and non-invasively determined ultrasonographic flow profiles.

## Materials and methods

All procedures were approved by the Ethical Committee of the Faculty of Veterinary Medicine, Ghent University (EC 2016/104). Five warmblood horses were investigated, mean age 18 ± 3 years and mean body weight 648 ± 47 kg. All horses were scheduled for euthanasia because of non-cardiovascular reasons. One horse was privately owned (informed owner consent was obtained), the remaining four horses were experimental horses owned by the Faculty of Veterinary Medicine, Ghent University. For euthanasia the following protocol was applied: premedication with detomidine 0.02mg/kg; induction with a combination of ketamine 2.2mg/kg I.V. and midazolam 0.04mg/kg I.V.; and finally euthanasia with 6 ml/50 kg T61 (Intervet International GmbH, Unterschleissheim, Germany), containing 24mg/kg embutramide, 6 mg/kg mebezoniumjodide and 0,6 mg/kg tetracaïnehydrochloride.

### In vivo measurements

#### *Ultrasound*

Ultrasound imaging was performed (Vivid IQ, GE Healthcare) on all 5 standing, non-sedated horses. Different regions along the arterial tree were examined: the aorta from a left and right parasternal position, the right common carotid artery 15 cm cranial to the thoracic inlet, the right external iliac artery from the inguinal region and the right median artery just proximal to the carpus on the medial side of the leg. 2D B-mode images were collected, using a 9 MHz linear transducer (9L-RS, GE Healthcare) for the common carotid and the median artery, a 6

MHz phased array probe (6S-RS,GE Healthcare) for the external iliac artery and a 5 MHz phased array probe (M5Sc-RS, GE Healthcare) for the aorta. Mean values were obtained from 3 consecutive cardiac cycles at a heart rate between 35-45 beats per minute. Measurements were performed off-line (Echopac version 201, GE Healthcare). Diastolic diameters were measured from a transverse image for the carotid and external iliac artery, and from a longitudinal image for the aorta and the median artery. Pulsed wave Doppler images were collected at every location, using a 6 MHz phased array probe (6S-RS,GE Healthcare) for the common carotid and the external iliac artery, a 5 MHz phased array probe (M5Sc-RS GE Healthcare) for the aorta, and a 9 MHz linear probe (9L-RS,GE Healthcare) for the median artery. Angle correction was set at 45° for every image at all locations. Using this fixed angle correction, images were optimised to align with the flow direction.

***Invasive blood pressure***

In all 5 horses, the blood pressure at the level of the common carotid artery was measured invasively in the standing, awake animal. The right common carotid artery was punctured aseptically under ultrasound guidance (Vivid IQ, GE Healthcare; 9L-RS, GE Healthcare), using an 18 gauge 90mm needle (Terumo spinal needle, Terumo) placed in the middle of the lumen and kept in place for at least 20 consecutive heart cycles. The needle was connected with a fluid filled pressure transducer (MLT0699 Disposable BP Transducer, ADInstruments) interfacing with a digital acquisition station (PowerLab 8, ADInstruments), blood pressure curves were recorded for offline analysis (LabChart, ADInstruments). For each horse the systolic, diastolic and mean arterial pressure was calculated automatically as the mean of 20 consecutive heart beats (heart rate between 35-45 bpm).

In one horse, scheduled for euthanasia, invasive blood pressure measurements over the whole length of the thoracic and abdominal aorta were performed under general anaesthesia (pre-medication: detomidine 0.02mg/kg; induction: combination of ketamine 2.2mg/kg I.V. and midazolam 0.04mg/kg I.V.) with the horse in the dorsal recumbent position. After chirurgical exposure of the right common carotid artery, a 72cm steerable 8.5Fr sheath (Zurpaz, Boston Scientific) was introduced using the Seldinger technique. Under transthoracic ultrasound guidance (Vivid IQ, GE Healthcare; M5Sc-RS, GE Healthcare) the sheath was introduced retrogradely through the brachiocephalic trunk, into the ascending part of the aorta. Once in place, a custom-made pressure tip catheter (Gaeltec) was introduced and advanced to the most caudal end of the aorta under transrectal ultrasound guidance. Blood pressures were recorded (PowerLab 8, ADInstruments) at the most caudal site and subsequently at every 10 cm during step-wise pulling back of the catheter until the ascending part of the aorta was reached. An ECG was recorded simultaneously. At each location, an ensemble-averaged

waveform was constructed from at least 5 cardiac cycles. The ensemble-average was aligned in time relative to the peak of the R-wave of the ECG. Pulse wave velocity was calculated from the relation between inter-measurement distance and time delay. The time delay was calculated from delays in the peak of the 2$^{nd}$ derivative of pressure, assumed to represent the foot of the pressure wave. After the procedure the horse was euthanized while still under general anaesthesia with 6 ml/50 kg bodyweight T61 (Intervet International GmbH, Unterschleissheim, Germany) containing 24mg/kg bodyweight embutramide, 6 mg/kg bodyweight mebezoniumjodide and 0,6 mg/kg bodyweigth tetracaïnehydrochloride.

**Ex vivo measurements**

Necropsy of 4 out of 5 horses was performed within 12 hours after euthanasia. A dissection was completed on the aorta and the most important (left sided) side branches and morphometric data (length, diameter and branching angle) were recorded. Arterial length was measured using a tape measure and diameters were measured in the middle of each segment by introducing custom-made iron rods of different diameters into the explored arterial lumen. Subsequently, post-mortem diameters were scaled to the *in vivo* diameters, using the *in vivo* ultrasound measurements of common carotid artery, external iliac artery and median artery as a reference. Angles of the different arterial segments in the 1-dimensional plane were measured using anatomical images of the equine arterial tree[21]. Lengths of terminal segments were only measured in one horse. Right sided circulation was assumed to be the same as the left sided arterial circulation, except for the right sided subclavian circulation (as the branching pattern is different), which was measured separately in one of the horses. All investigated arterial branches and their corresponding average length and diameter are displayed in Table 1. Note that in the mathematical model vessel tapering will be included, meaning that average segment diameters will be adjusted to minimize forward reflections (see chapter ‘Distal boundary conditions and bifurcations’).

**Mathematical model**

The mathematical model is based on a previously published and validated 1D arterial network model in humans[22; 23]. Main differences between the human and the adapted equine model are described below. The system of nonlinear equations is solved using in-house MatLab code. For the solution an implicit finite difference scheme was chosen, with second order of accuracy for the temporal and spatial domains. Forward, central and backward difference approximations of the spatial derivative were used for the proximal, middle and distal nodes in each segment, respectively. The arterial tree was initialized with a pressure of 100 mmHg and a flow of 1ml/s. The solution was found over 8 cardiac cycles yielding pressure and flow

waveforms over the entire arterial tree. For more details on the modelling aspects and the mathematical equations, we refer the interested reader to Ref. [22].

***Governing equations***

The main branches of the equine arterial tree were divided into 117 interconnected straight cylindrical arterial segments and inserted in the mathematical model (Fig. 1, Table 1). The integrated forms of the continuity and momentum equations of the Navier-Stokes equations were solved in each of these segments for pressure (P), flow (Q) and cross-sectional area (A),

$$\frac{\partial A}{\partial t} + \frac{\partial Q}{\partial x} = -\psi \tag{1}$$

$$\frac{\partial Q}{\partial t} + \frac{\partial}{\partial x}\left(\int_A u^2 dA\right) = -\frac{A}{\rho}\frac{\partial P}{\partial x} - 2\pi R \frac{\mu}{\rho}\frac{\partial u}{\partial r}\Big|_{r=R} + Ag\cos\theta \tag{2}$$

where $x$ and $t$ are the spatial and temporal variables, $u$ is the longitudinal velocity component, and $R$ is the lumen radius. Given that measurements in animals, used as input into the model, were acquired in standing, awake animals, as well as in anesthetized and supine animals, we expect effects of gravity to be important given the height of the animal. We therefore accounted for the effects of gravity including the body forces term in the momentum equation, with $g$=9.81 m/s$^2$, the gravitational acceleration constant, and $\theta$, the projection angle on the vertical axis. Results will be further reported for both situations, considering the effects of gravity and neglecting gravitational body forces. Blood was assumed to be an incompressible Newtonian fluid with density ρ=1050 kg/m$^3$ and dynamic viscosity μ=0.004 Pa · s. Given the large arterial diameters in horses, the Witzig-Womersley correction (see section 'Velocity profile') was used to approximate the convective acceleration term ($\frac{\partial}{\partial x}\left(\int_A u^2 dA\right)$) and the wall friction term ($\tau = \mu\frac{\partial u}{\partial r}\Big|_{r=R}$), both present in the momentum equation.

Fig. 1. Schematic representation of the left sided arterial tree of the horse. Numbers agree with the numbers displayed in Table 1.

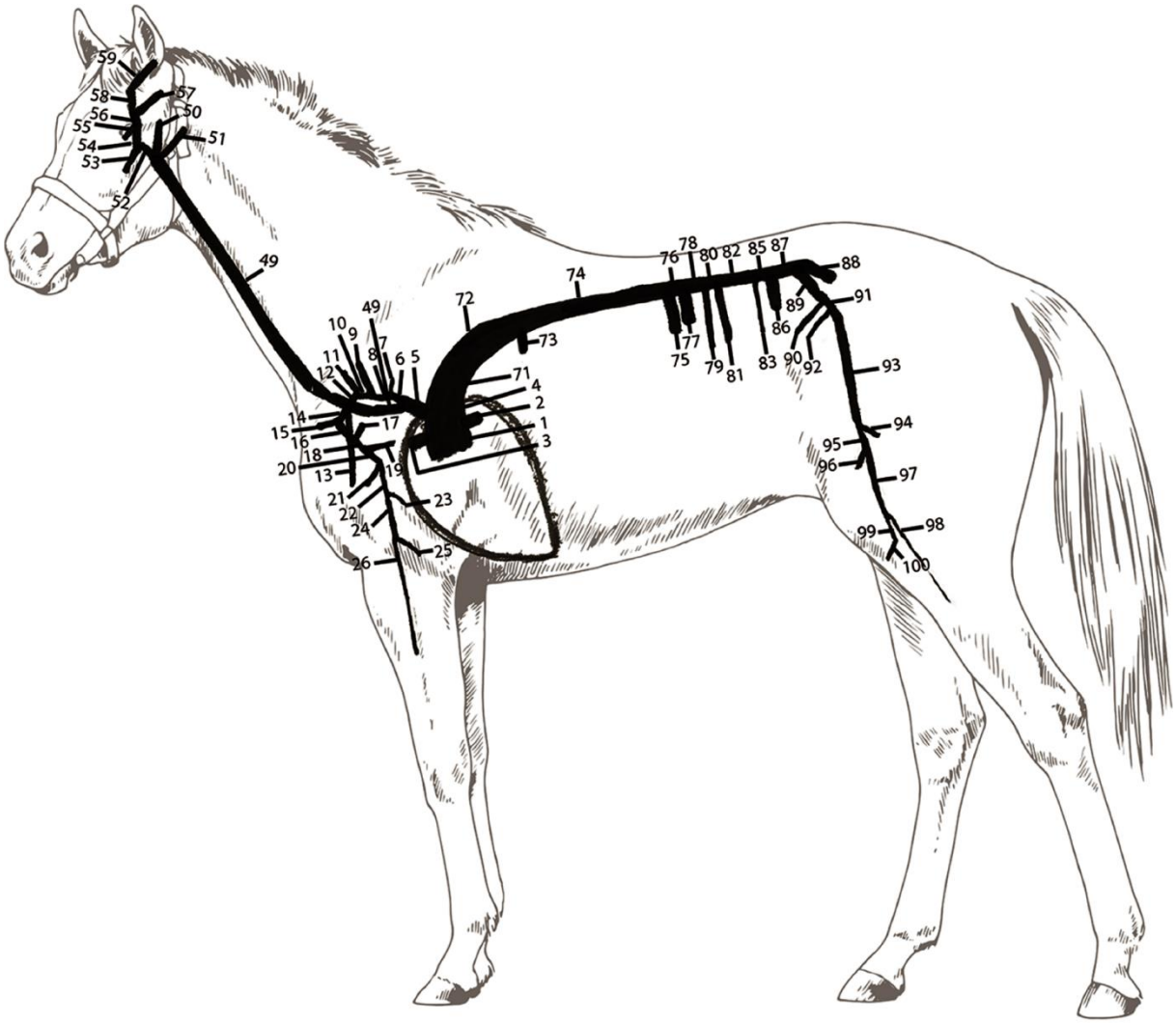

Table 1. Anatomical data of the equine arterial tree.

| Artery | Arterial Segment Number | Angle in the 1D plane (degrees) | Mean Length (mm) | SD | Mean diameter (mm) | SD | Tapering | | Distensibility $10^{-3}$ 1/mmHg |
|---|---|---|---|---|---|---|---|---|---|
| | | | | | | | Proximal lumen diameter (mm) | Distal lumen diameter (mm) | |
| Aorta ascendens 1 | 1 | 90 | 18 | 9 | 68 | 6 | 68.18 | 67.39 | 6.85 |
| A coronaria sinistra | 2 | 180 | 20 | / | 19 | 6 | 23.638 | 12.10 | 3.17 |
| A coronaria dextra | 3 | 0 | 20 | / | 19 | 6 | 23.638 | 12.10 | 3.17 |
| Aorta ascendens 2 | 4 | 90 | 64 | 9 | 67 | 6 | 67.22 | 66.82 | 6.80 |
| Truncus brachiocephalicus 1 | 5 | 160 | 38 | 26 | 39 | 9 | 38.882 | 38.88 | 4.90 |
| A subclavia sinistra 1 | 6 | 155 | 39 | 24 | 26 | 11 | 25.332 | 25.33 | 3.79 |
| Truncus costocervicalis sinister | 7 | 90 | 10 | / | 11 | 5 | 12.102 | 10.50 | 2.34 |
| A subclavia sinistra 2 | 8 | 155 | 19 | 13 | 24 | 8 | 24.11 | 24.11 | 3.68 |
| A cervicalis profunda sinistra | 9 | 115 | 70 | / | 3 | 1 | 2.82 | 2.82 | 0.87 |
| A subclavia sinistra 3 | 10 | 155 | 14 | 8 | 24 | 8 | 24.11 | 24.11 | 3.68 |
| A vertebralis sinistra | 11 | 135 | 95 | / | 12 | 5 | 14.17 | 9.98 | 2.45 |
| A subclavia sinistra 4 | 12 | 240 | 40 | 6 | 23 | 6 | 22.89 | 22.89 | 3.57 |
| A thoracica interna sinistra | 13 | 280 | 137 | / | 12 | 4 | 12.11 | 12.11 | 2.44 |
| A subclavia sinistra 5 | 14 | 240 | 7 | 8 | 23 | 6 | 22.89 | 22.89 | 3.57 |
| A cervicalis superficialis sinistra | 15 | 180 | 80 | / | 8 | 2 | 10.31 | 4.79 | 1.90 |
| A axillaris sinistra 1 | 16 | 310 | 62 | 25 | 21 | 6 | 21.50 | 20.37 | 3.38 |
| A suprascapularis sinistra | 17 | 70 | 15 | / | 6 | 0 | 7.68 | 3.52 | 1.59 |
| A axillaris sinistra 2 | 18 | 310 | 58 | 45 | 20 | 8 | 19.90 | 19.90 | 3.28 |
| A subscapularis sinistra | 19 | 10 | 10 | / | 17 | 7 | 16.80 | 16.80 | 2.96 |
| A axillaris sinistra 3 | 20 | 310 | 23 | 18 | 18 | 5 | 18.02 | 18.02 | 3.09 |
| A circumflexa humeri cranialis sinistra | 21 | 230 | 30 | / | 5 | 2 | 6.11 | 2.79 | 1.39 |
| A axillaris sinistra 4 | 22 | 270 | 70 | 28 | 17 | 3 | 17.05 | 17.05 | 2.99 |
| A profunda brachii sinistra | 23 | 325 | 5 | / | 11 | 5 | 11.281 | 9.60 | 2.23 |
| A axillaris sinistra 5 | 24 | 270 | 82 | 11 | 14 | 1 | 15.35 | 12.79 | 2.67 |
| A collateralis ulnaris sinistra | 25 | 320 | 5 | / | 6 | 2 | 8.60 | 4.92 | 1.75 |
| A mediana sinistra | 26 | 270 | 145 | / | 7 | 3 | 10.01 | 5.30 | 1.90 |
| Truncus brachiocephalicus 2 | 27 | 160 | 50 | / | 39 | / | 38.88 | 38.88 | 4.90 |
| Truncus costocervicalis dexter | 28 | 90 | 10 | / | 11 | 6 | 14.38 | 7.07 | 2.34 |
| Truncus brachiocephalicus 3 | 29 | 160 | 10 | / | 39 | / | 38.88 | 38.88 | 4.90 |
| A cervicalis profunda dextra | 30 | 115 | 70 | / | 3 | 2 | 2.81 | 2.81 | 0.87 |
| Trunucus brachiocephalicus 4 | 31 | 160 | 10 | / | 39 | / | 38.88 | 38.88 | 4.90 |
| A vertebralis dextra | 32 | 135 | 95 | / | 12 | 5 | 16.95 | 7.12 | 2.54 |
| Truncus brachiocephalicus 5 | 33 | 160 | 20 | / | 26 | / | 26.96 | 25.00 | 4.24 |
| A subclavia dextra 1 | 34 | 240 | 30 | / | 26 | 11 | 25.00 | 25.00 | 3.76 |
| A thoracica interna dextra | 35 | 280 | 137 | / | 11 | 5 | 12.12 | 12.10 | 2.44 |
| A cervicalis superficialis dextra | 36 | 180 | 80 | / | 3 | 1 | 8.07 | 8.02 | 1.90 |
| A axillaris dextra 1 | 37 | 310 | 62 | 25 | 21 | 6 | 20.95 | 20.94 | 3.38 |
| A suprascapularis | 38 | 70 | 15 | / | 6 | 0 | 6.43 | 5.47 | 1.59 |
| A axillaris dextra 2 | 39 | 310 | 58 | 45 | 20 | 8 | 19.90 | 19.90 | 3.28 |
| A subscapularis dextra | 40 | 10 | 10 | / | 17 | 7 | 16.80 | 16.80 | 2.96 |
| A axillaris dextra 3 | 41 | 310 | 23 | 18 | 18 | 5 | 18.02 | 18.02 | 3.09 |
| A circumflexa humeri cranialis dextra | 42 | 230 | 30 | / | 5 | 2 | 6.115 | 2.79 | 1.39 |
| A axillaris dextra 4 | 43 | 270 | 70 | 28 | 17 | 3 | 17.05 | 17.05 | 2.99 |
| A profunda brachii dextra | 44 | 325 | 5 | / | 11 | 5 | 10.47 | 10.47 | 2.23 |
| A axillaris dextra 5 | 45 | 270 | 82 | 11 | 14 | 1 | 17.05 | 10.42 | 2.67 |
| A collateralis ulnaris dextra | 46 | 320 | 5 | / | 6 | 2 | 8.60 | 4.92 | 1.75 |
| A mediana dextra | 47 | 270 | 145 | / | 7 | 3 | 10.00 | 5.30 | 1.90 |
| Truncus bicaroticus | 48 | 165 | 78 | 91 | 22 | 19 | 22.06 | 21.26 | 3.45 |
| A carotis communis sinistra | 49 | 110 | 710 | 59 | 12 | 1 | 13.45 | 10.35 | 2.42 |
| A carotis interna sinistra | 50 | 90 | 120 | / | 4 | 1 | 4.43 | 3.53 | 1.25 |

| | | | | | | | | | |
|---|---|---|---|---|---|---|---|---|---|
| A occipitalis sinistra | 51 | 60 | 45 | / | 5 | 2 | 4.94 | 4.13 | 1.35 |
| A carotis externa sinistra 1 | 52 | 130 | 65 | 41 | 10 | 3 | 10.04 | 10.04 | 2.18 |
| Truncus linguofacialis sinister | 53 | 180 | 80 | / | 6 | 3 | 6.54 | 5.50 | 1.60 |
| A carotis externa sinistra 2 | 54 | 90 | 41 | 11 | 9 | 2 | 9.22 | 8.83 | 2.04 |
| Ramus massetericus sinister | 55 | 255 | 20 | / | 2 | 1 | 2.51 | 1.21 | 0.82 |
| A carotis externa sinistra 3 | 56 | 90 | 13 | 3 | 9 | 2 | 8.56 | 8.55 | 1.98 |
| A auricularis caudalis sinistra | 57 | 55 | 10 | / | 3 | 2 | 3.953 | 1.74 | 1.07 |
| A carotis externa sinistra 4 | 58 | 90 | 23 | 3 | 7 | 3 | 8.56 | 5.15 | 1.76 |
| A temporalis superficialis sinistra | 59 | 60 | 20 | / | 2 | 2 | 3.44 | 2.48 | 1.05 |
| A carotis externa sinistra 5 | 58b* | 90 | 5 | / | 5 | / | 5.15 | 5.15 | 1.46 |
| A carotis communis dextra | 60 | 110 | 710 | 59 | 12 | 1 | 13.45 | 10.35 | 2.42 |
| A carotis interna dextra | 61 | 90 | 120 | / | 4 | 1 | 4.43 | 3.53 | 1.25 |
| A occipitalis dextra | 62 | 60 | 45 | / | 5 | 2 | 4.94 | 4.13 | 1.35 |
| A carotis externa dextra 1 | 63 | 130 | 65 | 41 | 10 | 3 | 10.04 | 10.04 | 2.18 |
| Truncus linguofacialis dexter | 64 | 180 | 80 | / | 6 | 3 | 6.54 | 5.50 | 1.60 |
| A carotis externa dextra 2 | 65 | 90 | 41 | 11 | 9 | 2 | 9.22 | 8.83 | 2.04 |
| Ramus massetericus dexter | 66 | 255 | 20 | / | 2 | 1 | 2.51 | 1.21 | 0.82 |
| A carotis externa dextra 3 | 67 | 90 | 13 | 3 | 9 | 2 | 8.56 | 8.55 | 1.98 |
| A aurocularis caudalis dextra | 68 | 55 | 10 | / | 3 | 2 | 3.95 | 1.74 | 1.07 |
| A carotis externa dextra 4 | 69 | 90 | 23 | 3 | 7 | 3 | 8.56 | 5.15 | 1.76 |
| A temporalis superficialis dextra | 70 | 60 | 20 | / | 2 | 2 | 3.44 | 2.48 | 1.05 |
| A carotis externa dextra 5 | 69b* | 90 | 5 | / | 5 | / | 5.15 | 5.15 | 1.46 |
| Arcus aortae (lig. Art Botalli) | 71 | 45 | 77 | 26 | 54 | 10 | 58.07 | 49.53 | 5.97 |
| Aorta descendens 1 | 72 | 45 | 105 | 5 | 45 | 11 | 48.21 | 40.62 | 5.32 |
| A broncho-oesophagea | 73 | 270 | 66 | / | 11 | 2 | 13.71 | 6.31 | 2.26 |
| Aorta descendens 2 | 74 | 0 | 486 | 69 | 36 | 1 | 38.44 | 32.28 | 4.64 |
| A coeliaca | 75 | 270 | 20 | / | 15 | 3 | 19.31 | 9.24 | 2.78 |
| Aorta descendens 3 | 76 | 0 | 48 | 26 | 29 | 6 | 28.70 | 28.70 | 4.09 |
| A mesenterica cranialis | 77 | 270 | 20 | / | 11 | 7 | 13.48 | 7.56 | 2.29 |
| Aorta descendens 4 | 78 | 0 | 30 | 35 | 29 | 10 | 28.70 | 28.70 | 4.09 |
| A renalis dextra | 79 | 270 | 30 | / | 11 | 2 | 13.26 | 7.21 | 2.26 |
| Aorta descendens 5 | 80 | 0 | 20 | 19 | 29 | 5 | 28.70 | 28.70 | 4.09 |
| A renalis sinistra | 81 | 270 | 30 | / | 11 | 2 | 13.26 | 7.21 | 2.26 |
| Aorta descendens 6 | 82 | 0 | 104 | 60 | 29 | 6 | 28.70 | 28.70 | 4.09 |
| A ovarica sinistra | 83 | 270 | 300 | / | 3 | 1 | 2.76 | 2.76 | 1.00 |
| A ovarica dextra | 84 | 270 | 300 | / | 3 | 1 | 2.76 | 2.76 | 1.00 |
| Aorta descendens 7 | 85 | 0 | 40 | 27 | 29 | 6 | 28.70 | 28.70 | 4.09 |
| A mesenterica caudalis | 86 | 270 | 10 | / | 8 | 3 | 9.78 | 4.63 | 1.85 |
| Aorta descendens 8 | 87 | 0 | 63 | 12 | 29 | 6 | 28.70 | 28.70 | 4.09 |
| A iliaca interna sinistra | 88 | 330 | 30 | 10 | 18 | 6 | 20.19 | 15.12 | 0.92 |
| A iliaca externa sinistra 1 | 89 | 315 | 30 | / | 17 | 2 | 16.93 | 16.24 | 0.88 |
| A circumflexa iliumprofunda sinistra | 90 | 240 | 160 | / | 6 | 2 | 7.58 | 3.66 | 0.48 |
| A iliaca externa sinistra 2 | 91 | 280 | 29 | 19 | 16 | 3 | 15.99 | 15.54 | 0.86 |
| A uterina sinistra | 92 | 260 | 200 | / | 3 | 2 | 3.19 | 3.19 | 0.33 |
| A iliaca externa sinistra 3 | 93 | 280 | 230 | 54 | 15 | 3 | 15.30 | 15.30 | 0.84 |
| A profunda femoris sinistra | 94 | 335 | 30 | / | 8 | 2 | 7.93 | 7.23 | 0.55 |
| A femoralis sinistra 1 | 95 | 280 | 51 | 14 | 15 | 3 | 15.26 | 14.27 | 0.82 |
| A circumflexa femoris lateralis sinistra | 96 | 240 | 30 | / | 6 | 3 | 7.69 | 3.62 | 0.48 |
| A femoralis sinistra 2 | 97 | 280 | 180 | 56 | 11 | 1 | 10.78 | 10.78 | 0.68 |
| A saphena sinistra | 98 | 285 | 625 | / | 3 | 3 | 2.59 | 2.59 | 0.29 |
| A femoralis sinistra 3 | 99 | 280 | 25 | 26 | 10 | 1 | 10.78 | 9.71 | 0.66 |
| A genus descendens sinistra | 100 | 260 | 25 | / | 3 | 1 | 4.46 | 3.47 | 0.38 |
| A femoralis sinistra 4 | 99b* | 280 | 5 | / | 10 | / | 9.71 | 9.71 | 0.64 |
| A iliaca interna dextra | 101 | 330 | 30 | 10 | 18 | 6 | 20.19 | 15.12 | 0.92 |
| A iliaca externa dextra 1 | 102 | 315 | 30 | / | 17 | 2 | 16.98 | 16.19 | 0.88 |
| A uterina dextra | 103 | 260 | 200 | / | 6 | 2 | 3.19 | 3.19 | 0.33 |
| A iliaca externa dextra 2 | 104 | 280 | 29 | 19 | 16 | 3 | 15.97 | 15.56 | 0.86 |
| A circumflexa iliumprofunda dextra | 105 | 240 | 160 | / | 3 | 2 | 7.52 | 3.77 | 0.48 |

| | | | | | | | | | |
|---|---|---|---|---|---|---|---|---|---|
| A iliaca externa dextra 3 | 106 | 280 | 230 | 54 | 15 | 3 | 15.30 | 15.30 | 0.84 |
| A profunda femoris dextra | 107 | 335 | 30 | / | 8 | 2 | 7.93 | 7.23 | 0.55 |
| A femoralis dextra 1 | 108 | 280 | 51 | 14 | 15 | 3 | 15.26 | 14.27 | 0.82 |
| A circumflexa femoris lateralis dextra | 109 | 240 | 30 | / | 6 | 3 | 7.69 | 3.62 | 0.48 |
| A femoralis dextra 2 | 110 | 280 | 180 | 56 | 11 | 1 | 10.78 | 10.78 | 0.68 |
| A saphena dextra | 111 | 285 | 625 | / | 3 | 3 | 2.59 | 2.59 | 0.29 |
| A femoralis dextra 3 | 112 | 280 | 25 | 26 | 10 | 1 | 10.78 | 9.71 | 0.66 |
| A genus descendens dextra | 113 | 260 | 25 | / | 3 | 1 | 4.46 | 3.47 | 0.38 |
| A femoralis dextra 4 | 112b * | 280 | 5 | / | 1 | / | 9.71 | 9.71 | 0.64 |

SD: standard deviation

/: no SD could be obtained, because the measurement was only performed in one horse

* An additional terminal segment, which was not measured on necropsy, with an artificial length of 5 cm was implemented in the model.

***Modelling of the arterial wall***

A constitutive equation is needed to account for the elastic properties of the arterial wall, relating the dependency in intra-arterial pressure with the cross-sectional area. The nonlinear elastic behaviour of the arterial wall is assumed with an expression of area compliance ($C_A$)[22], as the product of a location-dependent function, $C_d(\bar{d}, P_{ref})$, and a pressure-dependent function, $C_p(P)$.

$$C_A(\bar{d}, P) = \underbrace{\frac{A}{\rho \cdot PWV^2(\bar{d}, P_{ref})}}_{C_d(\bar{d}, P_{ref})} \cdot \underbrace{\left[a_1 + \frac{b_1}{1+\left[\frac{P-P_{maxC}}{P_{width}}\right]^2}\right]}_{C_p(P)} \tag{3}$$

The function $C_d(\bar{d}, P_{ref})$ gives the compliance for a given local mean arterial lumen diameter, $\bar{d}$, at a given reference pressure value, $P_{ref}$ =100 mmHg. Reymond et al.[22] fitted an empirical inverse power curve for PWV as a function of $\bar{d}$, from human data reported in the literature.

$$PWV(\bar{d}) \approx \frac{a_2}{\bar{d}^{b_2}} \tag{4}$$

To the best of our knowledge, measurements of the pressure and diameter dependency of the compliance in horses are lacking in literature but it can be assumed that the intrinsic building blocks (elastin, collagen, smooth muscle cells, proteoglycans) and their organization, and hence the overall mechanical behaviour, is similar as in humans. Initially, following Reymond et al.[22], we used the fitted values on humans for the pressure dependency of the compliance. However, these parameters were subsequently adapted to obtain values of pulse pressure close to the value reported by Boegli et al.[23] for healthy horses, resulting in $a_1$=0.76, $b_1$=5, $P_{maxC}$=10 mmHg and $P_{width}$=21 mmHg. We also applied the fit obtained from human data to describe the relation between local diameter and compliance (for $a_2$=13.3 and $b_2$=0.3).

Nonetheless, we did tune the arterial distensibilities to the equine physiology, by multiplying the distensibilities of all vessels of the 1D model by a common factor with value 0.75. That factor was determined such that in resting conditions, we obtained a value of PWV close to the PWV computed from invasive blood pressure measurements over the abdominal aorta of an anesthetized horse; keeping in mind that differences may arise between an anesthetized and a conscious animal.

***Velocity profile***

The Witzig-Womersley theory describes the effect of flow pulsatility and inertia on the velocity profile. This oscillatory flow theory was needed to calculate the terms of convective acceleration and wall shear stress in the momentum equation derived from the Navier-Stokes equations, given that both terms depend on the instantaneous velocity profile. The Witzig-Womersley theory requires the knowledge of the local flow profile across the arterial lumen over the entire heart cycle, which is a priori unknown in the 1D model. This difficulty was overcome assuming that the solution is periodic; the flow waveform from the previous heart cycle was used to calculate the velocity profile and the wall shear stress using the formulations:

$$\mathrm{u}(r,t) = \frac{2}{\pi R^2}\left(1-\frac{r^2}{R^2}\right)Q_1 + \sum_{n=2}\mathrm{Real}\left\{\frac{Q_n}{\pi R^2}\frac{1-\frac{J_0\left(\alpha i^{3/2} r/R\right)}{J_0\left(\alpha i^{3/2}\right)}}{1-\frac{2J_1\left(\alpha i^{3/2}\right)}{\alpha i^{3/2} J_0\left(\alpha i^{3/2}\right)}}e^{i\omega t}\right\} \quad (5)$$

$$\tau(t) = -\frac{4\mu}{\pi R^3}Q_1 + \sum_{n=2}\mathrm{Real}\left\{\frac{\mu}{\pi R^3}Q_n \alpha i^{3/2}\frac{\frac{J_1\left(\alpha i^{3/2}\right)}{J_0\left(\alpha i^{3/2}\right)}}{1-\frac{2J_1\left(\alpha i^{3/2}\right)}{\alpha i^{3/2} J_0\left(\alpha i^{3/2}\right)}}e^{i\omega t}\right\} \quad (6)$$

The velocity profile ($\mathrm{u}$) and the wall friction term ($\tau$) are calculated as a Fourier series with harmonics ($n$) and depend on the harmonic-specific Womersley's number $\alpha = \mathrm{R}\sqrt{\rho 2\pi \mathrm{f}/\mu}$, where $\mathrm{R}$ is the artery radius and $\mathrm{f}$ the frequency, $r/R$ is the relative radial position, $Q_n$ is the $n^{\text{th}}$ harmonic of the flow pulse, and $J_0$ and $J_1$ are the Bessel functions of first kind of order 0 and 1, respectively. The oscillatory flow theory is taken into account for vessels with $\alpha > 3$ (75% of the total number of arterial segments), where the wall friction and convective acceleration are related as independent terms in the 1D momentum equation; the solution described by Stergiopulos et al.[3] is considered otherwise. The solution is found solving in time a number of repeating cycles until convergence.

***Distal boundary conditions and bifurcations***

For the terminal nodes a 3-element Windkessel model was used, to account for the cumulative effect of all distal vessels beyond the terminal sites [3, 22]. The equation takes the form:

$$\frac{\partial \mathrm{Q}}{\partial \mathrm{t}} = \frac{1}{\mathrm{R}_1}\frac{\partial \mathrm{P}}{\partial \mathrm{t}} + \frac{\mathrm{P}}{\mathrm{R}_1\mathrm{R}_2\mathrm{C}_\mathrm{T}} - \left(1 + \frac{\mathrm{R}_1}{\mathrm{R}_2}\right)\frac{\mathrm{Q}}{\mathrm{R}_1\mathrm{C}_\mathrm{T}} \quad (7)$$

where $\mathrm{R}_1$ is the proximal resistance, $\mathrm{R}_2$ is the distal resistance, and $\mathrm{C}_\mathrm{T}$ is the terminal compliance. Total peripheral resistances $\mathrm{R}_\mathrm{T} = \mathrm{R}_1 + \mathrm{R}_2$, were estimated taking into account both the distribution of flow described in the literature [24] and our own measurements of flow at specific locations from ultrasound data. A total resistance parallel combination of about 0.14 mmHg*s/ml was assumed. The values of $\mathrm{R}_1$ were estimated assuming minimal reflection at high frequencies, with the condition $\mathrm{R}_1 = \mathrm{Z}_\mathrm{c}$, where $\mathrm{Z}_\mathrm{c} = \rho \cdot \mathrm{PWV}/\mathrm{A}$ is the characteristic impedance of the terminal segments. The values of distal resistance were then calculated as $\mathrm{R}_2 = \mathrm{R}_\mathrm{T} - \mathrm{R}_1$.

Terminal compliance was estimated following Reymond et al.[22], where the terminal compliance of each terminal vessel, $\mathrm{C}_{\mathrm{T},i}$, was assumed to be proportional to the area compliance, $\mathrm{C}_{\mathrm{A},i}$, at the distal end of the terminal vessels:

$$\mathrm{C}_{\mathrm{T},i} \cong \mathrm{C}_\mathrm{T}\frac{\mathrm{C}_{\mathrm{A},i}}{\sum \mathrm{C}_{\mathrm{A},i}} \quad (8)$$

with $\mathrm{C}_\mathrm{T} = \sum \mathrm{C}_{\mathrm{T},i}$ the part of the total volume compliance attributed to peripheral vessels not included in the arterial tree model, assumed to be in the order of 20% of the total systemic vascular compliance. The total systemic vascular compliance is the sum of the volume compliance of all vessels and compliance of the terminal beds, so that $\mathrm{C}_\mathrm{V} = \sum_n^i \mathrm{C}_{\mathrm{V},i} + \sum_m^i \mathrm{C}_{\mathrm{T},i}$, where n=117 is the total number of arterial segments and m=62 is the number of terminal segments. To obtain volume compliance of each segment, the area compliance given by equation (3) is integrated over the segment length. All values of terminal resistance and compliance can be found in S1 Table. Continuity of pressure and flow was imposed throughout the arterial network at bifurcations. Forward wave reflections were minimized by adapting the characteristic impedance of the tributaries so that the absolute value of the reflection coefficient was < 0.2 at all bifurcations. The cross-sectional area of the vessels was therefore slightly adjusted resulting in tapered-structure segments. Cross-sectional areas were determined by minimizing the reflection coefficient, subject to three conditions: (i) measured area is the average between the input and output areas ($A_{in}$ and $A_{out}$ respectively); (ii) $A_{in}$ of tributaries is lower or equal to $A_{out}$ of the parent, and (iii) for each segment $A_{out} \leq A_{in}$. Initial searching points were obtained by assuming linear tapering. The forward wave reflection coefficient is calculated as:

$$\Gamma = \frac{Z_{\text{parent}}^{-1} - \sum Z_{\text{daughter}}^{-1}}{Z_{\text{parent}}^{-1} + \sum Z_{\text{daughter}}^{-1}} \quad (9)$$

where $\mathrm{Z}$ is the characteristic impedance of the parent and daughter vessels.

### *Heart model*

A model of the left ventricle (LV) was used at the proximal end of the arterial tree (root of the ascending aorta), simulating the blood flow pumped out of the LV. The LV model is based on the time-varying elastance model, which describes the variation of LV pressure ($P_{LV}$) and volume ($V_{LV}$) during a cardiac cycle.

$$E(t) = \frac{P_{LV}(t)}{V_{LV}(t) - V_0} \tag{10}$$

The interaction between the ventricle and the arterial tree is mainly produced during the ejection phase, when the aortic valve is open. To improve the simulation of the wave reflection phenomena that occur during this period between the ventricle and the aorta, an internal resistance of the LV was introduced. Taking this into consideration, the varying elastance model originally suggested by Sagawa[25] was adapted by Reymond et al.[22], leading to the following expression for the varying elastance of an ejecting heart:

$$E(t) = E^*(t)[1 - \kappa Q(t)] \tag{11}$$

where $E^*$ is the elastance that would be measured during a nonejecting isovolumic contraction, and $\kappa$ a constant relating the internal resistance of the LV to the ventricular pressure during the same cardiac phase. Assuming that the elastance curve (when normalized with respect to its peak value) is similar in shape for all mammals, a normalized isovolumic elastance, $E^*$, can be derived from equation (11) using the global normalized elastance curves, $E$, reported by Senzaki et al.[26]. The constant $\kappa$ was derived iteratively by minimizing the difference between the elastance curve resultant from the 1D model and the original elastance curve reported by Senzaki et al.[26]. The value of $\kappa$ obtained was 55E-06 s/ml. Due to the lack of detailed horse data in current literature, assumptions needed to be made to set most of the input parameters necessary for the heart model. The value of end-diastolic pressure was taken as, $P_{end\text{-}dias}$=16 mmHg, according to the value reported by Brown and Holmes[27] for a normal horse and well within the standard range (12-24 mmHg) reported in the literature for horses[28], whereas the end-systolic pressure was 113 mmHg[27]. The value of the dead volume of the LV was set to $V_0$=0 ml. Initial reference values for stroke volume ($SV$=900 ml/min) and ejection fraction ($EF$=60 %) were used to estimate the end-diastolic volume (EDV) and the end-systolic volume (ESV), wherewith initial values of minimal and maximal elastance were derived considering equation (10). These values were further tuned to obtain a close match between the simulated aortic flow velocity and the aortic flow velocity measured from ultrasound imaging, which resulted in final values of $E_{min}$=0.01 mmHg/ml and $E_{max}$=0.26 mmHg/ml. The standard heart rate was set to 40 bpm, a normal physiological value for the horse at rest, whereas systolic duration was set to 478 ms [29].The heart model simulates the four main phases of the cardiac cycle, starting

the loop at the onset of the isovolumic contraction phase, where the volume in the LV equals EDV (derived in the simulation from equation (10), for a LV pressure equal $P_{end\text{-}dias}$). With the contraction, the pressure in the ventricle rises over the aortic pressure, which causes the opening of the aortic valve and the start of the ejection phase. During this period, the ventricle-arterial interaction is described by the combination of equations (10) and (11). When the flow becomes negative, end systole is reached (aortic valve closes) and the relaxation phase takes place. The filling phase is set when the pressure in the ventricle drops below the initially assumed $P_{end\text{-}dias}$, and the filling flow is modelled from the internal resistance of the LV (assumed as 0.003 mmHg·s·ml$^{-1}$). The solution of the heart model is periodic; at the start of every cardiac cycle, EDV takes the value derived from the previous cardiac cycle.

#### *Coronary model*

Coronary arteries were modelled following Reymond et al.[22], assuming that changes in compliance, distensibility and resistance are proportional to the local time varying elastance of each vessel. For the right coronary, it was additionally assumed that the effect of the right ventricular contraction is smaller by a factor proportional to the ratio of maximal pressure in the two ventricles (PLV,max/PRV,max ≈ 3 [28]).

#### Hemodynamic and Wave Reflection Analysis using Wave Power

Wave power analysis (WPA) [30] was applied in different locations to study the dynamics of the waves. The method defines the wave power, $d\pi$, as the product of the changes in pressure ($dP$) and flow ($dQ$), and equals the energy carried by the wave which is conserved at junctions. Wave power can be separated into its forward and backward components (subscripts (+) and (-), respectively), $d\pi = d\pi_+ + d\pi_-$, where $d\pi_+ = 1/(4 \cdot Z_c)(dP + Z_c dQ)^2$ and $d\pi_- = -1/(4 \cdot Z_c)(dP - Z_c dQ)^2$. The concept of wave power is analogous to wave intensity analysis [31], with $d\pi > 0$ indicating dominant forward waves and $d\pi < 0$ indicating dominant backward waves. The distance travelled by the waves to their reflection points can be estimated as the product of the transit time between a wave and its reflection and the local theoretical PWV. Since the wave travels twice the same distance, the final distance can be computed as $L = (\Delta t \cdot PWV_{theor})/2$.

## Results

#### General physiological parameters

Running the model without including gravity revealed a cardiac output of 33 L/min, an ejection fraction of 65 % and a stroke volume 820 ml. Systolic/diastolic pressure in the aortic root was 114/70 mmHg, with a pulse pressure of 44 mmHg and a mean arterial pressure of 93 mmHg.

Taking gravity into account, cardiac output was reduced to 30 L/min, with an ejection fraction of 59 % and a stroke volume of 740 ml, whereas systolic/diastolic pressure increased to 131/88 mmHg, resulting in an almost unaltered pulse pressure of 43 mmHg and an increased mean arterial pressure of 111 mmHg. The distribution of cardiac output derived from the model for both configurations is summarized in Table 2. Table 3 shows the values of the Womersley number, maximum shear stress, mean values of the convective acceleration approximation and the Reynolds number, derived from the model at different locations in the arterial network, including and neglecting gravity for both configurations of the model. On the other hand, the total vascular resistance resulted in a value of 0.17 mmHg*s/ml for the model without gravity, and 0.22 mmHg*s/ml for the model with gravity. Note that these values differ from the total combination of resistances in parallel, since the total vascular resistance also account for the resistances in series in the vessels.

Table 2. Distribution of cardiac output (CO) in the model.

| **Body parts** | **Model without gravity CO distribution (%).** | **Model with gravity CO distribution (%).** | **Reference [24] CO distribution (%).** |
|---|---|---|---|
| **Heart** | 4.2 | 5.4 | 5 |
| **Brain** | 15.4 | 10.5 | 10 |
| **Muscle** | 7.7 | 11.3 | 15 |
| **Kidney** | 18.2 | 20.7 | 20 |
| **Splanchnic** | 28.3 | 32.6 | 30 |
| **Other** | 26.2 | 19.5 | 20 |

Table 3. Womersley number, maximum shear stress, mean convective acceleration and Reynolds numbers, derived from the model with and without gravity at different locations along the equine arterial tree.

| **Artery** | | **Prox Ao** | **Dist Ao** | **CCA** | **MA** | **EIA** |
|---|---|---|---|---|---|---|
| **Womersley number $\alpha$** | | 35.47 | 15.05 | 6.02 | 3.78 | 8.02 |
| **Maximum shear stress ($\tau_{max}$ in Pa)** | **With gravity** | 2.72 | 2.89 | 2.28 | 1.74 | 1.50 |
| | **Without gravity** | 3.05 | 3.11 | 2.09 | 1.79 | 1.70 |
| **Mean convective acceleration ($\frac{\partial}{\partial x}\left(\int_A u^2 dA\right)$ $10^{-5}$ in $m^3/s^2$)** | **With gravity** | 57.32 | -27.75 | -0.12 | 0.27 | -1.02 |
| | **Without gravity** | 68.67 | -31.55 | 6.79 | 0.06 | -1.32 |
| **Reynolds number** | **With gravity** | 2404 | 870 | 1160 | 98 | 278 |
| | **Without gravity** | 2660 | 749 | 2312 | 68 | 195 |

Prox Ao: proximal aorta; Dist Ao: distal aorta; CCA: common carotid artery; MA: median artery; EIA: external iliac artery

**Effects of gravity**

To assess the importance of considering gravity in the model, the distribution of pressure and flow velocity was plotted all over the arterial tree, both with and without taking gravity into account (Fig. 2). Considerable differences in pressure were most evident in the limb arteries, carotid arteries and the arteries of the head. Because of pressure amplification, systolic pressures were relatively high in the front and hind legs (>160 mmHg) when gravity was neglected while mean pressures were almost unaltered over the whole arterial tree. Considering gravity, systolic pressures in the front legs became even higher, whereas systolic pressures in the arteries of the head became low (<100 mmHg) and mean pressures increased from the head to the legs. Mean flow velocity distribution was similar for both configurations, with higher values for vessels in the splanchnic region and toward the head. A more direct comparison on the features of waveforms is displayed in Fig. 3, with evident discrepancies in flow waveforms of the common carotid artery and in pressure waveforms for the proximal aorta, common carotid artery and median artery.

Fig. 2. Distribution of systolic pressure, mean blood pressure and mean flow velocity over the complete arterial tree, comparing the model including gravity with the model neglecting gravity. Lower and higher values are indicated with colours varying from light to dark tones, respectively.

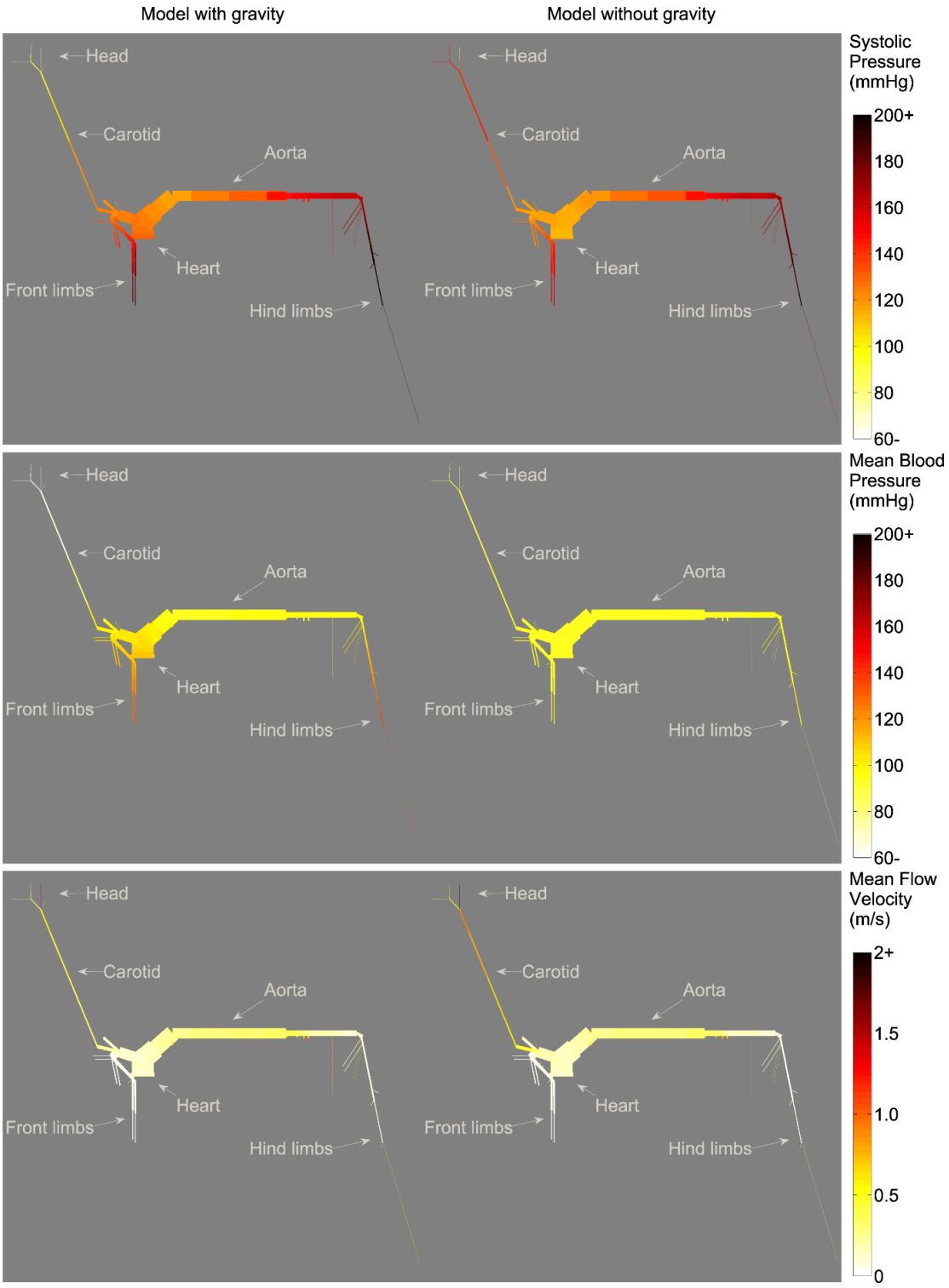

Fig. 3. Model results (with and without gravity) of pressure and flow waveforms at various arterial locations: common carotid artery, proximal aorta, distal aorta, median artery and external iliac artery.

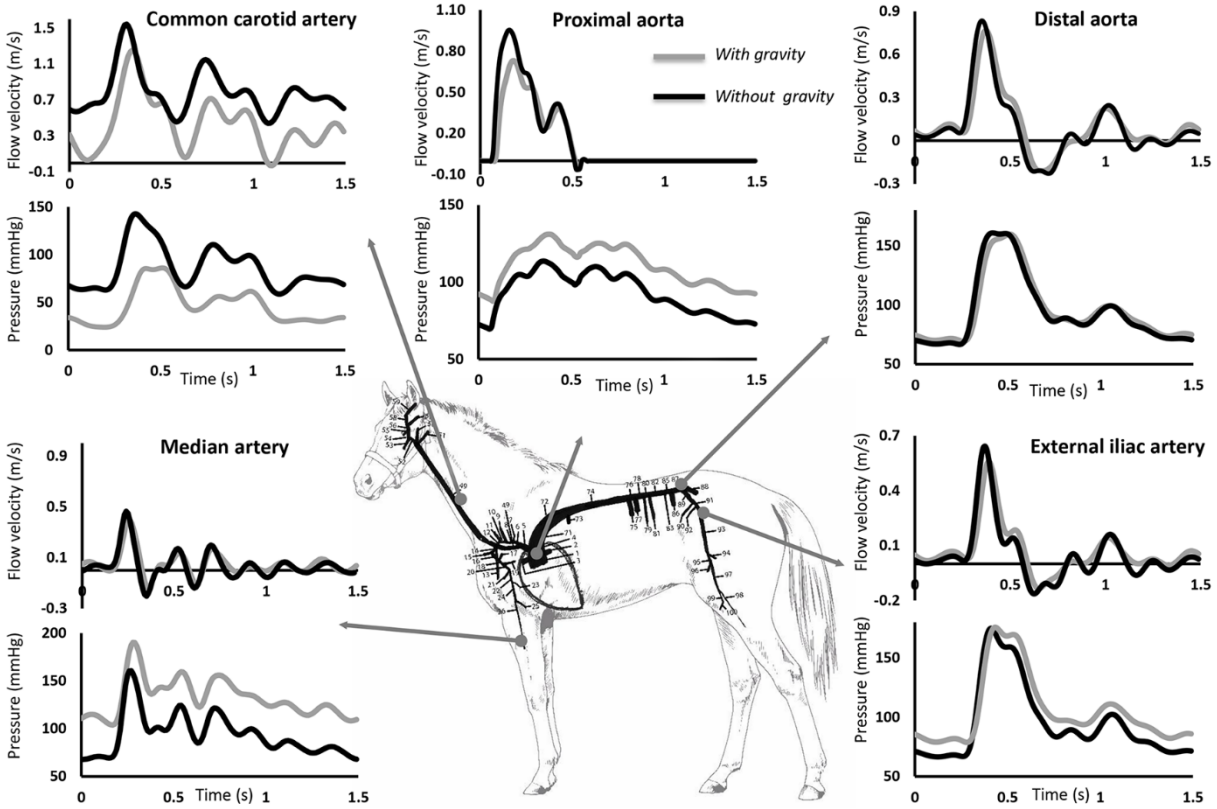


**Model predictions vs. *in vivo* measurements**

Table 4 presents peak blood flow velocities and pressure data estimated from the 1D model in both situations, including and neglecting gravity, along with available *in vivo* measurements. Of note is the higher pulse pressure predicted by both models, in combination with the amplification of pulse pressure towards the periphery. Moreover, both models reveal an amplification in pressure along the aorta. An increase in systolic pressure from the ascending aorta to the iliac artery of ~54 % was found for the model neglecting gravity, while it was reduced to ~34 % when gravitational forces are included.

Fig. 4 displays the modelled blood flow velocity waveforms, both with and without including gravitational forces, for the ascending aorta, common carotid artery and the main limb arteries (median artery and external iliac artery), compared with the measured waveforms in standing horses, derived using pulsed wave Doppler ultrasound. A relatively good similarity in waveform shape and their amplitude was found at all arterial locations, with relative errors for peak flow velocity between *in vivo* data, in the standing awake animal, and simulations without including gravitational forces of 29% for the ascending aorta, 82% for the common carotid artery, 15 %

for the external iliac artery and 40 % for the median artery. When gravitational forces are included, relative errors improved to 2%, 48%, 2% and 23%, respectively.

Fig. 5 compares *in vivo* invasively measured pressure waveforms along the thoracic and abdominal aorta (horse under general anaesthesia in dorsal recumbent position), with modelled pressure waveforms at the same locations (simulations resemble a non-anaesthetised horse), with and without considering gravitational forces. The effect of wave propagation is well captured by the model. Modelled mean, systolic and diastolic arterial pressures in the proximal aorta showed relative errors of 11 %, 3% and 25 %, respectively, compared to the invasively recorded pressure measurements (recorded under general anaesthesia with the horse in dorsal recumbent position). When gravitational forces are included relative errors changed to 6% for mean pressure, 12% for systolic pressure and 5% for diastolic pressure. For the distal aorta relative errors were slightly higher, 21% for mean pressure, 20% for systolic pressure and 40% for diastolic pressure. Including gravity had almost no influence on the derived pressures and thus the relative errors. Aortic PWV determined from the simulation was 5.3 m/s when gravity is neglected, changing to 5.2 m/s considering gravity, whereas the value obtained from *in vivo* data was 5.27 m/s (difference of ~0.6 % when comparing with the model neglecting gravity, and ~-1.3% when comparing with the model including gravity).

Table 4. Pressure and blood flow velocity predictions derived from the model with and without gravity and corresponding in vivo measurements at different locations along the equine arterial tree.

| **Artery** | | **Prox Ao** | **Dist Ao** | **CCA** | **MA** | **EIA** |
|---|---|---|---|---|---|---|
| **Segment number** | | 1 | 87 | 49 | 26 | 93 |
| **Peak flow velocity (m/s)** | *In vivo* | 0.742* | NA | 0.846* | 0.403* | 0.457* |
| | Model without gravity | 0.955 | 0.834 | 1.544 | 0.464 | 0.642 |
| | Relative error (without gravity)° | 29% | NA | 82% | 15% | 40% |
| | Model with gravity | 0.731 | 0.765 | 1.253 | 0.395 | 0.560 |
| | Relative error (with gravity)° | 2% | NA | 48% | 2% | 23% |
| **Mean pressure (mmHg)** | *In vivo* | 104.5** | 119.7** | 116.9* | NA | NA |
| | Model without gravity | 92.82 | 94.63 | 88.61 | 93.54 | 94.77 |
| | Relative error (without gravity)° | 11% | 21% | 24% | NA | NA |
| | Model with gravity | 110.74 | 95.74 | 64.04 | 132.34 | 105.54 |
| | Relative error (with gravity)° | 6% | 20% | 45% | NA | NA |
| **Systolic pressure (mmHg)** | *In vivo* | 116.7** | 134.4** | 134.8* | NA | NA |
| | Model without gravity | 113.62 | 160.76 | 145.08 | 160.68 | 174.93 |
| | Relative error (without gravity)° | 3% | 20% | 8% | NA | NA |
| | Model with gravity | 131.11 | 159.78 | 103.44 | 190.17 | 175.73 |
| | Relative error (with gravity)° | 12% | 19% | 23% | NA | NA |
| **Diastolic pressure (mmHg)** | *In vivo* | 92.2** | 109.8** | 101.9** | NA | NA |
| | Model without gravity | 69.50 | 66.70 | 61.00 | 67.70 | 66.38 |
| | Relative error (without gravity)° | 25% | 40% | 40% | NA | NA |
| | Model with gravity | 87.75 | 69.30 | 44.63 | 103.78 | 78.61 |
| | Relative error (with gravity)° | 5% | 37% | 56% | NA | NA |
| **Pulse Pressure (mmHg)** | *In vivo* | 24.0** | 24.2** | 32.8** | NA | NA |
| | Model without gravity | 44.12 | 94.06 | 84.08 | 92.97 | 108.55 |
| | Relative error (without gravity)° | 83% | 288% | 156% | NA | NA |
| | Model with gravity | 43.36 | 90.47 | 58.81 | 86.39 | 97.13 |
| | Relative error (with gravity)° | 81% | 274% | 79% | NA | NA |

Prox Ao: proximal aorta; Dist Ao: distal aorta; CCA: common carotid artery; MA: median artery; EIA: external iliac artery; NA: not applicable

*Measured in standing, non-sedated horses; mean of all investigated horses

**Measured in the anesthetised horse in dorsal recumbency; values of only 1 horse µ°Relative error was calculated as | (in vivo measured value – Modelled value) | / in vivo measured value.

Fig. 4. Model results (with and without gravity) compared with the averaged flow waveforms of all investigated horses at various arterial locations: common carotid artery, ascending aorta, median artery and external iliac artery.

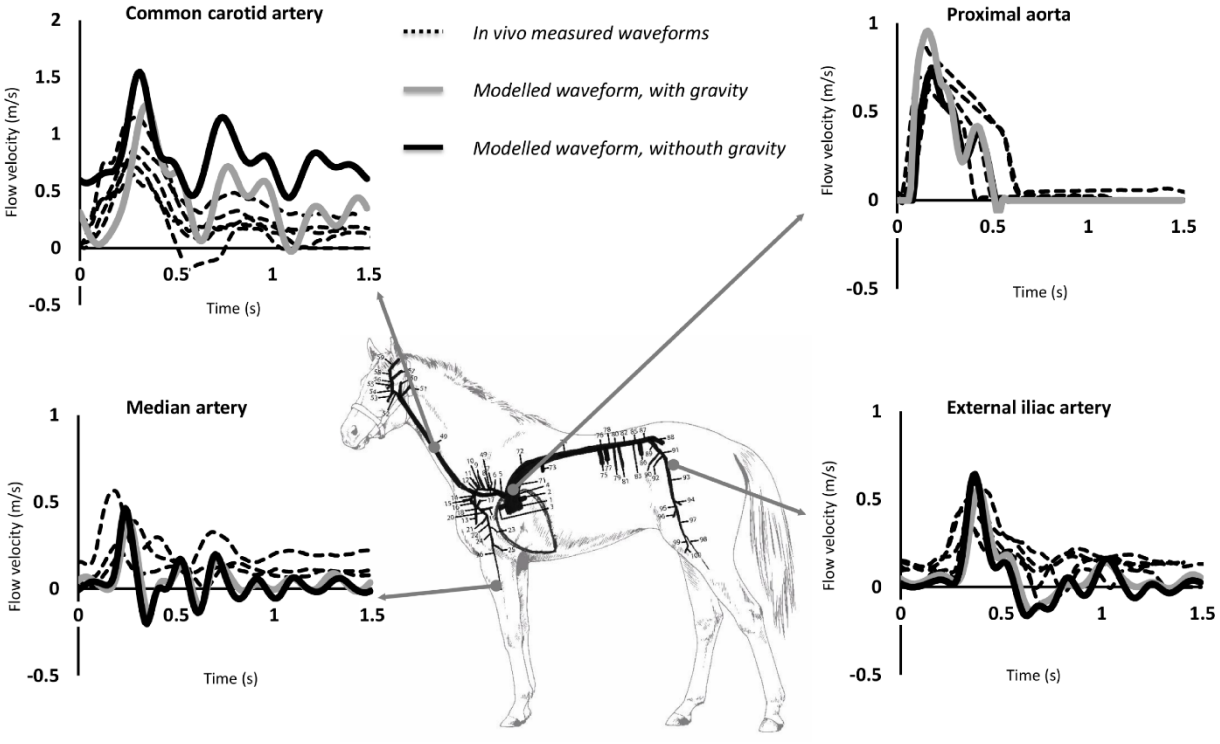


Fig. 5. In vivo pressure waveforms compared with simulations, at seven locations along the aorta. Distances are expressed in centimetres distal from the aortic root.

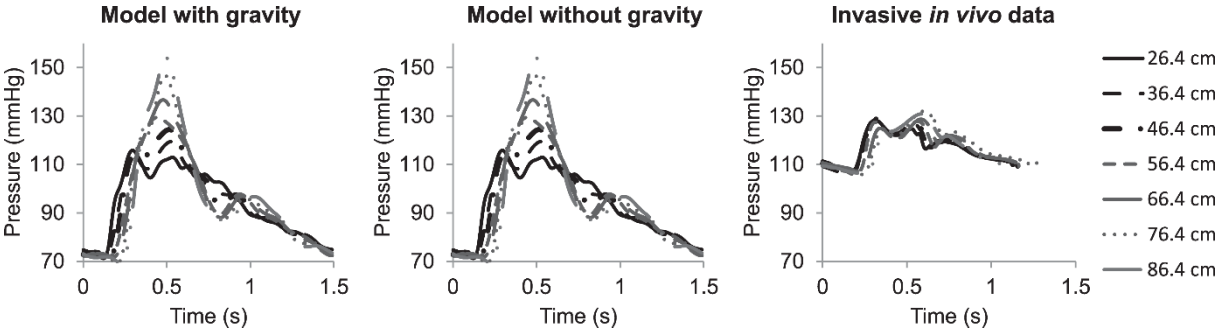


### Wave power analysis

WPA is shown in Fig. 6 for the proximal aorta, common carotid, median and external iliac artery. Models with and without including gravitational forces are compared. In both situations, the proximal aorta shows the three typical peaks: i) a forward compression (FC) wave generated by the systolic ejection, ii) a backward compression (BC) wave as the result of peripheral reflection, and iii) a forward expansion (FE) wave due to the slowing of ventricular contraction. Besides these normal peaks, a small FE can be visible at the different locations in mid-systole. The timing of occurrence of this wave coincides with the drop in flow signals for

the median and iliac arteries. For all the considered locations, wave power was lower when gravitational forces were included. The largest difference between both situations is observed at the carotid artery, where for the configuration without gravity, a mid-systolic FE wave combines with the typical FE from the ventricular contraction, resulting in a wide FE wave; and this in a more drastic drop in the carotid systolic pressure of the model without gravity than the model with gravity (Fig. 3).

Fig. 6. Wave power analysis at several locations of the arterial tree, comparing the model including gravity, with the model neglecting gravity. (FC: forward compression; FE: forward expansion; BC: backward compression; BE: backward expansion; 〖dπ〗_+ and 〖dπ〗_-: forward and backward components of wave power, respectively).

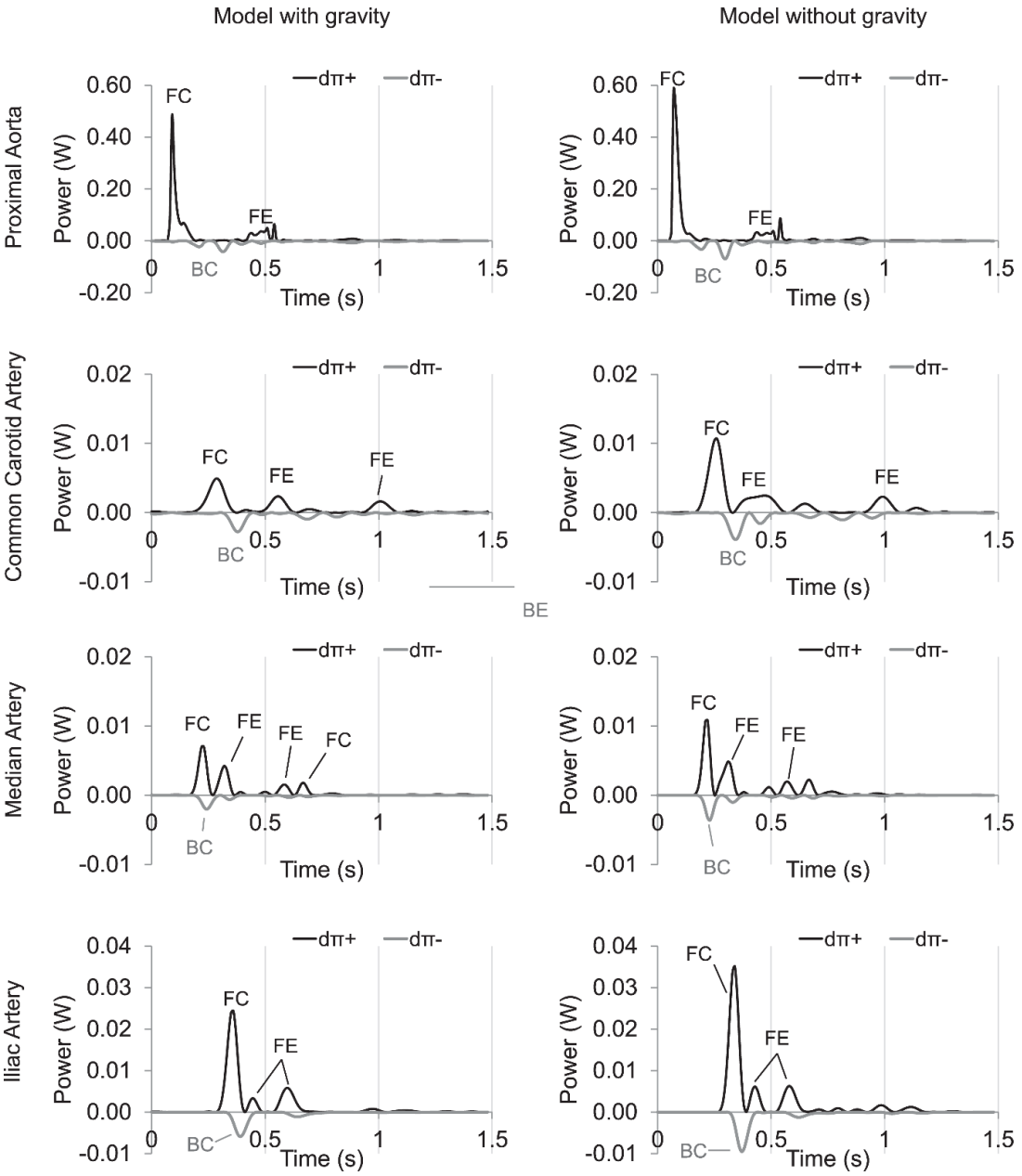

## Discussion

Current literature provides only limited information on arterial hemodynamics in horses. In-depth fundamental research into equine intra-arterial pressures and flows is therefore expected to increase the understanding of aortic and arterial rupture in this species[14-17]. Today, due to technical limitations it is difficult to assess pressure and flow in the centrally located arteries and therefore peripheral measurements are usually extrapolated to the rest of the vascular network. The present study aimed to develop a 1D computer model for the equine arterial circulation comprising all major vessels of the arterial tree. The original 1D human model on which this equine model is based, has been validated and is used as a research tool in many studies[5, 32-35]. Recently, it formed the basis for the development of a 1D model in mice[36]. As aortic branching pattern of horses is completely different compared to humans, arterial segments needed to be redefined. *Ex vivo* measurements (diameter, length and branching angle) of each arterial segment along the equine arterial tree resulted in a unique dataset of the equine arterial anatomy (Table 1). Dimensions (lengths and diameters) of the equine arterial tree are much bigger than those of humans. Moreover, equine heart rate is lower at rest (28-45 bpm in horses and 60-100 bpm in humans) and the heart mass is much larger compared to humans (>1% of the body mass in horses and ~0.5% of the body mass in humans [24]). Both elements imply a much higher cardiac output in horses (~35 L/min compared with ~7 L/min in humans). Of note is the higher Womersley number in the horse, implying a considerably higher impact of inertia on the flow velocity profile, leading to flatter velocity profiles with steeper velocity gradients near the wall than those predicted by Poiseuille flow. As this leads to an improved estimation of viscous friction, it was important to include the Witzig-Womersley correction factor in the momentum equation.

### Importance of gravity

Existing 1D models usually ignore the effects of gravity, because most physiological measurements in humans are performed in supine position, with the heart being at the same level as the rest of the arterial tree. In horses most blood flow velocity and pressure measurements are performed on standing patients, and therefore the effect of gravity was incorporated in the present model. The gradient of pressure in the arterio-venous system, which causes flow, does not fluctuate considerably for the body in the supine position compared with that in the standing position; thus overall flow is similar in both situations. The transmural pressures on the contrary, are strongly different. Given the nonlinear pressure dependency of arterial stiffness, gravity was expected to exert an effect on wave propagation and wave morphology. This was indeed confirmed by our results.

In order to assess the impact of gravitation, two configurations of the model (with and without gravity) were compared (Fig. 2 - 6). Taking into account gravity generally improved predicted peak flows. Relative errors improved from 15-82% for the model without gravity to 2-48% for the model including gravity. While peak flow predictions improved when including gravity into the model, relative error for mean pressure, diastolic pressure and systolic pressure did not improve when gravity was included, with relative errors ranging from 3-40% without gravity and 5-56% with gravity included. Fig. 2 shows that, when gravity is neglected, mean blood pressure is practically the same in all conduit arteries. As was expected, including gravity into the model revealed more variability in mean pressure throughout the arterial tree, with lower values toward the head and higher values toward the limbs. Fig. 5 clearly shows the similarities in pressure waveforms of the descending aorta with and without gravity. These similarities in pressure waveforms are due to the assumption of a horizontal motion of blood (angle=0) in the descending aorta, causing no influence of gravity.

**Wave power analysis**

As changes in arterial pressure waves are associated with alterations in the contour of the arterial flow profiles[37], the pronounced oscillations during flow wave measurements at different arteries in horses probably indicate pressure waves returning from the periphery at multiple reflection sites, starting during systole and continuing during diastole. Wave power analysis performed at several locations revealed important wave reflections mainly during systole. Wave power patterns were most complex for the common carotid artery, which also displayed the biggest delay between the first FC wave and its peripheral reflection (BC wave) coming from the head. This was somewhat expected considering that the wave has to travel forth and back along the carotid artery. The reflection of the first forward peak at the peripheral site in the head was higher when gravity was included in the model (~56 % with gravity vs. ~36 % without gravity). The presence of a mid-systolic forward expansion wave immediately after the first peak generated by the heart ejection (Fig. 6), was responsible for the drop of pressure and flow velocity that resulted in narrow systolic peaks in pressure and flow waveforms of the investigated vessels. In order to understand the origin of this suction wave, we estimated the distance travelled by the wave to the site of re-reflection. By combining the time difference measured from the foot of the waves with the local theoretical PWV in the involved segments, very short distances were derived. These re-reflections might be occurring locally in the network rather than at the heart level, and may be related to a mismatch of junctions in the peripheral branches. Higher efforts to minimize forward wave reflections at these sites are needed.

**Limitations and future work**

In general flow waveform patterns (morphology) are well captured by the model, especially by the one including gravity while discrepancies in amplitude are quite obvious (Fig. 4), this is probably due to several limitations of this model, which will be explained clearly in this section.

Since the present model is based on averaged data, it enables us to predict generic local pressures and flow profiles in all investigated arterial segments. A fully quantitative validation, however, would require a detailed horse-specific approach, tuning of all input parameters that define the model to each specific animal (such as geometry, elastic properties, peripheral resistance, and cardiac parameters) and comparing the outcomes of the model with *in vivo* measurements in that specific animal. Such an approach is technically challenging and almost impossible. Therefore, even if we consider the present model to be representative for the average healthy horse, waveforms should only be compared qualitatively and not quantitatively to individual measurements.

The lack of literature data on equine hemodynamics was the major challenge to develop an equine 1D model. Tuning the model parameters was based on plausible assumptions and scaling factors between human and equine patients. Further fine-tuning of the input parameters to equine physiology will be necessary to obtain a closer match with *in vivo* flow profiles. Branching pattern and dimensions of the arterial tree, both largely defining flow wave patterns, are well integrated in this model. However, branching patterns and arterial dimensions can vary significantly between individual horses. Other important parameters, influencing flow velocity and pressure waves morphology are arterial elasticity and peripheral resistance. Both, arterial elasticity and peripheral resistance largely define diastolic flow[38] and pulse pressure[33], two parameters still showing large differences between measured values and modelled ones, with relative errors for diastolic pressure ranging from 5-60% and for pulse pressure ranging from 81 to 288%. Equine arterial elasticity and peripheral vascular resistance are therefore interesting criteria to further unravel in the future. In addition, in our simulations the compliance distribution and peripheral resistances remain the same for both, the model with gravity and the model without gravity. Neglecting the autoregulation mechanisms that lead to a cardiovascular response to control blood flow and pressure levels during postural changes, can also partially explain the differences found in our simulations and *in vivo* data.

The limited research possibilities in equines form another restrictive factor in the development of the equine 1D model. Due to ethical concerns, invasive aortic blood pressure was only collected in one horse, which is a limitation of this study. Moreover these aortic blood pressures were collected in anaesthetized, dorsally recumbent animals, while ultrasound and pressure

measurements at the carotid artery were performed in non-sedated, standing horses. This complicates comparison between *in vivo* measurements and modelled findings. The present model does not yet account for the changes in physiological parameters due to anaesthesia or dorsal recumbent position. Anaesthesia tends to slow down heart rate, reduce both cardiac output and pulse pressure and likely leads to modulations in resistance of vascular beds and mechanical properties of arteries. Changes in smooth muscular tone modulate distensibility and stiffness. The recumbent position of the horse has a huge effect on intrathoracic and arterial transmural pressure, modulating stiffness and leading to important volume shifts of blood affecting cardiac filling and preload and, via the Frank-Starling mechanism, cardiac contractility. In addition, the model does not include physiological control mechanisms such as the baroreflex that neurologically modulates cardiovascular function via sympathetic/parasympathetic mechanisms. When a body changes from the supine to the standing position, these baroreceptor control mechanisms are activated to limit mean arterial pressure decrease to only a few mmHg. The restoring mechanisms include an increase in cardiac output (mainly an increase in heart rate), as well as an increase in systemic vascular resistance.

Next to this, discrepancies in pressure and flow waveforms between measured and obtained modelled values may be affected by angle correction. In order to obtain standardised images, angle correction was set at 45° when collecting flow velocity profiles in the standing horse. Measurements were optimized for alignment with the flow but this alignment was not always perfect and flow was probably not always captured in the centre of the artery, which implies that captured flow velocities are only an approximation of the true flow profiles.

Discrepancies in pressure and flow waveforms may also be affected by the exclusion of the entire systemic and pulmonary circulation, making the model an open loop system that requires boundary conditions: a cardiac time-varying elastance model at the inlet, and the Windkessel model at the terminal ends. Moreover, the cerebral arterial tree is not included in detail in the equine model, only a simplified representation containing the major vessels that supply the cerebral circulation. A more detailed description of the cerebral arterial tree may provide better predictions of pressure and flow waveforms in the carotid artery and smaller vessels of the head circulation, as has been previously shown for the human and murine models [39]. Furthermore, in the present design, the model used for coronary arteries is simplistic. Last but not least, development of the present model was based on data obtained on a limited number of horses, without accounting for cardiovascular variations due to age or gender.

Nevertheless, despite individual differences in absolute values of flow velocities and arterial pressures, flow wave morphology is well captured by the model as shown in Fig. 4. Fig. 5

evidences the effect of wave propagation along the aorta both in the measured and the modelled pressure profiles. This indicates the added value of the model for studying trends in arterial flow dynamics in horse populations.

In the future this computer model may be useful to predict changes in flow profiles and local pressures under specific circumstances or conditions (age, exercise). During high-intensive exercise, heart rate may rise up to 8 times above the resting rate and total aerobic capacity can reach a 40-fold increase, which is much greater compared to human athletes. By altering input parameters of the horse-specific model, this model might predict local pressures and flow profiles during these extreme circumstances and contribute to the understanding of the relatively high incidence of sudden death during exercise due to arterial rupture[14-17]. As increasing age increases the risk of arterial disorders (arterial rupture during exercise, during parturition or after phenylephrine administration)[14, 18-20], it might also be interesting to use the present model to study the effect of age on arterial hemodynamics. Moreover the development and adjustment of this kind of computer models, could lead to a better understanding of some intensively studied, but poorly understood clinical situations such as exercise induced pulmonary hemorrhage.

## Conclusions

A 1D computer model for the equine arterial circulation has been developed and this provided a unique anatomical dataset for horses. *Ex vivo* anatomical measurements were combined both with literature data and physiological information from ultrasound analysis in order to predict pressure and flow waveforms in the equine arterial tree by means of 1D modelling. The qualitative validation of the model was carried out by comparing the results with average flow velocities and pressures measured *in vivo* in horses. Despite its generic character and limitations, outcomes from the model showed plausible predictions of pressure and flow waveforms throughout the considered arterial tree. Simulated flow waveforms reproduce important features observed in ultrasound Doppler images, especially the oscillating pattern (most pronounced at the external iliac artery, median artery and common carotid artery). Adapting the model by taking into account gravity further improved predicted waveforms. Thanks to wave power analysis, the contours of the arterial flow profiles could be explained. Despite the shortcomings of *in vivo* measured pressures (aortic pressures measured under general anaesthesia with the horse in dorsal recumbent position), modelled pressure data seem in line with invasive measurements. We believe that the present model may be useful, not only to explain flow wave patterns in horses, but also to predict changes in flow profiles and local pressures as a result of strenuous exercise or altered arterial wall properties related to age, breed or gender.

## Acknowledgements

None

## References

1. Mynard JP, Smolich JJ. One-Dimensional Haemodynamic Modeling and Wave Dynamics in the Entire Adult Circulation. Ann Biomed Eng. 2015;43(6):1443-60. doi: 10.1007/s10439-015-1313-8. PubMed PMID: WOS:000355924000016.
2. Bessems D, Rutten M, Van De Vosse F. A wave propagation model of blood flow in large vessels using an approximate velocity profile function. J Fluid Mech. 2007;580:145-68. doi: 10.1017/S0022112007005344. PubMed PMID: WOS:000247055900006.
3. Stergiopulos N, Young DF, Rogge TR. Computer-Simulation of Arterial Flow with Applications to Arterial and Aortic Stenoses. J Biomech. 1992;25(12):1477-88. doi: Doi 10.1016/0021-9290(92)90060-E. PubMed PMID: WOS:A1992JZ89500010.
4. Wemple RR, Mockros LF. Pressure and Flow in Systemic Arterial System. J Biomech. 1972;15(6):629-&. PubMed PMID: WOS:A1972N941700009.
5. Vardoulis O, Coppens E, Martin B, Reymond P, Tozzi P, Stergiopulos N. Impact of Aortic Grafts on Arterial Pressure: A Computational Fluid Dynamics Study. Eur J Vasc Endovasc. 2011;42(5):704-10. doi: 10.1016/j.ejvs.2011.08.006. PubMed PMID: WOS:000297238900026.
6. Avolio AP. Multi-Branched Model of the Human Arterial System. Med Biol Eng Comput. 1980;18(6):709-18. doi: Doi 10.1007/Bf02441895. PubMed PMID: WOS:A1980KS09500003.
7. Sherwin SJ, Franke V, Peiro J, Parker K. One-dimensional modelling of a vascular network in space-time variables. J Eng Math. 2003;47(3-4):217-50. doi: DOI 10.1023/B:ENGI.0000007979.32871.e2. PubMed PMID: WOS:000187200200004.
8. Epstein S, Willemet M, Chowienczyk PJ, Alastruey J. Reducing the number of parameters in 1D arterial blood flow modeling: less is more for patient-specific simulations. Am J Physiol-Heart C. 2015;309(1):H222-H34. doi: 10.1152/ajpheart.00857.2014. PubMed PMID: WOS:000357502700022.
9. Dobroserdova T, Simakov S, Gamilov T, Pryamonosov R, Sakharova E. Patient-specific blood flow modelling for medical applications. Matec Web Conf. 2016;76. doi: UNSP 0500110.1051/matecconf/20167605001. PubMed PMID: WOS:000392332200127.
10. Gamilov T, Ivanov Y, Kopylov P, Simakov S, Vassilevski Y. Patient Specific Haemodynamic Modeling after Occlusion Treatment in Leg. Math Model Nat Pheno. 2014;9(6):85-97. doi: 10.1051/mmnp/20149607. PubMed PMID: WOS:000346401500007.
11. Willemet M, Lacroix V, Marchandise E. Validation of a 1D patient-specific model of the arterial hemodynamics in bypassed lower-limbs: simulations against in vivo measurements. Med Eng Phys. 2013;35(11):1573-83. doi: 10.1016/j.medengphy.2013.04.012. PubMed PMID: 23701843.
12. Ploeg M, Saey V, van Loon G, Delesalle C. Thoracic aortic rupture in horses. Equine Vet J. 2017;49(3):269-74. doi: 10.1111/evj.12641. PubMed PMID: 27783422.
13. Ploeg M, Saey V, de Bruijn CM, Grone A, Chiers K, van Loon G, et al. Aortic rupture and aorto-pulmonary fistulation in the Friesian horse: characterisation of the clinical and gross post mortem findings in 24 cases. Equine Vet J. 2013;45(1):101-6. doi: 10.1111/j.2042-3306.2012.00580.x. PubMed PMID: 22607232.
14. Lyle CH, Blissitt KJ, Kennedy RN, Mc Gorum BC, Newton JR, Parkin TD, et al. Risk factors for race-associated sudden death in Thoroughbred racehorses in the UK (2000-2007). Equine Vet J. 2012;44(4):459-65. doi: 10.1111/j.2042-3306.2011.00496.x. PubMed PMID: 22128788.
15. Lyle CH, Uzal FA, McGorum BC, Aida H, Blissitt KJ, Case JT, et al. Sudden death in racing Thoroughbred horses: An international multicentre study of post mortem findings. Equine Vet J. 2011;43(3):324-31. doi: 10.1111/j.2042-3306.2010.00164.x. PubMed PMID: WOS:000289523600012.

16. Gelberg HB, Zachary JF, Everitt JI, Jensen RC, Smetzer DL. Sudden-Death in Training and Racing Thoroughbred Horses. Journal of the American Veterinary Medical Association. 1985;187(12):1354-6. PubMed PMID: WOS:A1985AVW9900006.
17. Platt H. Sudden and Unexpected Deaths in Horses - a Review of 69 Cases. Brit Vet J. 1982;138(5):417-29. PubMed PMID: WOS:A1982PJ83500006.
18. Ueno T, Nambo Y, Tajima Y, Umemura T. Pathology of lethal peripartum broad ligament haematoma in 31 Thoroughbred mares. Equine Vet J. 2010;42(6):529-33. doi: 10.1111/j.2042-3306.2010.00090.x. PubMed PMID: 20716193.
19. Williams NM, Bryant UK. Periparturient Arterial Rupture in Mares: A Postmortem Study. J Equine Vet Sci. 2012;32(5):281-4. doi: 10.1016/j.jevs.2011.11.002. PubMed PMID: WOS:000303966300005.
20. Frederick J, Giguere S, Butterworth K, Pellegrini-Masini A, Casas-Dolz R, Turpin MM. Severe phenylephrine-associated hemorrhage in five aged horses. J Am Vet Med Assoc. 2010;237(7):830-4. doi: 10.2460/javma.237.7.830. PubMed PMID: 20919849.
21. Barone R. Tome 5 - Angiologie In: Vigot E, editor. Anatomie comparée des mammifères domestiques 2011.
22. Reymond P, Merenda F, Perren F, Rüfenacht D, Stergiopulos N. Validation of a one-dimensional model of the systemic arterial tree. Am J Physiol Heart Circ Physiol 2009;297(1):H208–H22. doi: 10.1152/ajpheart.00037.2009.
23. Boegli J, Schwarzwald CC, Mitchell KJ. Diagnostic value of noninvasive pulse pressure measurements in Warmblood horses with aortic regurgitation. J Vet Intern Med. 2019;33(3):1446-55. doi: 10.1111/jvim.15494. PubMed PMID: 30938891; PubMed Central PMCID: PMCPMC6524107.
24. Poole DC, Erickson HH. Highly athletic terrestrial mammals: Horses and Dogs. Comprehensive Physiology. 2011;1:1-37. doi: 10.1002/cphy.c091001.
25. Sagawa K. Cardiac contraction and the pressure-volume relationship. Oxford, UK: Oxford University Press; 1988. 15 p.
26. Senzaki H, Chen C-H, Kass DA. Single-Beat Estimation of End-Systolic Pressure-Volume Relation in Humans. A New Method With the Potential for Noninvasive Application. Circulation. 1996;94(10): 2497-506. doi: 10.1161/01.CIR.94.10.2497.
27. Brown CM, Holmes JR. Haemodynamics in the horse: 2. Intracardiac, pulmonary arterial and aortic pressures. Equine Vet J. 1978;10(4):207-15. PubMed PMID: 738261.
28. Reed SM, Bayly WM, Sellon DC. Equine Internal Medicine-E-Book: Elsevier Health Sciences; 2017. 418 p.
29. Brown CM, Holmes JR. Haemodynamics in the horse: 3. Duration of the phases of the cardiac cycle. Equine Vet J. 1978;10(4):216-23. PubMed PMID: 738262.
30. Mynard JP, Smolich JJ. Novel wave power analysis linking pressure-flow waves, wave potential, and the forward and backward components of hydraulic power. Am J Physiol Heart Circ Physiol. 2016;310(8):H1026-38. doi: 10.1152/ajpheart.00954.2015. PubMed PMID: 26873972.
31. Parker KH, Jones CJ. Forward and backward running waves in the arteries: analysis using the method of characteristics. J Biomech Eng. 1990;112(3):322-6. PubMed PMID: 2214715.
32. Swillens A, Lanoye L, De Backer J, Stergiopulos N, Verdonck PR, Vermassen F, et al. Effect of an abdominal aortic aneurysm on wave reflection in the aorta. IEEE Trans Biomed Eng. 2008;55(5):1602-11. doi: 10.1109/TBME.2007.913994. PubMed PMID: 18440906.
33. Reymond P, Westerhof N, Stergiopulos N. Systolic hypertension mechanisms: effect of global and local proximal aorta stiffening on pulse pressure. Ann Biomed Eng. 2012;40(3):742-9. doi: 10.1007/s10439-011-0443-x. PubMed PMID: 22016326.
34. Obeid H, Soulat G, Mousseaux E, Laurent S, Stergiopulos N, Boutouyrie P, et al. Numerical assessment and comparison of pulse wave velocity methods aiming at measuring aortic stiffness. Physiol Meas. 2017;38(11):1953-67. doi: 10.1088/1361-6579/aa905a. PubMed PMID: 28968226.
35. Campos Arias D, Londono F, Rodriguez Moliner T, Georgakopoulos D, Stergiopulos N, Segers P. Hemodynamic Impact of the C-Pulse Cardiac Support Device: A One-Dimensional

Arterial Model Study. Artif Organs. 2017;41(10):E141-E54. doi: 10.1111/aor.12922. PubMed PMID: 28548693.
36. Aslanidou L, Trachet B, Reymond P, Fraga-Silva RA, Segers P, Stergiopulos N. A 1D model of the arterial circulation in mice. ALTEX. 2016;33(1):13-28. doi: 10.14573/altex.1507071. PubMed PMID: 26555250.
37. O'Rourke MF. Pressure and flow waves in systemic arteries and the anatomical design of the arterial system. J Appl Physiol. 1967;23(2):139-49. doi: 10.1152/jappl.1967.23.2.139. PubMed PMID: 5340142.
38. Belz GG. Elastic properties and Windkessel function of the human aorta. Cardiovasc Drugs Ther. 1995;9(1):73-83. PubMed PMID: 7786838.
39. Reymond P, Merenda F, Perren F, Rüfenacht D, Stergiopulos N.Validation of a one-dimensional model of the systemic arterial tree. Am J Physiol Heart Circ Physiol. 2009;297(1):H208-22. doi: 10.1152/ajpheart.00037.2009 9, 33].PubMed PMID 19429832

## Supporting information

S1 Table. Terminal impedance data.

| Arterial Segment Number | Terminal resistance mmHg*s/ml | Terminal compliance $10^{-2}$ ml/mmHg |
|---|---|---|
| **2** | 7.22 | 14.36 |
| **3** | 7.22 | 14.36 |
| **7** | 32.80 | 7.97 |
| **9** | 29.82 | 0.05 |
| **11** | 10.98 | 7.53 |
| **13** | 32.80 | 11.01 |
| **15** | 55.44 | 1.34 |
| **17** | 55.44 | 0.61 |
| **19** | 55.44 | 25.80 |
| **21** | 55.44 | 0.33 |
| **23** | 55.44 | 6.34 |
| **25** | 67.61 | 1.31 |
| **26** | 64.46 | 1.65 |
| **28** | 32.80 | 3.62 |
| **30** | 29.82 | 0.05 |
| **32** | 10.98 | 3.98 |
| **35** | 55.44 | 11.00 |
| **36** | 55.44 | 3.78 |
| **38** | 55.44 | 1.46 |
| **40** | 55.44 | 25.80 |
| **42** | 55.44 | 0.33 |
| **44** | 61.60 | 7.55 |
| **46** | 67.61 | 1.31 |
| **47** | 64.46 | 1.65 |
| **50** | 1.10 | 0.48 |
| **51** | 8.55 | 0.71 |
| **53** | 8.55 | 1.50 |
| **55** | 8.62 | 0.04 |
| **57** | 8.92 | 0.10 |
| **58b** | 9.00 | 1.19 |
| **59** | 9.08 | 0.20 |

| | | |
|---|---|---|
| **61** | 1.10 | 0.48 |
| **62** | 8.55 | 0.71 |
| **64** | 8.55 | 1.50 |
| **66** | 8.62 | 0.04 |
| **68** | 8.92 | 0.10 |
| **70** | 9.08 | 0.20 |
| **73** | 3.55 | 2.78 |
| **75** | 1.96 | 7.34 |
| **77** | 3.03 | 4.04 |
| **79** | 1.80 | 3.62 |
| **81** | 1.80 | 3.63 |
| **83** | 22.55 | 0.24 |
| **84** | 22.55 | 0.24 |
| **86** | 3.51 | 1.22 |
| **88** | 5.52 | 21.68 |
| **90** | 47.31 | 0.66 |
| **92** | 23.13 | 0.12 |
| **94** | 47.31 | 2.97 |
| **96** | 47.31 | 0.65 |
| **79b** | 9.00 | 1.20 |
| **98** | 47.31 | 0.07 |
| **99b** | 57.70 | 6.21 |
| **100** | 57.70 | 0.47 |
| **101** | 5.52 | 21.68 |
| **103** | 23.13 | 0.12 |
| **105** | 55.02 | 0.70 |
| **107** | 47.31 | 2.97 |
| **109** | 47.31 | 0.65 |
| **111** | 47.31 | 0.07 |
| **112b** | 57.70 | 6.21 |
| **113** | 52.57 | 0.47 |

# CHAPTER 4:

# AORTIC, COMMON CAROTID AND EXTERNAL ILIAC ARTERY ARTERIAL WALL STIFFNESS PARAMETERS IN HORSES: INTER-DAY AND INTER-OBSERVER AND INTRA-OBSERVER MEASUREMENT VARIABILITY

# Aortic, common carotid and external iliac artery arterial wall stiffness parameters in horses: inter-day and inter-observer and intra-observer measurement variability

Lisse Vera[1], Dominique De Clercq[1], Ellen Paulussen[1], Glenn van Steenkiste[1], Annelies Decloedt[1], Koen Chiers[2] and Gunther van Loon[1]

[1] Equine Cardioteam Ghent University, Department of Large Animal Internal Medicine, Faculty of Veterinary Medicine, Ghent University

[2] Department of Pathology, Bacteriology and Poultry Diseases, Faculty of Veterinary Medicine, Ghent University

**Ethical animal research**

The study was approved by the ethical committee of the Faculty of Veterinary Medicine and Bioscience Engineering (EC 2016/104).

**Acknowledgements**

None

Adapted from:

**Lisse Vera**, Dominique De Clercq, Ellen Paulussen, Glenn Van Steenkiste, Annelies Decloedt, Koen Chiers, and Gunther van Loon. 2020. “Aortic, Common Carotid and External Iliac Artery Arterial Wall Stiffness Parameters in Horses : Inter-Day and Inter-Observer and Intra-Observer Measurement Variability.” *EQUINE VETERINARY JOURNAL*. 52(3):471-47

**Abstract**

**Background:** In human medicine, local and regional arterial wall stiffness (AWS) parameters are routinely used to assess vascular health. In horses, information regarding reproducibility of ultrasonographically derived AWS parameters are lacking. **Objectives**: To evaluate the inter-day and inter-observer and intra-observer measurement variability of both local and regional AWS parameters in horses. **Study Design:** Prospective study. **Methods:** In ten healthy, adult Warmblood horses, B-, M-mode and pulsed wave Doppler ultrasound images were collected on two different days from aorta, cranial and caudal common carotid artery and external iliac artery. Heart rate and non-invasive blood pressure were recorded simultaneously. From blinded data, diastolic and systolic vessel lumen areas and diameters were measured from B/M-mode images and the velocity of the pressure wave was determined by pulsed wave Doppler. From each horse, one examination was measured again by the same observer and by a second, independent observer. Afterwards local and regional AWS parameters were calculated and inter-day and inter-observer and intra-observer measurement coefficients of variation (CV) were assessed. **Results:** Low CV were found for both arterial diameter and lumen area measurements. Moderate to high CV were found for local AWS parameters, while regional AWS parameters showed low CV. **Main Limitations**: The number of horses investigated was too low to obtain reference values. The inter-operator variability was not evaluated. **Conclusions:** Our results show good reproducibility of aortic, carotid and external iliac artery diameter and area measurements using both B- and M-mode ultrasonography. Nevertheless, the variability of the derived local AWS parameters was relatively high. Therefore local AWS parameters might be less suitable for follow-up studies, although they might be useful for population studies. On the other hand, regional AWS parameters showed low CV, making them valuable for both follow-up and population studies.

## Introduction

The arterial wall stiffness (AWS) is a measure of the ability of the arterial wall to expand and recoil during the cardiac cycle. In human medicine measurements of AWS are used for diagnosis and progression of vascular changes. Stiffening of the arterial wall is an important independent predictor of cardiovascular mortality in humans[1] and is known to be associated with age[2], gender[3], race[4] and training level[5]. In horses, little is known about the AWS. Nevertheless, measurement of AWS might be important in horses as an independent predictor of cardiovascular risk, especially when arterial rupture is considered. Measurement of AWS might contribute to the understanding of the underling conditions leading to arterial rupture in horses, a poorly understood but mostly fatal condition, not only affecting animal-welfare but

also rider-safety[6]. Arterial rupture in horses is known to be associated with foaling[7], intensive exercise[8] and the administration of α1-agonists for treatment of left dorsal displacement of the large colon (nephrosplenic entrapment)[9], especially in older animals[8]. Males (gelded or entire) more often present exercise-related arterial rupture compared to females[6; 10] and Friesian horses are predisposed to aortic rupture and aortopulmonary fistulation[11]. These clinical findings suggest that, age, gender and breed might affect AWS, and as such play a role in the aetiology of arterial rupture.

In human medicine, the AWS can be assessed both regionally (over a certain length of the arterial tree) and locally (at one specific arterial location). The pulse wave velocity (PWV), indicating how fast a pressure wave travels over a certain length of the arterial tree, is considered as the gold standard method to assess regional aortic AWS[12; 13]. Various non-invasive techniques, including tonometry and pulsed wave Doppler ultrasound, enable to capture the pulse wave[13]. A stiffer artery will result in a higher PWV. To estimate local AWS of large, elastic arteries, ultrasound measurements of lumen area or diameter and derived AWS parameters in relation to distending pressures can be used[13]. A larger lumen area and diameter change throughout the cardiac cycle, indicates a more compliant artery. In horses, information regarding reproducibility of ultrasonographically derived arterial diameter or area measurements and the derived AWS parameters is limited. Therefore this study describes the reliability of both regional and local AWS parameters of the aorta and common carotid artery and local AWS parameters of the external iliac artery.

## Materials and methods

### Horses

Cardiovascular ultrasound was performed in 10 Warmblood horses, owned by the Faculty of Veterinary Medicine, Ghent Univeristy. The horses were aged (mean±SD) 13±5 years, weighing 590±42 kg with a height at the withers of 164±3 cm. Five horses were mares, the other 5 geldings. All horses were evaluated with auscultation and echocardiographic and electrocardiographic examination. None of the horses showed arrhythmias on the electrocardiogram during a 15 min recording at rest, no systolic or diastolic murmur was found and no more than a trace valvular regurgitation was present on ultrasound. Five necropsied Warmblood horses were used to determine real arterial lengths between investigated arterial locations. These animals did not show cardiovascular disease and were euthanized for reasons not related to this study.

### Blood pressure

The systolic (SAP), diastolic (DAP) and mean (MAP) arterial blood pressure were measured non-invasively, simultaneously with the ultrasound images, using an oscillometric device (Cardell Veterinary Monitor, 9401[a]), with a cuff placed over the coccygeal artery around the base of the tail. To correct readings to the level of the heart base, a correction factor of 0.77 mmHg was added for every cm in difference between the right atrium (estimated at the height of the shoulder) and the cuff[14]. The mean of 5 consecutive, consistent measurements was taken. In each horse tail circumference was measured to assure a cuff width-to-tail circumference ratio between 0.4 and 0.6[14].

### Ultrasound

Ultrasound imaging was performed (Vivid IQ[b]) on the standing, non-sedated horse with simultaneous electrocardiogram recording. Images were only collected with a heart rate (HR) below 50 beats per minute. All images were stored for off-line analysis (Echopac software version 203[b]).

#### *B- and M-mode*

To calculate local AWS parameters 4 arterial locations were examined: the aorta from a right parasternal position, the right caudal common carotid artery (15 cm cranial to the thoracic inlet), the cranial common carotid artery (45 cm cranial to the thoracic inlet) and the right external iliac artery from the inguinal region just proximal to the side branch ‘arteria profunda femoris’. For the aorta a right parasternal left ventricular outflow tract view was collected, using a 1.5-4.6 MHz phased array probe (M5Sc-RS[b]). For the cranial and caudal carotid artery, cross-sectional B- and M-mode images were collected using a 3.5-10 MHz linear transducer (9L-RS[b]). For the external iliac artery cross-sectional B-mode images and longitudinal M-mode images, both using a 2.7-8 MHz phased array probe (6S-RS[b]) were collected.

#### *Pulsed wave Doppler*

Pulsed wave Doppler was performed to capture the pulse wave non-invasively. A 2.7-8 MHz phased array probe (6S-RS)[b] was used for the carotid and external iliac artery and a 1.5–4.6 MHz phased array probe (M5Sc-R)[b] for the aorta (left parasternal view). Angle correction was set at 45° for every image at all locations. Using this fixed angle correction, probe orientation was optimised to align with the flow direction.

### Local arterial wall stiffness

All diameters were measured from inner edge to inner edge. For the aorta, diameters were measured at the sinotubular junction. Means were calculated from 3 consecutive beats. For

the cranial and caudal common carotid artery, diameters were measured from cross-sectional M-mode images, while areas were measured from cross-sectional B-mode images. For the external iliac artery, diameters were measured from longitudinal M-mode images and areas from cross-sectional B-mode images. For the cranial and caudal carotid and external iliac artery, means were calculated from 9 measurements, performed on 3 loops of 3 consecutive heart cycles each. For all arteries, diastolic measurements were performed on the R peak of the simultaneously recorded electrocardiogram (base-apex configuration) and systolic measurements were performed at maximal dilation. Measurements were never performed on a heart cycle following a second degree atrioventricular block.

***Arterial diameter and lumen area change***

The arterial diameter ($\Delta D$) or lumen area change ($\Delta A$) represent the change in diameter (D) or lumen area (A) between systole (s) and diastole (d)[13].

$\Delta D = Ds - Dd$

$\Delta A = As - Ad$

***Arterial diameter and lumen area strain***

The arterial diameter ($S_D$) or lumen area strain ($S_A$) represent the relative change in diameter (D) or lumen area (A) during the cardiac cycle[15].

$S_D\ (\%) = \Delta D/Dd$

$S_A\ (\%) = \Delta A/Ad$

***Arterial distensibility***

The arterial distensibility coefficient represents the relative diameter ($DC_D$) or area change ($DC_A$) for a pressure increment[16].

$DC_D = (\Delta D/Dd)/\Delta P$

$DC_A = (\Delta A/Ad)/\Delta P$

$\Delta P$ is the pulse pressure defined as SAP-DAP.

***Arterial compliance***

The arterial compliance coefficient represents the absolute diameter ($CC_D$) or area change ($CC_A$) for a pressure increment[13].

$CC_D = \Delta D/\Delta P$

$CC_A = \Delta A/\Delta P$

### *Stiffness index*

The stiffness index represents the ratio of the natural logarithm (systolic/diastolic pressure) to the relative change in diameter[17].

SI=ln(SAP/DAP)/(∆D/Dd)

### Regional arterial wall stiffness

Regional AWS was assessed using PWV. The PWV represents how fast the pressure wave travels through the arteries and is calculated as the difference in distance between two measurement points (∆Dist) divided by the difference in time delay (∆t)[12; 13]. For the latter, at every location (aorta, cranial and caudal common carotid artery and external iliac artery), the time delay (ms) between the R wave of the synchronised electrocardiogram and the onset (foot) of the waveform, captured using pulsed wave Doppler was measured and a mean value was calculated from 3 times 3 consecutive beats. The difference in time delay (∆t), was calculated by subtracting the mean time delay at the location the closest to the heart (shortest time delay) from the mean time delay at the location the furthest away from the heart (longest time delay).

#### *Caudal carotid to cranial carotid artery pulse wave velocity ($PWV_{c-c}$)*

$PWV_{c-c}$ represents how fast the pressure wave travels between the caudal common carotid artery and the cranial common carotid artery and describes the regional stiffness of the common carotid artery.

$PWV_{c-c}(m/s)=\Delta Dist_{c-c}(m)/\Delta t_{c-c}(s)$, wherein $\Delta Dist_{c-c}(m)$ represents the difference in distance relative to the aortic root between the caudal and cranial common carotid artery. A fixed distance between both measuring places of 0.3 m was taken.

#### *Aorta to external iliac artery pulse wave velocity ($PWV_{a-e}$)*

$PWV_{a-e}$ represents how fast the pressure wave travels from the aortic valve to the external iliac artery and describes the regional stiffness of the aorta.

$PWV_{a-e}(m/s)=\Delta Dist_{a-e}(m)/\Delta t_{a-e}(s)$, wherein $\Delta Dist_{a-e}$ represents the distance between the aortic valve and the external iliac artery. This distance was estimated based on measurements performed on 5 other horses (mean ±SD bodyweight: 633±112kg, height at the withers: 166±10cm) at necropsy. The distance between the aortic valve and the external iliac artery was measured and related to the length of the horse (measured from the most cranial point of the shoulder to the tuber ischiadicum). This distance was approximately 0.62 (range 0.55-0.66) times the length of the horse. Therefore, $\Delta Dist_{a-e}(m)$=length of the horse(m) x 0.62.

***Carotid to external iliac artery pulse wave velocity ($PWV_{c-e}$)***

$PWV_{c-e}$ represents how fast the pressure wave travels between the caudal common carotid artery and the external iliac artery.

$PWV_{c-e}(m/s)=\Delta Dist_{c-e}(m)/\Delta t_{c-e}(s)$, wherein $\Delta Dist_{c-e}$ represents the difference in distance relative to the aortic root between the caudal carotid and external iliac artery. To estimate this distance, in the same 5 horses on necropsy the distance between the aortic valve and the caudal carotid artery was measured and was found to be on avarage 0.40 m (range 0.37-0.52 m). Because the pressure wave travels from the aortic valve at the same time cranially (towards the caudal carotid artery) and caudally (towards the external iliac artery), this distance was subtracted from the estimated distance between the aorta and external iliac artery. Therefore $\Delta Dist_{c-e}(m)$=length of the horse (m) x 0.62 - 0.40 m.

**Statistics, assessment of variability**

A paired-samples t-test was performed to compare SAP, DAP, MAP, ΔP and HR between day one and day 2. Inter-day variability was obtained by comparing measurements performed by observer 1 (LV) from images collected on day 1 and day 2, in a one way ANOVA with horse as a unit of repeated measure. The coefficients of variation (CV) were calculated by dividing the square root of the mean square error by the grand mean, multiplied by 100 (SPSS statistics 25[c])[18; 19]. Similarly, inter-observer measurement variability was obtained by comparing measurements from images collected on day 1 performed by observer 1 (LV) with measurements performed by observer 2 (EP) on the same images. Next intra-observer measurement variability was obtained comparing 2 repeated independent measurements performed by observer 1 (LV) on the images collected on day 1. A CV lower than 15% was considered as low, 15-25% as moderate and higher than 25% as high[20]. At any time, observers were blinded to horse, day and previous results.

## Results

All horses tolerated the procedure well. Pulse pressure, SAP, DAP and MAP, collected simultaneously with the ultrasound images did not differ significantly between day 1 and day 2, while HR did differ significantly between both days. Detailed information can be found in Table 1.

Table 1. Systolic, diastolic, mean arterial blood pressure, pulse pressure and heart rate on day 1 and day 2. Values are calculated over 5 cardiac cycles.

| | Day 1 | | Day 2 | | |
|---|---|---|---|---|---|
| | Mean | SD | Mean | SD | p-value |
| SAP (mmHg) | 129 | 17 | 130 | 14 | 0.773 |
| DAP (mmHg) | 88 | 11 | 85 | 9 | 0.483 |
| MAP (mmHg) | 103 | 13 | 102 | 10 | 0.894 |
| ΔP (mmHg) | 40 | 9 | 45 | 10 | 0.183 |
| HR (bpm) | 38 | 7 | 34 | 5 | 0.048 |

SAP= systolic arterial pressure; DAP= diastolic arterial pressure; MAP=mean arterial pressure; ∆P= pulse pressure; HR= heart rate

All diameter and area measurements, together with their derived local and regional AWS parameters and their CV can be found in Table 2. CV for arterial diameter and lumen area measurements were low to moderate (1-16%), with the lowest CV for diameter measurements (1-7%). Inter-day and inter-observer and intra-observer measurement CV for local AWS parameters ranged from low to high (10-68%) for all investigated arteries, with the lowest values for intra-observer variability (10-63%) and the highest values for inter-day variability (22-68%), especially for area measurements. AWS parameters derived from lumen area measurements showed higher CV (21-68%) compared to the ones derived from diameter measurements (2-69%), with the highest values for the external iliac artery. The $PWV_{c\text{-}c}$, describing the regional stiffness of the common carotid artery, showed moderate to high CV (20-25%), while both the $PWV_{a\text{-}e}$ and the $PWV_{c\text{-}e}$, describing the regional stiffness of the aorta showed low CV (3-15%).

Table 2. Systolic and diastolic arterial diameter and area and derived local and regional AWS parameters of the aorta, cranial common carotid artery, caudal common carotid artery and external iliac artery, together with their coefficients of variation.

| | | Mean† | SD† | Inter-Observer measurement CV (%) | Inter-day CV (%) | Intra-Observer measurement CV (%) |
|---|---|---|---|---|---|---|
| Arterial diameter measurements | | | | | | |
| Aorta | Dd Ao (mm) | 62 | 5 | 2 | 6 | 2 |
| | Ds Ao (mm) | 67 | 5 | 4 | 7 | 2 |
| Cranial carotid artery | Dd CrCCA (mm) | 10.3 | 1.1 | 4 | 6 | 1 |
| | Ds CrCCA (mm) | 10.8 | 1.1 | 4 | 6 | 1 |
| Caudal carotid artery | Dd CaCCA (mm) | 11.7 | 1.1 | 1 | 5 | 2 |
| | Ds CaCCA (mm) | 12.5 | 1.0 | 2 | 6 | 1 |
| External iliac artery | Dd EIA (mm) | 12.1 | 1.2 | 1 | 6 | 1 |
| | Ds EIA (mm) | 12.4 | 1.2 | 1 | 6 | 1 |
| Arterial lumen area measurements | | | | | | |
| Cranial carotid artery | Ad CrCCA ($mm^2$) | 74.4 | 12.2 | 7 | 11 | 3 |
| | As CrCCA ($mm^2$) | 83.0 | 11.8 | 6 | 10 | 3 |
| Caudal carotid artery | Ad CaCCA ($mm^2$) | 107.8 | 20.2 | 7 | 11 | 3 |
| | Ad CaCCA ($mm^2$) | 119.0 | 21.3 | 6 | 10 | 3 |
| External iliac artery | Ad EIA ($mm^2$) | 125.5 | 19.3 | 4 | 5 | 3 |
| | As EIA ($mm^2$) | 133.6 | 16.9 | 4 | 16 | 3 |
| Local arterial wall stiffness parameters calculated from diameter measurements | | | | | | |
| Aorta | ΔD Ao (mm) | 5.4 | 2.2 | 31 | 41 | 16 |
| | $S_D$ Ao | $8.8x10^{-2}$ | $3.7x10^{-2}$ | 33 | 42 | 2 |
| | $DC_D$ Ao (/mmHg) | $2.5X10^{-03}$ | $1.8X10^{-03}$ | 31 | 52 | 17 |
| | $CC_D$ Ao (mm/mmHg) | $1.6x10^{-01}$ | $1.1x10^{-01}$ | 29 | 47 | 17 |
| | SI Ao | 5.1 | 2.6 | 20 | 57 | 23 |
| Cranial carotid artery | ΔD CrCCA (mm) | $5.0x10^{-01}$ | $2.4x10^{-01}$ | 32 | 43 | 11 |
| | $S_D$ CrCCA | $4.9x10^{-2}$ | $2.6x10^{-2}$ | 32 | 45 | 12 |
| | $DC_D$ CrCCA (/mmHg) | $1.3x10^{-03}$ | $7.1x10^{-04}$ | 34 | 42 | 10 |
| | $CC_D$ CrCCA (mm/mmHg) | $1.3x10^{-02}$ | $0.7x10^{-02}$ | 35 | 40 | 10 |
| | SI CrCCA | 8.3 | 4.8 | 32 | 57 | 24 |

| | | | | | | |
|---|---|---|---|---|---|---|
| Caudal carotid artery | ΔD CaCCA (mm) | $7.8x10^{-01}$ | $2.0x10^{-01}$ | 15 | 24 | 15 |
| | $S_D$ CaCCA | $6.8x10^{-2}$ | $1.9x10^{-2}$ | 14 | 22 | 14 |
| | $DC_D$ CaCCA (/mmHg) | $1.7x10^{-03}$ | $0.6x10^{-03}$ | 14 | 32 | 19 |
| | $CC_D$CaCCA (mm/mmHg) | $2.0x10^{-02}$ | $7.4x10^{-03}$ | 15 | 36 | 20 |
| | SI CaCCA | 6.1 | 2.4 | 14 | 51 | 25 |
| External iliac artery | ΔD EIA (mm) | $3.2x10^{-01}$ | $1.6x10^{-01}$ | 27 | 40 | 40 |
| | $S_D$ EIA | $2.7x10^{-02}$ | $1.3x10^{-02}$ | 29 | 43 | 40 |
| | $DC_D$ EIA (/mmHg) | $7.2x10^{-04}$ | $4.0x10^{-04}$ | 32 | 42 | 44 |
| | $CC_D$ EIA (mm/mmHg) | $8.8x10^{-03}$ | $5.3x10^{-03}$ | 55 | 42 | 45 |
| | SI EIA | 19.2 | 15.1 | 69 | 64 | 63 |
| Local arterial wall stiffness parameters calculated from lumen area measurements | | | | | | |
| Cranial carotid artery | ΔA CrCCA ($mm^2$) | 8.6 | 3.1 | 27 | 32 | 24 |
| | $S_A$ CrCCA | $1.9x10^{-1}$ | $0.5x10^{-1}$ | 32 | 37 | 27 |
| | $DC_A$ CrCCA (/mmHg) | $3.2x10^{-03}$ | $1.7x10^{-03}$ | 25 | 31 | 23 |
| | $CC_A$ CrCCA ($mm^2$/mmHg) | $2.3x10^{-01}$ | $1.2x10^{-01}$ | 32 | 33 | 21 |
| Caudal carotid artery | ΔA CaCCA ($mm^2$) | 11.2 | 4.3 | 22 | 42 | 35 |
| | $S_A$ CaCCA | $1.1\ x10^{-1}$ | $0.4\ x10^{-1}$ | 30 | 39 | 28 |
| | $DC_A$ CaCCA (/mmHg) | $2.7x10^{-03}$ | $1.2x10^{-03}$ | 26 | 49 | 25 |
| | $CC_A$ CaCCA ($mm^2$/mmHg) | $3.0x10^{-01}$ | $1.4x10^{-01}$ | 21 | 48 | 21 |
| External iliac artery | ΔA EIA ($mm^2$) | 8.2 | 4.0 | 59 | 52 | 25 |
| | $S_A$ EIA | $6.9x10^{-2}$ | $3.9x10^{-2}$ | 58 | 50 | 25 |
| | $DC_A$ EIA (/mmHg) | $1.8x10^{-03}$ | $1.1x10^{-03}$ | 56 | 52 | 27 |
| | $CC_A$ EIA ($mm^2$/mmHg) | $2.1x10^{-01}$ | $1.2x10^{-01}$ | 56 | 68 | 26 |
| Regional arterial wall stiffness parameters | | | | | | |
| Carotid artery | $PWV_{c-c}$ (m/s) | 7.8 | 2.7 | 20 | 37 | 25 |
| Aorta | $PWV_{a-e}$ (m/s) | 9.2 | 2.0 | 15 | 15 | 4 |
| | $PWV_{c-e}$ (m/s) | 5.9 | 0.6 | 12 | 8 | 3 |

Dd= diastolic diameter; Ds= systolic diameter; Ad= diastolic Area; As= systolic Area; ΔD= arterial diameter change; $S_D$= arterial diameter strain; $DC_D$= arterial distensibility coefficient derived from the diameter; $CC_D$= arterial compliance coefficient derived from the diameter change; SI= stiffness index; ΔA= arterial lumen area change; $S_A$= arterial lumen area strain; $DC_A$= arterial distensibility coefficient derived from the area change; $CC_A$= arterial compliance coefficient derived from the lumen area change; $PWV_{c-c}$= caudal carotid to cranial carotid artery pulse wave velocity; $PWV_{a-e}$=aorta to external iliac artery pulse wave velocity; $PWV_{c-e}$= carotid

to external iliac artery pulse wave velocity; Ao= Aorta; CrCCA= cranial common carotid artery; CaCCA= caudal common carotid artery; EIA= external iliac artery; CV= coefficient of variation.

† Means and SD are displayed for measurements on day 1, performed by observer 1.

## Discussion

This study revealed good inter-day, inter-observer and intra-observer measurement reproducibility of ultrasonographic arterial diameter and area measurements, derived both from M- and B-mode images, respectively. In this study inter-operator variability was not evaluated. CV lower than 15% were considered as acceptable, as also in human medicine variability of AWS parameters varies from 10 up to 15%[21].For the common carotid artery cross-sectional M-mode images were chosen to measure diameters, as the intima was more clearly visible. For the external iliac artery longitudinal M-mode images were collected, instead of cross-sectional ones, as cross-sectional images were more difficult to collect in the inguinal region. In general CV were higher for area compared to diameter measurements. Therefore M-mode diameter measurements seem superior to B-mode area measurements to calculate local AWS parameters. Although the repeatability of arterial diameter and area measurements were good (1-16%), CV for derived local AWS parameters ranged from low (2%) to extremely high (69%). Overall, the highest values were found for inter-day variability, as a result of the highest variability in diameter and area measurements. The high values for the inter-day variability might be related to the significant difference in HR between day 1 and day 2, as increased HR leads to stiffer behaviour of arteries[22]. This also implies that HR should be in the same range for follow-up studies of patients. Although not significantly different, the variation in arterial blood pressure and $\Delta P$ between day 1 and day 2 might have affected the inter-day variability. Because an artery consists of non-linear elastic material, meaning that it behaves differently depending on distending pressure, elasticity will decrease as distending pressure increases[23]. Relatively high CV were found for the inter-observer measurement variability. This suggests that follow-up measurements of individual patients should ideally be performed by the same observer. Remarkably, very high (27-69%) inter-day CV were found for external iliac artery AWS parameters. This is probably due to the difficulty of collecting perfect transverse or longitudinal images. The high variability in local AWS parameters of all investigated arteries may be a significant confounder for follow-up studies of individual patients that aim to detect changes in AWS over time, nevertheless they might be useful to study differences in AWS between different populations[21]. Therefore in future, these local AWS parameters might be useful to assess the influence of age, gender, breed, and training on the arterial wall in horses, but cannot be used to monitor the AWS of individual patients.

Regional aortic AWS parameters, $PWV_{a-e}$ and $PWV_{c-e}$, showed good repeatability, with CV ≤15%. The low variability of these regional aortic AWS parameters makes them valuable for both follow-up of individual patients over time and population research. These parameters might be similar as the carotid to femoral PWV ($PWV_{c-f}$) in humans, which is generally accepted as the most simple, non-invasive, robust, and reproducible method to determine AWS[13; 16]. Indeed, the aorta contributes largely to the arterial buffering capacity and aortic PWV is an independent predictor of cardiovascular mortality in human patients[1], which underlines the importance of $PWV_{c-f}$. In human medicine, the pulse wave can be captured both using tonometry and ultrasonography (pulsed wave Doppler)[13]. In this study, to capture the pulse wave non-invasively, pulsed wave Doppler was used, as a preliminary study indicated that applanation tonometry was technically difficult in horses.

To calculate the PWV and allow for comparison between different studies, the travelled distance should be measured in a standard way. In human medicine, the direct surface distance between the carotid and the femoral artery is used, in combination with a correction factor to estimate the real distance[24; 25]. In horses, no information about true dimensions of the arterial tree in relation to measured surface distances is available. Due to the size of an adult horse, MRI cannot be performed to visualize the whole arterial tree and invasive arterial measurements are technically difficult to obtain. Therefore, in this study relations were studied on necropsy of 5 (other) horses that had been euthanized for non-cardiovascular reasons. As the measurement of the surface distance between the carotid and external iliac artery is technically difficult, we chose to measure the length of the horse between the most cranial point of the shoulder and the tuber ischiadicum, which is an established measurement to assess horse size[26].

The authors suggest the use of $PWV_{a-e}$ to describe aortic AWS over $PWV_{c-e.}$ The $PWV_{c-e}$ assumes that the pulse wave travels at the same speed towards the carotid and the external iliac artery, while our study proves that AWS and thus PWV can differ a lot between different arteries. Similarly, in human medicine the aortic PWV (measured from the root of the left subclavian artery to the bifurcation of the abdominal aorta) is chosen over the $PWV_{c-f}$ to more accurately assess the aortic AWS itself, although it is more difficult to perform the measurements. In contrast to $PWV_{c-e}$ and $PWV_{a-e}$, the $PWV_{c-c}$ describing the regional stiffness of the common carotid artery, revealed moderate to high CV. This could be explained by the relatively small distance resulting in a larger absolute error in determining transit time[13]. Moreover, the exact distance of 0.3 m between the caudal and cranial carotid artery was difficult to assure because of the oblique probe position in order to align with the flow.

Although the current study provides guiding values for all measured variables and calculated AWS parameters (Table 2), real reference values should be defined in a larger, homogeneous study population. Another limitation of this study, is that although measurements were performed by 2 independent observers, all images were collected by the same operator and thus inter-operator variability was not assessed.

## Conclusion

Inter-day and inter-observer and intra-observer measurement variability of arterial diameter and lumen area measurements, derived from M- and B-mode respectively, were fairly low for all investigated arteries. Inter-operator variability was not assessed. Diameter measurements are preferred over lumen area measurements, as they show lower CV. Nevertheless, most local AWS parameters showed relatively high variability, especially those of the external iliac artery. Therefore local AWS parameters might not be suitable for individual follow-up studies, evaluating AWS over time, but can have and added value in population studies. Regional aortic AWS parameters such as $PWV_{c\text{-}e}$ and $PWV_{a\text{-}e}$, reveal low inter-day, inter-observer and intra-observer measurement variability. Further studies should be performed to evaluate the applicability of local and regional AWS parameters for assessment of age, gender, breed, and training effects on arterial wall properties in horses.

## Manufacturers addresses

[a] Midmark, Versailles, Ohio, USA

[b] GE Healthcare, Diegem, Belgium

[c] SPSS Statistics, Chicago, Illinois, USA

## References

[1] Laurent, S., Boutouyrie, P., Asmar, R., Gautier, I., Laloux, B., Guize, L., Ducimetiere, P. and Benetos, A. (2001) Aortic stiffness is an independent predictor of all-cause and cardiovascular mortality in hypertensive patients. *Hypertension* **37**, 1236-1241.
[2] O'Rourke, M.F. and Nichols, W.W. (2005) Aortic diameter, aortic stiffness, and wave reflection increase with age and isolated systolic hypertension. *Hypertension* **45**, 652-658.
[3] Rossi, P., Frances, Y., Kingwell, B.A. and Ahimastos, A.A. (2011) Gender differences in artery wall biomechanical properties throughout life. *J Hypertens* **29**, 1023-1033.
[4] Ferreira, A.V., Viana, M.C., Mill, J.G., Asmar, R.G. and Cunha, R.S. (1999) Racial differences in aortic stiffness in normotensive and hypertensive adults. *J Hypertens* **17**, 631-637.
[5] Seals, D.R., Nagy, E.E. and Moreau, K.L. (2019) Aerobic exercise training and vascular function with aging in healthy men and women. *J Physiol*.
[6] de Solis, C.N., Althaus, F., Basieux, N. and Burger, D. (2018) Sudden death in sport and riding horses during and immediately after exercise: A case series. *Equine Vet J* **50**, 644-648.

[7] Williams, N.M. and Bryant, U.K. (2012) Periparturient Arterial Rupture in Mares: A Postmortem Study. *J Equine Vet Sci* **32**, 281-284.
[8] Lyle, C.H., Blissitt, K.J., Kennedy, R.N., Mc Gorum, B.C., Newton, J.R., Parkin, T.D., Stirk, A. and Boden, L.A. (2012) Risk factors for race-associated sudden death in Thoroughbred racehorses in the UK (2000-2007). *Equine Vet J* **44**, 459-465.
[9] Frederick, J., Giguere, S., Butterworth, K., Pellegrini-Masini, A., Casas-Dolz, R. and Turpin, M.M. (2010) Severe phenylephrine-associated hemorrhage in five aged horses. *J Am Vet Med Assoc* **237**, 830-834.
[10] Lyle, C.H., Uzal, F.A., McGorum, B.C., Aida, H., Blissitt, K.J., Case, J.T., Charles, J.T., Gardner, I., Horadagoda, N., Kusano, K., Lam, K., Pack, J.D., Parkin, T.D., Slocombe, R.F., Stewart, B.D. and Boden, L.A. (2011) Sudden death in racing Thoroughbred horses: an international multicentre study of post mortem findings. *Equine Vet J* **43**, 324-331.
[11] Ploeg, M., Saey, V., de Bruijn, C.M., Grone, A., Chiers, K., van Loon, G., Ducatelle, R., van Weeren, P.R., Back, W. and Delesalle, C. (2013) Aortic rupture and aorto-pulmonary fistulation in the Friesian horse: characterisation of the clinical and gross post mortem findings in 24 cases. *Equine Vet J* **45**, 101-106.
[12] Van Bortel, L.M., Laurent, S., Boutouyrie, P., Chowienczyk, P., Cruickshank, J.K., De Backer, T., Filipovsky, J., Huybrechts, S., Mattace-Raso, F.U., Protogerou, A.D., Schillaci, G., Segers, P., Vermeersch, S., Weber, T., Artery, S., European Society of Hypertension Working Group on Vascular, S., Function and European Network for Noninvasive Investigation of Large, A. (2012) Expert consensus document on the measurement of aortic stiffness in daily practice using carotid-femoral pulse wave velocity. *J Hypertens* **30**, 445-448.
[13] Laurent, S., Cockcroft, J., Van Bortel, L., Boutouyrie, P., Giannattasio, C., Hayoz, D., Pannier, B., Vlachopoulos, C., Wilkinson, I., Struijker-Boudier, H. and European Network for Non-invasive Investigation of Large, A. (2006) Expert consensus document on arterial stiffness: methodological issues and clinical applications. *Eur Heart J* **27**, 2588-2605.
[14] Heliczer, N., Lorello, O., Casoni, D. and Navas de Solis, C. (2016) Accuracy and Precision of Noninvasive Blood Pressure in Normo-, Hyper-, and Hypotensive Standing and Anesthetized Adult Horses. *J Vet Intern Med* **30**, 866-872.
[15] Ohyama, Y., Redheuil, A., Kachenoura, N., Venkatesh, B.A. and Lima, J.A.C. (2018) Imaging Insights on the Aorta in Aging. *Circ-Cardiovasc Imag* **11**.
[16] Messas, E., Pernot, M. and Couade, M. (2013) Arterial wall elasticity: state of the art and future prospects. *Diagn Interv Imaging* **94**, 561-569.
[17] O'Rourke, M.F., Staessen, J.A., Vlachopoulos, C., Duprez, D. and Plante, G.E. (2002) Clinical applications of arterial stiffness; definitions and reference values. *American Journal of Hypertension* **15**, 426-444.
[18] Decloedt, A., Verheyen, T., Sys, S., De Clercq, D. and van Loon, G. (2013) Two-dimensional speckle tracking for quantification of left ventricular circumferential and radial wall motion in horses. *Equine Vet J* **45**, 47-55.
[19] Schwarzwald, C.C., Schober, K.E., Berli, A.S.J. and Bonagura, J.D. (2009) Left Ventricular Radial and Circumferential Wall Motion Analysis in Horses Using Strain, Strain Rate, and Displacement by 2D Speckle Tracking. *Journal of Veterinary Internal Medicine* **23**, 890-900.
[20] Schwarzwald, C.C., Schober, K.E. and Bonagura, J.D. (2007) Methods and reliability of echocardiographic assessment of left atrial size and mechanical function in horses. *Am J Vet Res* **68**, 735-747.
[21] Godia, E.C., Madhok, R., Pittman, J., Trocio, S., Ramas, R., Cabral, D., Sacco, R.L. and Rundek, T. (2007) Carotid artery distensibility: a reliability study. *J Ultrasound Med* **26**, 1157-1165.
[22] Tan, I., Butlin, M., Liu, Y.Y., Ng, K. and Avolio, A.P. (2012) Heart Rate Dependence of Aortic Pulse Wave Velocity at Different Arterial Pressures in Rats. *Hypertension* **60**, 528-533.
[23] von Maltzahn, W.W., Besdo, D. and Wiemer, W. (1981) Elastic properties of arteries: a nonlinear two-layer cylindrical model. *J Biomech* **14**, 389-397.
[24] Huybrechts, S.A., Devos, D.G., Vermeersch, S.J., Mahieu, D., Achten, E., de Backer, T.L., Segers, P. and van Bortel, L.M. (2011) Carotid to femoral pulse wave velocity: a

comparison of real travelled aortic path lengths determined by MRI and superficial measurements. *J Hypertens* **29**, 1577-1582.
[25] Weber, T., Ammer, M., Rammer, M., Adji, A., O'Rourke, M.F., Wassertheurer, S., Rosenkranz, S. and Eber, B. (2009) Noninvasive determination of carotid-femoral pulse wave velocity depends critically on assessment of travel distance: a comparison with invasive measurement. *J Hypertens* **27**, 1624-1630.
[26] Carroll, C.L. and Huntington, P.J. (1988) Body Condition Scoring and Weight Estimation of Horses. *Equine Vet J* **20**, 41-45

# CHAPTER 5:

# DIFFERENCES IN ULTRASOUND-DERIVED ARTERIAL WALL STIFFNESS PARAMETERS AND NON-INVASIVE BLOOD PRESSURE BETWEEN FRIESIAN HORSES AND WARMBLOOD HORSES

# Differences in ultrasound-derived arterial wall stiffness parameters and non-invasive blood pressure between Friesian horses and Warmblood horses

Lisse Vera[1], Dominique De Clercq[1], Glenn Van Steenkiste[1], Annelies Decloedt[1], Koen Chiers[2] and Gunther van Loon[1]

[1] Equine cardioteam Ghent University, Department of Large Animal Internal Medicine, Faculty of Veterinary Medicine, Ghent University

[2] Department of Pathology, bacteriology and poultry diseases, Faculty of Veterinary Medicine, Ghent University

**Institutional Animal Care and Use Committee (IACUC) or Other Approval Declaration:** The study was approved by the ethical committee of the Faculty of Veterinary Medicine and Bioscience Engineering (EC2018/111).

Adapted from:

**Lisse Vera**, Dominique De Clercq, Glenn Van Steenkiste, Annelies Decloedt, Koen Chiers, and Gunther van Loon. 2020. “Differences in Ultrasound-Derived Arterial Wall Stiffness Parameters and Noninvasive Blood Pressure between Friesian Horses and Warmblood Horses.” *JOURNAL OF VETERINARY INTERNAL MEDICINE*, 34(2):893-901

**Abstract**

**Background:** Aortic rupture is more common in Friesians compared to Warmbloods, which might be related to differences in arterial wall composition and as such, arterial wall stiffness (AWS). Currently, nothing is known about differences in AWS between both breeds. **Objectives:** Comparison of AWS parameters and non-invasive blood pressure between Friesians and Warmbloods. **Animals:** One-Hundred healthy Friesians and 101 age-matched healthy Warmbloods. **Methods:** Two-dimensional and pulsed-wave Doppler ultrasound examination was performed of the aorta, common carotid artery and external iliac artery to define local and regional AWS parameters. Regional aortic AWS was estimated using aortic-to-external iliac artery pulse wave velocity ($PWV_{a-e}$) and carotid-to-external iliac artery pulse wave velocity ($PWV_{c-e}$). Non-invasive blood pressure and heart rate were recorded simultaneously. **Results:** Systolic, diastolic and mean arterial blood pressure and pulse pressure were significantly higher in Friesians compared to Warmbloods. No significant difference in heart rate was found. Most local AWS parameters (diameter change, compliance coefficient, distensibility coefficient) were significantly lower in Friesians compared to Warmbloods, indicating a stiffer aorta in Friesians. This difference could be confirmed by the regional stiffness parameters. A higher $PWV_{a-e}$ and $PWV_{c-e}$ was found in Friesians. For the cranial and caudal common carotid artery and external iliac artery, most local AWS parameters were not significantly different. **Conclusions and clinical importance:** Results indicate that aortic AWS differs between Friesian and Warmblood horses. Friesians seem to have a stiffer aorta, which might be related to the higher incidence of aortic rupture in Friesians.

## Introduction

In Friesian horses, aortic rupture is more common compared to Warmblood horses[1]. In contrast to Warmblood horses[2-4], aortic rupture in Friesian horses typically occurs close to the ligamentum arteriosum with formation of a pseudoaneurysm and aortopulmonary fistulation[5; 6]. The reason why Friesians are predisposed to aortic rupture at this specific location remains unknown. An embryological defect occurring during fusion of the proximal aorta with the heart base has been hypothesized. However, valvular abnormalities, which would be expected with an embryological disorder, are not described in affected Friesians[1]. In human medicine, aortic rupture- usually is preceded by aortic aneurysm formation, which is not the case in Friesians[7]. In human patients, elastin and especially collagen have been shown to be important factors contributing to aortic aneurysm formation[8; 9]. Collagen fibrils, together with smooth muscle cells and elastin, form the primary load-bearing components of the aortic wall. Both collagen and elastin are responsible for the tensile strength and the elasticity of the aortic wall. Collagen is essential to prevent over-stretching and rupture,

whereas elastin is essential for stretching and recoil of the artery, in order to buffer differences in pressure between systole and diastole[9]. Previous post mortem studies identified differences in composition[10; 11] and relative amounts[12] of collagen and elastin between unaffected Friesian horses, affected Friesian horses and Warmblood horses, which might be related to the predisposition of Friesian horses to aortic rupture. Moreover medial necrosis is found at the site of rupture in affected Friesians[13], that might be related to connective tissue disorders[14], hypertension[15], ischemia[6] or inflammation[16]. In addition to medial necrosis, disorganization and fragmentation of elastic laminae, aortic medial smooth muscle cell hypertrophy and accumulation of mucoid material can be found histologically at the rupture site in affected Friesians[7].

In human medicine, arterial wall stiffness (AWS) is known to be an independent predictor of cardiovascular mortality[17-21] and can be assessed both regionally and locally. Measurement of carotid-to-femoral artery pulse wave velocity ($PWV_{c-f}$) generally is accepted as the most simple, non-invasive, robust, and reproducible method to determine regional AWS, and is therefore used as the gold standard method[22-27]. The pulse wave velocity (PWV) represents how fast a pressure wave travels over a certain length of the arterial tree. The pressure wave can be captured non-invasively using tonometry or pulsed wave Doppler ultrasound[27; 28]. The PWV is calculated as the difference in travelled distance ($\Delta$Dist) between 2 recording sites (e.g. carotid and femoral artery) divided by the time delay ($\Delta$t) between the 2 waveforms: PWV (m/s) = $\Delta$Dist (m) / $\Delta$t (s). The stiffer the artery, the higher the PWV. Ultrasonographic evaluation of lumen area or diameter change in relation to distending pressures can be used to estimate local AWS [22; 25; 26]. Larger diameter and lumen area change indicates a more compliant artery.

To further understand the underlying cause of the predisposition of the Friesian breed to aortic rupture, we assessed both regional and local AWS parameters of the aorta, cranial and caudal common carotid artery and external iliac artery *in vivo*, comparing Friesian horses to Warmblood horses. All AWS parameters were derived using vascular ultrasound examination. We hypothesized that Friesians would have stiffer arteries, which may predispose them to aortic rupture.

## Materials and methods

Cardiovascular ultrasound examination was performed in 101 healthy Friesian horses (mean age ± SD, 12 ± 6 years) and 101 age-matched, healthy Warmblood horses (mean age, 11 ± 5 years). Friesians consisted of 73 mares, 23 geldings and 5 stallions. Warmblood horses consisted of 57 mares and 44 geldings. All horses were privately owned and informed consent was obtained. The study was approved by the ethical committee of the Faculty of Veterinary

Medicine and Bioscience Engineering (EC2018/111). In every horse, height at the withers, tail circumference, chest circumference and length, defined as the length between the most cranial point of the shoulder and the tuber ischiadicum, was measured. Body weight was calculated as length (cm) x (chest circumference)$^2$ (cm) / 11900.[29] In all horses, auscultation, echocardiography and ECG were performed. Inclusion criteria were: no more than a 2/6 left- or right-sided systolic or diastolic murmur on auscultation, no more than mild valvular regurgitation visible with Doppler ultrasound examination, and absence of atrial and ventricular premature beats during a 15 min ECG recording at rest.

**Blood pressure**

Systolic (SAP), diastolic (DAP) and mean (MAP) arterial blood pressure were measured non-invasively, simultaneously with acquisition of ultrasound images, using an oscillometric device (Cardell Veterinary Monitor, 9401, Midmark), with a cuff placed around the base of the tail. To correct readings to the level of the heart base, a correction factor of 0.77 mmHg was added for every cm in difference between the right atrium (estimated at the height of the shoulder) and the cuff [30]. As recommended[31], the mean of 5 consecutive, consistent measurements was taken. In all horses, a cuff width of 9 cm was used. Tail circumference was measured to calculate the cuff width-to-tail circumference ratio. A cuff width-to-tail circumference ratio between 0.4 and 0.6 [32; 33] was achieved in all horses except for 3 Friesians in which tail circumference was slightly too large, resulting in a cuff width-to-tail circumference ratio of 0.3.

**Ultrasound**

Ultrasound imaging was performed (Vivid IQ, GE Healthcare) in the standing, non-sedated horse. Images only were collected with a heart rate (HR) < 50 beats per minute. Stroke volume (SV) was calculated as pulsed wave Doppler-derived aortic velocity time integral (left parasternal view) multiplied by aortic valve cross sectional area (right parasternal view)[34]. Cardiac output (CO) was determined as SV x HR.

**Ultrasonographic measurements**

***B- and M-mode images***

Ultrasound examination was performed from 4 different arterial locations to calculate AWS: the aorta from a right parasternal position, the right caudal common carotid artery (15 cm cranial to the thoracic inlet), the right cranial common carotid artery (30 cm more cranially) and the right external iliac artery, from the inguinal region (Fig.1) just proximal to the side branch, deep femoral artery (arteria profunda femoris). For the aorta, a 1.5 - 4.6 MHz phased array probe (M5Sc-RS, GE Healthcare) was used to obtain a right parasternal left ventricular outflow tract view (frequency 4.0 MHz / 8 MHz, depth 26 cm, gain 10 dB). A 3.5 - 10 MHz linear

transducer (9L-RS, GE Healthcare) was used to collect cross-sectional B- and M-mode images from the cranial and caudal carotid artery (frequency 4.0 MHz / 8.0 MHz, depth 4 cm, gain 16 dB). For the external iliac artery, a 2.7 - 8 MHz phased array probe (6S-RS,GE Healthcare) was used to obtain longitudinal M-mode images and cross-sectional B-mode images (gain 3.5 MHz / 7.0 MHz, depth 7 cm, gain 4 dB). All images were stored for off-line analysis (Echopac version 203, GE Healthcare).

Fig. 1. Exact probe location to collect images of the external iliac artery from the inguinal region.

***Pulsed wave Doppler***

The pulse wave was captured non-invasively using pulsed wave Doppler. For the carotid and external iliac artery, a 2.7 - 8MHz phased array probe (6S-RS,GE Healthcare, frequency: 4 MHz, depth 7 cm, gain 5 dB, sample size 5 mm) was used and a 1.5 - 4.6 MHz phased array probe (M5Sc-RS GE Healthcare, frequency 2 MHz, depth 26 cm, gain 10 dB, sample size 5 mm) was used for the aorta (left parasternal view). At all locations, angle correction was set at 45° and images were optimized to align with flow direction. All images were stored for off-line analysis (Echopac version 203, GE Healthcare).

**Local measurements of arterial wall stiffness**

Aortic diameters were measured at the sinotubular junction from a right parasternal left ventricular outflow tract view. Mean aortic diameters were calculated from 3 consecutive cycles. Diameters were measured from cross-sectional M-mode images for the cranial and caudal common carotid artery. On the other hand, areas were measured from cross-sectional B-mode images. For the external iliac artery, diameters were measured from longitudinal M-mode images and areas from cross-sectional B-mode images. Mean carotid and external iliac artery diameters were calculated from 3 times 3 consecutive heart cycles (9 in total). For all arteries, diastolic measurements were performed on the R peak of the simultaneously recorded ECG (base-apex configuration) and systolic measurements were performed at maximal dilatation (Fig.2).

Fig. 2. M-mode systolic (Ds) and diastolic (Dd) diameter measurement at the level of the cranial common carotid artery. Diastolic measurements were performed at the time of the R peak of the simultaneously recorded ECG and systolic measurements were performed at maximal dilation.

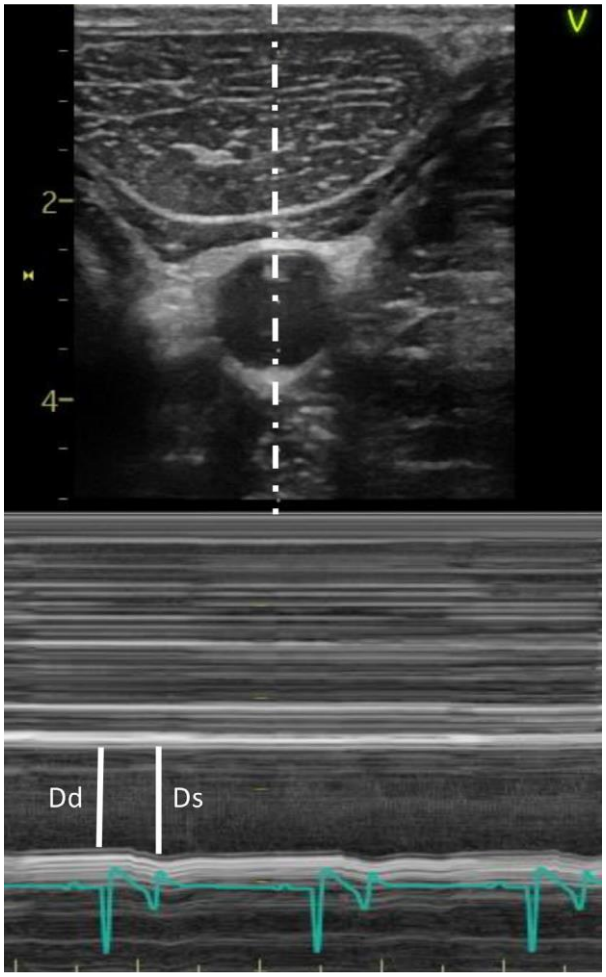

***Arterial diameter and lumen area change***

The change in diameter or lumen area between systole (s) and diastole (d) is defined as the arterial diameter change ($\Delta D = Ds - Dd$) or lumen area change ($\Delta A = As - Ad$), respectively.

***Arterial diameter and lumen area strain***

The relative change in diameter or lumen area during the cardiac cycle is defined as the arterial diameter strain ($S_D = \Delta D / Dd$) or lumen area strain ($S_A = \Delta A / Ad$), respectively.

***Arterial distensibility***

The relative diameter or area change for a pressure increment is defined as the arterial distensibility coefficient ($DC_D = [\Delta D / Dd] / PP$; $DC_A = [\Delta A / Ad] / PP$, respectively). Pulse pressure (PP) is defined as SAP - DAP.

***Arterial compliance***

The absolute diameter/area change for a pressure increment is defined as the arterial compliance coefficient ($CC_D = \Delta D / PP$ ; $CC_A = \Delta A / PP$, respectively).

***Stiffness index***

The ratio of the natural logarithm (systolic/diastolic pressure) to the relative change in diameter is defined as the stiffness index ($SI = \ln [SAP / DAP] / [\Delta D / Dd]$).

**Regional measurements of arterial wall stiffness**

The time delay (ms) between the R wave of the synchronised electrocardiogram and the onset (foot) of the waveform, captured using pulsed wave Doppler, was measured at every investigated location. Means were calculated from 3 times 3 consecutive beats (9 in total). The mean time delay at the location nearest to the heart (shortest time delay) was subtracted from the mean time delay at the location the farthest away from the heart (longest time delay) to calculate the difference in time delay ($\Delta t$; Fig.3).

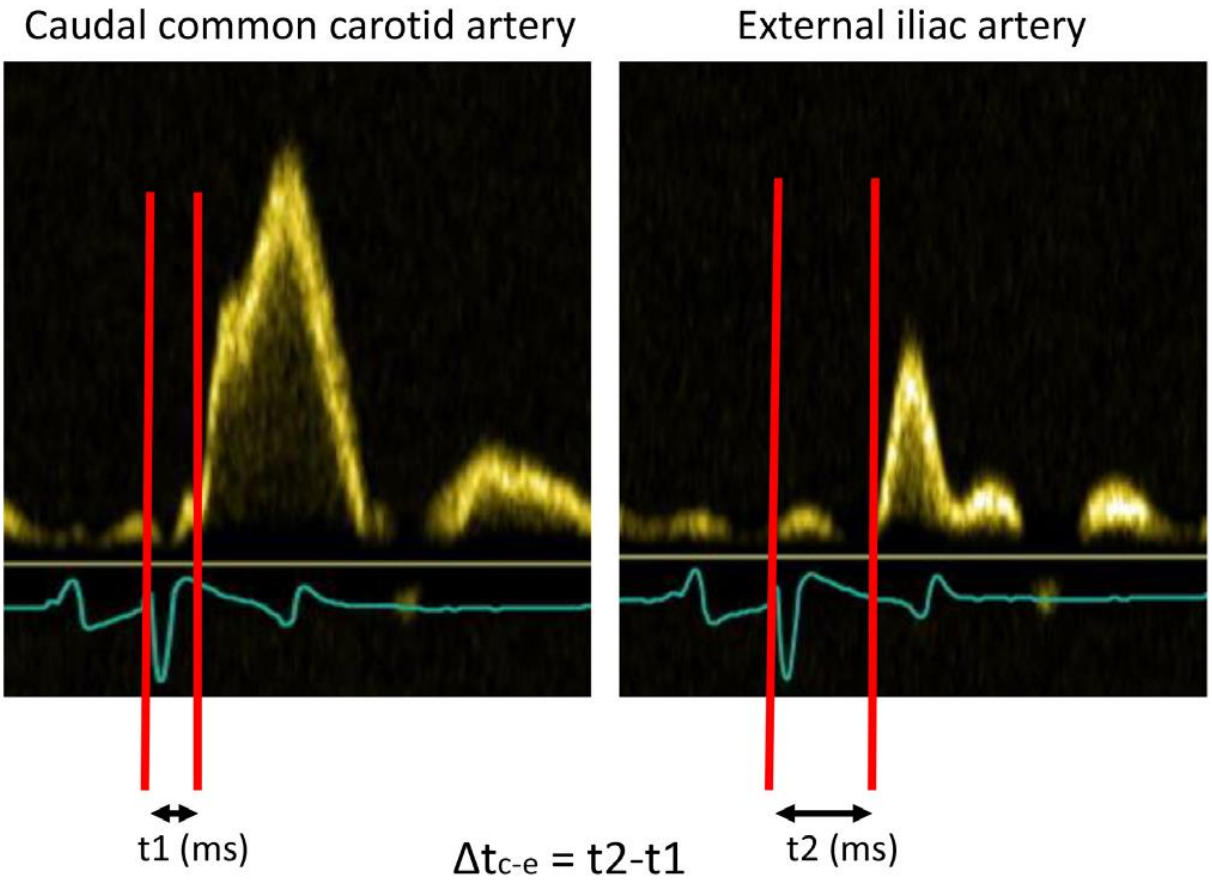


Fig. 3. Measurement of the time it takes for the pressure wave to travel from the caudal carotid artery to the external iliac artery using pulsed wave Doppler. The time delay between the R wave of the synchronised ECG and the onset of the waveform is measured both at the level of the caudal common carotid artery (t1) and at the level of the external iliac artery (t2). To calculate the difference in time delay (Δt), the time delay at the location nearest to the heart (shortest time delay, t1) was subtracted from the mean time delay at the location the furthest away from the heart (longest time delay, t2).

***Caudal carotid-to-cranial carotid artery pulse wave velocity***

The velocity at which the pressure wave travels between the caudal and cranial common carotid artery is defined as the caudal carotid-to-cranial carotid artery pulse wave velocity ($PWV_{c\text{-}c}$ [m/s] = $\Delta Dist_{c\text{-}c}$ [m] / $\Delta t_{c\text{-}c}$ [s]). A fixed distance of 0.3 m between both measuring places ($\Delta Dist_{c\text{-}c}$) was taken.

***Aorta-to-external iliac artery pulse wave velocity***

The velocity at which the pressure wave travels between the aorta and the external iliac artery is defined as the aorta-to-external iliac artery pulse wave velocity ($PWV_{a\text{-}e}$ [m/s] = $\Delta Dist_{a\text{-}e}$ [m] / $\Delta t_{a\text{-}e}$ [s]). The $\Delta Dist_{a\text{-}e}$ represents the distance between the aortic valve and the external iliac artery. This distance was estimated based on measurements performed on 5 Warmblood horses (mean ± SD body weight, 633 ± 112 kg; height at the withers, 166 ± 10 cm) at necropsy. The distance between the aortic valve and the external iliac artery was measured and related

to the length of the horse (measured from the most cranial point of the shoulder to the tuber ischiadicum). The mean value for this distance estimate was 0.62 times the length of the horse (range, 0.55-0.66). Therefore, $\Delta Dist_{a-e}$ (m) = length of the horse (m) x 0.62.

***Carotid-to-external iliac artery pulse wave velocity***

The velocity at which the pressure wave travels between the caudal common carotid artery and the external iliac artery is defined as the carotid-to-external iliac artery pulse wave velocity ($PWV_{c-e}$ [m/s] = $\Delta Dist_{c-e}$ [m] / $\Delta t_{c-e}$ [s]). The $\Delta Dist_{c-e}$ represents the difference in distance relative to the aortic root between the caudal carotid and external iliac arteries. To estimate this distance, in the same 5 horses at necropsy, the distance between the aortic valve and the caudal carotid artery was measured and was found to average 0.40 m (range, 0.37-0.52 m). Because the pressure wave simultaneously travels from the aortic valve cranially (toward the caudal carotid artery) and caudally (toward the external iliac artery), this distance was subtracted from the estimated distance between the aorta and external iliac artery. Therefore, $\Delta Dist_{c-e}$ (m) = length of the horse (m) x 0.62 - 0.40 m.

**Statistical analysis of data**

Normality of all variables and derived AWS parameters was evaluated graphically. Arterial diameters and areas, arterial blood pressures, PWV, HR and CO were compared between Friesians and Warmbloods using an independent samples t test. For derived local stiffness values, a univariate model was built including breed (Friesian or Warmblood) and location (cranial carotid artery, caudal carotid artery, aorta and external iliac artery) as fixed factors and horse as random factor. Interaction was found between location and breed, therefore a univariate model, including location*breed as a fixed factor and horse as a random factor with post hoc Bonferroni correction for multiple comparisons was applied. P values <.05 were considered significant.

## Results

Although all horses tolerated the procedure well, images of the external iliac artery, especially transverse images, were the most difficult to obtain. The distance of 0.3 m between the caudal and cranial common carotid artery was difficult to define, because of the oblique probe position needed to align with flow direction.

Friesians were significantly less tall (height at the withers [mean ± SD], 162 ± 4 cm vs. 167 ± 5cm; p<.001), but longer (length of the horse, 188 ± 11 cm vs. 180 ± 9 cm; p<.001), with a larger chest circumference (199 ± 7 cm vs. 195 ± 8 cm; p<.001) and a larger calculated weight (627 ± 61 kg vs. 575 ± 63 kg; p<.001) compared to Warmblood horses.

Friesians had significantly (p<.001) higher SAP (146 ± 18 mmHg vs. 135± 14 mmHg), DAP (97 ± 12 vs. 91 ± 10 mmHg), MAP (115 ±15mmHg vs. 106 ± 13 mmHg) and PP (49 ± 9 mmHg vs. 44 ± 9 mmHg) in comparison with Warmblood horses. No significant differences in HR or CO were found. Results are represented in Table 1. The mean tail circumference of the Friesians horses was significantly higher (25 ± 1 cm) in comparison with the Warmblood horses (22 ± 2 cm; p<.001), but both were within the reference range for the cuff used (17-25 cm). The only exceptions were 3 Friesians for which tail circumference was slightly too large for the cuff used (26 cm in 1 horse and 27 cm in 2 horses).

Table 1. Comparison of systolic, diastolic and mean arterial blood pressure and pulse pressure in Friesian horses and Warmblood horses

| | Friesian (mean±SD) | Warmblood (mean±SD) | p-value |
|---|---|---|---|
| SAP (mmHg) | 146±18 | 135±14 | <.001 |
| DAP (mmHg) | 97±12 | 91±10 | <.001 |
| MAP (mmHg) | 115±15 | 106±13 | <.001 |
| PP (mmHg) | 49±9 | 44±9 | <.001 |
| HR (bpm) | 37±5 | 36±6 | .139 |
| CO (L/min) | 34.18±7.66 | 36.32±8.88 | .086 |

SAP, systolic arterial pressure; DAP, diastolic arterial pressure; MAP, mean arterial pressure; PP, pulse pressure; HR, heart rate; CO, cardiac output

All measured arterial diameters and areas are presented in Table 2. Overall, arterial diameters and areas of all investigated arteries were smaller (2-20%) in Friesian horses compared to Warmblood horses. A detailed overview of all derived AWS parameters is found in Table 3. The AWS parameters indicate that Friesian horses might have a stiffer aorta. The $PWV_{a-e}$ and $PWV_{c-e}$, both regional aortic AWS parameters covering a large part of the aorta, were significantly higher in Friesian horses compared to Warmblood horses, indicating a stiffer aorta. The arterial diameter change, distensibility coefficient and the compliance coefficient, all three local aortic AWS parameters, were significantly lower in Friesian horses compared to Warmblood horses, also suggesting a stiffer aorta. For the cranial and caudal common carotid artery and the external iliac artery, most local AWS parameters were not significantly different between breeds, except for a higher diameter strain of the cranial carotid artery, a higher area strain of the caudal common carotid artery and a lower stiffness index of the external iliac artery in Friesians compared to Warmblood horses.

Table 2. Comparison of internal diastolic and systolic diameters and areas of the aorta, the cranial and caudal common carotid artery and the external iliac artery between Friesian horses and Warmblood horses.

| | Friesian (mean±SD) | Warmblood (mean±SD) | p-value |
|---|---|---|---|
| Dd(Ao) (mm) | 59±5 | 62±5 | .001 |
| Ds(Ao) (mm) | 65±6 | 68±6 | <.001 |
| Dd(CrCCA) (mm) | 10.1±.9 | 10.5±.9 | .006 |
| Ds(CrCCA) (mm) | 10.8±1.0 | 11.00±1.0 | .125 |
| Ad(CrCCA) ($mm^2$) | 78.1±14.6 | 84.8±18.6 | .005 |
| As(CrCCA) ($mm^2$) | 86.8±16.0 | 93.1±20.2 | .015 |
| Dd(CaCCA) (mm) | 11.6±1.1 | 11.9±1.4 | .042 |
| Ds(CaCCA) (mm) | 12.5±1.1 | 12.8±1.4 | .103 |
| Ad(CaCCA) ($mm^2$) | 108.8±19.62 | 120.1±26.0 | .001 |
| As(CaCCA) ($mm^2$) | 122.8±20.9 | 132.3±27.6 | .006 |
| Dd(EIA) (mm) | 10.8±1.1 | 11.8±1.2 | <.001 |
| Ds(EIA) (mm) | 11.2±1.1 | 12.2±1.2 | <.001 |
| Ad(EIA) ($mm^2$) | 107.2±21.3 | 133.3±28.9 | <.001 |
| As(EIA) ($mm^2$) | 116.9±22.4 | 143.4±30.5 | <.001 |

Ao, aorta; CaCCA, caudal common carotid artery; CrCCA, cranial common carotid artery; EIA, external iliac artery; Dd, diastolic diameter; Ds, systolic diameter; Ad, diastolic area; As, systolic area;

Table 3. Comparison of arterial wall stiffness parameters for the aorta, the cranial and caudal common carotid artery and the external iliac artery between 101 Friesian horses and 101 Warmblood horses.

| | Friesian (mean ±SD) | Warmblood (mean ±SD) | p-value |
|---|---|---|---|
| Regional stiffness parameters | | | |
| $PWV_{a-e}$ (m/s) | 6.52±.90 | 5.95±.94 | <.001 |
| $PWV_{c-e}$ (m/s) | 7.06±1.60 | 5.79±1.43 | <.001 |
| $PWV_{c-c}$ (m/s) | 7.96±3.16 | 8.02±3.58 | .915 |
| Local stiffness parameters | | | |
| Aorta | | | |
| ΔD(Ao) (mm) | 5.8±2.1 | 6.3±2.0 | .013 |
| $S_D$(Ao) | $9.9x10^{-02}$ ±$3.9x10^{-02}$ | $10.3x10^{-02}$±$3.5x10^{-02}$ | 1.000 |

| | | | |
|---|---|---|---|
| $DC_D$(Ao) (/mmHg) | $2.1x10^{-03}$±$1.0x10^{-03}$ | $2.5x10^{-03}$±$1.0x10^{-03}$ | .005 |
| $CC_D$(Ao) (mm/mmHg) | $1.2x10^{-01}$±$.6x10^{-01}$ | $1.5x10^{-01}$±$.6x10^{-01}$ | <.001 |
| SI (Ao) | 4.9±2.5 | 4.4±2.2 | 1.000 |
| Cranial carotid artery | | | |
| ∆D(CrCCA) (mm) | $6.8x10^{-01}$±$2.7x10^{-01}$ | $5.3x10^{-01}$±$2.2x10^{-01}$ | 1.000 |
| $S_D$(CrCCA) | $6.8x10^{-02}$±$2.8x10^{-02}$ | $5.1x10^{-02}$±$2.1x10^{-02}$ | <.001 |
| $DC_D$(CrCCA) (/mmHg) | $1.5x10^{-03}$±$.7x10^{-03}$ | $1.2x10^{-03}$±$.7x10^{-03}$ | .138 |
| $CC_D$(CrCCA) (mm/mmHg) | $1.5x10^{-02}$±$.7x10^{-02}$ | $1.3x10^{-02}$±$.7x10^{-02}$ | 1.000 |
| SI (CrCCA) | 7.1±3.9 | 9.6±5.9 | .439 |
| ∆A(CrCCA) ($mm^2$) | 8.7±3.5 | 8.4±3.8 | 1.000 |
| $S_A$(CrCCA) | $1.1x10^{-01}$±$.4x10^{-01}$ | $1.0x10^{-01}$±$.4x10^{-01}$ | 1.000 |
| $DC_A$(CrCCA) (/mmHg) | $2.5x10^{-03}$±$1.1x10^{-03}$ | $2.4x10^{-03}$±$1.3x10^{-03}$ | 1.000 |
| $CC_A$(CrCCA) ($mm^2$/mmHg) | $1.9x10^{-01}$±$1.0x10^{-01}$ | $2.1x10^{-01}$±$1.2x10^{-01}$ | 1.000 |
| Caudal carotid artery | | | |
| ∆D(CaCCA) (mm) | $9.3x10^{-01}$±$2.9x10^{-01}$ | $8.7x10^{-01}$±$3.3x10^{-01}$ | 1.000 |
| $S_D$(CaCCA) | $8.2x10^{-02}$±$2.7x10^{-02}$ | $7.4x10^{-02}$±$3.0x10^{-02}$ | .890 |
| $DC_D$(CaCCA) (/mmHg) | $1.7x10^{-03}$±$.7x10^{-03}$ | $1.8x10^{-03}$±$.9x10^{-03}$ | 1.000 |
| $CC_D$(CaCCA) (mm/mmHg) | $2.0x10^{-02}$±$.7x10^{-02}$ | $2.1x10^{-02}$±$1.0x10^{-02}$ | 1.000 |
| SI(CaCCA) | 5.6±2.6 | 7.1±9.2 | 1.000 |
| ∆A(CaCCA) ($mm^2$) | 14.0±5.5 | 12.2±5.4 | 1.000 |
| $S_A$(CaCCA) | $1.3x10^{-01}$±$.5x10^{-01}$ | $1.0x10^{-01}$±$.5x10^{-01}$ | <.005 |
| $DC_A$(CaCCA) (/mmHg) | $2.8x10^{-03}$±$1.4x10^{-03}$ | $2.5x10^{-03}$±$1.3x10^{-03}$ | 1.000 |
| $CC_A$(CaCCA)($mm^2$/mmHg) | $3.0x10^{-01}$±$1.5x10^{-01}$ | $2.9x10^{-01}$±$1.5x10^{-01}$ | 1.000 |
| External iliac artery | | | |
| ∆D(EIA) (mm) | $3.9x10^{-01}$±$1.6x10^{-01}$ | $3.9x10^{-01}$±$1.8x10^{-01}$ | 1.000 |
| $S_D$(EIA) | $3.6x10^{-02}$±$1.5x10^{-02}$ | $3.3x10^{-02}$±$1.6x10^{-02}$ | 1.000 |
| $DC_D$(EIA) (/mmHg) | $7.8x10^{-04}$±$3.5x10^{-04}$ | $7.9x10^{-04}$±$4.5x10^{-04}$ | 1.000 |
| $CC_D$(EIA) (mm/mmHg) | $8.2x10^{-03}$±$3.8x10^{-03}$ | $9.3x10^{-03}$±$5.0x10^{-03}$ | 1.000 |
| SI(EIA) | 12.3±10.6 | 16.5±14.8* | .021 |
| ∆A(EIA) ($mm^2$) | 9.7±4.8 | 10.1±3.8 | 1.000 |
| $S_A$(EIA) | $9.4x10^{-02}$±$5.1x10^{-02}$ | $7.7x10^{-02}$±$2.9x10^{-02}$ | .991 |
| $DC_A$(EIA) (/mmHg) | $2.0x10^{-03}$±$1.3x10^{-03}$ | $1.9x10^{-03}$±$.8x10^{-03}$ | 1.000 |
| $CC_A$(EIA) ($mm^2$/mmHg) | $2.0x10^{-01}$±$1.2x10^{-01}$ | $2.4x10^{-01}$±$1.3x10^{-01}$ | 1.000 |

Ao, Aorta; CrCCA, cranial common carotid artery; CaCCA, caudal common carotid artery; EIA, external iliac artery; $PWV_{c-c}$, caudal carotid to cranial carotid artery pulse wave velocity; $PWV_{a-e}$,aorta to external iliac artery pulse wave velocity; $PWV_{c-e}$, carotid to external iliac artery pulse wave velocity; ∆D, arterial diameter change; $S_D$, arterial diameter strain; $DC_D$, arterial

distensibility coefficient calculated from diameter change; $CC_D$, arterial compliance coefficient, calculated from diameter change; SI, stiffness index; $\Delta A$, arterial lumen area change; $S_A$, arterial lumen area strain; $DC_A$, arterial distensibility coefficient calculated from area change; $CC_A$, arterial compliance coefficient calculated from lumen area change.

## Discussion

In our study, both regional and local AWS parameters were determined echocardiographically as described previously[35]. Regional AWS parameters describe the stiffness of an artery over a certain length, whereas local AWS parameters consider only a specific location of the arterial tree. In our study, echocardiographic measurements were performed at 4 arterial locations that met the following criteria: large, superficial arteries that are relatively easy to image using ultrasound. Therefore, the proximal aorta, the cranial and caudal common carotid artery and the external iliac artery were chosen. Regional AWS parameters were only assessed for the aorta and the common carotid artery because a large distance between 2 measuring sites, preferably on the same artery, is necessary to measure PWV reliably[26].

The aorta is of major interest when assessing AWS because the aorta makes a substantial contribution to the arterial buffering capacity[36]. In this study, both regional and local AWS parameters indicated a stiffer aorta in Friesian horses compared to Warmbloods. In accordance with the $PWV_{c\text{-}f}$ in human medicine, in our study the $PWV_{c\text{-}e}$ was calculated to assess the stiffness of the aorta. Although in human medicine $PWV_{c\text{-}f}$ is used as the gold standard method, we also calculated the $PWV_{a\text{-}e}$ to more accurately assess aortic stiffness. The $PWV_{c\text{-}e}$ assumes that the pulse wave travels at the same speed cranially (toward the carotid artery) and caudally (toward the external iliac artery), whereas our study shows that stiffness, and thus the velocity of the pulse wave, can differ substantially among different arteries. The $PWV_{a\text{-}e}$ on the other hand considers only the aorta itself and a very small part of the external iliac artery. Ideally, the aortic PWV should be measured between the proximal aorta and the aortic bifurcation into the external and internal iliac arteries. To examine the aortic bifurcation, transrectal ultrasonography would need to be performed. However, to avoid effects of stress on HR and BP, no transrectal ultrasound examination was performed, and the external iliac artery was examined instead. The $PWV_{a\text{-}e}$ as well as $PWV_{c\text{-}e}$ were significantly higher in Friesian horses compared to Warmbloods, indicating a stiffer aorta in Friesians. These higher PWV were not caused by a higher HR[37], because the HR in Friesians was not significantly different from that of Warmbloods. The stiffer aorta could be confirmed by local AWS parameters of the aorta: arterial diameter change, arterial compliance coefficient and arterial distensibility coefficient all were lower in Friesians. Arterial diameter strain also was lower and the stiffness index was higher in Friesians compared to Warmblood, but not

significantly. For the local AWS parameters of the cranial and caudal common carotid artery and the external iliac artery, most parameters did not differ significantly, indicating no difference in AWS of these vessels between Friesians and Warmbloods. Also the $PWV_{c\text{-}c}$, describing the regional AWS of the common carotid artery, wasn't significantly different between the breeds. These results suggest that in Friesians a difference in AWS is only present at the aortic level.

Systolic arterial blood pressure, DAP, MAP and PP were significantly higher in Friesian horses compared to Warmblood horses. Therefore, AWS parameters, especially those that do not include pressure, should be interpreted with caution. Whether the higher blood pressure in Friesians was the cause or the consequence of stiffer arteries cannot be determined from our results. In human medicine, primary hypertension is known to lead to an increase in collagen density, associated with an increase in AWS[9; 38]. Although the results found in our study did not indicate true hypertension, the continuously increased blood pressure in Friesians might lead to an increased amount of collagen in the Friesian aortic wall. Indeed, Friesians are known to have an increased amount of collagen in the tunica media of the aorta compared to Warmblood horses[12], in combination with a different collagen cross-linking pattern[10; 11]. As previously shown, an oversized cuff will underestimate blood pressure, whereas using a too small cuff in relation to tail circumference will overestimate it[39; 40]. In our study, tail circumference was significantly larger in Friesian horses (24.5 ± 1.1 cm) compared to Warmblood horses (22.3 ± 1.7 cm). The cuff bladder used was suitable for a tail circumference of 17-25 cm, ensuring a width-to-tail circumference ratio between 0.4 and 0.6. The only exceptions were 3 Friesians in which the tail circumference was slightly higher (26 cm in 1 horse and 27 cm in 2 horses), which could have led to slightly overestimated blood pressure. However, even when those 3 horses were excluded, MAP, SAP, DAP and PP remained significantly higher in the Friesian horses. Only 1 of the 3 horses had considerably higher blood pressure (SAP, 182 mmHg; DAP, 106 mmHg; MAP, 134 mmHg), but also a high PP (76 mmHg). The latter is not influenced by width-to-tail circumference ratio and therefore suggests that the pressure differences were not a measurement artifact. Also, CO and systemic vascular resistance (SVR) may affect BP. Cardiac output however was not different between breeds. Systemic vascular resistance was not measured in our study, but increased SVR can lead to a higher DAP[41], which was found in these Friesian horses. On the other hand, stiffer arteries will result in higher SAP and PP[32; 41], which also was found in our study. Friesians might therefore have a combination of increased AWS and increased SVR.

Another reason why AWS parameters should be interpreted with caution is the different body conformation of Friesian horses compared to Warmblood horses. Although differences were relatively small, investigated Friesians had significantly smaller height at the withers compared to Warmbloods (162 ± 4 cm vs. 167 ± 5 cm, respectively), whereas total body length (188 ±

11 cm vs. 180 ± 9 cm, respectively) and chest circumference (199 ± 7 cm vs. 195 ± 8 cm, respectively) were significantly larger. The smaller height at the withers of the Friesians might explain smaller blood vessel size. Because of this difference in diameter, relative stiffness parameters, such as arterial strain ($S_A$, $S_D$), distensibility coefficient ($DC_A$, $DC_D$) and stiffness index (SI), are preferred over absolute stiffness parameters, such as arterial diameter and area change ($\Delta D$; $\Delta A$) and compliance coefficient ($CC_D$, $CC_A$). The smaller arteries of Friesian horses, may lead to smaller absolute differences in area and lumen change during the cardiac cycle, which would wrongly suggest that arteries in Friesians are stiffer compared to Warmbloods when only absolute stiffness parameters would be considered.

Our study had a number of limitations. A major limitation was that only a small number of Warmblood horses were used to study the relation between *in vivo* horse length and *ex vivo* determined distance between the investigated arteries, and that no Friesian horses were included in this part of the study. As mentioned previously, Friesian horses have a different body conformation compared to Warmblood horses. Friesians are not only smaller with a larger chest circumference, but they also are longer compared to Warmblood horses. Friesians may have different arterial lengths in relation to body length, which may affect the calculated PWV and thus regional AWS results. An *ex vivo* study with more horses and including a group of Friesian horses would allow better definition of breed specific data and also would account for anatomical variations.

Another limitation of our study is the use of non-invasively determined arterial blood pressure. A previous study showed that non-invasively collected SAP, MAP and DAP correlated well with invasive measurements at the level of the facial or transverse facial artery, corrected to the level of the heart base, in the standing, normotensive, non-sedated horse[32]. Results found in our study, both for Friesians and Warmblood horses, were almost all within normal limits and thus can be considered representative of actual central blood pressure. In our study, coccygeal PP was used for calculation of aortic, common carotid and external iliac artery local AWS parameters, but PP is known to vary over the arterial tree[30] and might have been slightly different for the carotid artery, external iliac artery and aorta compared to the coccygeal artery. Nevertheless, the same method was used in both breeds, making comparison possible.

Overall, we conclude that Friesians have higher arterial blood pressure compared to Warmblood horses, in combination with a stiffer aorta. The higher SAP and PP, in combination with a higher DAP suggests that Friesians might have a combination of increased AWS and increased SVR. Whether the increased blood pressure is the cause or a consequence of the increased aortic AWS cannot be concluded from our study. These findings, in combination with the previously shown differences in amount and cross-linking pattern of collagen, make it highly

probable that the predisposition of Friesians to aortic rupture is, at least partially, related to increased AWS of the aorta. Additional *in vitro* biomechanical testing, should provide more insight.

## References

[1] Ploeg, M., Saey, V., van Loon, G. and Delesalle, C. (2017) Thoracic aortic rupture in horses. *Equine Vet J* **49**, 269-274.
[2] Sleeper, M.M., Durando, M.M., Miller, M., Habecker, P.L. and Reef, V.B. (2001) Aortic root disease in four horses. *J Am Vet Med Assoc* **219**, 491-496.
[3] Marr, C.M., Reef, V.B., Brazil, T.J., Thomas, W.P., Knottenbelt, D.C., Kelly, D.F., Baker, J.R., Reimer, J.M., Maxson, A.D. and Crowhurst, J.S. (1998) Aorto-cardiac fistulas in seven horses. *Vet Radiol Ultrasound* **39**, 22-31.
[4] Shirai, W., Momotani, E., Sato, T., Kashima, T., Saito, T. and Itoi, Y. (1999) Dissecting aortic aneurysm in a horse. *J Comp Pathol* **120**, 307-311.
[5] Ploeg, M., Saey, V., de Bruijn, C.M., Grone, A., Chiers, K., van Loon, G., Ducatelle, R., van Weeren, P.R., Back, W. and Delesalle, C. (2013) Aortic rupture and aorto-pulmonary fistulation in the Friesian horse: characterisation of the clinical and gross post mortem findings in 24 cases. *Equine Vet J* **45**, 101-106.
[6] van der Linde-Sipman, J.S., Kroneman, J., Meulenaar, H. and Vos, J.H. (1985) Necrosis and rupture of the aorta and pulmonary trunk in four horses. *Vet Pathol* **22**, 51-53.
[7] Ploeg, M., Saey, V., Delesalle, C., Grone, A., Ducatelle, R., de Bruijn, M., Back, W., van Weeren, P.R., van Loon, G. and Chiers, K. (2015) Thoracic Aortic Rupture and Aortopulmonary Fistulation in the Friesian Horse: Histomorphologic Characterization. *Veterinary Pathology* **52**, 152-159.
[8] Dobrin, P.B., Baker, W.H. and Gley, W.C. (1984) Elastolytic and collagenolytic studies of arteries. Implications for the mechanical properties of aneurysms. *Arch Surg* **119**, 405-409.
[9] Berillis, P. (2013) The Role of Collagen in the Aorta's Structure. *Open Circ and Vasc J* **6**, 1-8.
[10] Ploeg, M., Grone, A., van de Lest, C.H.A., Saey, V., Duchateau, L., Wolsein, P., Chiers, K., Ducatelle, R., van Weeren, P.R., de Bruijn, M. and Delesalle, C. (2017) Differences in extracellular matrix proteins between Friesian horses with aortic rupture, unaffected Friesians and Warmblood horses. *Equine Vet J* **49**, 609-613.
[11] Saey, V., Tang, J., Ducatelle, R., Croubels, S., De Baere, S., Schauvliege, S., van Loon, G. and Chiers, K. (2018) Elevated urinary excretion of free pyridinoline in Friesian horses suggests a breed-specific increase in collagen degradation. *Bmc Vet Res* **14**, 139.
[12] Saey, V., Ploeg, M., Delesalle, C., van Loon, G., Grone, A., Ducatelle, R., Duchateau, L. and Chiers, K. (2016) Morphometric Properties of the Thoracic Aorta of Warmblood and Friesian Horses with and without Aortic Rupture. *J Comp Pathol* **154**, 225-230.
[13] Ploeg, M., Saey, V., Delesalle, C., Grone, A., Ducatelle, R., de Bruijn, M., Back, W., van Weeren, P.R., van Loon, G. and Chiers, K. (2015) Thoracic aortic rupture and aortopulmonary fistulation in the Friesian horse: histomorphologic characterization. *Vet Pathol* **52**, 152-159.
[14] Yuan, S.M. and Jing, H. (2011) Cystic medial necrosis: pathological findings and clinical implications. *Rev Bras Cir Cardiovasc* **26**, 107-115.
[15] Schlatmann, T.J. and Becker, A.E. (1977) Histologic changes in the normal aging aorta: implications for dissecting aortic aneurysm. *Am J Cardiol* **39**, 13-20.
[16] Vine, N. and Powell, J.T. (1991) Metalloproteinases in degenerative aortic disease. *Clin Sci (Lond)* **81**, 233-239.
[17] Blacher, J., Guerin, A.P., Pannier, B., Marchais, S.J., Safar, M.E. and London, G.M. (1999) Impact of aortic stiffness on survival in end-stage renal disease. *Circulation* **99**, 2434-2439.

[18] Cruickshank, K., Riste, L., Anderson, S.G., Wright, J.S., Dunn, G. and Gosling, R.G. (2002) Aortic pulse-wave velocity and its relationship to mortality in diabetes and glucose intolerance: an integrated index of vascular function? *Circulation* **106**, 2085-2090.
[19] Laurent, S., Boutouyrie, P., Asmar, R., Gautier, I., Laloux, B., Guize, L., Ducimetiere, P. and Benetos, A. (2001) Aortic stiffness is an independent predictor of all-cause and cardiovascular mortality in hypertensive patients. *Hypertension* **37**, 1236-1241.
[20] Inoue, N., Maeda, R., Kawakami, H., Shokawa, T., Yamamoto, H., Ito, C. and Sasaki, H. (2009) Aortic pulse wave velocity predicts cardiovascular mortality in middle-aged and elderly Japanese men. *Circ J* **73**, 549-553.
[21] Safar, M.E., Henry, O. and Meaume, S. (2002) Aortic pulse wave velocity: an independent marker of cardiovascular risk. *Am J Geriatr Cardiol* **11**, 295-298.
[22] Messas, E., Pernot, M. and Couade, M. (2013) Arterial wall elasticity: state of the art and future prospects. *Diagn Interv Imaging* **94**, 561-569.
[23] Davies, J.I. and Struthers, A.D. (2003) Pulse wave analysis and pulse wave velocity: a critical review of their strengths and weaknesses. *J Hypertens* **21**, 463-472.
[24] Van Bortel, L.M., Laurent, S., Boutouyrie, P., Chowienczyk, P., Cruickshank, J.K., De Backer, T., Filipovsky, J., Huybrechts, S., Mattace-Raso, F.U., Protogerou, A.D., Schillaci, G., Segers, P., Vermeersch, S., Weber, T., Artery, S., European Society of Hypertension Working Group on Vascular, S., Function and European Network for Noninvasive Investigation of Large, A. (2012) Expert consensus document on the measurement of aortic stiffness in daily practice using carotid-femoral pulse wave velocity. *J Hypertens* **30**, 445-448.
[25] Hoeks, A.P.G., Brands, P.J., Willigers, J.M. and Reneman, R.S. (1999) Non-invasive measurement of mechanical properties of arteries in health and disease. *Proceedings of the Institution of Mechanical Engineers Part H-Journal of Engineering in Medicine* **213**, 195-202.
[26] Laurent, S., Cockcroft, J., Van Bortel, L., Boutouyrie, P., Giannattasio, C., Hayoz, D., Pannier, B., Vlachopoulos, C., Wilkinson, I., Struijker-Boudier, H. and European Network for Non-invasive Investigation of Large, A. (2006) Expert consensus document on arterial stiffness: methodological issues and clinical applications. *Eur Heart J* **27**, 2588-2605.
[27] Jiang, B., Liu, B., McNeill, K.L. and Chowienczyk, P.J. (2008) Measurement of pulse wave velocity using pulse wave Doppler ultrasound: comparison with arterial tonometry. *Ultrasound Med Biol* **34**, 509-512.
[28] Calabia, J., Torguet, P., Garcia, M., Garcia, I., Martin, N., Guasch, B., Faur, D. and Valles, M. (2011) Doppler ultrasound in the measurement of pulse wave velocity: agreement with the Complior method. *Cardiovasc Ultrasound* **9**, 13.
[29] Carroll, C.L. and Huntington, P.J. (1988) Body Condition Scoring and Weight Estimation of Horses. *Equine Veterinary Journal* **20**, 41-45.
[30] Izzo, J.L., Jr. (2014) Brachial vs. central systolic pressure and pulse wave transmission indicators: a critical analysis. *Am J Hypertens* **27**, 1433-1442.
[31] O'Rourke, M.F., Staessen, J.A., Vlachopoulos, C., Duprez, D. and Plante, G.E. (2002) Clinical applications of arterial stiffness; definitions and reference values. *Am J Hypertens* **15**, 426-444.
[32] Heliczer, N., Lorello, O., Casoni, D. and Navas de Solis, C. (2016) Accuracy and Precision of Noninvasive Blood Pressure in Normo-, Hyper-, and Hypotensive Standing and Anesthetized Adult Horses. *J Vet Intern Med* **30**, 866-872.
[33] Boegli, J., Schwarzwald, C.C. and Mitchell, K.J. (2019) Diagnostic value of noninvasive pulse pressure measurements in Warmblood horses with aortic regurgitation. *J Vet Intern Med* **33**, 1446-1455.
[34] Ven, S., Decloedt, A., Van der Vekens, N., De Clercq, D. and van Loon, G. (2016) Assessing aortic regurgitation severity from 2D, M-mode and pulsed wave Doppler echocardiographic measurements in horses. *Veterinary Journal* **210**, 34-38.
[35] Vera, L., De Clercq, D., Paulussen, E., Broux, B., Ven, S., Van Steenkiste, G. and van Loon, G. (2019) Measurement of aortic, common carotid artery and external iliac artery arterial wall stiffness in horses: inter-day, inter-observer and intra-observer variability. *Equine Veterinary Journal*.

[36] Lyle, A.N. and Raaz, U. (2017) Killing Me Unsoftly Causes and Mechanisms of Arterial Stiffness. *Arterioscl Throm Vas* **37**, E1-E11.
[37] Tan, I., Butlin, M., Liu, Y.Y., Ng, K. and Avolio, A.P. (2012) Heart Rate Dependence of Aortic Pulse Wave Velocity at Different Arterial Pressures in Rats. *Hypertension* **60**, 528-533.
[38] von Maltzahn, W.W., Besdo, D. and Wiemer, W. (1981) Elastic properties of arteries: a nonlinear two-layer cylindrical model. *J Biomech* **14**, 389-397.
[39] Hatz, L.A., Hartnack, S., Kummerle, J., Hassig, M. and Bettschart-Wolfensberger, R. (2015) A study of measurement of noninvasive blood pressure with the oscillometric device, Sentinel, in isoflurane-anaesthetized horses. *Vet Anaesth Analg* **42**, 369-376.
[40] Taylor, P.M. (1981) Techniques and clinical application of arterial blood pressure measurement in the horse. *Equine Vet J* **13**, 271-275.
[41] Oliver, J.J. and Webb, D.J. (2003) Noninvasive assessment of arterial stiffness and risk of atherosclerotic events. *Arterioscler Thromb Vasc Biol* **23**, 554-566.

# CHAPTER 6:

# AGE-RELATED DIFFERENCES IN BLOOD PRESSURE, ULTRASOUND-DERIVED ARTERIAL DIAMETERS AND ARTERIAL WALL STIFFNESS PARAMETERS IN HORSES

# Age-related differences in blood pressure, ultrasound-derived arterial diameters and arterial wall stiffness parameters in horses

Lisse Vera[1], Glenn Van Steenkiste[1]; Annelies Decloedt[1], Koen Chiers[2], Gunther van Loon[1]

[1]Equine Cardioteam Ghent University, Department of Large Animal Internal Medicine, Faculty of Veterinary Medicine, Ghent University, Merelbeke, Belgium

[2]Department of Pathology, Bacteriology and Poultry Diseases, Faculty of Veterinary Medicine, Ghent University, Merelbeke, Belgium

**Ethical animal research**

The study was approved by the ethical committee of the Faculty of Veterinary Medicine and Bioscience Engineering (EC 2018/111). Horses were privately owned and for all examinations informed owner consent was obtained.

**Acknowledgements**

We want to acknowledge the owners for letting their horses participate in our study.

Adapted from:

**Lisse Vera**, Glenn Van Steenkiste, Annelies Decloedt, Koen Chiers and Gunther van Loon. 2020. “Age-related Differences in Blood Pressure, Ultrasound-Derived Arterial Diameters and Arterial Wall Stiffness Parameters in Horses.” EQUINE VETERINARY JOURNAL. (Online ahead of print; doi: 10.1111/evj.13263)

## Abstract

**Background:** Arterial rupture mainly affects older horses. The reason why older horses are more prone to arterial rupture and which underlying vascular changes predispose older horses to aortic rupture is still unclear. **Objectives:** To investigate the effect of ageing on the equine arterial wall and blood pressure. **Study design:** Cohort study. **Methods**: Non-invasive blood pressure measurement using a tail cuff and vascular ultrasound from aorta, common carotid artery and external iliac artery was performed in 50 healthy young (3-7 years) and 50 healthy old Warmblood horses (>18 years). Arterial diameters and cross-sectional areas, and arterial wall thickness were measured offline. Regional arterial wall stiffness of the aorta and common carotid artery was assessed using pulse wave velocity, while lumen area/diameter change, strain, compliance and distensibility were calculated to assess local arterial wall stiffness. **Results:** No difference in blood pressure was found between old and young horses. All arterial dimensions and intima-media thickness of the common carotid artery were significantly larger in old horses. A significantly higher local arterial wall stiffness was found for the aorta and the caudal common carotid artery in older horses. For the external iliac artery, no significant differences in arterial wall stiffness were found. Both aortic and carotid pulse wave velocity were higher in older horses compared to younger horses. **Main limitations:** Blood pressure was measured non-invasively. **Conclusions:** In horses, arteries stiffen with age, in combination with luminal enlargement and arterial wall thickening. This might, at least partially, explain the increased incidence of arterial rupture in older horses.

## Introduction

In human medicine, the arterial wall is known to stiffen with age, together with luminal enlargement and arterial wall thickening [1; 2]. This increased stiffness is a significant predictor of cardiovascular disease, independent of other cardiovascular risk factors [3]. The most important structural changes leading to progressive stiffening of large arteries are a reduction in medial vascular smooth muscle cells and medial degeneration with fragmentation of elastic laminae and sclerosis due to repetitive pulsations (around 21 million pulsations/year) [1; 3; 4]. Another important factor in the ageing process is the glycation of collagen and elastin, leading to the formation of advanced glycation end-products and related molecular cross-links, which modifies the mechanical properties of the arterial wall [1; 5].

There are several non-invasive methods to evaluate regional (over a certain length of the arterial tree) and local (at one specific place of the arterial tree) arterial wall stiffness. The gold standard method to assess regional arterial wall stiffness in human patients is pulse wave velocity. The pulse wave velocity is calculated as the distance travelled by the pulse wave divided by the time it takes to travel that distance [6]. Increased arterial wall stiffness, indicating

stiffer arteries, will lead to an increased pulse wave velocity. Calculation of the local arterial wall stiffness is based on variations in vascular size during the cardiac cycle [7]. The smaller the variation between systolic and diastolic measurements, the stiffer the investigated artery.

In horses, little is known about the alteration in vascular properties due to ageing. Nevertheless, arterial rupture is known to occur more often in older horses, especially associated with parturition in mares [8] or coitus in stallions [9], intense exercise or the administration of α1-agonists for treatment of left dorsal displacement of the large colon (nephrosplenic entrapment) [10]. This might imply that structural changes of the arterial wall due to ageing are likely to be one of the contributing factors leading to arterial rupture. Therefore, we hypothesised that horses show age-related stiffening of the arterial wall.

## Materials and methods

### Horses

Cardiovascular ultrasound was performed in 50 young (3-7 years) and 50 old (>18 years) healthy Warmblood horses. Exclusion criteria were: more than a 2/6 left- or right-sided systolic or diastolic murmur on auscultation, more than a mild regurgitation visible using colour Doppler ultrasound or presence of atrial or ventricular premature beats during a 15 min electrocardiogram recording at rest. In all horses, height at the withers, chest circumference, tail circumference and length of the horse, between the most cranial point of the shoulder and the tuber ischiadicum, were measured. Body weight was calculated as length x (chest circumference)$^2$ / 11900 [11].

### Blood pressure

Systolic (SAP), diastolic (DAP) and mean (MAP) arterial blood pressure were measured non-invasively (Cardell Veterinary Monitor[a]) and at the same time ultrasonography was performed. A cuff with a width of 9 cm was placed around the base of the tail, ensuring a width to tail circumference ratio between 0.4 and 0.6 [12; 13]. Readings were corrected to the level of the heart base by adding a correction factor of 0.77 mmHg for every cm difference between the right atrium (estimated at the height of the shoulder) and the cuff [12]. The average of 5 consistent measurements was taken.

### Ultrasound

Ultrasound images (Vivid IQ[b]) were collected in the standing, non-sedated horse, with a heart rate (HR) below 50 beats per minute. Stroke volume (SV) was calculated as pulsed-wave Doppler derived aortic velocity time integral (left parasternal view) multiplied by aortic valve cross-sectional area (right parasternal view) [14]. Cardiac output (CO) was determined as SV

x HR. For determining the arterial wall stiffness, ultrasound images of the aorta, the right caudal and cranial common carotid artery and the right external iliac artery were collected as described previously [15; 16]. In brief, a right ventricular outflow tract view was obtained to measure aortic diameters. From the caudal (15 cm before the thoracic inlet) and cranial common carotid artery (45 cm before the thoracic inlet), cross-sectional B- and M-mode images were recorded in order to calculate arterial areas and diameters, respectively, and for the external iliac artery cross-sectional B- and longitudinal M-mode images were obtained from the inguinal region for calculation of arterial areas and diameters, respectively. Diastolic measurements were performed on the R peak of the simultaneously recorded electrocardiogram (base-apex configuration) and systolic measurements were performed at maximal dilation. Measurements were never performed in a cardiac cycle following a second-degree atrioventricular block. Arterial wall thickness was evaluated by measuring the intima-media thickness (IMT) during maximal dilation from longitudinal images of the caudal common carotid artery. For each data point, averages were calculated from 3 consecutive beats.

**Local arterial wall stiffness**

All local arterial wall stiffness parameters were calculated as described previously [15; 16].

The arterial diameter ($\Delta D$) or lumen area change ($\Delta A$) describes the difference between the systolic (s) and diastolic (d) diameter (D) or area (A).

$\Delta D = Ds - Dd$; $\Delta A = As - Ad$

The arterial diameter ($S_D$) or lumen area strain ($S_A$) describes the relative change in diameter or lumen area during the cardiac cycle.

$S_D = \Delta D/Dd$; $S_A = \Delta A/Ad$

The arterial diameter distensibility coefficient ($DC_D$) or arterial lumen area distensibility coefficient ($DC_A$) describes the relative diameter or area change in relation to pulse pressure (PP). The PP is defined as SAP – DAP.

$DC_D = (\Delta D/Dd)/PP$; $DC_A = (\Delta A/Ad)/PP$.

The arterial diameter compliance coefficient ($CC_D$) or arterial lumen area compliance coefficient ($CC_A$) describes the absolute diameter/area change in relation to pulse pressure (PP).

$CC_D = \Delta D/PP$; $CC_A = \Delta A/PP$

The stiffness index describes the ratio of the natural logarithm (systolic/diastolic pressure) to the relative change in diameter.

SI = ln (SAP/DAP)/(∆D/Dd).

**Regional arterial wall stiffness**

All regional arterial wall stiffness parameters were calculated as described previously[15; 16].

Regional arterial wall stiffness was assessed using pulse wave velocity. The pulse wave velocity represents how fast the pressure wave travels between two locations along the arterial tree and is calculated as the difference in distance between the two investigated arteries (∆Dist) divided by the difference in time delay (∆t) [6; 17]. As described previously, pulsed wave Doppler was used to measure the pulse wave velocity [15; 16]. The difference in time delay (∆t), at every location (aorta, cranial and caudal common carotid artery, and external iliac artery), was calculated as time delay (ms) between the R wave of the synchronised electrocardiogram and the onset (foot) of the waveform. The mean time delay (calculated from 3 times 3 consecutive beats) at the location closest to the heart (shortest time delay) was subtracted from the mean time delay at the location most distant from the heart (longest time delay).

The caudal to cranial common carotid artery pulse wave velocity ($PWV_{c-c}$) represents the velocity at which the pressure wave travels from the caudal to cranial common carotid artery.

$PWV_{c-c}$ (m/s) = $\Delta Dist_{c-c}$ (m)/$\Delta t_{c-c}$ (s). A fixed distance of 0.3 m between both measuring places ($\Delta Dist_{c-c}$) was taken [15].

The aorta to external iliac artery pulse wave velocity ($PWV_{a-e}$) represents the velocity at which the pressure wave travels between the aorta and the external iliac artery.

$PWV_{a-e}$ (m/s) = $\Delta Dist_{a-e}$ (m)/$\Delta t_{a-e}$ (s). $\Delta Dist_{a-e}$ represents the distance between the aortic valve and the external iliac artery and was calculated as length of the horse(m) x 0.62 [15].

The carotid to external iliac artery pulse wave velocity ($PWV_{c-e}$) represents the velocity at which the pressure wave travels between the caudal common carotid artery and the external iliac artery.

$PWV_{c-e}$ (m/s) = $\Delta Dist_{c-e}$ (m)/$\Delta t_{c-e}$ (s). $\Delta Dist_{c-e}$ represents the difference in distance relative to the aortic root between the caudal carotid and external iliac artery and was calculated as length of the horse (m)x0.62 – 0.40 m [15].

**Data analysis**

Normality of all variables and derived arterial wall stiffness parameters was checked graphically, using Q-Q plots. Arterial diameters and areas, arterial blood pressures, pulse wave velocity, CO and HR were compared between young and old Warmblood horses using an

independent samples t-test. For derived local stiffness values, a univariate model was built including age (young or old) and location (aorta, caudal common carotid artery, cranial common carotid artery and external iliac artery) as fixed factors and horse as a random factor. Interaction was found between location and age, therefore a univariate model, including location*age as a fixed factor and horse as a random factor with post hoc Bonferroni correction for multiple comparisons was applied (SPSS Statistics 25[c]). P-values ≤0.05 were considered statistically significant.

## Results

Mean ± SD age was 5 ± 1 years for the young horses and 21 ± 3 year for the old horses. Mean ± SD body weight of the old horses (558 ± 109 kg) was not significantly different compared to the young horses (535 ± 51 kg; P=0.19), neither was the height at the withers (167 ± 5 cm vs. 168 ± 5 cm; P=0.44). Mean SAP (131 ± 16 mmHg vs. 134 ± 15 mmHg; P=0.44), DAP (86 ± 15 mmHg vs. 91 ± 11 mmHg; P=0.09) and MAP (101 ± 16 mmHg vs. 106 ± 12 mmHg; P=0.08) were not significantly different between old and young horses, respectively. Also, the PP was not significantly different in the older horses (45 ± 9 mmHg) compared to the younger horses (43 ± 9 mmHg; P=0.27). Cardiac output was significantly lower in older horses (34.04 ± 13.97 L/min) compared to younger horses (40.12 ± 11.55 L/min; P=0.02), while no significant difference in HR was found (37 ± 6 bpm vs. 36 ± 7 bpm; P=0.38, respectively).

All systolic and diastolic arterial diameters and areas were significantly larger in the old horses compared to the young horses, in combination with an enlarged IMT of the caudal common carotid artery. Details can be found in Table 1. For the aorta all derived local arterial wall stiffness parameters, namely the diameter change ($\Delta D$), the strain ($S_D$), the distensibility coefficient ($DC_D$) and compliance coefficient ($CC_D$) were significantly lower in old compared to young horses, in combination with a higher stiffness index (SI). For the caudal common carotid artery, most of the local arterial wall stiffness parameters, namely the strain ($S_D$ and $S_A$), the distensibility coefficient ($DC_D$ and $DC_A$) and the compliance coefficient ($CC_A$) were significantly lower in old horses, in combination with a significantly higher stiffness index (SI). For the cranial common carotid artery, only the strain ($S_A$) was significantly lower in the old horses group. No significant differences in local arterial wall stiffness parameters were found at the level of the external iliac artery. Overall, differences between local arterial wall stiffness parameters indicated that the arterial elasticity significantly decreased from the central arteries (aorta) towards the more peripheral arteries (caudal common carotid artery, cranial common carotid artery and external iliac artery). All local arterial wall stiffness parameters and their mutual relations can be found in Table 2. All considered regional arterial wall stiffness parameters

($PWV_{c-e}$, $PWV_{a-e}$ and $PWV_{c-c}$) were higher in old compared to young horses. All derived regional arterial wall stiffness parameters can be found in Table 3.

Table 1. Comparison of (mean ± SD) internal diastolic and systolic diameters and areas of the aorta, the caudal and cranial common carotid artery and the external iliac artery and the intima-media thickness of the caudal common carotid artery between young (3-7 years) horses and old (>18 years) horses.

| | | Young | Old | P-value |
|---|---|---|---|---|
| Aorta | Dd (mm) | 59 ± 5 | 65 ± 6 | <0.001 |
| | Ds (mm) | 65 ± 5 | 70 ± 6 | <0.001 |
| Caudal common carotid artery | Dd (mm) | 11.2 ± 1 | 12.3 ± 1.4 | <0.001 |
| | Ds (mm) | 12.2 ± 1.1 | 13.1 ± 1.4 | 0.001 |
| | Ad ($mm^2$) | 105.5 ± 21.1 | 129.1 ± 29.7 | <0.001 |
| | As ($mm^2$) | 119.8 ± 23.6 | 141.7 ± 31.6 | <0.001 |
| | IMT (mm) | $7.2x10^{-2} \pm 1.0x10^{-2}$ | $8.8x10^{-2} \pm 1.5x10^{-2}$ | <0.001 |
| Cranial common carotid artery | Dd (mm) | 9.8 ± 0.8 | 10.7 ± 1.0 | <0.001 |
| | Ds (mm) | 10.3 ± 0.9 | 11.2 ± 1.0 | <0.001 |
| | Ad ($mm^2$) | 71.7 ± 13.3 | 92.0 ± 19.3 | <0.001 |
| | As ($mm^2$) | 79.2 ± 14.0 | 99.6 ± 20.0 | <0.001 |
| External iliac artery | Dd (mm) | 11.5 ± 1.1 | 12.0 ± 1.4 | 0.028 |
| | Ds (mm) | 11.9 ± 1.2 | 12.3 ± 1.4 | 0.032 |
| | Ad ($mm^2$) | 122.3 ± 28.2 | 135.3 ± 28.4 | <0.001 |
| | As ($mm^2$) | 131.6 ± 30.2 | 144.8 ± 28.9 | <0.001 |

Table 2. Comparison of local arterial wall stiffness parameters (mean (SD)) for the aorta, the caudal (CaCCA) and cranial common carotid artery (CrCCA) and the external iliac artery (EIA) between young horses and old horses.

| | | ΔD (mm) | $S_D$ | $DC_D$ (/mmHg) | $CC_D$ (mm/mmHg) | SI | ΔA ($mm^2$) | $S_A$ | $DC_A$ (/mmHg) | $CC_A$ ($mm^2$/mmHg) |
|---|---|---|---|---|---|---|---|---|---|---|
| Aorta | Young | **6.5** A | **$1.1x10^{-1}$** A | **$2.8x10^{-3}$** A | **$1.6x10^{-1}$** A | **2.7** A | NA | NA | NA | NA |
| | | (2.1) | ($0.4x10^{-1}$) | ($1.1x10^{-3}$) | ($0.7x10^{-1}$) | (0.4) | | | | |
| | Old | **5.5** B | **$0.8x10^{-1}$** B | **$2.0x10^{-3}$** B | **$1.3x10^{-1}$** B | **3.0** B | NA | NA | NA | NA |
| | | (1.7) | ($0.3x10^{-1}$) | ($0.8x10^{-3}$) | ($0.5x10^{-1}$) | (0.4) | | | | |
| | P-value | <0.001 | <0.001 | <0.001 | <0.001 | 0.015 | NA | NA | NA | NA |
| CaCCA | Young | 1.0 A | **$9.0x10^{-2}$** A,C | **$2.2x10^{-3}$** A,C | $2.5x10^{-2}$ A | **2.9** C | 14.3 A | $1.4x10^{-1}$ A | $3.5x10^{-3}$ A | $3.7x10^{-1}$ A |
| | | (0.03) | ($3.0x10^{-2}$) | ($1.1x10^{-3}$) | ($1.2x10^{-2}$) | (0.3) | (6.4) | ($0.6x10^{-1}$) | ($2.3x10^{-3}$) | ($2.9x10^{-1}$) |
| | Old | 0.8 B | **$6.5x10^{-2}$** B,D | **$1.6x10^{-3}$** B,D | $1.9x10^{-2}$ | **3.3** D | 12.6 B | $1.0x10^{-1}$ B | $2.3x10^{-3}$ | $1.9x10^{-1}$ |
| | | (0.3) | ($2.6x10^{-2}$) | ($0.8x10^{-3}$) | ($1.0x10^{-2}$) | (0.4) | (5.6) | ($0.4x10^{-1}$) | ($1.0x10^{-3}$) | ($1.1x10^{-1}$) |
| | P-value | 1 | <0.001 | <0.001 | 1 | <0.001 | 0.703 | <0.001 | <0.001 | 0.035 |
| CrCCA | Young | $5.5x10^{-1}$ A | $5.6x10^{-2}$ A,C,E | $1.4x10^{-3}$ A,C,E | $1.4x10^{-2}$ A | 3.4 A,C,E | 7.5 A | $1.1x10^{-1}$ B,C | $2.7x10^{-3}$ A,B | $1.9x10^{-1}$ A |
| | | ($1.5x10^{-1}$) | ($1.5x10^{-2}$) | ($0.5x10^{-3}$) | ($0.6x10^{-2}$) | (0.3) | (3.0) | ($0.4x10^{-1}$) | ($1.5x10^{-3}$) | ($1.1x10^{-1}$) |
| | Old | $5.1x10^{-1}$ B | $4.9x10^{-2}$ B,D,F | $1.1x10^{-3}$ B,D | $1.2x10^{-2}$ **B** | 3.6 B,D,F | 7.3 B | $8.8x10^{-2}$ | $2.0x10^{-3}$ | $1.8x10^{-1}$ |
| | | ($1.6x10^{-1}$) | ($1.7x10^{-2}$) | ($0.5x10^{-3}$) | ($0.5x10^{-2}$) | (0.4) | (3.2) | ($4.6x10^{-2}$) | ($1.0x10^{-3}$) | ($0.9x10^{-1}$) |
| | P-value | 1 | 1 | 1 | 1 | 0.458 | 1 | 0.402 | 0.045 | 1 |
| EIA | Young | $4.4x10^{-1}$ A | $3.9x10^{-2}$ A,C,E | $9.3x10^{-4}$ A,C,E | $1.0x10^{-2}$ A | 3.9 A,C,E | 9.3 A | $7.6x10^{-2}$ A,C | $1.9x10^{-3}$ A,B | $2.3x10^{-1}$ A |
| | | ($3.0x10^{-1}$) | ($2.6x10^{-2}$) | ($6.2x10^{-4}$) | ($0.7x10^{-2}$) | (0.7) | (3.6) | ($2.3x10^{-2}$) | ($0.8x10^{-3}$) | ($1.1x10^{-1}$) |
| | Old | $3.8x10^{-1}$ B | $3.2x10^{-2}$ B,D,F | $7.5x10^{-4}$ B,D | $0.9x10^{-2}$ B | 4.0 B,D,F | 9.5 B | $7.3x10^{-2}$ B | $1.7x10^{-3}$ | $2.2x10^{-1}$ |
| | | ($1.7x10^{-1}$) | ($1.5x10^{-2}$) | ($3.9x10^{-4}$) | ($0.5x10^{-2}$) | (0.5) | (3.4) | ($2.9x10^{-2}$) | ($0.7x10^{-3}$) | ($1.0x10^{-1}$) |
| | P-value | 1 | 1 | 1 | 1 | 1 | 1 | 1 | 1 | 1 |

$\Delta D$, arterial diameter change; $S_D$, arterial diameter strain; $DC_D$, arterial distensibility coefficient calculated from diameter change; $CC_D$, arterial compliance coefficient calculated from diameter change; SI, stiffness index; $\Delta A$, arterial lumen area change; $S_A$, arterial lumen area strain; $DC_A$, arterial distensibility coefficient calculated from area change; $CC_A$, arterial compliance coefficient calculated from lumen area change;

Bold values indicate significant difference between young and old horses. For each parameter, similar superscripts indicate a significant difference between locations within the young or within the old horses for the investigated parameter.

Table 3. Comparison of regional arterial wall stiffness parameters for the aorta, and the common carotid artery between young horses and old horses.

| | Young | | Old | | |
|---|---|---|---|---|---|
| | Mean | SD | Mean | SD | P-value |
| PWVc-c (m/s) | 6.5 | 2.2 | 9.5 | 8.1 | 0.014 |
| PWVa-e (m/s) | 5.3 | 0.6 | 6.2 | 1.3 | <0.001 |
| PWVc-e (m/s) | 4.6 | 0.8 | 6.0 | 2.2 | <0.001 |

$PWV_{c\text{-}c}$, caudal carotid to cranial carotid artery pulse wave velocity; $PWV_{a\text{-}e}$, aorta to external iliac artery pulse wave velocity; $PWV_{c\text{-}e}$, carotid to external iliac artery pulse wave velocity.

## Discussion

In this study, horses from 3-7 years of age were included in the young group, while horses > 18 years were included in the old group. The limit of 3 years was set in order to avoid the increasing elasticity phase as seen in not fully grown, pubertal children[18]. An obvious age-related decline in elasticity was found in humans after 50 years of age[19], which is about 62% of the life expectancy[20]. Therefore, in this study, horses were considered old if > 18 years, which is about 62% of the life expectancy in horses[21].

In human medicine, the arterial wall stiffens with age[1; 2], mainly affecting the large, central arteries[22]. Our study demonstrates similar age-related changes in horses. Stiffer arteries were found in older horses. This effect was also most pronounced in the central arteries, namely the aorta and the caudal common carotid artery, compared to the more peripheral arteries, such as the cranial common carotid artery and the external iliac artery. The significantly stiffer aorta in older horses was demonstrated by a lower diameter change, strain, distensibility and compliance and a higher stiffness index, in combination with higher values for $PWV_{a\text{-}e}$ and $PWV_{c\text{-}e}$. For the common carotid artery, the $PWV_{c\text{-}c}$ was significantly higher in old horses, while only the local arterial wall stiffness parameters of the caudal common carotid artery, and not the more peripheral cranial common carotid artery, indicated increased stiffness. For the external iliac artery, the most peripheral artery included in this study, local arterial wall stiffness parameters didn't show any significant difference between young and old horses.

In human patients differences in arterial wall composition between central and more peripheral arteries have been well studied. Central arteries are known to contain a higher percentage of elastic fibres and therefore have better elastic capacities[23]. Previously, the amount of elastin in the medial layer of the mid-thoracic aortic wall in Warmblood horses has been shown to be

around 42%[24], but to the best of our knowledge, nothing is known about the difference in composition between other arteries. Results of our study indicate that, irrespective of age, the larger central arteries are more compliant compared to the smaller, more peripheral arteries, probably due to a higher elastin content. Local stiffness of the arterial wall increased significantly from the aorta, over the caudal common carotid artery and the cranial carotid artery to the external iliac artery.

In Warmblood horses, aortic rupture itself is mostly observed in aged stallions, during coitus or shortly thereafter[9], while also the smaller, more peripheral arteries seem to be susceptible to arterial rupture due to ageing, for example uterine artery rupture in older mares [8] or phenylephrine-associated haemorrhage in aged horses[8; 10]. In racehorses post mortem examinations of sudden deaths during intense exercise reveal arterial rupture of smaller, more peripheral arteries as a common cause of sudden death, while aortic rupture itself is rather rare [25].Results of our study reveal significant age-related differences in arterial wall stiffness at the level of the aorta and the caudal common carotid artery, but not at the level of the cranial common carotid and the external iliac artery. Nevertheless, larger arterial diastolic and systolic areas and diameters were found for all investigated arteries, indicating age-related breakdown of the elastic laminae in all investigated arteries[26]. These findings suggest that ageing occurs in peripheral arteries but that the process is less pronounced in the already stiffer vessels. Age-related increase in IMT could only be confirmed for the caudal common carotid artery, as the IMT of the aorta and external iliac artery were not evaluated due to insufficient image quality which did not allow for wall layer differentiation. The IMT of the cranial common carotid artery could have been assessed, but was not included in this study.

This intima-media thickening can be explained by peripheral arterial remodelling, due to changes in aortic stiffness. In human medicine, it is known that in the elderly changes in large artery stiffness lead to systolic hypertension in combination with a widened PP[27]. The arterial pressure wave is the result of the forward pressure wave (arising from left ventricular systole), and the backward, reflected pressure wave. The backward reflection wave normally arrives at the aortic root during diastole, increasing the DAP and supporting coronary circulation. Due to increased aortic stiffness, the reflection wave may arrive earlier at the aortic root, even during systole. This will increase SAP but also decrease DAP, resulting in a wider PP. This wider PP will be transmitted to the peripheral arteries, causing arterial remodelling, namely intima-media thickening, due to accumulation of collagen and proteoglycans in the tunica intima[28], and further stiffening of the arterial wall in a vicious circle[29]. Moreover, the elevated SAP will induce left ventricular hypertrophy and the increased left ventricular afterload will increase myocardial oxygen demand. However, myocardial blood supply will decrease due to reduced diastolic pressure. Therefore, in human patients, myocardial infarction, chronic ischemic heart

disease or sudden cardiac death due to arrhythmia may occur[30]. In our study, despite the difference in arterial wall stiffness, no differences in SAP, DAP or PP were found between old and young horses. The rather small increase in aortic stiffness found in horses (35% increase in $PWV_{c-e}$), compared to the increase observed in human patients (around 50%[31; 32]), makes it probable that the backward pressure wave arrived in early diastole, rather than during systole. This finding, in combination with a similar decrease in CO (18% found in this study vs. 22% in human patients[33]) might explain why no increase in SAP, nor a decrease in DAP and thus no widening in the PP was found in our study. This decrease in CO can be explained by the lower plasma volume[34] and altered ventricular function in older horses[35]. A limitation of our study, which can also explain why small differences in blood pressure might be not detected, is the non-invasive measurement of the arterial blood pressure. Heliczer et al. [12], however, showed that non-invasively collected SAP, MAP and DAP correlated well with invasive measurements, in the standing, normotensive, non-sedated horse.

Overall, our results indicate that horses present age-related arterial wall stiffening, in combination with luminal enlargement and arterial wall thickening, which might be related to the higher incidence of arterial rupture in older horses. Moreover, results reveal that arterial compliance decreases towards the periphery. Histologic examination of the arterial wall should be performed to investigate local differences in arterial wall composition and the effect of ageing on arterial wall morphology.

## Manufacturers' addresses

[a] Midmark, Versailles, Ohio, USA

[b] GE Healthcare, Diegem, Belgium

[c] SPSS Statistics, Chicago, Illinois, USA

## References

[1] Lee, H.Y. and Oh, B.H. (2010) Aging and arterial stiffness. *Circ J* **74**, 2257-2262.
[2] Mikael, L.R., Paiva, A.M.G., Gomes, M.M., Sousa, A.L.L., Jardim, P., Vitorino, P.V.O., Euzebio, M.B., Sousa, W.M. and Barroso, W.K.S. (2017) Vascular Aging and Arterial Stiffness. *Arq Bras Cardiol* **109**, 253-258.
[3] O'Rourke, M.F. and Hashimoto, J. (2007) Mechanical factors in arterial aging - A clinical perspective. *Journal of the American College of Cardiology* **50**, 1-13.
[4] Lee, S.J. and Park, S.H. (2013) Arterial Ageing. *Korean Circulation Journal* **43**, 73-79.
[5] Atanasova, M., Dimitrova, A., Ruseva, B., Stoyanova, A., Georgieva, M. and Konova, E. (2012) Quantification of Elastin, Collagen and Advanced Glycation End Products as Functions of Age and Hypertension In: *Senescence* Ed: T. Nagata, InTech. p 850.
[6] Laurent, S., Cockcroft, J., Van Bortel, L., Boutouyrie, P., Giannattasio, C., Hayoz, D., Pannier, B., Vlachopoulos, C., Wilkinson, I., Struijker-Boudier, H. and European Network for Non-invasive Investigation of Large, A. (2006) Expert consensus document on arterial stiffness: methodological issues and clinical applications. *Eur Heart J* **27**, 2588-2605.

[7] Messas, E., Pernot, M. and Couade, M. (2013) Arterial wall elasticity: state of the art and future prospects. *Diagn Interv Imaging* **94**, 561-569.
[8] Williams, N.M. and Bryant, U.K. (2012) Periparturient Arterial Rupture in Mares: A Postmortem Study. *Journal of Equine Veterinary Science* **32**, 281-284.
[9] Rooney, J.R., Prickett, M.E. and Crowe, M.W. (1967) Aortic ring rupture in stallions. *Pathol Vet* **4**, 268-274.
[10] Frederick, J., Giguere, S., Butterworth, K., Pellegrini-Masini, A., Casas-Dolz, R. and Turpin, M.M. (2010) Severe phenylephrine-associated hemorrhage in five aged horses. *J Am Vet Med Assoc* **237**, 830-834.
[11] Carroll, C.L. and Huntington, P.J. (1988) Body Condition Scoring and Weight Estimation of Horses. *Equine Veterinary Journal* **20**, 41-45.
[12] Heliczer, N., Lorello, O., Casoni, D. and Navas de Solis, C. (2016) Accuracy and Precision of Noninvasive Blood Pressure in Normo-, Hyper-, and Hypotensive Standing and Anesthetized Adult Horses. *J Vet Intern Med* **30**, 866-872.
[13] Boegli, J., Schwarzwald, C.C. and Mitchell, K.J. (2019) Diagnostic value of noninvasive pulse pressure measurements in Warmblood horses with aortic regurgitation. *J Vet Intern Med* **33**, 1446-1455.
[14] Ven, S., Decloedt, A., Van Der Vekens, N., De Clercq, D. and van Loon, G. (2016) Assessing aortic regurgitation severity from 2D, M-mode and pulsed wave Doppler echocardiographic measurements in horses. *Vet J* **210**, 34-38.
[15] Vera, L., De Clercq, D., Paulussen, E., Van Steenkiste, G., Decloedt, A., Chiers, K. and van Loon, G. (2019) Aortic, common carotid and external iliac artery arterial wall stiffness parameters in horses: Inter-day and inter-observer and intra-observer measurement variability. *Equine Vet J*.
[16] Vera, L., De Clercq, D., Van Steenkiste, G., Decloedt, A., Chiers, K. and van Loon, G. (2020) Differences in ultrasound-derived arterial wall stiffness parameters and noninvasive blood pressure between Friesian horses and Warmblood horses. *J Vet Intern Med*.
[17] Van Bortel, L.M., Laurent, S., Boutouyrie, P., Chowienczyk, P., Cruickshank, J.K., De Backer, T., Filipovsky, J., Huybrechts, S., Mattace-Raso, F.U., Protogerou, A.D., Schillaci, G., Segers, P., Vermeersch, S., Weber, T., Artery, S., European Society of Hypertension Working Group on Vascular, S., Function and European Network for Noninvasive Investigation of Large, A. (2012) Expert consensus document on the measurement of aortic stiffness in daily practice using carotid-femoral pulse wave velocity. *J Hypertens* **30**, 445-448.
[18] Marlatt, K.L., Steinberger, J., Dengel, D.R., Sinaiko, A., Moran, A., Chow, L.S., Steffen, L.M., Zhou, X. and Kelly, A.S. (2013) Impact of pubertal development on endothelial function and arterial elasticity. *J Pediatr* **163**, 1432-1436.
[19] Nethononda, R.M., Lewandowski, A.J., Stewart, R., Kylinterias, I., Whitworth, P., Francis, J., Leeson, P., Watkins, H., Neubauer, S. and Rider, O.J. (2015) Gender specific patterns of age-related decline in aortic stiffness: a cardiovascular magnetic resonance study including normal ranges. *J Cardiovasc Magn Reson* **17**, 20.
[20] Ho, J.Y. and Hendi, A.S. (2018) Recent trends in life expectancy across high income countries: retrospective observational study. *BMJ* **362**, k2562.
[21] Comfort, A. (1961) The life span of animals. *Sci Am* **205**, 108-119.
[22] Fjeldstad, A.S. and Bemben, D. (2007) Large and small arterial elasticity in healthy active and sedentary premenopausal women. *J Sports Sci Med* **6**, 250-253.
[23] Atienza, J.M., Guinea, G.V., Rojo, F.J., Burgos, R.J., Garcia-Montero, C., Goicolea, F.J., Aragoncillo, P. and Elices, M. (2007) [The influence of pressure and temperature on the behavior of the human aorta and carotid arteries]. *Rev Esp Cardiol* **60**, 259-267.
[24] Saey, V., Ploeg, M., Delesalle, C., van Loon, G., Grone, A., Ducatelle, R., Duchateau, L. and Chiers, K. (2016) Morphometric Properties of the Thoracic Aorta of Warmblood and Friesian Horses with and without Aortic Rupture. *J Comp Pathol* **154**, 225-230.
[25] Lyle, C.H., Uzal, F.A., McGorum, B.C., Aida, H., Blissitt, K.J., Case, J.T., Charles, J.T., Gardner, I., Horadagoda, N., Kusano, K., Lam, K., Pack, J.D., Parkin, T.D., Slocombe, R.F., Stewart, B.D. and Boden, L.A. (2011) Sudden death in racing Thoroughbred horses: an international multicentre study of post mortem findings. *Equine Vet J* **43**, 324-331.

[26] Pyo, R., Lee, J.K., Shipley, J.M., Curci, J.A., Mao, D., Ziporin, S.J., Ennis, T.L., Shapiro, S.D., Senior, R.M. and Thompson, R.W. (2000) Targeted gene disruption of matrix metalloproteinase-9 (gelatinase B) suppresses development of experimental abdominal aortic aneurysms. *J Clin Invest* **105**, 1641-1649.
[27] Pinto, E. (2007) Blood pressure and ageing. *Postgraduate Medical Journal* **83**, 109-114.
[28] von Maltzahn, W.W., Warriyar, R.G. and Keitzer, W.F. (1984) Experimental measurements of elastic properties of media and adventitia of bovine carotid arteries. *J Biomech* **17**, 839-847.
[29] Dao, H.H., Essalihi, R., Bouvet, C. and Moreau, P. (2005) Evolution and modulation of age-related medial elastocalcinosis: Impact on large artery stiffness and isolated systolic hypertension. *Cardiovascular Research* **66**, 307-317.
[30] Mattace-Raso, F.U.S., van der Cammen, T.J.M., Hofman, A., van Popele, N.M., Bos, M.L., Schalekamp, M.A.D.H., Asmar, R., Reneman, R.S., Hoeks, A.P.G., Breteler, M.M.B. and Witteman, J.C.M. (2006) Arterial stiffness and risk of coronary heart disease and stroke - The Rotterdam Study. *Circulation* **113**, 657-663.
[31] Alecu, C., Labat, C., Kearney-Schwartz, A., Fay, R., Salvi, P., Joly, L., Lacolley, P., Vespignani, H. and Benetos, A. (2008) Reference values of aortic pulse wave velocity in the elderly. *Journal of Hypertension* **26**, 2207-2212.
[32] Hidvegi, E.V., Illyes, M., Benczur, B., Bocskei, R.M., Ratgeber, L., Lenkey, Z., Molnar, F.T. and Cziraki, A. (2012) Reference values of aortic pulse wave velocity in a large healthy population aged between 3 and 18 years. *Journal of Hypertension* **30**, 2314-2321.
[33] Houghton, D., Jones, T.W., Cassidy, S., Siervo, M., MacGowan, G.A., Trenell, M.I. and Jakovljevic, D.G. (2016) The effect of age on the relationship between cardiac and vascular function. *Mechanisms of Ageing and Development* **153**, 1-6.
[34] McKeever, K.H. and Kearns, C.F. (2001) Aging-Induced Alterations in Plasma Volume in Horses. *Med Sci Sport Exer* **33**, S257-S257.
[35] Gehlen, H. and Bildheim, L.M. (2018) Evaluation of age-dependent changes of myocardial velocity using pulsed wave and colour tissue Doppler imaging in adult warmblood horses. *J Anim Physiol Anim Nutr (Berl)* **102**, 1731-1742.

# CHAPTER 7:

# HISTOLOGICAL AND BIOMECHANICAL PROPERTIES OF SYSTEMIC ARTERIES IN YOUNG AND OLD WARMBLOOD HORSES

# Histological and biomechanical properties of systemic arteries in young and old Warmblood horses

Lisse Vera[1*], Sofie Muylle[2], Glenn Van Steenkiste[1], Patrick Segers[3], Annelies Decloedt[1], Koen Chiers[4], Gunther van Loon[1]

[1] Equine Cardioteam Ghent University, Department of Large Animal Internal Medicine, Faculty of Veterinary Medicine, Ghent University, Merelbeke, Belgium

[2] Department of Morphology, Faculty of Veterinary Medicine, Ghent University, Merelbeke, Belgium

[3] IBiTech-bioMMeda, Ghent University, Ghent, Belgium

[4] Department of Pathology, Bacteriology and Poultry Diseases, Faculty of Veterinary Medicine, Ghent University, Merelbeke, Belgium

Submitted for publication in Plos One

## Abstract

Arterial rupture is a well-recognized cause of sudden death in horses, which mostly affects older horses. The arterial wall is known to stiffen with age, although the underlying age-related histological and biomechanical changes remain unclear. The purpose of this study was to investigate the effect of aging by analysing the arterial wall histologically and to examine the biomechanical properties of the arterial wall using an inflation-extension test. Entire circular samples of the cranial and caudal common carotid artery, proximal and distal aorta, external iliac, femoral and median artery were collected from 6 young (3-7 years) and 14 old horses (≥15 years). Samples of all arteries were histologically examined and intima media thickness as well as area % of elastin, smooth muscle actin and collagen type I and III were determined. Old horses had a significantly larger intima media thickness and a significantly higher area % of smooth muscle actin compared to young horses. Samples of the proximal and distal aorta, the carotid and the external iliac artery were biomechanically assessed using an inhouse developed inflation-extension device using ultrasound analysis. Rupture occurred in a minority of arteries (8/78) at high pressures (250-300 mmHg), and mostly occurred in old horses (7/8). Pressure-area, pressure-compliance and pressure-distensibility curves were constructed. A significant difference in the pressure-area curves of the distal aorta, common carotid artery and external iliac artery, the pressure-compliance curves of the proximal aorta and carotid artery and the pressure-distensibility curve of the proximal aorta was observed between young and old horses. Results demonstrate an effect of age on the histological and biomechanical properties of the arterial wall, which might explain why arterial rupture occurs more often in older horses.

## Introduction

Conduit arteries in mammals are compliant by nature and provide a low resistance path for the blood supply to the visceral organs and the limbs while cushioning the pulsatile action of the heart and keeping systolic and diastolic pressure within physiological limits[1]. The key structural components contributing to the compliance of the arterial wall are elastin fibres, collagen fibres, smooth muscle cells and cross-linking matrix constituents[1; 2]. In humans, conduit arteries are known to stiffen with age, resulting in luminal enlargement and arterial wall thickening[3; 4]. The arterial compliance at physiological pressures and the pressure at which compliance is maximal decrease with age, meaning a shift of the pressure-compliance curve to lower pressures[5]. These mechanical alterations are due to major structural changes. Structural changes are characterised by a proinflammatory profile, collagen deposition and fragmentation and thinning of elastin fibres[1; 3; 6; 7]. The elastin fragmentation causes luminal enlargement[8] and leads to a transfer of a part of the mechanical load to the collagen fibres,

which are 100 to 1000 times stiffer compared to elastin fibres[1]. Due to calcification[1; 3; 6] and the accumulation of advanced glycation end products (AGEs)[1; 3] the elastin fibres become stiffer. The formation of AGEs is not limited to elastin fibres but also occurs in collagen fibres[1]. In the aged vascular wall, the intima is infiltrated by vascular smooth muscle cells from the adjacent tunica media. Vascular smooth muscle cells, switched from the contractile to the synthetic phenotype, are capable of migration towards the intima. Once in the tunica intima they start to proliferate and synthesise extracellular matrix[9-11], causing thickening of the arterial wall[1].

In equine medicine a recent non-invasive, ultrasound study demonstrated stiffening of the conduit arteries with age, in combination with luminal enlargement and arterial wall thickening[12]. The objective of the current study was to determine whether age-related functional changes found in the *in vivo* study in horses can be supported by structural and biomechanical differences, using histology and an *ex vivo* inflation-extension test with ultrasound analysis.

## Materials and methods

### Sample collection and preparation

Arterial tissue was collected from old (≥15 years) and young (3-7 years) Warmblood horses, euthanized for non-cardiovascular reasons. For each horse, 10 cm long cylindrical tissue samples from the entire arterial wall were collected at seven topographical locations. The left common carotid artery was sampled at the level of the thoracic inlet (caudal common carotid artery) and 30 cm more cranially (cranial common carotid artery). The aorta was sampled just distal to the sinotubular junction (proximal aorta) and just cranial from the bifurcation into the external and internal iliac arteries (distal aorta). The left external iliac artery was sampled proximal to the arteria profunda femoris and the left femoral artery was sampled 20 cm distal to the arteria profunda femoris. The left median artery was sampled proximal to the carpus (Fig 1). All samples were collected within 12 hours post euthanasia. From the caudal common carotid artery, the proximal and distal aorta and the external iliac artery 5-7 cm of the arterial sample was immediately frozen at -80°C for the *ex vivo* inflation-extension test. The remaining part of these samples, as well as the samples of the cranial common carotid, femoral artery and median artery were fixed in buffered 4% formaldehyde solution for 24 hours, routinely embedded in paraffin wax and cut into 5 µm longitudinal and cross-sectional sections for histological examination. Sections were stained with haematoxylin and eosin to evaluate the different layers of the arterial wall. Immunohistochemistry was performed for demonstration of smooth muscle cells, elastin, collagen type I and collagen type III. Smooth muscle cells were visualised using mouse anti-smooth muscle actin (1/200, DakoCytomation). The presence of

elastin was demonstrated using a monoclonal mouse anti-human anti-elastin antibody BA-4 (1/600, Leica Biosystems) in combination with a standard avidin-biotin complex method with diaminobenzidine as chromogen for visualization (Envision, Dako). For both smooth muscle cells and elastin, immunolabeling was achieved using a high-sensitive horseradish peroxidase diaminobenzidine kit (Envision DAB+ kit, Dako) in an immunostainer (Cytomation S/N S38-7410-01, Dako). Samples were labelled with monoclonal rabbit anti-collagen type I (1/100, ABCAM 138492) and III (1/200, ABCAM 7778). Visualization was obtained using peroxidase labelled polymer conjugated to goat anti-rabbit immunoglobulins (Agilent, K400311-2, Dako) and biotinylated polyclonal goat anti-rabbit immunoglobulins (Agilent, E043201-8, Dako), respectively, in combination with a peroxidase diaminobenzidine kit (DAB+ Liquid, K346811-2, Agilent).

Fig. 1. Schematic overview of the locations at which samples were collected.

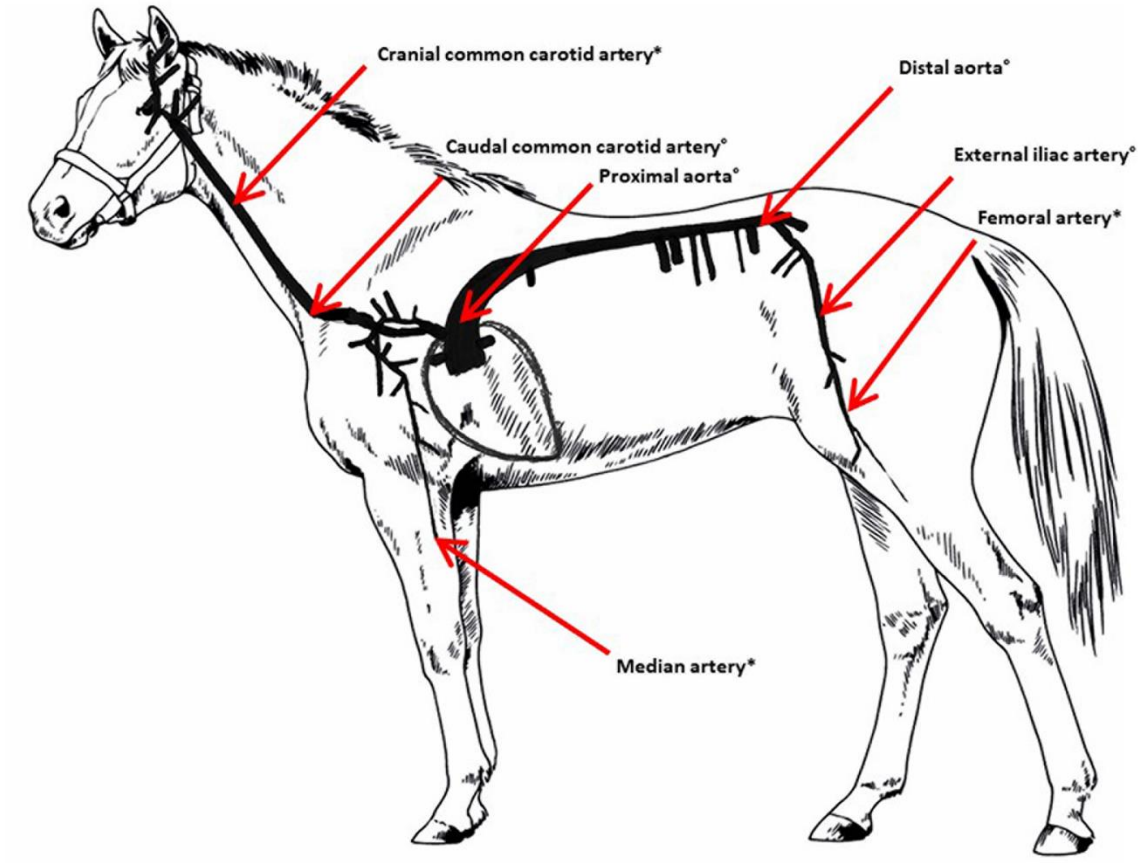


*: samples of 14 old and 6 young horses were collected for histology

°: samples of 14 old and 6 young horses were collected for histology and biomechanical testing

### *Histology*

All sections were randomised and blindly analysed. Haematoxylin eosin sections were used to measure the combined thickness of the tunica intima and the tunica media and to screen for arterial wall lesions and mineralisations. A low power magnification was used to measure the intima media thickness as the perpendicular distance between the endothelial layer and the transition tunica media – tunica adventitia. For each section five measurements were carried out at randomly chosen locations over the entire arterial wall cross-section and the mean of those values was calculated. The intima media thickness of the proximal aorta was not assessed, as wall thickness exceeded the measurement capacity. The area % of elastin, smooth muscle actin, collagen type I and collagen type III was determined using image analysis. The area % was determined using a Leica Camera DFC320 (Leica Microsystems Ltd) coupled to a computer-based image analysis system LAS v.3.8. (Leica Microsystems Ltd.) at 400x magnification[13]. For each slide, five randomly selected image frames from just underneath the endothelium until the transition tunica media – tunica adventitia were analysed and the mean area % of the five image frames was calculated. In many cases the tunica media consisted of two separate layers. If so, image analysis was performed separately for both layers and the thickness of each layer was measured. To calculate the overall area % of elastin, smooth muscle actin and collagen type I and III, the following formula was applied:

$$overall\ area\ \% = mean\ area\ \%\ in\ layer\ 1 * \left(\frac{mean\ thickness\ of\ layer\ 1}{mean\ total\ thickness}\right) + mean\ area\ \%\ in\ layer\ 2 * \left(\frac{mean\ thickness\ of\ layer\ 2}{mean\ total\ thickness}\right).$$

### *Inflation-extension test*

For the *ex vivo* inflation-extension test, samples were thawed at room temperature. Loose connective tissue was removed and all side branches were ligated. Subsequently, the vessel was vertically mounted onto a custom-made pressurisation-system (Fig 2) with adaptable connectors depending on the size of the arterial segment. Each vessel side was fixed using either two ligatures (common carotid artery and external iliac artery) or a tie strap (proximal and caudal aorta) (Fig 3). During the entire experiment each vessel was fixed at the stretching-length obtained with an internal pressure of 120 mmHg. The fixed vessel was placed in a 0.9% NaCl water bath at a constant temperature of 37°C. Before starting all vessels were gradually pre-stretched three times to a pressure of 120 mmHg. Afterwards all vessels were gradually pressurised using a pressure reservoir containing 0.9% NaCl at 37°C, in which the pressure was manually regulated using a manometer. Pressure was monitored using a fluid filled pressure transducer (MLT0699 Disposable BP Transducer, ADInstruments) connected to the distal end of the arterial segment. The pressure was visualised using a digital acquisition station (PowerLab 8, ADInstruments). Measurements were sequentially performed at 15, 30,

45, 60, 80, 100, 125, 200, 250 and 300 mmHg. For each pressure point three B-mode longitudinal ultrasonographic video-loops were collected (Vivid IQ, GE Healthcare) through a silicone window in the water tank, using a 9 MHz linear probe (9L-RS, GE Healthcare). Longitudinal alignment of the probe was ensured by clearly visualising the intima of the arterial wall in both the near and the far field. All loops were digitally stored as raw data (Echopac version 203, GE Healthcare) and blinded for further offline analysis (MicroDicom viewer version 3.2.7). On each video loop inner arterial diameter was measured from inner edge to inner edge. For each pressure point the mean inner arterial diameter was calculated as the average of three measurements from separately obtained video loops.

Fig. 2. Schematic overview of the custom-made pressurisation system for the inflation-extension under ultrasound monitoring.

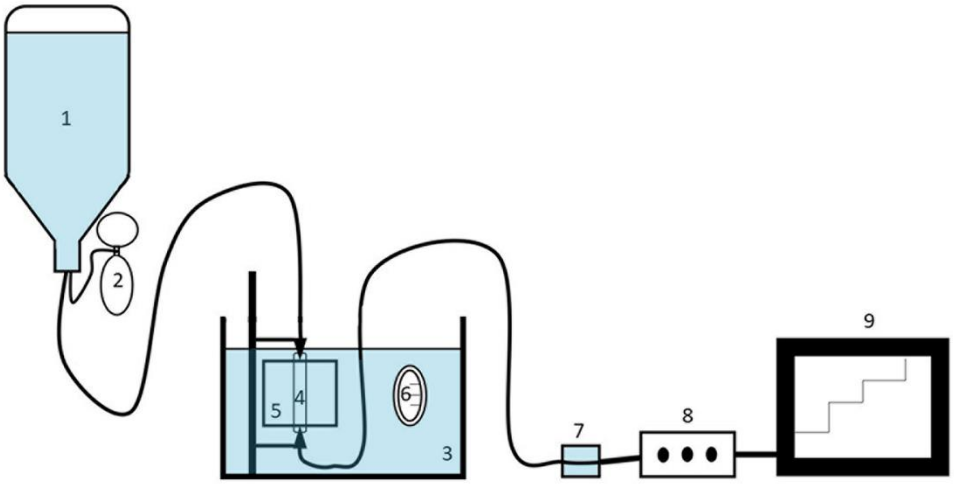


1: pressure reservoir containing 0.9% NaCl at 37°C; 2: manual manometer to adjust pressure; 3: water bath containing 0.9% NaCl at 37°C; 4: pressurised arterial sample; 5: silicone window in the water tank, through which ultrasound was performed; 6: bath thermometer; 7: fluid filled pressure transducer; 8: acquisition station; 9: visualisation of actual pressure in the arterial segment on screen.

Fig. 3. Example of the proximal aorta, mounted in the pressurisation system but out of the water bath, and derived ultrasound images at 30 (left) and 300 (right) mmHg.

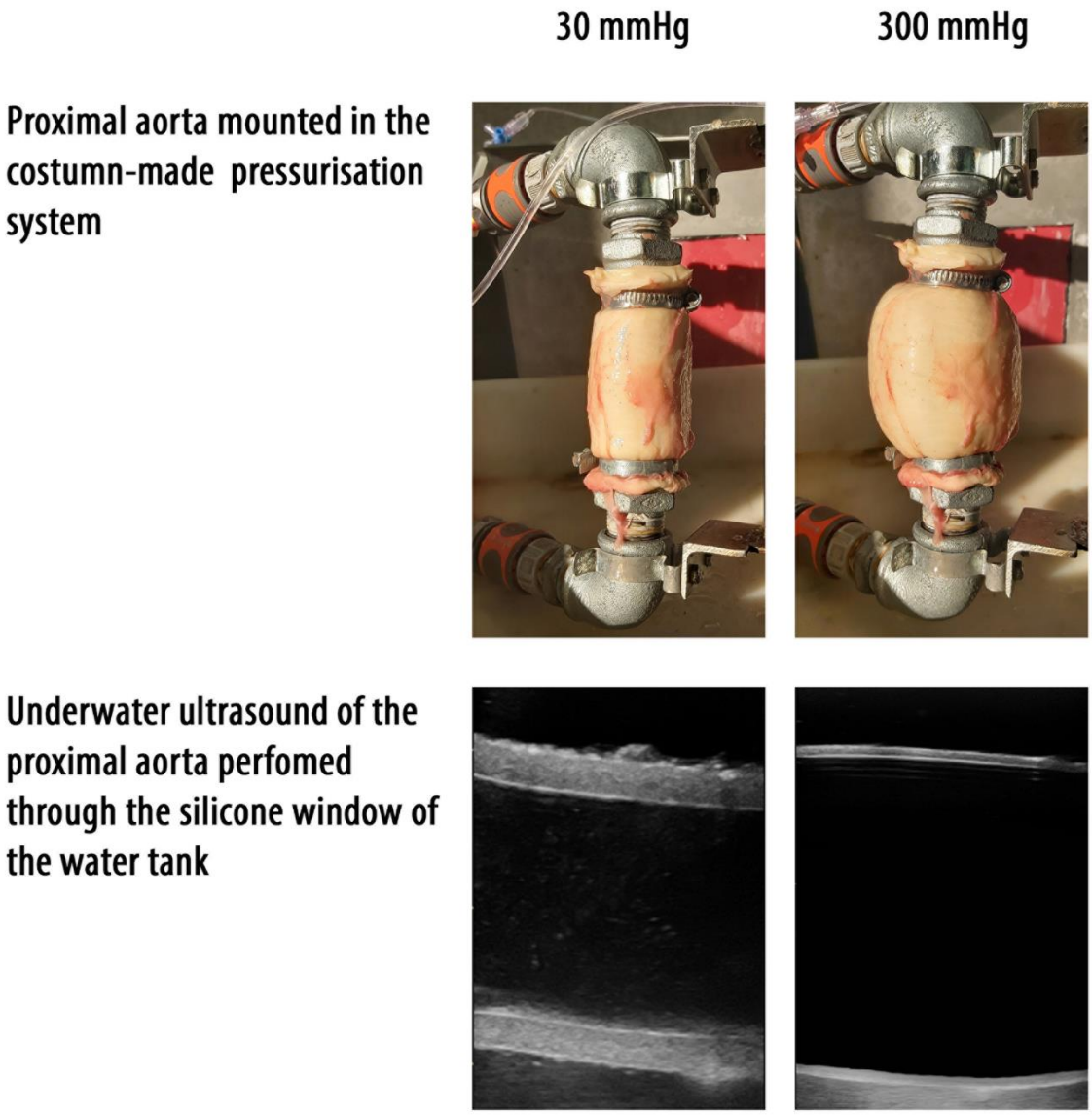


**Statistical analysis**

***Histology***

For the histological results normality of all variables was checked graphically using Q-Q plots. A multivariate ANOVA was used including age (young or old) and location (proximal and distal aorta, cranial and caudal common carotid artery, external iliac artery, femoral arteryand median artery) as fixed factors to compare the overall thickness, the overall area percentage of smooth muscle actin, elastin, collagen type I and collagen type III. For location, post-hoc

Bonferroni correction for multiple comparisons was applied. P-values ≤ 0.05 were considered statistically significant.

### *Inflation-extension test*

For the inflation—extension test, results were fitted to the arctangent model of Langewouters et al.[14] The area for a given pressure was calculated as $A\,(P) = A_m\left\{\frac{1}{2} + \frac{1}{\pi}\,tan^{-1}\left(\frac{P-P_0}{P_1}\right)\right\}$, $A_m$ represents the maximal cross-sectional area of the investigated artery, $P_0$ the pressure at which compliance is maximal and $P_1$ the half-width pressure. Corresponding compliance was calculated as $C_A\,(P) = \frac{\frac{A_m}{\pi P_1}}{1+\left(\frac{P-P_0}{P_1}\right)^2}$ and distensibility as $D_A(P) = \frac{C_A}{A}$. The effect of age (young or old) on the pressure-area, pressure-compliance and pressure-distensibility curves was tested by creating non-linear regression models. An F-test was used to determine whether there was an overall effect of age on the non-linear relationship.

Afterwards mean maximal area, maximal compliance and maximal distensibility were compared between young and old horses and between investigated vessels using a multivariate ANOVA including age (young, old) and location (proximal aorta, distal aorta, common carotid artery and external iliac artery) as fixed factors. Post-hoc Bonferroni correction was applied for multiple comparisons. P-values of ≤ 0.05 were considered statistically significant.

## Results

### Histological findings

Arterial wall tissue was collected from 20 Warmblood horses, six of them were categorised as young (mean age ± SD: 6±0 years) and 14 as old (mean age ± SD: 18±3 years). At the level of the proximal aorta, the tunica media consisted of one layer with an almost uniform distribution of fibres and smooth muscle cells. In 40% of the horses (5 old and 3 young horses), at the level of the distal aorta, two different layers within the tunica media could be distinguished. In the innermost layer (layer 1) the smooth muscle cell content was higher than the fibre content. The outer layer (layer 2) presented a large quantity of fibres with a very limited amount of smooth muscle cells. Also at the level of the cranial and caudal common carotid artery, the median artery, the external iliac artery and the femoral artery the tunica media presented these two clearly distinguishable layers in all horses.

No histological lesions were found, except for one horse (aged 18 years) in which the proximal aorta presented multifocal small mineralisations in the tunica media, close to the tunica adventitia. A Von Kossa staining indicated that the mineralisations were calcifications.

There was a significant effect of location on the overall arterial wall thickness, on the overall area % of elastin and on the overall area % of collagen type III (Table 1; Fig 4). The distal aorta showed a clearly thicker arterial wall (2273 ± 328 µm) compared to the other arteries. The highest overall amount of elastin was found in the proximal aorta (34 ± 3 %), whereas the median artery contained the lowest amount of elastin (8 ± 5 %). The highest overall amount of collagen type III was found in the femoral artery (28 ± 15 %) whereas the lowest overall amount of collagen type III was found in the proximal aorta (17 ± 7%), the median artery (17 ± 7%) and the cranial common carotid artery (18 ± 4%) (Fig 5).

Table 1. Overview of overall measured intima media thickness, area % of elastin, smooth muscle actin, collagen type I and collagen type III for the caudal and cranial common carotid artery, the proximal and distal aorta, the median artery, the external iliac artery and the femoral artery in old and young horses.

| | | Young | Old |
|---|---|---|---|
| Thickness (µm)* | Caudal common carotid artery[a] | 1654±145 | 1800±225 |
| | Cranial common carotid artery[b] | 1179±150 | 1405±246 |
| | Distal aorta[a,b,c,d,e] | 2219±361 | 2300±327 |
| | Median artery[c] | 1739±302 | 1383±370 |
| | External iliac artery[d] | 1655±360 | 1840±253 |
| | Femoral artery[e] | 1469±147 | 1870±325 |
| % Elastin | Caudal common carotid artery[f,h] | 16±7 | 15±7 |
| | Cranial common carotid artery[g,h] | 15±7 | 14±6 |
| | Proximal aorta[f,g,h] | 35±11 | 34±8 |
| | Distal aorta[h] | 15±5 | 15±7 |
| | Median artery[h,i] | 7±2 | 9±6 |
| | External iliac artery[h] | 11±5 | 11±7 |
| | Femoral artery[h,i] | 12±5 | 18±13 |
| % Smooth muscle actin* | Caudal common carotid artery | 43±6 | 51±16 |
| | Cranial common carotid artery | 43±2 | 50±6 |
| | Proximal aorta | 42±7 | 45±10 |
| | Distal aorta | 37±6 | 40±8 |
| | Median artery | 48±9 | 51±10 |
| | External iliac artery | 41±11 | 45±9 |

| | | | |
|---|---|---|---|
| | Femoral artery | 39±6 | 48±25 |
| % Collagen type I | Caudal common carotid artery | 17±5 | 23±24 |
| | Cranial common carotid artery | 20±8 | 23±14 |
| | Proximal aorta | 25±11 | 23±11 |
| | Distal aorta | 19±9 | 15±6 |
| | Median artery | 29±10 | 20±12 |
| | External iliac artery | 26±9 | 21±9 |
| | Femoral artery | 21±5 | 17±12 |
| % Collagen type III | Caudal common carotid artery | 18±2 | 23±11 |
| | Cranial common carotid artery[j] | 19±4 | 18±4 |
| | Proximal aorta[k] | 14±5 | 20±7 |
| | Distal aorta | 25±8 | 22±8 |
| | Median artery[l] | 19±4 | 16±8 |
| | External iliac artery | 23±1 | 23±6 |
| | Femoral artery[j,k,l] | 25±7 | 29±18 |

* indicates significant difference between young and old horses, independent from location; the same superscripts indicate a significant difference between locations.

Fig. 4. Overview of the overall mean intima media thickness, area % of elastin, area % of smooth muscle cells, area % of collagen type I and area % of collagen type III in young (blue) and old (red) horses, grouped by location.

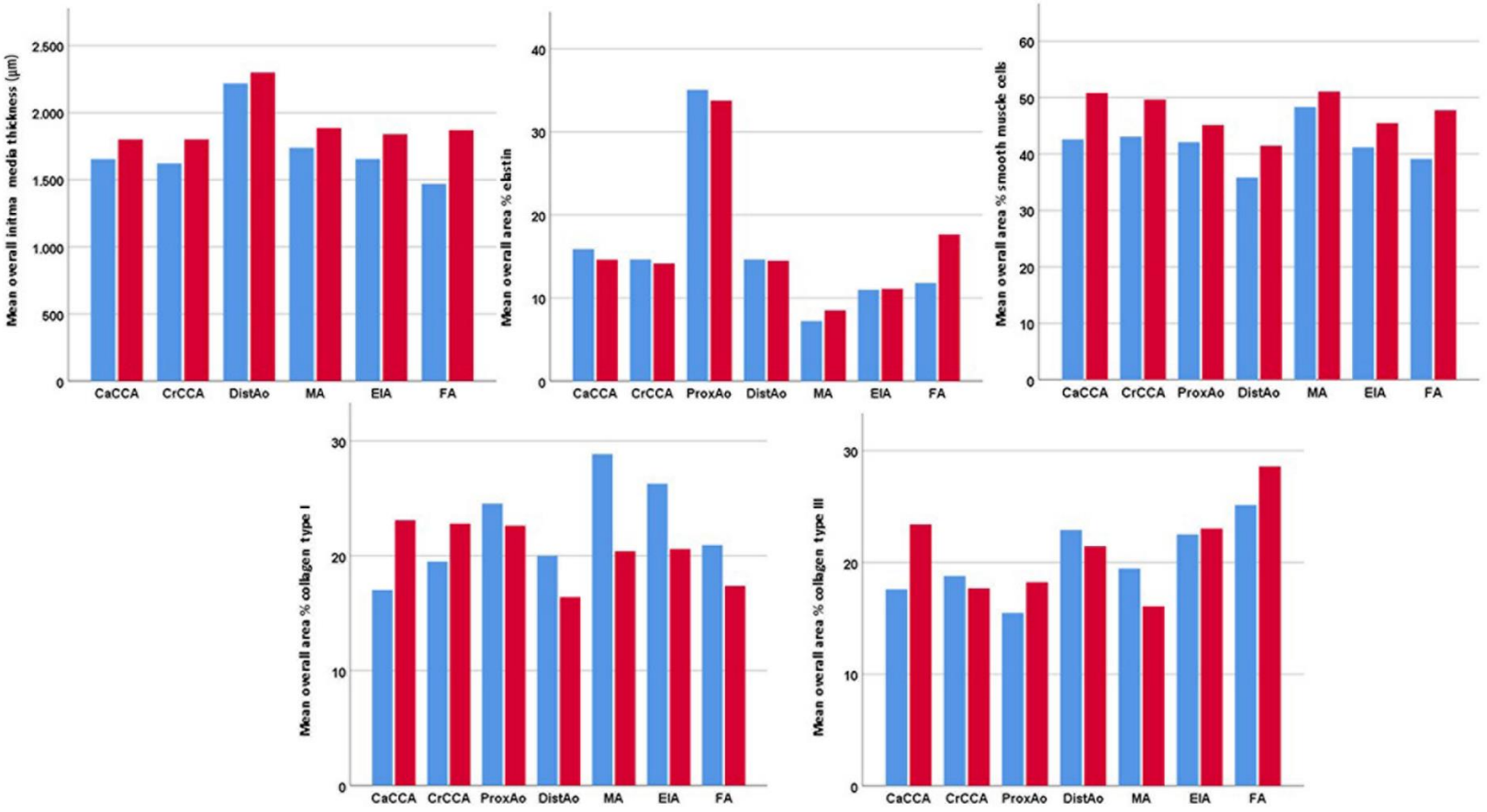


CaCCA: caudal common carotid artery; CrCCA: cranial common carotid artery; ProxAo: proximal aorta; DistAo: distal aorta; MA: median artery; EIA: external iliac artery; FA: femoral artery.

Fig. 5. Immunohistochemistry for elastin and collagen type III (brown) of longitudinal sections through the vessel wall.

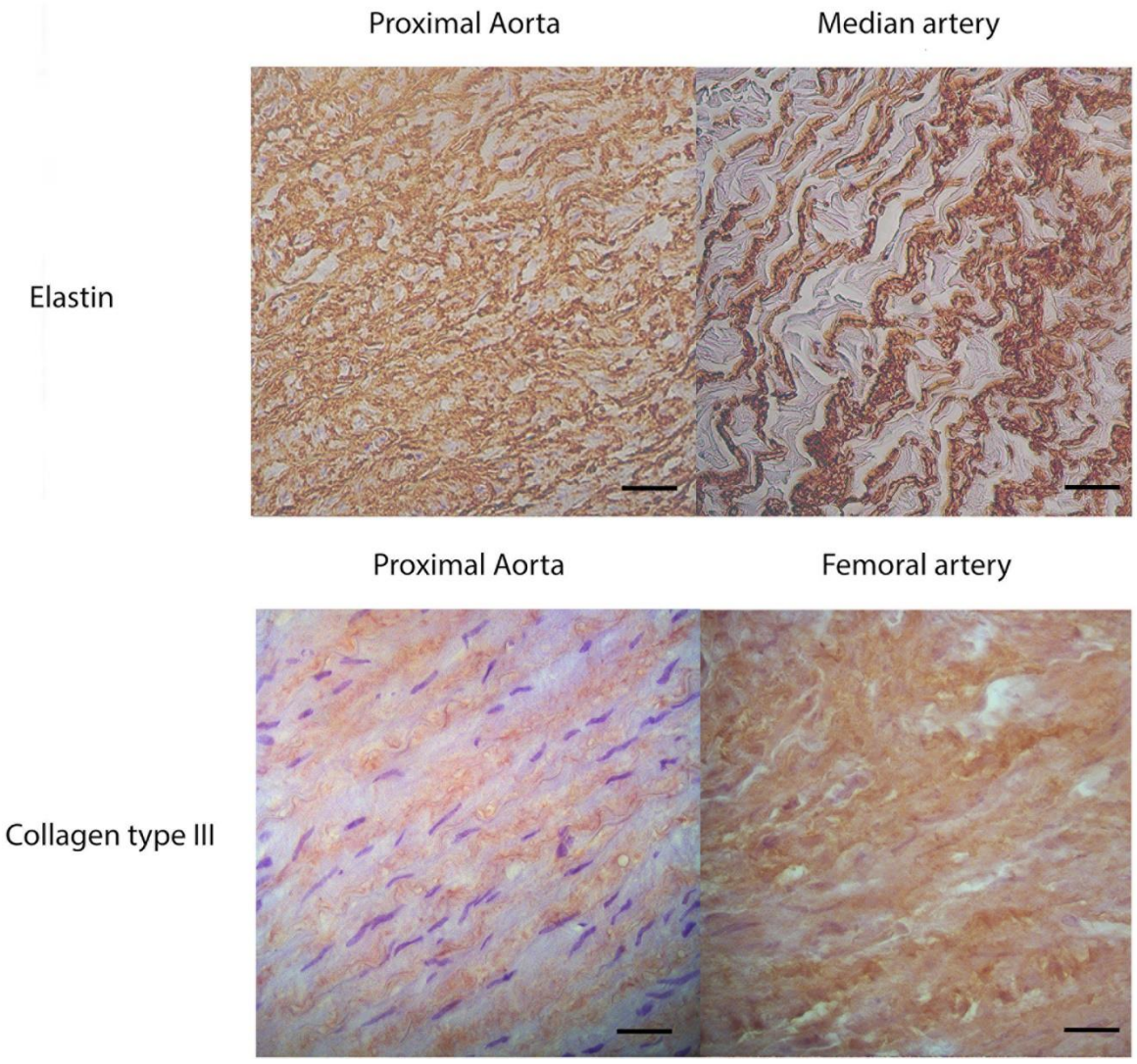


The proximal aorta contains a higher area % of elastin and a lower area % of collagen type III compared to peripheral arteries. Magnification x400; bar=250µm.

A significant effect of age was found for the overall arterial wall thickness and the overall area % of smooth muscle actin, independent from arterial location (Fig 4). The arterial wall thickness and the overall area % of smooth muscle actin were significantly higher in older horses when compared to younger animals. No significant difference was found for the overall area % of elastin nor for the overall area % of collagen type I and III. Details can be found in Table 1.

**Inflation-extension test**

During the inflation-extension test a total of eight arteries ruptured, five of them being proximal aortas. Three proximal aortas of old horses (aged 18, 23 and 25 years) ruptured at 250 mmHg pressure while the other two, of horses aged 6 and 15 years, ruptured at 300 mmHg. Rupture always occurred in cross-sectional direction, close to the strap securing the artery to the connector (Fig 6). Two distal aortas of old horses (aged 17 and 15 years) ruptured at the bifurcation of a ligated side branch, at a pressure of 250 and 300 mmHg. For the external iliac artery, two samples were not tested, as they could not be made leak proof. One external iliac artery of an old horse (20 years) ruptured at the bifurcation of a ligated side branch at a pressure of 250 mmHg.

Fig. 6. Typical cross-sectional rupture of the proximal aorta, close to the mounting side, which occurred predominantly in the older horses (> 15 years) at high pressures (250-300 mmHg).

Results from the inflation-extension test fitted the arctangent model well, with $R^2$ values (mean ± SD) of 0.990 ± 0.009 for the proximal aorta, 0.978 ± 0.025 for the distal aorta, 0.982 ± 0.247 for the carotid artery and 0.831 ± 0.271 for the external iliac artery.

There was a significant effect of location on the biomechanical properties of the arterial wall (Table 2). Largest mean maximal area was found for the proximal aorta (3202$mm^2$) whereas the smallest area was found for the caudal common carotid artery (109$mm^2$). The highest maximal compliance was found for the proximal aorta (17$mm^2$/mmHg) while the lowest maximal compliance was found for the caudal common carotid artery (0.7$mm^2$/mmHg) and the external iliac artery (0.7$mm^2$/mmHg). The highest maximal distensibility was found for the distal aorta (0.022/mmHg) but no significant difference in maximal distensibility was found within the other three arteries.

Table 2. Schematic overview of mean maximal area, compliance and distensibility of the proximal aorta, distal aorta, common carotid artery and external iliac artery.

| | | Young | Old |
|---|---|---|---|
| Maximal area ($mm^2$) | Proximal aorta | 3313±471 | 3154±852 |
| | Distal aorta | 1039±198 | 1132±279 |
| | Common carotid artery[a] | 100±14 | 114±27 |
| | External iliac artery[a] | 172±64 | 215±53 |
| Maximal compliance ($mm^2$/mmHg) | Proximal aorta | 18±5 | 17±6 |
| | Distal aorta | 10±4 | 10±5 |
| | Common carotid artery[b] | 0.7±0.3 | 0.8±0.3 |
| | External iliac artery[b] | 0.7±0.3 | 0.8±0.3 |
| Maximal distensibility (/mmHg) | Proximal aorta[c] | 0.008±0.001 | 0.008±0.002 |
| | Distal aorta[d] | 0.022±0.014 | 0.018±0.011 |
| | Common carotid artery[c,d] | 0.013±0.004 | 0.012±0.004 |
| | External iliac artery[c] | 0.006±0.003 | 0.006±0.004 |

The same superscripts indicate no significant difference between locations.

The pressure-area curve of the distal aorta ($p=0.048$), caudal common carotid artery ($p<0.001$) and external iliac artery ($p<0.001$) were significantly affected by age, showing larger areas at the same pressures in old horses. In the proximal aorta the pressure-compliance curve showed significant age-related differences ($p=0.001$) with lower maximal compliance at lower pressure in old horses. The pressure-compliance curve of the caudal common carotid artery was significantly affected by age ($p=0.038$) as well. Old horses presented a higher maximal compliance at low pressures and a lower compliance at physiological pressures. The pressure-distensibility curve of the proximal aorta was significantly different between old and young horses ($p<0.001$), showing a slightly higher distensibility in older horses at all pressures (Fig 7). Independent from location, there was no significant influence of age on the mean maximal area, maximal compliance or maximal distensibility (Table 2).

Fig. 7. Pressure-area, pressure-compliance and pressure-distensibility curves of the proximal aorta, distal aorta, common carotid artery and external iliac artery in young (blue) and old horses (red).

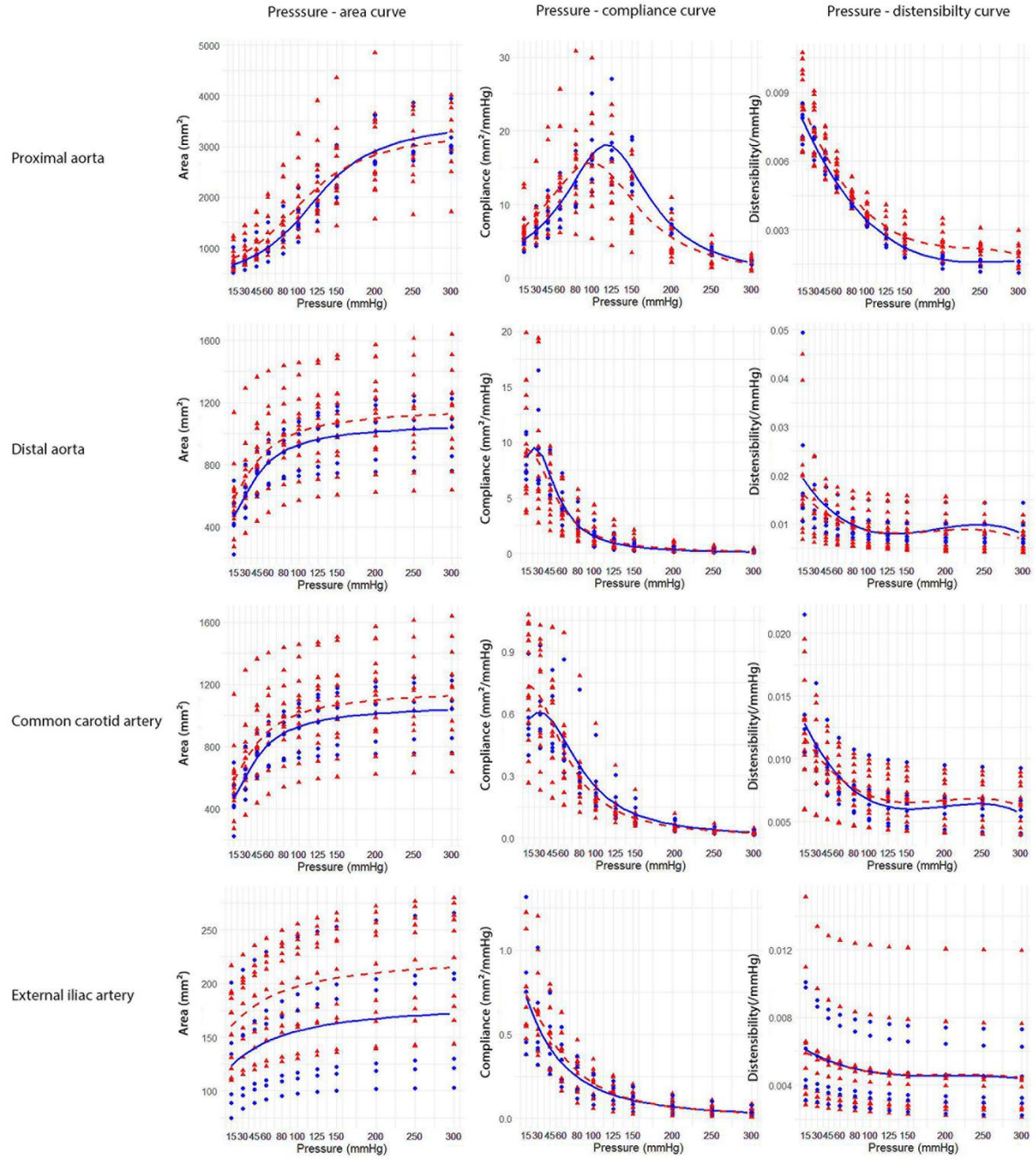


Dots and triangles represent individual values of young and old horses, respectively; full lines and dotted lines represent the fitted regression curves of young and old horses, respectively.

## Discussion

An arterial wall consists of three layers, from inner to outer side: the intima, the media and the adventitia. The present histological study focussed on the tunica intima and the tunica media, which is mainly responsible for arterial distensibility and resilience. Although the adventitia does contribute to arterial stiffness and compliance[1; 15; 16], this layer was not included in the present study because it occasionally got lost during sample processing.

In this study the tunica media presented two clearly distinguishable layers in 40% of the distal aortas and in all of the common carotid, median, external iliac and femoral arteries. When passing from more centrally located elastic arteries to more peripheral muscular arteries, in human medicine, the amount of elastin is known to reduce and the elastin fibres are known to become predominantly organised in the internal elastic lamina and the external elastic lamina with a clearly defined layer of smooth muscle cells in between. The inner layer of the tunica media (layer 1) in this study matches with the clearly defined zone of smooth muscle cells, while the outer layer (layer 2) can be considered as the external elastic lamina. A clear internal elastic lamina was not found, although in some arteries the amount of elastin was clearly higher at the most inner side of the tunica media.

The present study showed a significant effect of location on the amount of elastin in the arterial wall. The largest amount of elastin was found in the proximal aorta (34-35%), while the lowest amount was found in the median artery and the external iliac artery (7-11%). The highest area % of collagen type III on the other hand, was found at the level of the distal aorta (25±8%), external iliac artery (23±1%) and femoral artery (25±7%). Therefore a more elastic proximal aorta and a stiffer distal aorta and external iliac artery were suspected to be found in the *ex vivo* inflation-extension test. Nevertheless, the maximal distensibility, describing the maximal relative area change per mmHg, of the proximal aorta (0.008±0.001) and external iliac artery (0.006±0.003) was significantly lower compared to the distal aorta (0.022±0.14). The higher distensibility found at the level of the distal aorta compared to the external iliac artery is probably due to the significantly higher area % of elastin in the distal aorta (15±5% versus 11±5%). The low distensibility of the proximal aorta could not be explained based on current histological findings and might be related to the elastic properties of the tunica adventitia, which was not included in the histological study, but is known to contribute to arterial stiffness and compliance[1; 15; 16].

The present study also revealed age related arterial wall thickening in horses, a phenomenon that has been described in human patients[3; 4]. In humans this process is known to result from smooth muscle cell phenotype switch: smooth muscle cells switch from the contractile to the secretory phenotype and migrate from the media towards the intima. In the intima they

proliferate and start producing collagen and proteoglycans[10; 17-19]. In our study the increased arterial wall thickness was probably not due to smooth muscle cell phenotype switch, migration and proliferation as the overall area % of smooth muscle actin, which is only present in a very small amount in the secretory phenotype[20; 21], was increased in older horses. Moreover no indication of an increased amount of collagen or proteoglycans in the tunica intima was present. The increased amount of smooth muscle actin in older horses might be a compensatory mechanism for the decreased compliance that was found in the inflation-extension test and the known luminal enlargement in older horses. Passive expansion and recoil might as such be partially replaced by active vasoconstriction regulated by smooth muscle cells, in order to guarantee a maintenance of blood pressure. This hypothesis has not been described before and requires further investigation.

In humans an increase in collagen content associated with more cross-linking, a decrease in elastin content, elastin fragmentation and calcification are characteristics of vascular aging[1; 3; 6; 22]. In the current study, elastin fragmentation in combination with calcification was found in one horse (age 18) at the level of the proximal aorta. Age-related changes in the amount of collagen and elastin have been described in primates, birds, fish, mice, rats and dogs[23; 24] and are therefore expected to be present in horses too. In old mares histological changes have been described in the uterine artery[25] and an increased overall arterial wall stiffness has recently been demonstrated *in vivo* in old horses[12]. In the present study age-related differences were found in the area % of smooth muscle actin, but not in the amount of elastin and collagen. This could be ascribed to the small number of horses investigated in this study or to the fact that horses were considered old if aged over 15 years. If the chronological age, which refers to an animal's numerical age in relation their life expectancy, had been used, horses would have been considered old when aged >20 years, as the life expectancy of a horse is around 30 years of age[12; 26; 27].

Histology revealed no age-related difference in area % of collagen or elastin, but only an increased amount of smooth muscle actin in old horses. Smooth muscle cells are an active component, their mechanical properties depend on the state of contraction. For the inflation-extension test of our study, arterial tissue was frozen without cryoprotective agent, leading to smooth muscle cell death[28]. Therefore, no detectable effect of the increased amount of smooth muscle actin was suspected in the inflation-extension test. Nevertheless some changes in biomechanical function were found. The pressure-compliance curve was significantly different between young and old horses for the proximal aorta and the common carotid artery. For the proximal aorta, lower compliance in old horses was found in the higher pressure ranges. The maximal compliance was lower in older horses and was reached at lower pressure. The shift of maximal compliance to lower pressures is a known phenomenon in

human medicine. A remarkable difference between equine and human aortas is the higher pressure at which maximal compliance is achieved in horses (100-125 mmHg) compared to humans (0-40 mmHg)[5]. In humans, a clear difference in compliance can be found between low (0-60 mmHg) and physiological (60-200 mmHg) pressures: maximal compliance is found at low pressure ranges and is described to increase with increasing age, while in the physiological pressure ranges, compliance is known to decrease with increasing age [5; 29; 30]. This phenomenon of maximal compliance in the low pressure range was not found in the proximal aortal of horses. For the common carotid artery pressure-compliance curves behaved as expected: higher maximal compliance at low pressure (15-45mmHg) and lower compliance at physiological pressures were found in older horses compared to younger horses. No significant difference in pressure-distensibility curve was found, except for the proximal aorta, which, in contrast to human studies[5; 31; 32], showed slightly higher distensibility in older horses at all pressures. Freezing may not only cause smooth muscle cell death but may also result in loss of collagen[33]. However, the precise effects are not entirely clear as some studies showed ultimate tensile strength to be unchanged after freezing[34].

*In vivo*, arteries are longitudinally stretched and pressure-inflation tests should therefore be carried out at *in vivo* length, which normally corresponds to 1.6 times the unloaded length. As *in vivo* lengths were not determined, we decided to approach as much as possible the *in vivo* situation by fixating the samples at the length that the sealed-off but freely extensible vessel segments took when exposed to a static internal pressure of 120 mmHg, the mean arterial pressure in horses[35]. It was visually observed that such pressurisation induced an elongation in the order of 1.5-2 times the unloaded length. Thanks to this standardisation between arteries, results could be interpreted qualitatively in order to compare arteries of old and young horses.

Arteries were pressurized up to 300 mmHg, as horses may reach such high pressures during exercise[36]. Rupture occurred in a minority of arteries (8/78) at high pressures (250-300 mmHg) and mostly occurred in older horses (7/8 in old horses). Rupture occurred most frequently just underneath the mounting place. As mounting was the same in old and young horses, results indicate a predisposition of older horses to arterial rupture.

In conclusion, clear differences in histological and biomechanical properties of the arterial wall were found between the elastic central arteries and the more muscular, peripheral arteries**.** The proximal aorta contained the largest area % of elastin, while the distal aorta, external and femoral artery contained the highest area % of collagen type III. The highest distensibility was found for the distal aorta, and not for the proximal aorta as expected. Histological comparison of the arterial wall of old and young horses revealed a thicker arterial wall in old horses and a

higher area % of smooth muscle actin. An *ex vivo* inflation-extension test revealed larger areas in old horses compared to young horses at the same pressures. Lower maximal compliance at lower pressures in old horses was found for the proximal aorta, while higher maximal compliance at low pressures in combination with lower compliance at physiological pressures was found at the level of the common carotid artery.

## Acknowledgements

None.

## References

[1] Greenwald, S.E. (2007) Ageing of the conduit arteries. *J Pathol* **211**, 157-172.
[2] Harkness, M.L., Harkness, R.D. and McDonald, D.A. (1957) The collagen and elastin content of the arterial wall in the dog. *Proc R Soc Lond B Biol Sci* **146**, 541-551.
[3] Lee, H.Y. and Oh, B.H. (2010) Aging and arterial stiffness. *Circ J* **74**, 2257-2262.
[4] Mikael, L.R., Paiva, A.M.G., Gomes, M.M., Sousa, A.L.L., Jardim, P., Vitorino, P.V.O., Euzebio, M.B., Sousa, W.M. and Barroso, W.K.S. (2017) Vascular Aging and Arterial Stiffness. *Arq Bras Cardiol* **109**, 253-258.
[5] Langewouters, G.J. (1982) Visco-elasticity of the human aorta in vitro in relation to pressure and age
[6] O'Rourke, M.F. and Hashimoto, J. (2007) Mechanical factors in arterial aging - A clinical perspective. *Journal of the American College of Cardiology* **50**, 1-13.
[7] AlGhatrif, M. and Lakatta, E.G. (2015) The Conundrum of Arterial Stiffness, Elevated Blood Pressure, and Aging. *Curr Hypertens Rep* **17**.
[8] Pyo, R., Lee, J.K., Shipley, J.M., Curci, J.A., Mao, D., Ziporin, S.J., Ennis, T.L., Shapiro, S.D., Senior, R.M. and Thompson, R.W. (2000) Targeted gene disruption of matrix metalloproteinase-9 (gelatinase B) suppresses development of experimental abdominal aortic aneurysms. *J Clin Invest* **105**, 1641-1649.
[9] Monk, B.A. and George, S.J. (2015) The Effect of Ageing on Vascular Smooth Muscle Cell Behaviour--A Mini-Review. *Gerontology* **61**, 416-426.
[10] Lacolley, P., Regnault, V., Segers, P. and Laurent, S. (2017) Vascular Smooth Muscle Cells and Arterial Stiffening: Relevance in Development, Aging, and Disease. *Physiol Rev* **97**, 1555-1617.
[11] Lakatta, E.G., Wang, M.Y. and Najjar, S.S. (2009) Arterial Aging and Subclinical Arterial Disease are Fundamentally Intertwined at Macroscopic and Molecular Levels. *Med Clin N Am* **93**, 583-604.
[12] Vera, L., Van Steenkiste, G., Decloedt, A., Chiers, K. and van Loon, G. (2020) Age-related differences in blood pressure, ultrasound-derived arterial diameters and arterial wall stiffness parameters in horses. *Equine Vet J* **DOI10.1111/evj.13263**
[13] Saey, V., Ploeg, M., Delesalle, C., van Loon, G., Grone, A., Ducatelle, R., Duchateau, L. and Chiers, K. (2016) Morphometric Properties of the Thoracic Aorta of Warmblood and Friesian Horses with and without Aortic Rupture. *J Comp Pathol* **154**, 225-230.
[14] Langewouters, G.J., Wesseling, K.H. and Goedhard, W.J. (1984) The static elastic properties of 45 human thoracic and 20 abdominal aortas in vitro and the parameters of a new model. *J Biomech* **17**, 425-435.
[15] von Maltzahn, W.W., Warriyar, R.G. and Keitzer, W.F. (1984) Experimental measurements of elastic properties of media and adventitia of bovine carotid arteries. *J Biomech* **17**, 839-847.
[16] Xie, J., Zhou, J. and Fung, Y.C. (1995) Bending of blood vessel wall: stress-strain laws of the intima-media and adventitial layers. *J Biomech Eng* **117**, 136-145.

[17] Dinenno, F.A., Jones, P.P., Seals, D.R. and Tanaka, H. (2000) Age-associated arterial wall thickening is related to elevations in sympathetic activity in healthy humans. *Am J Physiol-Heart C* **278**, H1205-H1210.
[18] Lacolley, P., Regnault, V. and Avolio, A.P. (2018) Smooth muscle cell and arterial aging: basic and clinical aspects. *Cardiovasc Res* **114**, 513-528.
[19] Lee, S.J. and Park, S.H. (2013) Arterial Ageing. *Korean Circ J* **43**, 73-79.
[20] Beamish, J.A., He, P., Kottke-Marchant, K. and Marchant, R.E. (2010) Molecular regulation of contractile smooth muscle cell phenotype: implications for vascular tissue engineering. *Tissue Eng Part B Rev* **16**, 467-491.
[21] Rensen, S.S., Doevendans, P.A. and van Eys, G.J. (2007) Regulation and characteristics of vascular smooth muscle cell phenotypic diversity. *Neth Heart J* **15**, 100-108.
[22] Jani, B. and Rajkumar, C. (2006) Ageing and vascular ageing. *Postgrad Med J* **82**, 357-362.
[23] Mitchell, S.J., Scheibye-Knudsen, M., Longo, D.L. and de Cabo, R. (2015) Animal models of aging research: implications for human aging and age-related diseases. *Annu Rev Anim Biosci* **3**, 283-303.
[24] Kim, S.A., Lee, K.H., Won, H.Y., Park, S., Chung, J.H., Jang, Y. and Ha, J.W. (2013) Quantitative Assessment of Aortic Elasticity With Aging Using Velocity-Vector Imaging and Its Histologic Correlation. *Arterioscl Throm Vas* **33**, 1306-1312.
[25] Ueno, T., Nambo, Y., Tajima, Y. and Umemura, T. (2010) Pathology of lethal peripartum broad ligament haematoma in 31 Thoroughbred mares. *Equine Vet J* **42**, 529-533.
[26] McGowan, C. (2011) Welfare of Aged Horses. *Animals (Basel)* **1**, 366-376.
[27] Ireland, J.L., McGowan, C.M., Clegg, P.D., Chandler, K.J. and Pinchbeck, G.L. (2012) A survey of health care and disease in geriatric horses aged 30 years or older. *Veterinary Journal* **192**, 57-64.
[28] Delgadillo, J.O.V., Delorme, S., El-Ayoubi, R., DiRaddo, R. and Hatzikiriakos, S.G. (2010) Effect of freezing on the passive mechanical properties of arterial samples. *J. Biomedical Science and Engeneering* **3**, 645-652.
[29] Nakashima, T. and Tanikawa, J. (1971) A study of human aortic distensibility with relation to atherosclerosis and aging. *Angiology* **22**, 477-490.
[30] Gardner, A.W. and Parker, D.E. (2010) Association Between Arterial Compliance and Age in Participants 9 to 77 Years Old. *Angiology* **61**, 37-41.
[31] Hallock, P. and Benson, I.C. (1937) Studies on the Elastic Properties of Human Isolated Aorta. *J Clin Invest* **16**, 595-602.
[32] Butcher, H.R., Jr. and Newton, W.T. (1958) The influence of age, arteriosclerosis and homotransplantation upon the elastic properties of major human arteries. *Ann Surg* **148**, 1-20.
[33] Chow, M.J. and Zhang, Y.H. (2011) Changes in the Mechanical and Biochemical Properties of Aortic Tissue due to Cold Storage. *J Surg Res* **171**, 434-442.
[34] Stemper, B.D., Yoganandan, N., Stineman, M.R., Gennarelli, T.A., Baisden, J.L. and Pintar, F.A. (2007) Mechanics of fresh, refrigerated, and frozen arterial tissue. *J Surg Res* **139**, 236-242.
[35] Heliczer, N., Lorello, O., Casoni, D. and Navas de Solis, C. (2016) Accuracy and Precision of Noninvasive Blood Pressure in Normo-, Hyper-, and Hypotensive Standing and Anesthetized Adult Horses. *J Vet Intern Med* **30**, 866-872.
[36] Decloedt, A., De Clercq, D., Ven, S., Vera, L. and van Loon, G. (2017) Right ventricular function during pharmacological and exercise stress testing in horses. *Vet J* **227**, 8-14.

Supplementary Table. Measured thickness, area % of elastin, smooth muscle cells, collagen type I and collagen type III within layer 1 and layer 2 for the caudal and cranial common carotid artery, distal aorta, median artery, external iliac artery and femoral artery in young and old horses.

| | | Layer 1 | | Layer 2 | |
|---|---|---|---|---|---|
| | | Young | Old | Young | Old |
| Thickness (µm) | Caudal common carotid artery | 1209±153 | 1554±647 | 441±63 | 424±88 |
| | Cranial common carotid artery | 1179±152 | 1405±246 | 436±70 | 401±68 |
| | Distal aorta | 1673±434 | 1972±380 | 408±3 | 429±47 |
| | Median artery | 1367±253 | 1549±240 | 381±155 | 338±107 |
| | External iliac artery | 1275±253 | 1571±213 | 353±84 | 307±74 |
| | Femoral artery | 1127±162 | 1701±579 | 344±54 | 361±83 |
| % Elastin | Caudal common carotid artery | 14±6 | 10±4 | 21±10 | 23±8 |
| | Cranial common carotid artery | 12±4 | 12±5 | 22±9 | 23±8 |
| | Distal aorta | 17±2 | 17±13 | 29±12 | 23±9 |
| | Median artery | 1±1 | 4±6 | 30±6 | 28±6 |
| | External iliac artery | 8±5 | 8±6 | 24±6 | 24±7 |
| | Femoral artery | 7±4 | 12±5 | 29±11 | 28±8 |
| % Smooth muscle actin | Caudal common carotid artery | 57±7 | 60±7 | 3±3 | 1±1 |
| | Cranial common carotid artery | 59±4 | 63±7 | 1±1 | 2±4 |
| | Distal aorta | 44±13 | 46±11 | 2±2 | 2±2 |
| | Median artery | 61±9 | 62±11 | 2±2 | 2±2 |
| | External iliac artery | 53±12 | 52±10 | 1±1 | 4±3 |
| | Femoral artery | 51±6 | 50±7 | 1±1 | 2±3 |
| % Collagen type I | Caudal common carotid artery | 23±7 | 25±6 | 2±2 | 1±1 |
| | Cranial common carotid artery | 23±7 | 25±3 | 2±1 | 3±4 |

| | | | | | |
|---|---|---|---|---|---|
| | Distal aorta | 16±11 | 20±6 | 0±0 | 2±2 |
| | Median artery | 36±11 | 24±14 | 2±2 | 2±2 |
| | External iliac artery | 34±11 | 24±10 | 1±1 | 2±1 |
| | Femoral artery | 34±11 | 23±10 | 1±1 | 2±1 |
| % Collagen type III | Caudal common carotid artery | 14±2 | 20±7 | 29±5 | 27±6 |
| | Cranial common carotid artery | 15±3 | 15±5 | 29±5 | 27±6 |
| | Distal aorta | 28±4 | 26±10 | 42±5 | 27±10 |
| | Median artery | 17±5 | 14±8 | 29±8 | 28±9 |
| | External iliac artery | 20±2 | 22±6 | 32±5 | 26±4 |
| | Femoral artery | 25±10 | 23±5 | 28±6 | 27±7 |

# CHAPTER 8:

# DISCUSSION

## Blood pressure measurement in horses

### Invasive versus noninvasive blood pressure measurement

Blood pressure monitoring is important and routine practice during general anaesthesia and is usually performed invasively. Invasive blood pressure measurement requires peripheral artery puncture. In horses, the facial artery or transverse facial artery are most commonly used. The (transverse) facial artery is located superficially and can easily be cannulated. In standing, awake horses however, invasive blood pressure measurement is more challenging as placement and fixation of a (transverse) facial artery catheter is not easy[1]. Another possible location to measure the arterial blood pressure invasively is the common carotid artery. As described in Chapter 3 of this thesis, for short-time resting measurements in standing, awake horses the carotid artery can be punctured ultrasound guided, using a 18 G needle of 90 mm, which is kept in place for several cardiac cycles. For blood pressure monitoring, the common carotid artery is sometimes transferred superficially, the so called carotid loop. Unpublished data of our research group showed that blood pressure monitoring is also possible without carotid loop, using an 18 G, 18 cm arterial catheter, inserted in the carotid artery by the Seldinger technique, in combination with a fluid-filled connection to an external pressure transducer. Fluid-filled blood pressure monitoring is relatively cheap, but measurement errors up to 20 mmHg are reported due to overshoot or dampening caused by small air bubbles or blood clots. Catheter tip pressure transducers, where a pressure sensor is located on the tip of the catheter, are more precise but also more expensive. In horses those catheters are mostly used to monitor venous pressures and have a larger diameter, needing a 8-9 Fr introducer sheath. This increases the risk for hematoma formation after catheter removal. Very small pressure tip catheters, especially designed for arterial measurement in mice, do exist (up to 3-4 Fr), but are very expensive and still require a sheath for insertion into the artery. The small size of sheath and catheter include a high risk for kinking in the awake horse. As such these small catheter tip pressure transducers are rarely used in horses.

In standing, awake horses, blood pressure is mostly measured noninvasively, as invasive blood pressure measurement remains time consuming and labour intensive[2]. Oscillometry and Doppler ultrasound with a cuff placed around base of the tail (or the leg in anesthetized animals) can be applied. Only limited research has been performed to study the correlation between invasively and noninvasively measured blood pressure in the standing, awake horse[2; 3]. Most research has been performed in the anesthetized animal. Nevertheless, due to changes in physiological parameters and because the recumbent position alters blood pressure, studies in anesthetized animals can not necessarily be extrapolated to standing, awake animals. Heliczer et al. (2016)[2] found that the correlation between the invasively

measured blood pressure in the transverse facial or facial artery and the noninvasively measured blood pressure at the level of the tail was remarkably higher in anesthetized horses (0.76-0.92) compared to standing horses (0.45-0.58), when all pressure ranges were included. If only the normotensive range was considered correlation coefficients were high (0.72-0.85) in the standing horse group. Olsen et al.(2016)[3] only investigated standing horses and found that the percentage of error between invasively and noninvasively measured blood pressure over all pressure ranges was 15-28%. In our *in vivo* studies, blood pressure was measured noninvasively and correlation with invasive measurements was not assessed.

Appropriate cuff size is an important consideration when blood pressure is measured noninvasively. In human medicine, a cuff width approaching 40% of the arm circumference is generally accepted as the most suitable[4-7]. A too large cuff (overcuffing) will underestimate blood pressure in the range of 6/3 mmHg (systolic/diastolic pressure)[8], while a too small cuff (undercuffing) will overestimate blood pressure in the range of 10/2-8 mmHg[9], respectively. Similar to human medicine, in small animal medicine the 2018 ACVIM consensus statement on hypertension recommends the width of the cuff being 30-40% of the extremity circumference[10]. In horses, generally a cuff width-to-tail circumference ratio of 40-60% is used and is also recommended by the manufacturers[3; 11-13]. Nevertheless, in 2016 Tearney et al.[14] studied the equivalence between invasive and oscillometric blood pressure measurements at different anatomical locations, using different cuff sizes. In contradiction to what is generally used in horses and small animals, this study found a width-to-tail circumference ratio of 0.25 being the most appropriate for equivalence between invasively and noninvasively measured blood pressure in horses. The effect of over- or undercuffing is still poorly understood in horses. The effect of one cuff size too small or too large will probably be less than the movement effect, as even in humans talking or changing arm position can influence the blood pressure measurement with 10/10 mmHg (systolic/diastolic arterial pressure) and 1-8/5-11 mmHg, respectively[9]. In our *in vivo* studies, a cuff suitable for a tail circumference between 17-25 cm ensuring a width-to-tail circumference ratio of 40-60% was used. However, in the study investigating Friesians, three Friesians showed a slightly higher tail circumference (26 cm in one horse and 27 cm in two horses). As mentioned, the effect of this slightly undersized cuff was judged to be small. Indeed, only one of the three horses showed a higher blood pressure, with a systolic arterial blood pressure of 182 mmHg and diastolic arterial pressure of 106 mmHg. Also a higher pulse pressure (76 mmHg) was found in this horse. Pulse pressure is known to be independent of cuff size, therefore the elevated blood pressure was probably not due to an inappropriate cuff size.

**Extrapolation of peripherally measured blood pressure**

An important limitation of noninvasively and invasively measured blood pressure, is the extrapolation of locally measured blood pressure to other locations. The correction factor, used to correct for hydrostatic pressure difference between the proximal aorta and the tail artery is a first important point of discussion. In literature, values of 0.74-0.77 mmHg for every cm difference in height are used[2; 3; 11-14]. The hydrostatic pressure of 1 cm of water is 0.74 mmHg. Nevertheless blood has a higher density compared to water. Therefore the correct correction factor, which is used in all our *in vivo* studies, is 0.77 mmHg for every cm difference in height, as $\Delta bp = d_v \,.\, \frac{sg_b}{sg_m}$, where $\Delta bp$ represents the difference in blood pressure, $d_v$ the vertical distance from the measurement point to the heart in mm, $sg_b$ the specific gravity of blood (1.05)[15] and $sg_m$ the specific gravity of Hg (13.6)[16].

In our *in vivo* studies, blood pressure measured at the coccygeal artery and corrected to the heart level, was used to calculate pressure-dependent arterial wall stiffness parameters. Although measurements are corrected for the difference in height, measurements still do not represent the central arterial blood pressure. Hemodynamics of the arterial waveform and thus the blood pressure are known to differ substantially over the arterial tree. Diastolic pressure is known to be roughly the same over the whole arterial system, but systolic arterial pressure is influenced by the amplification phenomenon[17]. Firstly, arterial stiffness increases rapidly with increasing distance from the heart, which leads to an increased and narrowed pressure waveform during systole in the periphery, resulting in a higher arterial pressure and thus a higher pulse pressure. Secondly, there is also an effect of reflected pressure waves, originating from arterial bifurcations, side branches or sudden changes in lumen area. Those reflected waves will arrive earlier in the periphery, due to the reduced distance to the site of wave reflections, leading to a further increase in peripheral systolic pressure[18]. Therefore variables can be used to compare stiffness within populations, but do not represent the actual stiffness of that artery at a given pressure.

To resolve those limitations, central blood pressure can be measured accurately by invasively introducing a pressure transducer catheter in the ascending aorta, as performed in Chapter 3 under general anaesthesia. Nevertheless this technique cannot be routinely used in clinical patients. Alternatively, in human medicine the waveform is captured noninvasively at a peripheral artery using tonometry. Afterwards, the aortic waveform can be reconstructed from the peripherally captured waveform using established formulas[18]. In horses such formulas do not exist. Preliminary studies from our research group show that tonometry, to capture the pulse wave noninvasively, is not easy to perform in horses. A large artery, running close to the

skin, supported by a bony structure is necessary, which is not the case for the carotid or femoral artery.

### Blood pressure measurement during exercise

In human medicine blood pressure monitoring during health assessment exercise tests is routinely performed and is considered crucial for the patient's safety and the interpretation of the level of exercise performed[19]. Invasive blood pressure measurement is only used in laboratory settings, while noninvasive sphygmomanometry is routinely used during cycling stress-tests[19]. The major advantage of cycling is that only the legs move, while the arms stay in a fixed position, which allows noninvasive blood pressure measurement. To the best of our knowledge, noninvasive blood pressure measurement during exercise in horses has not been performed. As the tail moves during all types of exercise, movement artefacts are likely to hamper noninvasive blood pressure measurement. There are studies investigating invasively measured arterial pressures during exercise, but mostly in a small number of horses. Hornicke et al. (1977)[20] recorded systemic blood pressure invasively during rest and exercise from the carotid artery in three horses. Blood pressure values of 205±23 mmHg systolic pressure, 116±12 mmHg diastolic pressure, 160±20 mmHg mean pressure and 98±19 mmHg pulse pressure were recorded during galop at a heart rate of 184±23 beats/min. For those measurements, a carotid loop was created several months before the experiment, which is too invasive to perform in clinical patients[20]. Cannulation of the transverse facial artery is less invasive but dislocation of the catheter during exercise remains an important limitation[1].

### Added value of the equine 1-dimensional arterial network model in future

Mathematical models, as designed here in Chapter 3, might be a fair alternative to study arterial blood pressure of horses during exercise. At the moment, our model is based on resting physiology and still has limitations. As this model is based on average data of five horses, predictions of pressure and flow profiles can be made for the average healthy horse, but not on individual horse level. A horse-specific approach would require to adapt several input parameters of the model such as geometry, elastic properties and peripheral resistance to the individual values of each horse, which is challenging. Current discrepancies in pressure and flow waveforms could also be explained by the exclusion of the venous systemic and entire pulmonary circulation, making the model an open loop system that requires boundary conditions: a cardiac time-varying elastance model at the inlet, and the Windkessel model at the terminal ends. Moreover, the cerebral arterial tree is not included in detail in the equine model, only a simplified representation containing the major vessels that supply the cerebral circulation. A more detailed description of the cerebral arterial tree may provide better predictions of pressure and flow waveforms in the carotid artery and smaller vessels of the

head circulation, as has been previously shown for the human and murine models [21]. Nevertheless, as flow waveforms are well captured by the model, this model can be used in future to predict changes in flow profiles and pressure waves under different circumstances, without the need of invasive measurements. For example, local pressures may be predicted during intensive exercise, contributing to a better understanding of arterial rupture during exercise. In order to do so, several input parameters should be adapted. Next to the adjustment of the heart rate and cardiac output during exercise, also the distribution of the cardiac output should be adapted. As described by Poole et al.[22] the main change would be the amount of blood going to the muscles. At rest only 15% of the cardiac output is provided for the muscles, which increases to >80% during maximal exercise in horses, while only 3% would go to the splanchnic organs, instead of 30% during rest. Including the pulmonary arterial circulation into the model could lead to a better understanding of exercise induced pulmonary haemorrhage, an intensively studied but still poorly understood condition in horses. Last but not least, these models could also be used to study the effect of aging in horses on the pressure and flow waves, by altering the arterial compliance. Therefore, the changes in arterial compliance found in Chapter 6 could be used. In addition, this model was helpful in explaining the remarkably oscillating pattern of the ultrasonographic flow waveforms found in horses. On the other hand, by altering the input parameters, the model will allow us to predict changes in flow waveforms.

### Structural properties of the arterial wall in horses

In general the arterial system can be divided in two different types of arteries, the high-conductance elastic arteries, which are located near the heart and the high-resistance muscular arteries, being more peripherally located. In humans, the aorta and carotid artery are classified as elastic arteries, containing more elastin, while for example the femoral and the mesenteric arteries have a higher % of smooth muscle cells and are therefore called muscular arteries. These muscular arteries are capable of controlling blood distribution and blood pressure towards the periphery according to the needs. In equine medicine, research into the morphology of the equine arterial wall is limited. In 2016 Saey et al.[23] studied the morphometric properties of the thoracic aorta in Warmblood and Friesian horses. In 2017, Endoh et al.[24] studied morphometric changes in the aortic arch from fetal to mature state in Thoroughbred horses. When results of both studies are compared, remarkable differences are found. In general, area percentages of all components were higher in the study of Saey et al. The area % of elastin was found to be 49% by Saey et al., and only 15-29% by Endoh et al., while the % of smooth muscle actin was 41% and 22-26%, respectively. Saey et al. also investigated the area % of collagen type I and III, being 26 and 35%, respectively, while Endoh et al. only investigated the total amount of collagen, being only 13-29%, when horses of the same age group are considered. When these results are compared with those of the

morphometric study included in this thesis, results more closely match the finding of Saey et al., except for the area % of collagen type III. Results of our study revealed 34-35% elastin, 42-45% smooth muscle actin, 23-25% collagen type I and 14-20% collagen type III at the level of the proximal aorta. In addition, our study did not only investigate the proximal aorta, but also the distal aorta, the carotid artery , the external iliac artery, the femoral artery and the median artery. The amount of elastin clearly decreased from the proximal (34-35%) to the distal aorta (15%), while the amount of collagen type I (23-25% vs. 15-19%), type III (14-20% vs. 22-25%) and vascular smooth muscle actin (42-45% vs. 37-40%) showed smaller variation.

In the proximal aorta, the tunica media consisted of an almost uniform layer of elastin, collagen and smooth muscle cells, while from the distal aorta onwards two separate layers were distinguishable within the tunica media. These consisted of a muscular inner layer (predominance of smooth muscle cells) and an elastic outer layer (predominance of elastic fibres). When passing from more centrally located elastic arteries to more peripheral muscular arteries, in human medicine, the amount of elastin is known to reduce and the elastin fibres are known to become predominantly organised in the internal elastic lamina and the external elastic lamina with a clearly defined layer of smooth muscle cells in between. The outermost elastic layer of the tunica media found in our study resembles the tunica elastica externa while a tunica elastica interna was not clearly distinguishable in our study. However, in some arteries the inner side of the first layer contained more elastin compared to the rest of this layer.

A significant effect of location was found for the total area % of elastin and collagen type III. The largest amount of elastin was found in the proximal aorta (34-35%), while the lowest amount was found for the median artery and the external iliac artery (7-11%). Nevertheless, the area % of smooth muscle actin was not significantly different between the arteries, ranging from 37 to 51%. The amount of collagen type III did differ significantly between arterial locations, ranging from 14-20% in the proximal aorta, to 25-29% in the femoral artery. Surprisingly and in contrast to humans, the common carotid artery cannot be classified as an elastic artery, as it only contains a small amount of elastin (14-16%) compared to smooth muscle actin (43-51%). This is probably due to the continuously changing head position in horses (grazing versus head up), which means regulation of blood pressure by adapting vasomotor tone is necessary to prevent too low or too high cerebral pressures. The presence of a large amount of smooth muscle cells in the carotid artery is also described in giraffes[25].

## Biomechanical properties of the arterial wall in horses

The biomechanical properties of the arterial wall can be investigated using tensile tests, stretching the arterial wall in a controlled way, starting from a zero stress state. Saey et al. (2015)[26] investigated the biomechanical properties of the arterial wall in Friesians and

Warmblood horses, using a uniaxial tensile test, performed in the longitudinal and circumferential direction. Biaxial tests are preferred over uniaxial tests, as they simulate better the *in vivo* arterial behaviour. This technique is technically more difficult to perform, due difficulties in tissue fixation. In this thesis, arterial wall properties were studied using an inflation-extension test. This test is preferred over uni- or biaxial tensile tests, as it does not only take into account the longitudinal and circumferential characteristics of the arterial wall, but also the stress characterized by the sample curvature. Usually, optical measurement systems to monitor diameter changes are used[27]. A previous study showed good reproducibility of ultrasonographic assessment of tissue properties in porcine aortas[28], therefore, in our study ultrasonographic measurement of diameter change was performed. Areas were calculated from diameters measured on longitudinal images, as cross-sectional ultrasound images often had poor image quality at 4 and 8 o'clock[28]. Data derived from our inflation-extension test fitted the pressure-area relationship arctangent model of Langewouters et al.[29] well, indicating that the behaviour of equine arterial tissue with increasing pressure is similar compared to humans. Clear differences were found between different arterial segments, which has also been observed in human patients[29]. The pressure-compliance curve of the proximal aorta showed a completely different pattern compared to the other investigated arteries. For the proximal aorta, the highest compliance was found at a pressure of 100 mmHg. This is totally different compared to the distal aorta, common carotid artery and external iliac artery, where maximum compliance was found at the lowest investigated pressures of 15-30 mmHg. In humans, maximal aortic compliance is typically found at pressures around 50 mmHg for the proximal aorta[29], which is a remarkably lower pressure compared to horses (100 mmHg). For the abdominal aorta in humans, the pressure at maximal compliance is around 30 mmHg, which is the same as found in horses.

**Comparison of histological and biomechanical findings**

Significant histological differences were found between central and more peripheral arteries. The proximal aorta contained the highest area % of elastin (35±11%), while the external iliac artery, femoral artery and distal aorta showed the highest area % of collagen type III. Therefore a more elastic proximal aorta and a stiffer external iliac artery and distal aorta were suspected to be found in the *ex vivo* inflation-extension test. Nevertheless, the maximal distensibility, describing the maximal relative area change per mmHg, was significantly lower for the proximal aorta (0.008±0.001), compared to the distal aorta (0.022±0.14), which was at his turn significantly higher compared to the external iliac artery (0.006±0.003). The higher distensibility found at the level of the distal aorta compared to the external iliac artery is probably due to the significantly higher area % of elastin in the distal aorta (15±5% versus 11±5%). The low distensibility of the proximal aorta could not be explained based on current histological findings.

Whether or not the elastic properties of the tunica adventitia, which contributes to arterial stiffness and compliance[30-32], may have played a role could not be determined as it was not included in the histological study.

**The influence of freezing and thawing on arterial wall properties**

Tissue storage might have influenced the biomechanical properties of the arterial wall. Bovine arteries have been shown to change due to cold storage. Storage at -20 or -80°C is preferred over storage at 4°C, nevertheless, even at -80°C, as performed in our study, biomechanical changes have been described[33].

A loss of collagen has been described in frozen tissue. A normal stress-strain curve shows a knee-point, between the initial and the stiff slope. This knee-point is the point at which collagen fibres are being recruited to help bear the stress load, up till than carried by elastin. In thawed tissue, due to a loss of total collagen, the knee-point will shift to a higher strain (Fig. 1). This loss of total collagen is found in tissue stored at -20°C as well as at -80°C. The amount of collagen loss did not increase with increasing storage time[33]. Stemper et al. (2017)[34] found no difference in ultimate tensile strength between fresh porcine arterial tissue and frozen tissue at -20 and -80°C for 3 months, indicating a minimal effect of freezing on arterial tissue biomechanics. The elastin network, the most important in determining tissue compliance, seems to be not affected by freezing. In both studies, the initial slope, defined by the elastin network, was not affected by freezing. In contrary, Venkatasubramanian et al. (2006)[35] found clear differences between fresh and frozen arterial tissue in the lower strain region, indicating that freezing does also affect elastin. O'Leary et al. (2014)[36] on the other hand, demonstrated that porcine arterial tissue samples can be frozen without changes in biomechanical properties. The contrariety within these studies indicates that the exact effect of freezing is not totally clear yet. The preservation of smooth muscle cells during freezing depends on the freezing protocol and the applied medium. Without cryoprotective agent, freezing will decrease the volume of liquid water in the cells due to extracellular ice formation, leading to cellular dehydration, which might lead to a too high electrolyte concentration in the cell, resulting in smooth muscle cell death[37]. In our study, no cryoprotective medium was applied, as such probably leading to smooth muscle cell death. Cryopreservation in foetal calf serum, containing 1.8 M DMSO as cryoprotecting agent could have been applied as it is shown to preserve maximal contractile response after freezing for indefinite time. The serum is responsible for the maintenance of the endothelial function, while DMSO is necessary for the preservation of the smooth muscle cells itself[38]. Preservation of smooth muscle cells would lead to a horizontal shift of the pressure at which the compliance is maximal as shown in human medicine[39]. To test whether or not

smooth muscle cells were still intact, the effect of adding the α1-adrenergic agonist phenylephrine to the water bath could have been assessed.

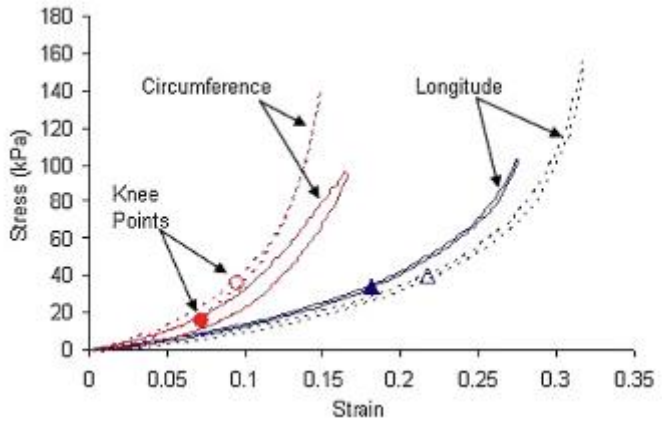


*Figure 1: Stress-strain curve from a bovine artery. Full lines represent fresh tissue, dotted lines represent frozen tissue (-20°C). The knee-points shift to higher strain in both directions due to freezing and thawing[33].*

***Comparison of biomechanical and in vivo findings***

Despite the freezing - thawing process, a similar compliance was found in the *ex vivo* study (Chapter 7) and compliance found in the *in vivo* study (Chapter 5) performed in 101 Warmblood horses, when values of the same pressure range are compared. With a mean arterial pressure of 106 mmHg the proximal aortic compliance was 15.50 $mm^2$/mmHg *in vivo*, compared to 15.95 $mm^2$/mmHg at a pressure of 100 mmHg in the *ex vivo* study. For the carotid artery, the *in vivo* compliance was 0.29 $mm^2$/mmHg vs. 0.20 $mm^2$/mmHg *ex vivo* and for the external iliac artery 0.24 $mm^2$/mmHg *in vivo* vs. 0.19 $mm^2$/mmHg *ex vivo*. This might indicate that, at rest, smooth muscle cells do not contribute substantially to the arterial wall stiffness. Nevertheless values considered here are mean values over multiple horses. In individual horses, differences would probably be larger due to the absence of intact smooth muscle cells in the frozen arteries and other freezing-caused damage.

In conclusion, this ‘novel’ type of inflation-extension test, performing underwater ultrasound of a pressurized artery is an easy and cheap method to reliably assess arterial wall biomechanical properties. Longitudinal images ensure precise diameter measurements, while immersion in physiological solution (0.9% NaCl) avoids drying out or swelling of the tissue, which would lead to stiffness alterations[28]. Also fixation of the artery onto the pressurisation system was relatively easy compared to clamping problems when thicker arterial tissue is tested in uni- or biaxial tensile tests. Therefore, this technique is probably also applicable to arterial tissue of other species.

## Feasibility and reliability of *in vivo* arterial wall stiffness measurement in horses

Chapter 4 describes the different investigated techniques of arterial wall stiffness measurement in horses and their repeatability. As far as the authors know, this is the first study describing the arterial wall stiffness in horses. In this study, the aortic wall stiffness, but also the wall stiffness of more peripheral arteries such as the common carotid artery and the external iliac artery were assessed.

### Regional arterial wall stiffness

Regional aortic arterial wall stiffness was assessed using the pulse wave velocity between the caudal carotid and the external iliac artery and the pulse wave velocity between the proximal aorta and external iliac artery. Both parameters did show low coefficients of variation (3-15%), making them both suitable for clinical use. The lowest values were found for the carotid to external iliac artery pulse wave velocity (3-12%). The higher coefficients of variation for proximal aorta to external iliac artery might be related to the fact that large horses with a tendency to obesity were used in our study which makes Doppler investigation of the proximal aorta more challenging. In addition, carotid to external iliac artery pulse wave velocity measurement is probably easier to perform in clinical practice as it does not require a low MHz cardiac ultrasound probe. Nevertheless, the proximal aorta to external iliac artery pulse wave velocity more precisely describes the compliance of the aorta itself. Indeed, the carotid to external iliac artery pulse wave velocity suggests a similar velocity in carotid artery and aorta, which is not the case. Taking into account the difference in elasticity between different arteries, the proximal to distal aortic pulse wave velocity would be ideal to study the stiffness of the aorta itself. Rectal ultrasound is, however, likely to result in increased heart rates and is not without risk. The technique could be useful in an experimental setting but seems less useful in practice.

A human study on short term repeatability of carotid to femoral pulse wave velocity showed comparable coefficients of variation ranging from 3.4-9.5%, using multiple synchronous or electrocardiogram (ECG)-based devices (e.g. the Complior, Sphymocor, Biopac,…). All devices applied in that study used algorithms to calculate the pulse wave velocity using the foot-to-foot method[40]. In our study in horses, no simultaneous recordings were made, and ECG-based measurements were performed manually. Using a manual technique introduces larger measurement errors and inter-observer variations. Indeed inter-observer coefficient of variations were the highest (up to 15%) but still acceptable. Another point which might introduce measurement error is the non-simultaneous recording of the flow profile at the two investigated locations as heart rate might slightly change. In dogs, Nogueira et al. found an inter- and intra-observer variability of 12% for carotid to femoral pulse wave velocity with

simultaneously recorded pulsed-wave Doppler signals in combination with manually measured transit time[41], comparable to our study in horses. This indicates that, although images were not collected simultaneously, this has not introduced large measurement errors in our study.

The caudal to cranial common carotid artery pulse wave velocity was also tested in our study. As this is a large, easily accessible artery, which can be examined at two different places on a relatively big distance from each other, carotid pulse wave velocity would be very useful to evaluate and monitor horses' arterial health, by means of arterial wall stiffness. Unfortunately, our study showed that carotid pulse wave velocity showed moderate to high (20-37%) coefficients of variation, which makes it not useful as a clinical parameter in horses. This is probably due to the difficulty of measuring accurately the exact distance between the two measuring places on the carotid artery. Probe angulation, necessary to align with the flow direction complicated estimation of investigated distance. Continuously changing head positions in some horses, complicated the distance determination even more. A device measuring the pulse wave velocity based on the time delay, picked up by tonometry, piezoelectric sensors, Doppler ultrasound, ultrasound wall tracking or photoplethysmography, between a fixed measurement distance could be a possible solution. Nevertheless, with the current knowledge we have now in horses (derived from our *ex vivo* study in Chapter 7), the large amount of smooth muscle cells in the equine carotid artery wall, the carotid artery cannot be considered as an elastic artery in horses and as such measurement of the carotid pulse wave velocity might not be a good option to estimate general arterial stiffness in horses.

***Measurement or calculation of the real travelled distance***

The most challenging part of aortic pulse wave velocity calculation remains the measurement or calculation of the real travelled distance of the pressure wave. In human medicine, multiple studies, including a large number of patients, have been performed using MRI or invasive measurements to predict real travelled distance based on surface measurements[42; 43]. Our study in horses was based on necropsy findings and included only five horses. Full body scans cannot be performed in adult horses as they do not fit in the gantry. Studies in foals or miniature horses were not considered as their body size cannot be transformed to adult size[44]. Invasive catheter based measurements might be an option but these are invasive and relatively difficult to perform. Therefore *ex vivo* measurement of the arterial tree in situ seemed the best option for comparison between surface measurements and real travelled distance. Data from more horses are needed as well as data from different breeds.

In human medicine, pulse wave velocity is independently associated with visceral fat. On the other hand, the travelled distance, measured over the body surface might be substantially overestimated in obese people, leading to falsely increased pulse wave velocities[45]. In none

of our studies body condition score was included. Including body condition score might have improved our studies. Nevertheless if body condition score would have been significantly associated with pulse wave velocity, it would still not be possible to define whether also in horses obesity contributes to increased arterial wall stiffness, or whether the pulse wave velocity would be overestimated by the higher measured surface distance. Another option would have been measuring the length of the horse in one straight line, 'birds eye view', without taking into account the body curves.

***Interspecies comparison of regional pulse wave velocity***

In our study in 101 normal, healthy Warmblood horses a mean carotid to external iliac artery pulse wave velocity of 5.8 m/s was found in horses aging 3-27 years. In humans, slightly higher normal values are reported ranging from 6.2 to 10.9 m/s in people from 30 years to 70 years old[46], while in healthy dogs of 1-8 years, normal values of 12-14 m/s were found[41]. This indicates a clearly stiffer aorta in dogs, compared to humans and equines. When interpreting these studies, measurement methods to estimate the real travelled distance should be kept in mind. All three studies use different methods. The study in dogs uses the uncorrected surface distance between the carotid and the femoral artery, which is an overestimation of the true travelled distance, leading to an overestimation of the pulse wave velocity. In the human study a correction factor of 0.8 was used. In our equine study, as described previously, the length of the horse (m) was multiplied with 0.62 and reduced with 0.40 m. The estimated difference in the human and equine study should more closely approach real travelled distance, and therefore calculated pulse wave velocity will more closely match true pulse wave velocity, compared to the study in dogs.

***Future applications of regional pulse wave velocity measurement***

In human medicine, pulse wave velocity or rather pulse transit time can be used to monitor blood pressure over a longer period of time. Multiple devices, such as ear-lobes[47] and armbands[48; 49] have been described. Those devices derive pulse transit time directly from a (built in) ECG and photoplethysmography, as the time between the R wave of the ECG and the arrival of the pulse wave. As such, blood pressure can be estimated based on pulse transit time. This technology is reliable, cost-efficient and easier to use compared to cuff-based blood pressure monitoring[48; 49]. This technique could also be applicable in horses. Armbands could be placed around the tail. The coccygeal artery runs superficially under the skin, making photoplethysmography, measuring local changes in blood volume, possible. The skin pigmentation at the level of the tail in most horses might be a compromising factor. Red light passes equally well through all skin tones. Nevertheless, compared to green light, of which the transmission through dark skin is known to be less than half compared to transmission through

lighter skin, red light gives poor performance in terms of errors caused by movement and ambient light. Further research to investigate the best type of light for use in horses is necessary. As mentioned previously blood pressure monitoring in the standing horse is not easy, especially not when long term follow-up of blood pressure is desirable. As such, this technique could be extremely useful for over-time blood pressure monitoring in critically ill horses, in order to rapidly notice a clinical important in- or decrease in blood pressure.

**Local arterial wall stiffness**

Local stiffness parameters including diameter/area change, strain, distensibility, compliance and stiffness index of the aorta, common carotid artery, median artery, external iliac artery and femoral artery revealed high coefficients of variation, up to 69%. These parameters are thus not useful as a clinical parameter, although they might be useful for populational research[50]. Calculations were based on diameter and area measurements. Diameter measurements showed clearly lower coefficients of variation compared to area measurements. Areas were more difficult to measure. The tunica intima was clearly visible at a perpendicular insonation angle in the near field and far field wall. Due to edge shadowing, the tunica intima was more difficult to identify at the edges because of a more parallel insonation angle, resulting in a weaker reflection. Therefore an assumption of the continuation of the intima at the side edges needed to be made, which probably introduced a significant measuring error. Carotid diameters were measured from transverse M-mode images. Similarly, the intima was clearly visible in the near field and far field wall, making measurements more precise. External iliac artery diameter measurements were performed from longitudinal M-mode images as transverse images were very difficult to obtain, due to difficulties with probe angulation. Nevertheless, diameter measurement of the external iliac artery showed the highest coefficients of variation, probably related to the more challenging image acquisition.

Images of the median artery, just proximal to the carpus at the medial side of the front leg were also collected. Local stiffness parameters could not be assessed, as in most horses a clear systolic dilation and diastolic collapse could not be identified. It should be noted that large individual differences in median artery diameter were found. This could have been related to a lower limb disease process as some of those horses had a known history of lameness. This was not further studied as it was beyond the scope of our study.

***Analysis of arterial wall motion by use of tissue Doppler***

Analysis of arterial wall motion by use of tissue Doppler imaging can be used to assess local arterial wall stiffness in humans[51; 52]. Tissue Doppler is a technique in which Doppler signals produced by tissue motion are filtered from blood-flow Doppler signals. Signals are filtered based on amplitude as tissue Doppler signals are about 40dB larger in amplitude compared to

blood-flow signals[51]. The sample volume is placed in the arterial wall of interest and peak systolic and diastolic movement can be registered. Echocardiographic measurements need to be made during apnoea, to eliminate the effect of respiration on the movement of the arterial wall[52]. This technique has been shown to be valuable for assessment of human arterial wall stiffness of the aorta and carotid artery[51-53]. This technique was also briefly evaluated on equine aorta, carotid and external iliac arteries. Because systolic and diastolic peaks were difficult to obtain and variable, partially due to motion artefacts, the technique was not further explored.

***Radiofrequency-based carotid wall tracking***

In human medicine, radiofrequency-based carotid arterial wall tracking is used to accurately assess the changes in arterial diameter during the cardiac cycle. The temporal and spatial resolution of routine ultrasound video images is not sufficient to follow the rapid changes of the arterial wall during the cardiac cycle. In order to be able to follow those rapid changes of the arterial wall, high-resolution wall tracking systems, analysing radiofrequency signals have been developed. These radiofrequency-based wall-tracking systems track the arterial wall movement and use calibrated distension waveforms to estimate pressure. The most known and most used, commercially available systems are the QAS software of Esaote and the E-track system of Aloka. These systems automatically calculate the beta-stiffness index and the arterial distention. The QAS software measures the changes in diameter simultaneously in 32 equidistant and parallel lines, while the E-track software evaluates the diameter along one single line[54]. We also evaluated the QAS software of Esaote for use in horses, but unfortunately this software was not able to track both the lateral and medial wall of the equine carotid artery, probably because the software is not designed for such a large and deep located arterial lumen. As far as we know, the E-track software has not been used in horses yet. A previous preliminary study of our research group showed that raw radiofrequency data of our ultrasound equipment (Vivid 7 in combination with a 12 MHz linear probe, GE Healthcare) could be used to track the arterial wall movement of the common carotid and femoral artery in awake and anesthetized horses. The raw data of six consecutive cardiac cycles of longitudinal B-mode images were exported to Matlab. The inner and the outer wall were tracked automatically throughout the cardiac cycles, producing arterial distension curves in order to derive arterial diameters and calculate absolute and relative arterial distension[55]. In the studies included in this thesis arterial diameters were measured from longitudinal (external iliac artery) or transverse (carotid artery) M-mode images, as dedicated raw data software was not available. M-mode images have the highest temporal resolution, therefore this mode was chosen to measure arterial diameters and derived arterial distention and compliance.

#### *Shear wave elastography*

Shear wave elastography is another, even newer technique to analyse local arterial wall stiffness. Ultrasonic shear waves are sent into the studied tissue. The propagation velocity of this shear wave is directly correlated with the stiffness of the investigated tissue, in this case the artery[56]. A commercially available example of shear wave technology to measure arterial wall stiffness is the Aixplorer (SuperSonic Imagine). Shear waves are created by a supersonic push, composed of three consecutive pushes of 100µs located 5 mm apart along the centreline of a region of interest selected manually by the sonographer. This region of interest needs to include the anterior and posterior wall of the carotid artery (Fig. 2). The propagation of the shear wave can be imaged over 5ms with a frame rate of 8000 images/s[57]. As far as the authors know, this technique has not been investigated in horses yet.

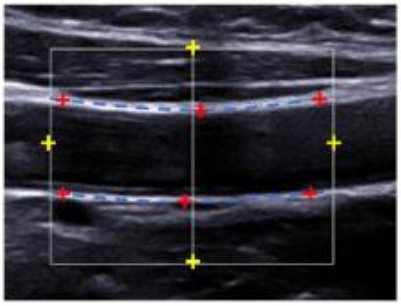

*Figure 2: Manual wall delineation used for shear wave elastography[57]*

## Factors that might influence arterial wall stiffness

### Breed

As mentioned in the introduction, in human medicine clear differences are found between black people, African people, Asian people and white people[58-62]. In this thesis, differences between Warmblood horses, the most prevalent horse type in Belgium and Friesian horses, which are prone to aortic rupture[63-65], were investigated. From this study we concluded that Friesian horses have a stiffer aorta, compared to Warmblood horses, as carotid to external iliac artery and aorta to external iliac artery pulse wave velocity were significantly higher in Friesian horses. Because Friesians have a totally different body composition results should be interpreted with caution. Friesians were less tall but had a bigger chest circumference and thus a higher calculated weight. Obesity can lead to an overestimation of the travelled distance, resulting in a falsely increased pulse wave velocity[45]. Moreover Friesians were longer compared to Warmblood horses. *Ex vivo* length determination of Friesian aortas however has not been investigated. Unpublished data of our study, revealed a significantly shorter transit time at the level of the external iliac artery in Friesian horses (258±25 ms) compared to Warmblood horses (278±28 ms; $p<0.001$). This means that, even if the travelled aortic distance

would have been the same in Friesian horses and Warmblood horse, the pulse wave velocity would still have been higher in Friesian horses. In addition, also local stiffness parameters of the aorta, the diameter change, distensibility coefficient and compliance coefficient were lower in Friesians compared to Warmblood horses, supporting the finding that Friesians do have a stiffer aorta.

Another important finding is that Friesians show a higher systolic, diastolic and mean arterial pressure in combination with a higher pulse pressure. Friesians had smaller arteries, but their cardiac output was the same as in Warmblood horses. The same blood volume traveling through smaller arteries might lead to a higher blood pressure and pulse wave velocity[66]. Nevertheless, this cannot explain the higher pulse pressure found in Friesians. The higher pulse pressure can only be explained by a higher arterial wall stiffness, as shown by both local and regional aortic stiffness parameters. Increased arterial wall stiffness however would only lead to an increased systolic arterial pressure and pulse pressure, in combination with a decreased diastolic arterial pressure, which was not the case in our study. Therefore we suggest that the increased diastolic arterial pressure is a consequence of a difference in systemic vascular resistance between Friesians and Warmblood horses, or that the increased diastolic pressure is indeed due to the same blood volume traveling through smaller arteries. Whether the higher systolic arterial pressure is the cause or the consequence of the increased arterial wall stiffness remains unclear. Increased arterial wall stiffness can lead to a higher blood pressure, but over time, a higher blood pressure can lead to increased arterial wall stiffness. This increase in arterial wall stiffness can be explained by a higher amount of collagen in the arterial wall induced by a constantly high blood pressure. This can be confirmed by the study of Saey et al[23], revealing that Friesians have a higher amount of collagen in the arterial wall compared to Warmblood horses. Probably the increased arterial wall stiffness and the increased blood pressure are part of a vicious circle.

In this thesis, only Friesians were compared with Warmblood horses, because they are known to be prone to aortic rupture. Nevertheless, there might also be important differences between other breeds. In literature, sudden death due to arterial rupture is more often described in Thoroughbred horses, compared to other horse breeds[67]. Whether this is a breed effect or an effect of training and exercise is not clear. As Thoroughbred horses in general perform at maximum cardiac and pulmonary capacity, an effect of the type of exercise performed is suggested over an effect of breed on the arterial wall stiffness predisposing these horses to arterial rupture. Further research examining Warmblood and Thoroughbred horses of a comparable training level, preferable untrained, or trained in the same stable, by the same trainer, following the same training protocol should be performed.

### Training

In human medicine, normal, regular, aerobic exercise is known to be inversely related to arterial wall stiffness[68-72]. Resistance exercise, however, a popular mode of exercise in humans, seems to increase the arterial wall stiffness, independent of age or gender[73; 74]. Resistance exercise is known as an anaerobic type of exercises. In horses the effect of training on the arterial wall stiffness has not been investigated, certainly not the effect of different types of exercise. The short-length high-intensity sprint types of exercise, like quarter horse races, barrel racing, timed events and draft horse pulls are known to be anaerobic types of exercise, probably comparable with resistance training in humans. In the race horse industry, resistance training is also used as a popular method to successfully train racehorses. A resistance cart is used or horses are trained uphill. This kind of resistance training is considered as an important part of successful racehorse training, but might have a negative effect on the arterial wall stiffness. The trotting or pacing races and the thoroughbred races can be considered as partially aerobic and partially anaerobic training. Up to a given point those horses perform aerobically, changing to anaerobic metabolism as time, distance and speed increases. Jumping and dressage can be considered as mostly aerobic exercises, but probably partially anaerobic too. Lastly endurance training, also known as sub-maximal exercise, relies mostly on aerobic metabolism[75]. The effect of training on arterial wall stiffness in horses might as such be very different depending on the discipline and training or competition scheme. The effect of training was not assessed in this thesis. To properly assess the effect of the different types of training, as previously suggested, horses should be trained following a strict training protocol and compared to non- or less trained horses of the same breed, same sex and same age category.

### Gender

In human medicine, gender is known to play an important role in arterial wall stiffening, as both testosterone and oestrogen have a protective role against arterial wall stiffening. Before puberty, females have less compliant arteries compared to males, which changes after puberty. Postmenopausal women in contrary, show an accelerated stiffening of the arterial wall due to a loss of oestrogen[76; 77]. Changes in postmenopausal women are shown to be comparable with the aging mare[78; 79]. Therefore the effect of aging on the arterial wall stiffness might also be comparable. Nevertheless horses are reproductively aged for a shorter period of time: above 20 years of age, while they have a life expectancy of only 29 years. Women are mostly in the menopause from the age of 50, which means for almost 40% of their lifespan. When stallions and mares would be compared, the same findings as in humans are suggested: less compliant arteries in mares before reproductive age compared to stallions. In

the reproductive stage of life, mares are expected to have more compliant arteries, while after the reproductive age, mares are suspected to develop a more rapid increase in arterial wall stiffness. In our study population, most of the males were castrated, which is fairly representative for the general equine (sport horse) population. As such the protective role of testosterone will disappear. Therefore we expect that both before and after puberty, mares might have more compliant arteries compared to geldings. In horses aged over 20 years, the effect of gender is difficult to predict, as both the protective roll of oestrogen and testosterone will not be present when mares and geldings are considered. In this thesis we did not succeed in collecting enough data from stallions and therefore the effect of gender was not assessed. To study this effect a sufficiently large group of mares, stallions and geldings of all age categories, before, during and after the reproductive stage (>20 years) should be included.

**Age**

Arterial aging is predominantly characterized by a decrease in arterial wall elasticity, in combination with luminal enlargement and arterial wall thickening[80-82]. As explained in the introduction this increased arterial wall stiffness will lead to an increased systolic and decreased diastolic pressure leading to an increased pulse pressure. Moreover, increased arterial wall stiffness will lead to a higher pulse wave velocity, increasing even more the systolic pressure, on his turn inducing increased arterial wall stiffness in a vicious circle[83].

***In vivo assessment of the effect of aging on the arterial wall***

This thesis includes an *in vivo* study of arterial wall stiffness measurement in 50 young and 50 aged horses. Our study did show enlarged arterial diameters, in combination with a thickened arterial wall. Moreover, all regional and most local arterial wall stiffness parameters indicated increased arterial wall stiffness in the older horses. Nevertheless, no difference in blood pressure was found between young and old horses. This might be explained by the lower cardiac output found in the older horse group. A lower stroke volume, traveling through larger arteries will result in a lower blood pressure. This lower cardiac output, in combination with a reduction in arterial compliance is also found in aged dogs[84]. Another important consideration is the arbitrary differentiation between adult and aged horses. Some studies consider horses >15 years as old, because the age at which one becomes demographically old is defined as the age at which there is only 25% survivorship[85]. Other authors in contrary, considered horses old if they were aged >20 years and very old as aged >30 years[86]. If the chronological age is used, which refers to an animal's numerical age in comparison with its life expectancy, an artificial age limit of 20 or even 30 years (in ponies) should be used, as some studies report life expectancies of 30 or even 40 years old[86-88]. In our study, horses were considered young from 3-7 years and old if aged >18 years, based on the life expectancy of

horses in comparison with humans and the onset of arterial aging in humans[89-91]. The mean age of our young population was five years and 21 years for the old population. This means a difference of 16 years, which is an apparently short period of time, but actually is 50% of the total lifespan of horses. Differences found in regional aortic stiffness reached from 25 to 35%, which is lower compared to humans, but still is a noteworthy increase, indicating that equine arteries, in absolute timespan, age more rapidly.

***Histological assessment of the effect of aging on the arterial wall***

In human medicine, the increased stiffness is known to be mainly caused by elastin fragmentation, elastin calcification and an increase in collagen content and cross-links, while the arterial wall thickening is known to result from smooth muscle cell migration and proliferation[82]. Elastin fragmentation was not clearly found in our study and aortic calcifications were found in only one of the aged horses. In contrast to what was expected, the area % of elastin and collagen type I and III did not differ between the age groups. Collagen cross-linking was not analysed in this thesis. To do so high-performance liquid chromatography should have been performed[92]. Enoh et al. (2017)[24] studied the composition of the equine arterial wall from foetal to adult and aged stage of life and did found differences in both elastin and collagen amount, but not in the amount of smooth muscle cells. The amount of collagen significantly increased from the preadult stage (≤2 years) to the adult stage (>10 years). If the same age groups as in our study are considered, no significant differences are found. The amount of elastin decreased significantly from the preadult stage (<2 years) to the elderly stage (>20 years). If the same age groups of our study are considered, no differences are found. Combining the results of Enoh's and our study suggests that differences in elastin and collagen content can only be found between not-fully grown horses and adult or even aged horses, but not between adult and aged horses.

Our study did show an increased arterial wall thickness in combination with an increased area % of smooth muscle actin in older horses. In the aging artery contractile smooth muscle cells are known to transform to the synthetic phenotype, migrating to the intima and producing proteoglycans and collagen[93]. This production of extracellular matrix and collagen by the vascular smooth muscle cells leads to an increased arterial wall thickness. In our study, increased arterial wall thickness could not be attributed to smooth muscle cell phenotype switch, migration and proliferation as the overall area % of smooth muscle actin, which is only present in a very small amount in the secretory phenotype[94; 95], was increased in older horses. Moreover, there was no indication of an increased amount of collagen or proteoglycans in the tunica intima. Authors suggest that the increased amount of smooth muscle actin in older horses might be to compensate the decreased compliance, as found in the inflation-extension

test. The larger diameter found in older horses, might as such be compensated by active vasoconstriction by smooth muscle cells, in order to guarantee a maintenance of blood pressure. The increased amount of smooth muscle actin might indicate an increased amount of smooth muscle cells, leading to increased arterial wall thickness, or an increased amount of smooth muscle actin within the same amount of smooth muscle cells. As the amount of smooth muscle cells itself was not assessed in this thesis, no definitive conclusion could be drawn.

***Biomechanical assessment of the effect of aging on the arterial wall***

In this thesis the effect of age on the biomechanical properties of the arterial wall was determined using an *ex vivo* inflation-extension test. In human medicine, the biomechanical effect of aging on the aortic wall is well reported. It is known that the compliance at a physiological pressure of 100 mmHg decreases significantly with age. Moreover, the pressure at which the compliance is maximal decreases with age, which means that the pressure-compliance curve shifts to lower pressures. In addition, the maximal compliance, found at low pressures, increases exponentially with increasing age[39]. In our equine study, for the proximal aorta lower compliance at 100 mmHg was found in older horses, together with a shift of maximal compliance to lower pressures. In contrary to humans, lower maximal compliance was found in older horses. For the common carotid artery on the other hand, higher maximal compliance in old compared to young horses at low pressure range (15-45 mmHg) and lower compliance in older horses at physiological pressures were found, similar to human medicine.

## General conclusion

This thesis aimed at gathering knowledge on equine arterial physiology in general and more specifically on factors that might influence arterial function as these may play a role in arterial rupture. The one-dimensional equine-specific mathematical model, the noninvasive technique to study arterial wall stiffness *in vivo* and the self-designed *ex vivo* inflation-extension test in combination with the structural analysis allowed us to get better insights in the dynamics of blood pressure and vascular wall properties over the arterial tree. First remarkable findings were that Friesians have a stiffer aorta, a higher arterial blood pressure and an elevated pulse pressure compared to Warmblood horses. These findings likely contribute to the increased prevalence of aortic rupture in Friesians. A second finding was that older horses have larger arteries with thicker and also stiffer arterial walls. These findings explain why old horses have an increased prevalence of arterial rupture. These new insights and investigational tools will allow us to further unravel arterial pathophysiology in horses.

## References

[1] Decloedt, A., De Clercq, D., Ven, S., Vera, L. and van Loon, G. (2017) Right ventricular function during pharmacological and exercise stress testing in horses. *Vet J* **227**, 8-14.
[2] Heliczer, N., Lorello, O., Casoni, D. and Navas de Solis, C. (2016) Accuracy and Precision of Noninvasive Blood Pressure in Normo-, Hyper-, and Hypotensive Standing and Anesthetized Adult Horses. *J Vet Intern Med* **30**, 866-872.
[3] Olsen, E., Pedersen, T.L., Robinson, R. and Haubro Andersen, P. (2016) Accuracy and precision of oscillometric blood pressure in standing conscious horses. *J Vet Emerg Crit Care (San Antonio)* **26**, 85-92.
[4] Stergiou, G.S., Alpert, B., Mieke, S., Asmar, R., Atkins, N., Eckert, S., Frick, G., Friedman, B., Grassl, T., Ichikawa, T., Ioannidis, J.P., Lacy, P., McManus, R., Murray, A., Myers, M., Palatini, P., Parati, G., Quinn, D., Sarkis, J., Shennan, A., Usuda, T., Wang, J.G., Wu, C.O. and O'Brien, E. (2018) A Universal Standard for the Validation of Blood Pressure Measuring Devices Association for the Advancement of Medical Instrumentation/European Society of Hypertension/International Organization for Standardization (AAMI/ESH/ISO) Collaboration Statement. *Hypertension* **71**, 368-374.
[5] Kirkendall, W.M., Burton, A.C., Epstein, F.H. and Freis, E.D. (1967) Recommendations for human blood pressure determination by sphygmomanometers. *Circulation* **36**, 980-988.
[6] Strugo, V., Glew, F.J., Davis, J. and Opie, L.H. (1990) Update: Recommendations for human blood pressure determination by sphygmomanometers. *Hypertension* **16**, 594.
[7] Bovet, P., Hungerbuhler, P., Quilindo, J., Grettve, M.L., Waeber, B. and Burnand, B. (1994) Systematic Difference between Blood-Pressure Readings Caused by Cuff Type. *Hypertension* **24**, 786-792.
[8] Ringrose, J., Millay, J., Babwick, S.A., Neil, M., Langkaas, L.A. and Padwal, R. (2015) Effect of overcuffing on the accuracy of oscillometric blood pressure measurements. *J Am Soc Hypertens* **9**, 563-568.
[9] Handler, J. (2009) The importance of accurate blood pressure measurement. *Perm J* **13**, 51-54.
[10] Acierno, M.J., Brown, S., Coleman, A.E., Jepson, R.E., Papich, M., Stepien, R.L. and Syme, H.M. (2018) ACVIM consensus statement: Guidelines for the identification, evaluation, and management of systemic hypertension in dogs and cats. *J Vet Intern Med* **32**, 1803-1822.
[11] Drynan, E.A., Schier, M. and Raisis, A.L. (2016) Comparison of invasive and noninvasive blood pressure measurements in anaesthetized horses using the Surgivet V9203. *Veterinary Anaesthesia and Analgesia* **43**, 301-308.
[12] Tunsmeyer, J., Hopster, K., Feige, K. and Kastner, S.B.R. (2015) Agreement of high definition oscillometry with direct arterial blood pressure measurement at different blood pressure ranges in horses under general anaesthesia. *Veterinary Anaesthesia and Analgesia* **42**, 286-291.
[13] Hatz, L.A., Hartnack, S., Kummerle, J., Hassig, M. and Bettschart-Wolfensberger, R. (2015) A study of measurement of noninvasive blood pressure with the oscillometric device, Sentinel, in isoflurane-anaesthetized horses. *Vet Anaesth Analg* **42**, 369-376.
[14] Tearney, C.C., Guedes, A.G.P. and Brosnan, R.J. (2016) Equivalence between invasive and oscillometric blood pressures at different anatomic locations in healthy normotensive anaesthetised horses. *Equine Veterinary Journal* **48**, 357-361.
[15] Trudnowski, R.J. and Rico, R.C. (1974) Specific gravity of blood and plasma at 4 and 37 degrees C. *Clin Chem* **20**, 615-616.
[16] Byrd, J.B. and Brook, R.D. (2014) Arm position during ambulatory blood pressure monitoring: a review of the evidence and clinical guidelines. *J Clin Hypertens (Greenwich)* **16**, 225-230.
[17] Izzo, J.L., Jr. (2014) Brachial vs. central systolic pressure and pulse wave transmission indicators: a critical analysis. *Am J Hypertens* **27**, 1433-1442.
[18] Tomlinson, L.A. and Wilkinson, I.B. (2012) Does it matter where we measure blood pressure? *Brit J Clin Pharmaco* **74**, 241-245.

[19] Griffin, S.E., Robergs, R.A. and Heyward, V.H. (1997) Blood pressure measurement during exercise: a review. *Med Sci Sports Exerc* **29**, 149-159.
[20] Hornicke, H., von Engelhardt, W. and Ehrlein, H.J. (1977) Effect of exercise on systemic blood pressure and heart rate in horses. *Pflugers Arch* **372**, 95-99.
[21] Reymond P, Merenda F, Perren F, Rüfenacht D, Stergiopulos N.Validation of a one-dimensional model of the systemic arterial tree. Am J Physiol Heart Circ Physiol. 2009;297(1):H208-22. doi: 10.1152/ajpheart.00037.2009 9, 33].PubMed PMID 19429832
[22] Poole, D.C. and Erickson, H.H. (2011) Highly athletic terrestrial mammals: Horses and Dogs. *Compr Physiol* **1**, 1-37.
[23] Saey, V., Ploeg, M., Delesalle, C., van Loon, G., Grone, A., Ducatelle, R., Duchateau, L. and Chiers, K. (2016) Morphometric Properties of the Thoracic Aorta of Warmblood and Friesian Horses with and without Aortic Rupture. *J Comp Pathol* **154**, 225-230.
[24] Endoh, C., Matsuda, K., Okamoto, M., Tsunoda, N. and Taniyama, H. (2017) Morphometric changes in the aortic arch with advancing age in fetal to mature thoroughbred horses. *J Vet Med Sci* **79**, 661-669.
[25] Kimani, J.K. (1987) Structural organization of the vertebral artery in the giraffe (Giraffa camelopardalis). *Anat Rec* **217**, 256-262.
[26] Saey, V., Famaey, N., Smoljkic, M., Claeys, E., van Loon, G., Ducatelle, R., Ploeg, M., Delesalle, C., Grone, A., Duchateau, L. and Chiers, K. (2015) Biomechanical and biochemical properties of the thoracic aorta in warmblood horses, Friesian horses, and Friesians with aortic rupture. *Bmc Vet Res* **11**.
[27] Macrae, R.A., Miller, K. and Doyle, B.J. (2016) Methods in Mechanical Testing of Arterial Tissue: A Review. *Strain* **52**, 380-399.
[28] Mascarenhas, E.J.S., Peters, M.F.J., Nijs, J., Rutten, M.C.M., van de Vosse, F.N. and Lopata, R.G.P. (2016) Assessment of mechanical properties of porcine aortas under physiological loading conditions using vascular elastography. *J Mech Behav Biomed* **59**, 185-196.
[29] Langewouters, G.J., Wesseling, K.H. and Goedhard, W.J. (1984) The static elastic properties of 45 human thoracic and 20 abdominal aortas in vitro and the parameters of a new model. *J Biomech* **17**, 425-435.
[30] Greenwald, S.E. (2007) Ageing of the conduit arteries. *J Pathol* **211**, 157-172.
[31] von Maltzahn, W.W., Warriyar, R.G. and Keitzer, W.F. (1984) Experimental measurements of elastic properties of media and adventitia of bovine carotid arteries. *J Biomech* **17**, 839-847.
[32] Xie, J., Zhou, J. and Fung, Y.C. (1995) Bending of blood vessel wall: stress-strain laws of the intima-media and adventitial layers. *J Biomech Eng* **117**, 136-145.
[33] Chow, M.J. and Zhang, Y.H. (2011) Changes in the Mechanical and Biochemical Properties of Aortic Tissue due to Cold Storage. *J Surg Res* **171**, 434-442.
[34] Stemper, B.D., Yoganandan, N., Stineman, M.R., Gennarelli, T.A., Baisden, J.L. and Pintar, F.A. (2007) Mechanics of fresh, refrigerated, and frozen arterial tissue. *J Surg Res* **139**, 236-242.
[35] Venkatasubramanian, R.T., Grassl, E.D., Barocas, V.H., Lafontaine, D. and Bischof, J.C. (2006) Effects of freezing and cryopreservation on the mechanical properties of arteries. *Ann Biomed Eng* **34**, 823-832.
[36] O'Leary, S.A., Doyle, B.J. and McGloughlin, T.M. (2014) The impact of long term freezing on the mechanical properties of porcine aortic tissue. *J Mech Behav Biomed Mater* **37**, 165-173.
[37] Delgadillo, J.O.V., Delorme, S., El-Ayoubi, R., DiRaddo, R. and Hatzikiriakos, S.G. (2010) Effect of freezing on the passive mechanical properties of arterial samples. *J. Biomedical Science and Engeneering* **3**, 645-652.
[38] Muller-Schweinitzer, E. (2009) Cryopreservation of vascular tissues. *Organogenesis* **5**, 97-104.
[39] Langewouters, G.J. (1982) Visco-elasticity of the human aorta in vitro in relation to pressure and age

[40] Grillo, A., Parati, G., Rovina, M., Moretti, F., Salvi, L., Gao, L., Baldi, C., Sorropago, G., Faini, A., Millasseau, S.C., Scalise, F., Carretta, R. and Salvi, P. (2018) Short-Term Repeatability of Noninvasive Aortic Pulse Wave Velocity Assessment: Comparison Between Methods and Devices. *American Journal of Hypertension* **31**, 80-88.
[41] Nogueira, R.B., Pereira, L.A., Basso, A.F., da Fonseca, I.S. and Alves, L.A. (2017) Arterial pulse wave propagation velocity in healthy dogs by pulse wave Doppler ultrasound. *Vet Res Commun* **41**, 33-40.
[42] Weber, T., Ammer, M., Rammer, M., Adji, A., O'Rourke, M.F., Wassertheurer, S., Rosenkranz, S. and Eber, B. (2009) Noninvasive determination of carotid-femoral pulse wave velocity depends critically on assessment of travel distance: a comparison with invasive measurement. *J Hypertens* **27**, 1624-1630.
[43] Huybrechts, S.A., Devos, D.G., Vermeersch, S.J., Mahieu, D., Achten, E., de Backer, T.L., Segers, P. and van Bortel, L.M. (2011) Carotid to femoral pulse wave velocity: a comparison of real travelled aortic path lengths determined by MRI and superficial measurements. *J Hypertens* **29**, 1577-1582.
[44] Brooks, S.A., Makvandi-Nejad, S., Chu, E., Allen, J.J., Streeter, C., Gu, E., McCleery, B., Murphy, B.A., Bellone, R. and Sutter, N.B. (2010) Morphological variation in the horse: defining complex traits of body size and shape. *Anim Genet* **41 Suppl 2**, 159-165.
[45] Canepa, M., AlGhatrif, M., Pestelli, G., Kankaria, R., Makrogiannis, S., Strait, J.B., Brunelli, C., Lakatta, E.G. and Ferrucci, L. (2014) Impact of central obesity on the estimation of carotid-femoral pulse wave velocity. *Am J Hypertens* **27**, 1209-1217.
[46] Mattace-Raso, F.U.S., Hofman, A., Verwoert, G.C., Witteman, J.C.M., Wilkinson, I., Cockcroft, J., McEniery, C., Yasmin, Laurent, S., Boutouyrie, P., Bozec, E., Hansen, T.W., Torp-Pedersen, C., Ibsen, H., Jeppesen, J., Vermeersch, S.J., Rietzschel, E., De Buyzere, M., Gillebert, T.C., Van Bortel, L., Segers, P., Vlachopoulos, C., Aznaouridis, C., Stefanadis, C., Benetos, A., Labat, C., Lacolley, P., Stehouwer, C.D.A., Nijpels, G., Dekker, J.M., Ferreira, I., Twisk, J.W.R., Czernichow, S., Galan, P., Hercberg, S., Pannier, B., Guerin, A., London, G., Cruickshank, J.K., Anderson, S.G., Paini, A., Rosei, E.A., Muiesan, M.L., Salvetti, M., Filipovsky, J., Seidlerova, J., Dolejsova, M. and Stiffnes, R.V.A. (2010) Determinants of pulse wave velocity in healthy people and in the presence of cardiovascular risk factors: 'establishing normal and reference values'. *European Heart Journal* **31**, 2338-2350.
[47] Inajima, T., Imai, Y., Shuzo, M., Lopez, G., Yanagimoto, S., Iijima, K., Morita, H., Nagai, R., Yahagi, N. and Yamasa, I. (2012) Relation Between Blood Pressure Estimated by Pulse WaveVelocity and Directly Measured Arterial Pressure. *Journal of Robotics ans Mechatronics* **24**, 811-819.
[48] Zheng, Y.L., Yan, B.P., Zhang, Y.T. and Poon, C.C.Y. (2014) An Armband Wearable Device for Overnight and Cuff-Less Blood Pressure Measurement. *Ieee T Bio-Med Eng* **61**, 2179-2186.
[49] Elgendi, M., Fletcher, R., Liang, Y.B., Howard, N., Lovell, N.H., Abbott, D., Lim, K. and Ward, R. (2019) The use of photoplethysmography for assessing hypertension. *Npj Digit Med* **2**.
[50] Godia, E.C., Madhok, R., Pittman, J., Trocio, S., Ramas, R., Cabral, D., Sacco, R.L. and Rundek, T. (2007) Carotid artery distensibility: a reliability study. *J Ultrasound Med* **26**, 1157-1165.
[51] Schmidt-Trucksass, A., Grathwohl, D., Schmid, A., Boragk, R., Upmeier, C., Keul, J. and Huonker, M. (1998) Assessment of carotid wall motion and stiffness with tissue Doppler imaging. *Ultrasound Med Biol* **24**, 639-646.
[52] Harada, K., Yasuoka, K. and Shimada, Y. (2004) Usefulness of tissue doppler imaging for assessing aortic wall stiffness in children with the Marfan syndrome. *Am J Cardiol* **93**, 1072-1075.
[53] Vitarelli, A., Giordano, M., Germano, G., Pergolini, M., Cicconetti, P., Tomei, F., Sancini, A., Battaglia, D., Dettori, O., Capotosto, L., De Cicco, V., De Maio, M., Vitarelli, M. and Bruno, P. (2010) Assessment of ascending aorta wall stiffness in hypertensive patients by tissue Doppler imaging and strain Doppler echocardiography. *Heart* **96**, 1469-1474.

[54] Palombo, C., Kozakova, M., Guraschi, N., Bini, G., Cesana, F., Castoldi, G., Stella, A., Morizzo, C. and Giannattasio, C. (2012) Radiofrequency-based carotid wall tracking: a comparison between two different systems. *J Hypertens* **30**, 1614-1619.
[55] van Loon, G., De Witte, M., Rossel, N., Decloedt, A., Verheyen, T., Declercq, D., Saey, V., Chiers, K. and Segers, P. (2012) Measurement of arterial diameter distention to assess arterial wall stifness in horses: preliminary results. In: *European College of Equine Internal Medicine*, Edinburgh, UK.
[56] Messas, E., Pernot, M. and Couade, M. (2013) Measuring the elasticity of the arterial wall: state of the art and perspectives. *J Radiol Diagn Inter* **94**, 577-585.
[57] Marais, L., Pernot, M., Khettab, H., Tanter, M., Messas, E., Zidi, M., Laurent, S. and Boutouyrie, P. (2019) Arterial Stiffness Assessment by Shear Wave Elastography and Ultrafast Pulse Wave Imaging: Comparison with Reference Techniques in Normotensives and Hypertensives. *Ultrasound Med Biol* **45**, 758-772.
[58] Baldo, M.P., Cunha, R.S., Ribeiro, A.L.P., Lotufo, P.A., Chor, D., Barreto, S.M., Bensenor, I.M., Pereira, A.C. and Mill, J.G. (2017) Racial Differences in Arterial Stiffness are Mainly Determined by Blood Pressure Levels: Results From the ELSA-Brasil Study. *J Am Heart Assoc* **6**.
[59] Chaturvedi, N., Bulpitt, C.J., Leggetter, S., Schiff, R., Nihoyannopoulos, P., Strain, W.D., Shore, A.C. and Rajkumar, C. (2004) Ethnic differences in vascular stiffness and relations to hypertensive target organ damage. *J Hypertens* **22**, 1731-1737.
[60] Goel, A., Maroules, C.D., Mitchell, G.F., Peshock, R., Ayers, C., McColl, R., Vongpatanasin, W. and King, K.S. (2017) Ethnic Difference in Proximal Aortic Stiffness An Observation From the Dallas Heart Study. *Jacc-Cardiovasc Imag* **10**, 54-61.
[61] Diemer, F.S., Baldew, S.M., Haan, Y.C., Karamat, F.A., Oehlers, G.P., van Montfrans, G.A., van den Born, B.H., Peters, R.J.G., Nahar-Van Venrooij, L.M.W. and Brewster, L.M. (2020) Aortic pulse wave velocity in individuals of Asian and African ancestry: the HELISUR study. *J Hum Hypertens* **34**, 108-116.
[62] Lefferts, W.K., Augustine, J.A., Spartano, N.L., Atallah-Yunes, N.H., Heffernan, K.S. and Gump, B.B. (2017) Racial Differences in Aortic Stiffness in Children. *J Pediatr* **180**, 62-67.
[63] Ploeg, M., Saey, V., de Bruijn, C.M., Grone, A., Chiers, K., van Loon, G., Ducatelle, R., van Weeren, P.R., Back, W. and Delesalle, C. (2013) Aortic rupture and aorto-pulmonary fistulation in the Friesian horse: characterisation of the clinical and gross post mortem findings in 24 cases. *Equine Vet J* **45**, 101-106.
[64] Ploeg, M., Saey, V., Delesalle, C., Grone, A., Ducatelle, R., de Bruijn, M., Back, W., van Weeren, P.R., van Loon, G. and Chiers, K. (2015) Thoracic Aortic Rupture and Aortopulmonary Fistulation in the Friesian Horse: Histomorphologic Characterization. *Veterinary Pathology* **52**, 152-159.
[65] Ploeg, M., Saey, V., van Loon, G. and Delesalle, C. (2017) Thoracic aortic rupture in horses. *Equine Vet J* **49**, 269-274.
[66] Painter, P.R. (2008) The velocity of the arterial pulse wave: a viscous-fluid shock wave in an elastic tube. *Theoretical Biology and Medical Modelling* **5**.
[67] Briceno, A.M., Mendez, A., Brewer, K., Hughes, C. and Tobin, T. (2015) Sudden death, aortic rupture in horses, literature review, case studies reported and risk factors. . *Braz J Vet Res Anim Sci* **52**, 298-309.
[68] Pugh, C.J.A., Stone, K.J., Stohr, E.J., McDonnell, B.J., Thompson, J.E.S., Talbot, J.S., Wakeham, D.J., Cockcroft, J.R. and Shave, R. (2018) Carotid artery wall mechanics in young males with high cardiorespiratory fitness. *Exp Physiol* **103**, 1277-1286.
[69] Ashor, A.W., Lara, J., Siervo, M., Celis-Morales, C. and Mathers, J.C. (2014) Effects of exercise modalities on arterial stiffness and wave reflection: a systematic review and meta-analysis of randomized controlled trials. *PLoS One* **9**, e110034.
[70] Tanaka, H., DeSouza, C.A. and Seals, D.R. (1998) Absence of age-related increase in central arterial stiffness in physically active women. *Arterioscler Thromb Vasc Biol* **18**, 127-132.

[71] Tanaka, H., Dinenno, F.A., Monahan, K.D., Clevenger, C.M., DeSouza, C.A. and Seals, D.R. (2000) Aging, habitual exercise, and dynamic arterial compliance. *Circulation* **102**, 1270-1275.
[72] Binder, J., Bailey, K.R., Seward, J.B., Squires, R.W., Kunihiro, T., Hensrud, D.D. and Kullo, I.J. (2006) Aortic augmentation index is inversely associated with cardiorespiratory fitness in men without known coronary heart disease. *American Journal of Hypertension* **19**, 1019-1024.
[73] Kawano, H., Tanimoto, M., Yamamoto, K., Sanada, K., Gando, Y., Tabata, I., Higuchi, M. and Miyachi, M. (2008) Resistance training in men is associated with increased arterial stiffness and blood pressure but does not adversely affect endothelial function as measured by arterial reactivity to the cold pressor test. *Exp Physiol* **93**, 296-302.
[74] Cortez-Cooper, M.Y., DeVan, A.E., Anton, M.M., Farrar, R.P., Beckwith, K.A., Todd, J.S. and Tanaka, H. (2005) Effects of high intensity resistance training on arterial stiffness and wave reflection in women. *Am J Hypertens* **18**, 930-934.
[75] Voltion, D. (2014) Metabolic responses to exercise training In: *Equine Sports Medicine and Surgery* Eds: K.W. Hinchliff, A.J. Kaneps and J.R. Geor, Elsevier Edinburg. pp 747-761.
[76] Ogola, B.O., Zimmerman, M.A., Clark, G.L., Abshire, C.M., Gentry, K.M., Miller, K.S. and Lindsey, S.H. (2018) New insights into arterial stiffening: does sex matter? *Am J Physiol-Heart C* **315**, H1073-H1087.
[77] DuPont, J.J., Kenney, R.M., Patel, A.R. and Jaffe, I.Z. (2019) Sex differences in mechanisms of arterial stiffness. *Br J Pharmacol* **176**, 4208-4225.
[78] Carnevale, E.M. (2008) The mare model for follicular maturation and reproductive aging in the woman. *Theriogenology* **69**, 23-30.
[79] Carnevale, E.M. (2017) The mare as an animal model for reproductive aging in woman In: *Animal models and human reproduction*, Eds: H. Schatten and C. G.M., Wiley Blackwell New Jersey. pp 235-246.
[80] Lee, H.Y. and Oh, B.H. (2010) Aging and arterial stiffness. *Circ J* **74**, 2257-2262.
[81] Mikael, L.R., Paiva, A.M.G., Gomes, M.M., Sousa, A.L.L., Jardim, P., Vitorino, P.V.O., Euzebio, M.B., Sousa, W.M. and Barroso, W.K.S. (2017) Vascular Aging and Arterial Stiffness. *Arq Bras Cardiol* **109**, 253-258.
[82] Wagenseil, J.E. and Mecham, R.P. (2012) Elastin in large artery stiffness and hypertension. *J Cardiovasc Transl Res* **5**, 264-273.
[83] Izzo, J.L., Jr. and Shykoff, B.E. (2001) Arterial stiffness: clinical relevance, measurement, and treatment. *Rev Cardiovasc Med* **2**, 29-34, 37-40.
[84] Haidet, G.C., Wennberg, P.W., Finkelstein, S.M. and Morgan, D.J. (1996) Effects of aging per se on arterial stiffness: systemic and regional compliance in beagles. *Am Heart J* **132**, 319-327.
[85] Mellor, D.J., Love, S., Gettinby, G. and Reid, S.W. (1999) Demographic characteristics of the equine population of northern Britain. *Vet Rec* **145**, 299-304.
[86] McGowan, C. (2011) Welfare of Aged Horses. *Animals (Basel)* **1**, 366-376.
[87] Ireland, J.L., McGowan, C.M., Clegg, P.D., Chandler, K.J. and Pinchbeck, G.L. (2012) A survey of health care and disease in geriatric horses aged 30 years or older. *Veterinary Journal* **192**, 57-64.
[88] Brosnahan, M.M. and Paradis, M.R. (2003) Assessment of clinical characteristics, management practices, and activities of geriatric horses. *J Am Vet Med Assoc* **223**, 99-103.
[89] Nethononda, R.M., Lewandowski, A.J., Stewart, R., Kylinterias, I., Whitworth, P., Francis, J., Leeson, P., Watkins, H., Neubauer, S. and Rider, O.J. (2015) Gender specific patterns of age-related decline in aortic stiffness: a cardiovascular magnetic resonance study including normal ranges. *J Cardiovasc Magn Reson* **17**, 20.
[90] Ho, J.Y. and Hendi, A.S. (2018) Recent trends in life expectancy across high income countries: retrospective observational study. *BMJ* **362**, k2562.
[91] Comfort, A. (1961) The life span of animals. *Sci Am* **205**, 108-119.
[92] Ploeg, M., Grone, A., van de Lest, C.H.A., Saey, V., Duchateau, L., Wolsein, P., Chiers, K., Ducatelle, R., van Weeren, P.R., de Bruijn, M. and Delesalle, C. (2017) Differences in

extracellular matrix proteins between Friesian horses with aortic rupture, unaffected Friesians and Warmblood horses. *Equine Vet J* **49**, 609-613.
[93] Lee, S.J. and Park, S.H. (2013) Arterial Ageing. *Korean Circ J* **43**, 73-79.
[94] Beamish, J.A., He, P., Kottke-Marchant, K. and Marchant, R.E. (2010) Molecular regulation of contractile smooth muscle cell phenotype: implications for vascular tissue engineering. *Tissue Eng Part B Rev* **16**, 467-491.
[95] Rensen, S.S., Doevendans, P.A. and van Eys, G.J. (2007) Regulation and characteristics of vascular smooth muscle cell phenotypic diversity. *Neth Heart J* **15**, 100-108.

# SUMMARY

In human medicine, vascular diseases are important and independently linked with mortality. Changes in arterial structure and function contribute to a poorer 'vascular health'. The latter is mainly assessed by determination of arterial wall stiffness, regionally and locally. Using different techniques it has been demonstrated that age, race and gender have an effect on the arterial wall stiffness. In horses, the most important, often fatal, vascular disorder is arterial rupture. This condition has been associated with breed (e.g. aortic rupture in Friesians), age, exercise, parturition, copulation and α1-agonist treatment. Nevertheless, knowledge of the pathophysiology of arterial rupture and the effect of age and breed remained very limited, since up till now, techniques to measure and assess arterial wall stiffness were not available.

**The General introduction** of this thesis gives an overview of normal and abnormal structural, biomechanical and functional properties of the arterial wall in humans and the current knowledge in equines. First the normal structure of the arterial wall is described, followed by an explanation of the physiological function of the arterial tree. This includes an overview of blood pressure regulation and different blood pressure measurement techniques, followed by a description of normal blood pressure in horses. Next, an outline of the biomechanical properties of the arterial wall is given, combined with possible *ex vivo* tests to describe these biomechanical properties. This is followed by a short description of the most used mathematical models that allow studying arterial tree flow dynamics and pressure waves. Measuring techniques for arterial wall stiffness assessment in human patients are described, together with the effect of aging, gender, training and race. Lastly, the most common arterial disorders in horses are described, including exercise-induced arterial rupture, aortocardiac fistulation, aortopulmonary fistulation in Friesians horses and arterial rupture associated with phenylephrine administration or parturition.

The first objective of this dissertation was to predict and understand flow profiles and pressures over the whole arterial tree of the healthy horse **(Chapter 3).** First, we have detailed the anatomy of the equine arterial tree (diameter, branch length and branching angle of 113 arterial segments). Based on these details, together with literature data, physiological data from ultrasound images and invasive blood pressure measurements, we have developed a mathematical one-dimensional model which mimics the arterial flow in horses. Adapting the model by taking into account gravity improved predicted flow waveform morphology. Outcomes of this model showed plausible predictions of pressures and flow waves throughout the arterial tree. Moreover, simulated flow waveforms showed a similar oscillating pattern as observed in ultrasound Doppler images. Wave power analysis helped to explain the contours of arterial flow profiles.

Techniques to reliably measure arterial wall stiffness in horses were developed and applied (**Chapter 4**). Regional arterial wall stiffness parameters, aortic to external iliac artery pulse wave velocity and carotid to external iliac artery pulse wave velocity calculated using pulsed wave Doppler, showed low coefficients of variation (3-15%). Local arterial wall stiffness parameters including diameter and lumen area change, diameter and lumen area strain, compliance, distensibility and stiffness index of the cranial and caudal common carotid artery, proximal aorta and external iliac artery showed low to high coefficients of variation (10-68%). We concluded that local arterial wall stiffness parameters are, in contrary to regional arterial wall stiffness parameters, not suitable for individual follow-up of patients, but can have an added value for population research.

In **Chapter 5**, the previously developed techniques were used to assess differences in arterial wall stiffness between Warmblood horses and Friesian horses, as Friesians are known to be predisposed to aortic rupture. Aortic to external iliac artery and carotid to external iliac artery pulse wave velocity were significantly higher in Friesians horses compared to Warmblood horses (6.52±2.51 and 7.06±1.60 m/s vs. 5.95±0.94 and 5.79±1.43 m/s), indicating a stiffer aorta in Friesians. This could be confirmed by lower local arterial wall stiffness parameters in Friesians. Additionally Friesian horses showed a significantly higher systolic (146±18 mmHg), diastolic (97±12 mmHg) and mean arterial blood pressure (115±15 mmHg) and a higher pulse pressure (49±9 mmHg) compared to Warmblood horses (135±14 mmHg, 91±10 mmHg, 106±13 mmHg and 44±9 mmHg, respectively). These findings, in combination with the previously described differences in collagen amount and cross-linking pattern, make it highly probable that the predisposition of Friesian horses to aortic rupture is, at least partially, related to increased arterial wall stiffness.

In **Chapter 6**, the effect of age on the arterial wall stiffness in horses was assessed using the same techniques. Older horses showed significantly larger arterial diameters compared to young horses, in combination with an increased arterial wall thickness. Aortic to external and carotid to external iliac artery pulse wave velocity were clearly higher in old horses (6.2±1.3 m/s and 6.0±2.2 m/s) compared to young horses (5.3±0.6 m/s and 4.6±0.8 m/s), in combination with lower local aortic and carotid arterial wall stiffness parameters, confirming stiffer arteries in older horses. No difference in blood pressure was found. Arterial compliance was maximal in the aorta and decreased towards the periphery. Results indicate that horses, in accordance with humans, present age-related arterial wall stiffening, in combination with luminal enlargement and arterial wall thickening.

In **Chapter 7** we aimed at investigating the structural and biomechanical effects of aging on the equine arterial wall. Histological findings showed a decrease in the amount of elastin from

the proximal aorta (34±3%) towards the peripheral arteries (8±5% in the median artery). A significant increase in wall thickness in aged horses was found, in combination with an increased area % of smooth muscle actin. Biomechanical properties were assessed using an inflation-extension test pressurising (15-300 mmHg) proximal aortas, distal aortas, common carotid arteries and external iliac arteries. Rupture occurred in a minority of arteries (8/78) at high pressures (250-300mmHg), and mostly occurred in older horses (7/8). Age significantly affected the pressure-area curve of the distal aorta, common carotid artery and external iliac artery, the pressure-compliance curve of the proximal aorta and the common carotid artery, and the pressure-distensibility curve of the proximal aorta. Larger vascular cross-sectional areas at the same pressure were found in older horses, combined with a lower compliance in older horses at physiological pressures. Results indicate structural and biomechanical arterial wall changes due to aging, which explain the *in vivo* differences in arterial wall stiffness between young and old horses.

As a general conclusion, by providing new insights in equine arterial physiology, this work contributes to the knowledge of the pathophysiology of arterial rupture in horses. A unique dataset of the equine arterial tree is provided, in combination with an equine specific mathematic model to study and predict the normal blood flow and pressure waves in horses. This model can be a starting point for studying arterial pathophysiology during hypertension, exercise or drug administration in future. A technique to study vascular health in the standing, unsedated horse by measuring local and regional arterial wall stiffness is described. We have demonstrated that age affects the arterial wall stiffness *in vivo* which corresponds to structural and biomechanical changes observed *ex vivo*. Furthermore, we have demonstrated that Friesians have a stiffer aorta, which could predispose this breed to aortic rupture. In future it would be useful to assess the effect of breed (other than Friesians), gender and training on the arterial wall stiffness, in order to further unravel the underlying causes of arterial rupture in horses.

# SAMENVATTING

Vasculaire aandoeningen zijn veel voorkomend in de humane geneeskunde en behoren tot de belangrijkste doodsoorzaken. Veranderingen in arteriële structuur en functie leiden tot een slechtere 'vasculaire gezondheid'. Eén belangrijke parameter die sterk geassocieerd wordt met deze vasculaire gezondheid is de arteriële wandstijfheid. Bij de mens werd aangetoond dat zowel leeftijd, afkomst, als geslacht een effect hebben op de arteriële wandstijfheid. Bij paarden is de meest voorkomende, vaak fatale vasculaire aandoening arteriële ruptuur. Arteriële ruptuur wordt in verband gebracht met ras (verhoogde prevalentie bij Friese paarden), leeftijd, inspanning, partus, copulatie en het gebruik van α1-agonisten. Toch blijft de kennis omtrent de pathofysiologie van arteriële ruptuur tot op heden heel beperkt. Dit is grotendeels het gevolg van het ontbreken van technieken die toelaten om de arteriële wandstijfheid bij paarden te meten.

**De algemene inleiding** van dit doctoraatsproefschrift geeft een overzicht van de normale en abnormale structurele, biomechanische en functionele eigenschappen van de arteriële wand bij mensen en de huidige kennis omtrent het paard. Eerst en vooral wordt de normale structuur van de arteriële wand beschreven, gevolgd door een weergave van de fysiologische functie van het arterieel systeem. Dit laatste bestaat uit een overzicht van de bloeddruk regulatie en de verschillende technieken om bloeddruk te meten, gevolgd door een beschrijving van de normale bloeddruk bij paarden. Daarnaast wordt een overzicht gegeven van de biomechanische eigenschappen van de arteriële wand, samen met de verschillende mogelijke *ex vivo* technieken om deze biomechanische eigenschappen in kaart te brengen. Dit wordt gevolgd door een korte beschrijving van de verschillende mathematische modellen die ons in staat stellen de dynamica van de arteriële bloedvloei en bloeddruk te bestuderen. Vervolgens worden de verschillende *in vivo* technieken om arteriële wandstijfheid bij humane patiënten te meten aangehaald, samen met het effect van ouderdom, geslacht, training en afkomst. Als laatste worden de meest voorkomende, vaak fatale arteriële aandoeningen bij het paard beschreven zoals arteriële ruptuur na inspanning, na toediening van fenylefrine, of tijdens de partus, en aortocardiale fistel en aortopulmonale fistel bij Friese paarden.

De eerste doelstelling van dit doctoraatsproefschrift was om de bloeddruk en het flowprofiel te analyseren en te voorspellen over de gehele arteriële boom van gezonde paarden (**Hoofdstuk 3**). Hiervoor werd eerst de arteriële anatomie van het paard in detail bestudeerd. De diameter en lengte van de voornaamste arteries en hun vertakkingen en de hoek tussen deze vertakkingen werd opgemeten, in totaal goed voor 113 arteriële segmenten. Gebaseerd op deze gegevens, in combinatie met bestaande literatuur data en fysiologische gegevens verkregen via echografische beelden en bloeddruk metingen, werd een wiskundig één-dimensioneel model ontworpen dat de arteriële bloedvloei bij paarden nabootst. Dit model gaf waarheidsgetrouwe resultaten over het gehele arteriële systeem. Wanneer in het model

eveneens rekening werd gehouden met de zwaartekracht, die een belangrijke rol speelt bij het rechtstaande paard, verbeterde de voorspelde morfologie van de flowprofielen. Bovendien vertoonden gesimuleerde flowprofielen een opmerkelijk oscillerend patroon, gelijkaardig aan de oscillerende flowprofielen die echografisch gevonden worden bij paarden. Analyse van de verschillende flowgolven kon de opvallende contouren van de flowprofielen verklaren.

In **Hoofdstuk 4** werden verschillende technieken ontwikkelend om de arteriële wandstijfheid op een betrouwbare manier te meten bij paarden. Pulsed Wave Doppler werd gebruikt om bloeddrukgolven te registreren op verschillende plaatsen. De berekende snelheid van de bloeddrukgolf is een indicator voor de regionale arteriële wandstijfheid. De snelheid van de bloeddrukgolf gemeten tussen de aorta en de arteria iliaca externa en deze tussen de arteria carotis communis en de arteria iliaca externa, vertoonde een lage variatiecoëfficiënt (3-15%). Parameters die de lokale wandstijfheid beschrijven, zoals de diameter en oppervlakte verandering, de compliantie, de distensibiliteit en de stijfheidsindex, vertoonden een hoge variatiecoëfficiënt (10-68%). Hieruit werd geconcludeerd dat parameters die de lokale wandstijfheid beschrijven, in tegenstelling tot parameters die de regionale wandstijfheid beschrijven, niet bruikbaar zijn voor onderzoek van individuele patiënten, maar wel een toegevoegde waarde hebben bij populatie-onderzoek.

In **Hoofdstuk 5** werden de technieken uit Hoofdstuk 4 gebruikt om het verschil in arteriële wandstijfheid tussen Friezen en Warmbloeden te achterhalen. De keuze voor het Friese paard was gebaseerd op zijn gevoeligheid voor aortaruptuur. De snelheid van de bloeddrukgolf gemeten tussen de aorta en de arteria iliaca externa en tussen de arteria carotis communis en arteria iliaca externa waren significant hoger bij Friese paarden in vergelijking met Warmbloeden (6.52±2.51 en 7.06±1.60 m/s vs. 5.95±0.94 en 5.79±1.43 m/s), wat wijst op een stijvere aorta bij Friese paarden. Deze bevinding kon gestaafd worden aan de hand van lokale stijfheidsparameters, dewelke lager waren bij Friezen in vergelijking met Warmbloeden. Daarenboven werd bij Friezen een significant hogere systolische (146±18 mmHg), diastolische (97±12 mmHg) en gemiddelde (115±15 mmHg) arteriële bloeddruk waargenomen, in vergelijking met Warmbloeden (135±14 mmHg, 91±10 mmHg en 106±13 mmHg respectievelijk). Deze bevindingen, in combinatie met de voordien reeds beschreven verschillen in de hoeveelheid collageen en de cross-linking ervan, wijzen erop dat de verhoogde prevalentie van aortaruptuur bij Friezen, tenminste deels toe te schrijven is aan een verhoogde arteriële wandstijfheid.

In **Hoofdstuk 6** werd het effect van leeftijd op de arteriële wandstijfheid bestudeerd, gebruik makend van de hierboven beschreven technieken. Significant grotere arteriële diameters werden waargenomen bij oudere paarden in vergelijking met jonge paarden, samen met een

verdikte arteriële wand. De snelheid van de bloeddrukgolf gemeten tussen de aorta en de arteria iliaca externa en tussen de arteria carotis communis en arteria iliaca externa waren significant hoger bij oude paarden (6.2±1.3 m/s en 6.0±2.2 m/s) in vergelijking met jonge paarden (5.3±0.6 m/s en 4.6±0.8 m/s). Er werd geen verschil in bloeddruk waargenomen. De arteriële elasticiteit bleek het grootst ter hoogte van de aorta en werd kleiner naar de periferie toe. Resultaten tonen aan dat, in overeenkomst met de humane geneeskunde, bij paarden eveneens leeftijds-gerelateerde verstijving van de arteriële wand optreedt, in combinatie met een toename in grootte van de het arteriële lumen en een verdikking van de arteriële wand.

In **Hoofdstuk 7** werden de structurele en biomechanische effecten van veroudering op de arteriële wand bestudeerd. Histologische bevindingen toonden een afnemende hoeveelheid van elastine aan van de proximale aorta (34±3%) naar de meer perifeer gelegen arteries (8±5% in de arteria mediana). Een significante toename van de arteriële wanddikte werd waargenomen bij oude paarden, tezamen met een toegenomen oppervlakte % van gladde spiercel actine. De biomechanische eigenschappen van de arteriële wand werden in kaart gebracht gebruik makend van een inflatie-extensie test. Hiervoor werd de proximale en distale aorta, de arteria carotis communis en de arteria iliaca externa *ex vivo* onder druk gezet (van 15 tot 300 mmHg). Arteriële ruptuur trad slechts op bij een beperkt aantal arteries (8/78), wanneer deze blootgesteld werden aan een hoge druk (250-300 mmHg) en dit voornamelijk bij oudere paarden (7/8). De leeftijd bleek de druk-oppervlakte curve van de distale aorta, arteria carotis communis en de arteria iliaca externa significant te beïnvloeden, evenals de druk-compliantie curve van de proximale aorta en de arteria carotis communis, en de druk-distensibiliteits curve van de proximale aorta. Bij oudere paarden werden grotere oppervlaktes waargenomen voor dezelfde drukken in vergelijking met jonge paarden, in combinatie met een lagere compliantie bij oude paarden bij fysiologische drukken.

Als algemene conclusie kunnen we stellen dat, dankzij het vergaren van nieuwe inzichten in de arteriële fysiologie, dit doctoraatsproefschrift bijdraagt tot de algemene kennis betreffende de pathofysiologie van arteriële ruptuur bij paarden. Een unieke dataset van de arteriële anatomie van het paard werd aangeleverd, in combinatie met een paard-specifiek wiskundig model dat het mogelijk maakt om de arteriële bloedvloei en bloeddruk over het gehele arterieel systeem te bestuderen. In de toekomst kan dit model dienen als basis voor het bestuderen van de arteriële fysiologie tijdens hypertensie, inspanning of na toediening van bepaalde medicatie. Technieken om de arteriële wandstijfheid te meten bij staande, ongesedeerde paarden, zowel regionaal als lokaal, werden op punt gezet. Met deze technieken kon aangetoond worden dat Friezen een stijvere aorta hebben in vergelijking met Warmbloeden, wat de verhoogde gevoeligheid van deze paarden voor aortaruptuur, op zijn minst deels, zou kunnen verklaren. Bovendien werd zowel *in vivo* als *ex vivo* aangetoond dat leeftijd de

structurele en biomechanische eigenschappen van de arteriële wand beïnvloedt. In de toekomst zou het nuttig zijn, bovenop de hier beschreven bevindingen, het effect van ras, geslacht en training op de arteriële wandstijfheid verder te onderzoeken, om zo de onderliggende mechanismen die leiden tot arteriële ruptuur beter te begrijpen.

# CURRICULUM VITAE

Lisse Vera werd geboren op 13 Augustus 1991 te Dendermonde. Na het beëindigen van het secundair onderwijs aan het Koninklijk Atheneum Dendermonde, richting Wetenschappen-talen, startte zij met de studies Diergeneeskunde aan de Universiteit Gent. In 2015 behaalde zij het diploma van dierenarts (optie Paard) met grote onderscheiding.

In Oktober van datzelfde jaar trad zij in dienst bij de vakgroep Inwendige ziekten van de grote huisdieren op de Faculteit Diergeneeskunde in Merelbeke als doctoraatsstudent, onder begeleiding van Prof. Dr. Gunther van Loon, in samenwerking met de vakgroep Pathologie, Bacteriologie en Pluimveeziekten, onder de begeleiding van Prof. Dr. Koen Chiers. In Februari 2016 kreeg Lisse Vera een beurs van het Fonds voor Wetenschappelijk onderzoek. Naast het cardiovasculair onderzoek bij paarden stond zij ook in voor het begeleiden van schrijfopdrachten van studenten en was zij betrokken bij de dienstverlening voor cardiologie patiënten.

Lisse Vera is eerste auteur van acht en medeauteur van zestien artikels in internationale tijdschriften (Q1) en gaf negen presentaties op verschillende nationale en internationale congressen. In 2019 won zij de “Voorjaarsdagen EFO Award” voor beste orale presentatie.

# BIBLIOGRAPHY

## Papers

**Lisse Vera**, Dominique De Clercq, Annelies Decloedt, Sofie Ven, and Gunther van Loon. 2015. “Hemothorax Bij Een Fries Paard : Niet Altijd Een Aortaruptuur!” *Vlaams Diergeneeskundig Tijdschrift* 84 (3): 142–146.

Annelies Decloedt, Dominique De Clercq, Sofie Ven, **Lisse Vera**, and Gunther van Loon. 2017. “Right Ventricular Function During Pharmacological and Exercise Stress Testing in Horses.” *Veterinary Journal* 227: 8–14.

Barbara Broux, Dominique De Clercq, Sofie Ven, **Lisse Vera**, Glenn Van Steenkiste, Annelies Decloedt, and Gunther van Loon. 2017. “Heart Rate Monitor Derived Heart Rate Variability to Diagnose Atrial Fibrillation in Horses.” In *Journal of Veterinary Internal Medicine*. Vol. 31.

Tim Vandecasteele, Stijn Schauvliege, Tim Boussy, Matthew Philpott, Eli Clement, **Lisse Vera**, Pieter Cornillie, Ward De Spiegelaere, Glenn Van Langenhove, Gunther van Loon, and Wim Van Den Broeck. 2017. “Immunohistochemical Identification of Stent-based Ablation Lesions in the Superior Vena Cava and Pulmonary Veins.” *Journal of Histology & Histopathology* 4 (1).

Alexander Dufourni, Dominique De Clercq, **Lisse Vera**, Barbara Broux, Laurence Lefère, Leslie Bosseler, Han Versnaeyen, and Gunther van Loon. 2017. “Pheochromocytoma in a Horse with Polymorphic Ventricular Tachycardia.” *Vlaams Diergeneeskundig Tijdschrift* 86 (4): 241–249.

Barbara Broux, Dominique De Clercq, Annelies Decloedt, Sofie Ven, **Lisse Vera**, Glenn Van Steenkiste, K Mitchell, C Schwarzwald, and Gunther van Loon. 2017. “Heart Rate Variability Parameters in Horses Distinguish Atrial Fibrillation from Sinus Rhythm Before and After Successful Electrical Cardioversion.” *Equine Veterinary Journal* 49 (6): 723–728.

**Lisse Vera**, Annelies Decloedt, Glenn Van Steenkiste, Dominique De Clercq, Jan Govaere, and Gunther van Loon. 2018. “Electrocardiographic Confirmation of a Twin Pregnancy in a Mare at 8 Months of Gestation.” *Journal of Veterinary Cardiology* 20 (4): 294–299.

Tim Vandecasteele, Stijn Schauvliege, Matthew Philpott, Eli Clement, Gunther van Loon, **Lisse Vera**, Tim Boussy, Thomas van Bergen, Wim Van Den Broeck, Pieter Cornillie, and Glenn Van Langenhove. 2018. “A Preliminary Study of Pulmonary Vein Implant Applicability and Safety as a Potential Ablation Platform in a Follow-up Study in Pigs.” *Pace-pacing and Clinical Electrophysiology* 41 (2): 167–171.

Tim Boussy, Tim Vandecasteele, **Lisse Vera**, Stijn Schauvliege, Matthew Philpott, Eli Clement, Gunther van Loon, Udi Willenz, Juan F Granada, Gregg W Stone, Vivek Y Reddy,

and Glenn Van Langenhove. 2018. “Isolation of Pulmonary Veins Using a Thermoreactive Implantable Device with External Energy Transfer : Evaluation in a Porcine Model.” *Pace-pacing and Clinical Electrophysiology* 41 (6): 603–610.

Sofie Ven, Annelies Decloedt, Dominique De Clercq, **Lisse Vera**, F Rademakers, and Gunther van Loon. 2018. “Detection of Subclinical Left Ventricular Dysfunction by Tissue Doppler Imaging in Horses with Aortic Regurgitation.” *Equine Veterinary Journal* 50 (5): 587–593.

Dominique De Clercq, Barbara Broux, **Lisse Vera**, Annelies Decloedt, and Gunther van Loon. 2018. “Measurement Variability of Right Atrial and Ventricular Monophasic Action Potential and Refractory Period Measurements in the Standing Non-sedated Horse.” *Bmc Veterinary Research* 14.

Annelies Decloedt, Barbara Broux, Dominique De Clercq, Piet Deprez, Glenn Van Steenkiste, **Lisse Vera**, Sofie Ven, and Gunther van Loon. 2018. “Effect of Sotalol on Heart Rate, QT Interval, and Atrial Fibrillation Cycle Length in Horses with Atrial Fibrillation.” *Journal of Veterinary Internal Medicine* 32 (2): 815–821.

Barbara Broux, Dominique De Clercq, **Lisse Vera**, Sofie Ven, Piet Deprez, Annelies Decloedt, and Gunther van Loon. 2018. “Can Heart Rate Variability Parameters Derived by a Heart Rate Monitor Differentiate Between Atrial Fibrillation and Sinus Rhythm?” *Bmc Veterinary Research* 14.

Barbara Broux, Dominique De Clercq, Annelies Decloedt, **Lisse Vera**, Mathias Devreese, R Gehring, Siska Croubels, and Gunther van Loon. 2018. “Pharmacokinetics and Electrophysiological Effects of Sotalol Hydrochloride in Horses.” *Equine Veterinary Journal* 50 (3): 377–383.

**Lisse Vera**, Daimé Campos Arias, Sofie Muylle, Nikos Stergiopulos , Patrick Segers, and Gunther van Loon. 2019. “A 1D Computer Model of the Arterial Circulation in Horses : An Important Resource for Studying Global Interactions between Heart and Vessels under Normal and Pathological Conditions.” *PLOS ONE* 14 (8).

**Lisse Vera**, Filip Boyen, Anneleen De Visscher, V Vandenbroucke, G Vanantwerpen, and Jan Govaere. 2019. “Limitations of a Chromogenic Agar Plate for the Identifying Bacteria Isolated from Equine Endometritis Samples.” *Equine Veterinary Journal* 51 (2): 266–269.

Glenn Van Steenkiste, Dominique De Clercq, **Lisse Vera**, Annelies Decloedt, and Gunther van Loon. 2019. “Sustained Atrial Tachycardia in Horses and Treatment by Transvenous Electrical Cardioversion.” *EQUINE VETERINARY JOURNAL* 51 (5): 634-640

**Lisse Vera**, Dominique De Clercq, Ellen Paulussen, Glenn Van Steenkiste, Annelies Decloedt, Koen Chiers, and Gunther van Loon. 2020. “Aortic, Common Carotid and External Iliac Artery Arterial Wall Stiffness Parameters in Horses : Inter-Day and Inter-Observer and Intra-Observer Measurement Variability.” *EQUINE VETERINARY JOURNAL* 34 (2): 893-901.

**Lisse Vera**, Dominique De Clercq, Glenn Van Steenkiste, Annelies Decloedt, Koen Chiers, and Gunther van Loon. 2020. “Differences in Ultrasound-Derived Arterial Wall Stiffness Parameters and Noninvasive Blood Pressure between Friesian Horses and Warmblood Horses.” *JOURNAL OF VETERINARY INTERNAL MEDICINE* 51 (5): 634–640.

Glenn Van Steenkiste, **Lisse Vera**, Annelies Decloedt, Stijn Schauvliege, T. Boussy, and Gunther van Loon. 2020. “Endocardial Electro-Anatomic Mapping in Healthy Horses : Normal Sinus Impulse Propagation in the Left and Right Atrium and the Ventricles.” *VETERINARY JOURNAL*. Published online

Glenn Van Steenkiste, Dominique De Clercq, Tim Boussy, **Lisse Vera**, Stijn Schauvliege, Annelies Decloedt, and Gunther van Loon. 2020. “Three Dimensional Ultra-high-density Electro-anatomical Cardiac Mapping in Horses : Methodology.” *EQUINE VETERINARY JOURNAL* 52 (5): 765-772

Ingrid Vernemmen, Dominique De Clercq, Annelies Decloedt, **Lisse Vera**, Glenn Van Steenkiste, and Gunther van Loon. 2020. “Atrial Premature Depolarisations Five Days Post Electrical Cardioversion Are Related to Atrial Fibrillation Recurrence Risk in Horses.” *EQUINE VETERINARY JOURNAL* 52 (3): 374-378

**Lisse Vera**, Sofie Muylle, Gunther van Loon, Laure Gatel, Ann Martens, and Katrien Vanderperren. 2020. “Internal jugular vein phlebectasia in a one-year-old Warmblood stallion.” *EQUINE VETERINARY EDUCATION*. Published online.

**Lisse Vera**, Glenn Van Steenkiste, Annelies Decloedt, Koen Chiers and Gunther van Loon. 2020. “Age-related Differences in Blood Pressure, Ultrasound-Derived Arterial Diameters and Arterial Wall Stiffness Parameters in Horses.” *EQUINE VETERINARY JOURNAL*. Published online.

## Presentations

Barbara Broux, Dominique De Clercq, **Lisse Vera**, Glenn Van Steenkiste, Annelies Decloedt, and Gunther van Loon. 2016. “Heart Rate Variability Parameters to Detect Atrial Fibrillation in Horses.” In *9th Congress of the European College of Equine Internal Medicine : Abstracts*, 97–97.

Barbara Broux, Dominique De Clercq, **Lisse Vera**, Glenn Van Steenkiste, Annelies Decloedt, Anneleen Watteyn, Mathias Devreese, Siska Croubels, and Gunther van Loon. 2016. “Pharmacokinetics and Electrophysiological Effects of Different Dosages of Oral Sotalol in Horses: Preliminary Results.” In *9th Congress of the European College of Equine Internal Medicine : Abstracts*.

**Lisse Vera**, Gunther van Loon, Laure Gatel, Sofie Muylle, Ann Martens, and Katrien Vanderperren. 2017. “Internal Jugular Vein Phlebectasia (IJVP) in a One Year Old Warmblood Horse.” In *10th Annual European College of Equine Internal Medicine Congress : Abstract Book*.

Sofie Ven, Annelies Decloedt, **Lisse Vera**, Dominique De Clercq, and Gunther van Loon. 2017. “Assessing Aortic Regurgitation Severity by Tissue Doppler Imaging in Horses.” In *Abstracts European Veterinary Conference Voorjaarsdagen 2017*.

Dominique De Clercq, Glenn Van Steenkiste, **Lisse Vera**, Stijn Schauvliege, Annelies Decloedt, and Gunther van Loon. 2017. “QRS Morphology Changes Depending on Site of Ventricular Pacing During High Resolution 3D Electro-anatomical Mapping in Adult Horses : Preliminary Results.” In *10th Annual European College of Equine Internal Medicine Congress : Abstract Book*.

Gunther van Loon, Tim Boussy, **Lisse Vera**, Dominique De Clercq, Stijn Schauvliege, Tim Vandecasteele, Annelies Decloedt, Glenn Van Steenkiste, and Glenn Van Langenhove. 2017. “Successful High Resolution 3D Electroanatomical Cardiac Mapping in Adult Horses in Sinus Rhythm.” In *Journal of Veterinary Internal Medicine*, 4.

**Lisse Vera**, Glenn Van Steenkiste, Dominique De Clercq, Annelies Decloedt, Bram Deserranno, and Gunther van Loon. 2018. “Right Atrial Related Structures in Horses, of Interest During Electrophysiological Studies.” In *Proceedings of the 11th European College of Equine Internal Medicine Congress*.

**Lisse Vera**, Dominique De Clercq, Barbara Broux, Sofie Ven, Glenn Van Steenkiste, and Gunther van Loon. 2018. “Inter-day, Inter-observer and Intra-observer Variability of Arterial

Pulse Wave Velocity Measurements Using Pulsed Wave Doppler in Healthy Horses." In *Abstracts European Veterinary Conference Voorjaarsdagen 2018*.

Daimé Campos Arias, **Lisse Vera**, Sofie Muylle, Nikos Stergiopoulos, Gunther van Loon, and Patrick Segers. 2018. "Arterial Hemodynamics in the Horse : Insights from a 1D Arterial Network Model." In *Biomechanics, 8th World Congress, Abstracts*.

**Lisse Vera**, Dominique De Clercq, Glenn Van Steenkiste, Annelies Decloedt, Koen Chiers, and Gunther van Loon. 2018. "Friesian Horses Show Higher Arterial Blood Pressure Compared to Warmbloods ." In *Proceedings of the 11th European College of Equine Internal Medicine Congress*.

Daimé Campos Arias, **Lisse Vera**, Sofie Muylle, Nikos Stergiopulos, Gunther van Loon, and Patrick Segers. 2018. "Arterial Wave Dynamics in the Horse : Insights Obtained from a 1D Arterial Network Model Simulation." In *Artery Research*, 24:120–120.

**Lisse Vera**, Dominique De Clercq, Annelies Decloedt, Glenn Van Steenkiste, and Gunther van Loon. 2018. "Reproducibility of Arterial Diameter Measurements Using B- and M-mode Ultrasonography in Standing Warmblood Horses." In *Proceedings of BEVA Congress 2018*, 308–309.

Sofie Ven, Annelies Decloedt, **Lisse Vera**, Glenn Van Steenkiste, Dominique De Clercq, and Gunther van Loon. 2018. "Cardiac Dimensions and Function in Matched Untrained Versus Endurance-trained Arabian Horses." In *Comparative Exercise Physiology*, 14:S78–S78.

Glenn Van Steenkiste, Dominique De Clercq, Annelies Decloedt, **Lisse Vera**, and Gunther van Loon. 2018. "Specific 12-lead ECG Characteristics That Help Localize the Anatomical Origin of Ventricular Ectopy in Horses : Preliminary Data." In *Proceedings of the 11th European College of Equine Internal Medicine Congress*.

Glenn Van Steenkiste, Mattias Duytschaever, Dominique De Clercq, Roger Tavernier, **Lisse Vera**, Anneleen Michielsen, Annelies Decloedt, Stijn Schauvliege, and Gunther van Loon. 2018. "First Successful Radiofrequency Ablation of Focal Atrial Tachycardia in a Horse Guided by a High Density 3D Electro-anatomical Mapping System (Rhythmia®)." In *Proceedings of the 11th European College of Equine Internal Medicine Congress*.

**Lisse Vera**, Glenn Van Steenkiste, Annelies Decloedt, Dominique De Clercq, and Gunther van Loon. 2019. "Comparison of Smartphone-based and Standard Electrocardiography in Healthy Horses." In *EQUINE VETERINARY JOURNAL*, 51:19–19.

**Lisse Vera**, Daimé Campos Arias, Sofie Muylle, Nikos Stergiopulos, Patrick Segers, and Gunther van Loon. 2019. "A Computer Model of the Equine Arterial Circulation to Gain Deeper

Insights into Equine Arterial Haemodynamics." In *EQUINE VETERINARY JOURNAL*, 51:20–20.

**Lisse Vera**, Dominique De Clercq, Glenn Van Steenkiste, Annelies Decloedt, Koen Chiers, and Gunther van Loon. 2019. "Differences in Cardiovascular Physiology Between Friesian Horses and Warmblood Horses." In *Abstracts European Veterinary Conference Voorjaarsdagen 2019*.

**Lisse Vera**, Dominique De Clercq, Glenn Van Steenkiste, Lisa De Lange, Annelies Decloedt, Zoé Neuckermans, Koen Chiers, and Gunther van Loon. 2019. "L'échographie Des Artères Principales Chez Les Chevaux Âgés Montre Un Diamètre Supérieur, Une Paroie plus Épaisse et plus Rigide Par Rapport à Des Jeunes Chevaux." In *Ateliers et Journées Annuelles AVEF, Tours, 2019*, 77–77.

Glenn Van Steenkiste, Dominique De Clercq, Annelies Decloedt, **Lisse Vera**, and Gunther van Loon. 2019. "A 12-lead Electrocardiogram Interpretation Algorithm to Determine the Anatomical Site of Origin of Atrial Premature Depolarizations in Horses : Preliminary Data." In *Abstracts European Veterinary Conference Voorjaarsdagen 2019*.

Alexander Dufourni, **Lisse Vera**, Annelies De Vos, Annelies Decloedt, Dominique De Clercq, and Gunther van Loon. 2019. "Ultrasonographic Assessment of Early Subclinical Cathether-Related Changes of the Jugular Vein in Hospitalized Horses." In *Proceedings of the 12th European College of Equine Internal Medicine Congress*.

Glenn Van Steenkiste, Dominique De Clercq, Annelies Decloedt, **Lisse Vera**, and Gunther van Loon. 2019. "Détection Fiable de La Fibrillation Atriale Chez Des Chevaux à l'aide d'apprentissage En Profondeur." In *Ateliers et Journées Annuelles AVEF, Tours, 2019*, 161–161.

Glenn Van Steenkiste, Dominique De Clercq, Annelies Decloedt, **Lisse Vera**, and Gunther van Loon. 2019. "A 12-lead Electrocardiogram Interpretation Algorithm to Determine the Anatomical Site of Origin of Atrial Premature Depolarizations in Horses : Preliminary Data." In *EQUINE VETERINARY JOURNAL*, 51:8–8.

Ingrid Vernemmen, Dominique De Clercq, Annelies Decloedt, **Lisse Vera**, Glenn Van Steenkiste, and Gunther van Loon. 2019. "Correlation between Atrial Premature Depolarisations after Electrical Cardioversion and Risk for Atrial Fibrillation Recurrence in Horses." In *EQUINE VETERINARY JOURNAL*, 51:18–18.

Glenn Van Steenkiste, **Lisse Vera**, Lisa De Lange, Annelies Decloedt, Dominique De Clercq, and Gunther van Loon. 2019. "Développement d'un Simulateur d'échocardiographie Équine

Basé Sur Des Images Tomographiques Dérivées à l'aide de Cœurs Moulés." In *Ateliers et Journées Annuelles AVEF, Tours, 2019*, 78–78.

Lisa De Lange , Dominique De Clercq, **Lisse Vera**, Glenn Van Steenkiste, Fe ter Woort, and Gunther van Loon. 2019. "Rupture Partielle de La Paroi de l'aorte Avec Dissection et Formation d'un Pseudo-Anévrisme Chez Un Étalon Frison de 10 Ans sans Symptômes Cliniques." In *Ateliers et Journées Annuelles AVEF, Tours, 2019*, 159–159.

Lisa De Lange, Glenn Van Steenkiste, **Lisse Vera**, Dominique De Clercq, Annelies Decloedt, Kristel MC Cromheeke, and Gunther van Loon. 2019. "First Succesful Applications of Closed Loop Stimulation Pacemakers with Remote Monitoring in Two Syncopal Miniature Donkeys." In *Proceedings of the 12th European College of Equine Internal Medicine Congress*.

Glenn Van Steenkiste, Tammo Delhaas, Ben Hermans, **Lisse Vera**, Ingrid Vernemmen, Annelies Decloedt, Dominique De Clercq, and Gunther van Loon. 2019. "Accuracy of Electrocardiographic and Vectorcardiographic Criteria to Identify the Anatomical Location of Ventricular Ectopy in Horses : Preliminary Data." In *EQUINE VETERINARY JOURNAL*, 51:17–17.

Gunther van Loon, Dominique De Clercq, Annelies Decloedt, **Lisse Vera**, Glenn Van Steenkiste, Marco De Bruijn, Margreet Ploeg, Willem Back, Catherine Delesalle, and Koen Chiers. 2019. "Ultrasound Approach to Diagnose Aortopulmonary Fistulation in Friesian Horses." In *ACVIM Forum 2019 Proceedings*, 184–184.

# DANKWOORD

Eigenlijk zou ik het heel kort kunnen houden, in één enkele zin kan ik namelijk alles zeggen: **“Success can’t be spelled without U!”**. Hierbij wil ik dan ook íedereen die van ver of heel dichtbij heeft bijgedragen aan dit doctoraat bedanken, zonder ieder van jullie had ik hier vandaag niet gestaan. (Voila, bij deze ben ik zéker niemand vergeten!)

Naar goede gewoonte wil ik starten met mijn promotoren te bedanken. **Gunther**, bedankt om mij deze kans te geven, bedankt om mee te denken en áltijd kritisch te zijn, bedankt voor onze discussies (want daar wordt een mens enkel wijzer van), bedankt om de puntjes op de i te zetten en mijn ellendig lange zinnen in te korten, kortom, bedankt voor alles! (PS: sorry, je gaat hier hele lange zinnen met heel veel komma’s moeten lezen)
**Koen**, ook jou wil ik bedanken om mee in dit project te stappen, al mijn schrijfsels na te lezen, mij te begeleiden op de vlakken waar ik totaal geen verstand van had (microscopen, histologie, immunohistochemie) en vooral het aanbrengen van nieuwe inzichten en ideeën, bedankt Koen!

Daarnaast wil ik alle leden van de examen commissie bedanken, evenals de voorzitter. **Jeroen**, bedankt om alles in goede banen te leiden!
**Patrick**, bedankt om in de commissie te willen zetelen, bedankt voor het grondig en kritisch nalezen van dit werk, bedankt voor onze fijne samenwerking gedurende mijn doctoraat, zonder jou biomechanisch inzicht waren het eerste en het laatste artikel nooit tot stand gekomen. Kortom Patrick, bedankt voor álles, hopelijk kan je samen met Gunther en één van mijn lieftallige collega’s nog een vervolg breien aan het 1D model, want wat wil ik graag weten hoe die bloeddrukken veranderen tijdens inspanning!
**Stijn**, bedankt om in de commissie te willen zetelen en dit werk tot in het kleinste detail na te lezen, niet enkel op inhoud, maar ook op schrijffouten. Daarnaast wil ik je ook bedanken voor de fijne samenwerking de afgelopen vijf jaar! De mappings, de magnesiumproeven, beiden leken ze soms eeuwig te duren, maar dankzij jouw fijn gezelschap en alles-overheersende-kalmte werd elke proef tot een goed einde gebracht! Stijn, bedankt!
**Pascale**, bedankt om in de commissie te willen zetelen, voor het nalezen van dit werk en voornamelijk voor je klinische kijk op deze materie. Eveneens bedankt voor de samenwerking gedurende de afgelopen jaren betreffende de kliniek patiënten: apparatuur uitlenen, kennis delen, elkaar uit de nood helpen, alles verliep altijd heel vlot! Pascale, bedankt!
**John**, excuse me that I’m writing this part of my thesis in Dutch, but I would also like to thank you for being a member of the exam committee, taking your time to read the manuscript carefully and joining the public defence (due to corona unfortunately online). Hopefully we’ll see each other later! John, thank you!

Daarnaast wil ik graag **ál mijn collega's van het 'team-inwendige', paard, rund én skillslab** evenals álle interns van de afgelopen vijf jaar bedanken. Ik ga geen namen noemen om zeker niemand te vergeten, maar weet dat het een eer en een genoegen was met jullie samen te mogen werken. Een ziek paardje? Breng maar mee! Een klinische vraag? Altijd paraat om te helpen! Een gezellige, grappige of soms gênante babbel onder de middag? Team-inwendige stond altijd klaar! Aan iedereen, bedankt! Ik ga jullie missen!
Alle collega's die deel uitmaakten van onze 'PhD-meetings' wil ik nog eens in het bijzonder bedanken. Corona maakte spijtig genoeg een eind aan onze gezellige babbels en uitwisseling van kennis en ervaringen, maar wat was/is dit een mooi initiatief! Ik zou zeggen, vooral mee blijven verder doen! (Dan kom ik misschien stiekem nog wel eens langs tijdens één van jullie meetings!)
PS Pia: heel veel succes met je kleine wondertje, we mikken op dezelfde datum hé?!

Ook de **collega's van heelkunde** wil ik graag bedanken, de **anesthesisten** en **chirurgen** voor de hulp tijdens de mappings, pacemaker implantaties en TVEC's, de samenwerking verliep altijd aangenaam en vlot, bedankt daarvoor! PS Lavina: special thanks to you! Maar ook de collega's van de **orthopedie** wil ik uitdrukkelijk bedanken, zoals ze het zelf zeggen: "veel paarden, altijd wel met ene miserie". Bedankt dat ik altijd bij jullie terecht kon met mijn paardjes! Kelly, Maarten en Michèle (in 't bijzonder!), bedankt!

Ook de **collega's van verloskunde** mogen zeker niet ontbreken in mijn dankwoord! Een lastige merrie dekken? Een gevaarlijke merrie vangen? Niets was teveel gevraagd! Bedankt allemaal, jullie hielpen twee pracht veulentjes van ons op de wereld! Eveneens bedankt voor het begeleiden van mijn masterproef (bij jullie begon dus mijn onderzoekscarrière), daarnaast schreven we samen ook twee mooie artikels, waarbij de samenwerking altijd probleemloos verliep, waarvoor speciale dank aan Jan!

Ook de **collega's van pathologie** mogen zeker niet in het lijstje ontbreken! Leen (x2), Laurien, Bart en Fréderic, bedankt voor de hulp en het geduld in de snijzaal! Delphine, Joachim en Christiaan bedankt voor het altijd zeer hartelijke onthaal en jullie bijdrage aan mijn doctoraat. Sarah, ongelooflijk hard bedankt voor je tijd én geduld met de immuno-kleuringen! Bedankt allemaal!

En dan, het **cardioteam**! Jullie dachten toch niet dat ik jullie vergeten was hé?! En deze keer ga ik wel (tijdsoverschrijdend zelf) namen noemen: Barbara, Sofie, Dominique, Gunther, Annelies, Glenn, Alex, Ellen, Ingrid, Eva, het cardioteam is over de jaren heen heel wat

veranderd, maar één ding blijft ‘only teamwork makes the dream work”. Bedankt allemaal voor jullie hulp en steun gedurende onze jaren samen!

**Barbara**, van jou leerde ik dat een doctoraat vooral doorzetten en geduld hebben is én dat het oké is om in het weekend je e-mails niet te lezen, bedankt!

**Sofie**, je was een zeer aangenaam persoon om mee samen te werken, waarvoor dank, en ik bewonder jou op vele vlakken. We hebben af en toe nog eens contact en ik hoop dat dit ook zo zal blijven! Heel veel succes nog in alles wat op je levenspad komt.

**Dominique**, woorden schieten tekort als ik jou wil bedanken en het afscheid van jou doet nog steeds pijn. Jij was mijn meter, maakte mij wegwijs in de cardio en in het kliniek-leven en ging uren mee Friezen en Warmbloeden echoën. Ook voor een deugddoende babbel privé of werk gerelateerd kon ik altijd bij jou terecht, Dominique bedankt! Ik wens je alle succes in de toekomst en hopelijk tot gauw!

**Gunther**, de geest en de motor achter dit team, ik heb je hierboven al uitgebreid bedankt, maar hier nogmaals: bedankt voor alles! PS: in’t leven moet je af en toe durven springen! Veel succes in de toekomst ik kijk vanop de zijlijn toe wat je allemaal nog in petto hebt!

**Annelies**, wat ben jij een voorbeeld voor zovelen! Áltijd klaar om íedereen te helpen, vriendelijk en professioneel. Bedankt dat ik jou bureau-maatje mocht zijn! Bedankt voor alle hulp, op alle vlak! Annelies, wat heb ik bewondering voor jou, wat kan en weet jij veel! Wat een top-vrouw! Ik wens je nog heel veel succes in de toekomst, met het skillslab en de cardio! Annelies, ik ga je missen!

**Glenn**, een onmisbaar lid van het cardioteam, maar toch sla ik je hier even over (always save the best for last!)

**Alex**, onze geschiedenis begint al in mijn laatste jaar, een héél heftig jaar voor jou, grotendeels als enige intern op de dienst inwendige! Korte (of geen) nachten, drukke dagen, vervelende student en toch áltijd vrolijk, goed gezind én klaar om uitleg te geven! Alex jij was een top-intern! ’t Jaar daarop werden we collega’s, ook als resident was jij altijd vrolijk en behulpzaam en je bleek niet enkel een top-intern maar ook een top-collega! Na veel zweten en zwoegen behaalde je, meer dan verdiend, je diplomate titel, en begint nu nog eens aan de lange weg tot doctor, chapeau! Alex, bedankt voor alles, heel veel succes met je doctoraat en blijf gewoon áltijd jezelf!

**Ellen,** net als Alex ben je nog maar recent ‘lid’ van het cardioteam, maar behoor je al heel lang tot de zotte bende van inwendige. Ook jij was een hele fijne collega en wat ben jij een straffe madam, diplomate, mama worden en nu nog eens een doctoraat beginnen! Heel veel succes, maak er iets moois van!

**Ingrid**, ook nog niet zo heel lang lid van ons cardioteam, maar al volledig ingeburgerd! Bedankt voor de fijne samenwerking i.v.m. het rechter atrium artikel en het friezen artikel. Ik wil je hierbij

dan ook nog heel veel succes wensen bij het verdere verloop van je doctoraat! Maak er een indrukwekkend stukje wetenschap van Ingrid!
**Eva**, jij staat nog maar aan het begin van je onderzoekscarrière, ik wil deze kans dan ook niet missen om je heel veel succes te wensen!

Nu we bijna aan het einde gekomen zijn wil ik nog enkele collega's in 't bijzonder bedanken…
**Sofie Muylle,** bedankt voor álle hulp! Je eindeloos geduld tijdens de dissecties, je talloze uren achter de microscoop, je kritische kijk op de artikels, en dit allemaal vrijwillig, zonder jou was mijn doctoraat nooit op tijd klaar geraakt! Ik kan je hiervoor niet genoeg bedanken! Bedankt Sofie!
**Zoé**, bedankt om de tijd te nemen om mijn doctoraat zo grondig na te lezen! Bedankt ook voor de fijne samenwerking de afgelopen jaren en het aangename gezelschap op de voorjaarsdagen! Ik wil je hierbij ook nog heel veel succes wensen met je residentie en je verdere carrière.
**Valentine**, jij werd nog niet zo heel lang geleden eveneens een bureau-maatje, direct werd duidelijk (babbelkousen als wij zijn) dat we het goed met elkaar konden vinden! Bedankt voor de steun en álle babbels, we spreken zeker nog eens af!
**Lisa**, alles begon toen ik in mijn laatste jaar zat met 'mag ik één euro lenen'… Niet veel later werden we collega's, het klikte van in het begin! Jij was er altijd voor mij, altijd paraat voor een babbel, een schouderklopje, een zucht, een lach en een traan! Al gauw deelden we al onze frustraties en geheimen! Lisa, hoe een collega zo een top-vriendin kan worden… ik heb er geen woorden voor. Dat ik met de tranen in mijn ogen zit als ik dit schrijf zegt genoeg: Lisa, wat ga ik je missen! Gelukkig ben ik ervan overtuigd dat wij elkaar nog heel veel gaan horen en hopelijk nog vaak gaan zien! Lisa, je bent een top-wijf! Nog heel veel succes met je residentie, je examen en je verdere carrière, ik ben er zeker van dat er nog een hele mooie toekomst op je wacht! Bedankt voor alles Lisa!!!
**Glenn**, een krop in mijn keel en tranen in mijn ogen bij het besef dat wij binnenkort geen collega's meer zijn, maar een lach bij het besef dat we voor altijd vrienden zullen blijven! Toen jij op onze dienst begon had ik nooit gedacht dat wij zo een hechte collega's zouden worden, maar je ziet, je kan je in mensen vergissen! Van een handige Harry en diegene die de computer problemen oploste, tot mijn partner-in-crime…Onze levens liepen zowel op professioneel vlak als op persoonlijk vlak vrijwel gelijk, waardoor we altijd bij elkaar terecht konden! Glenn, bedankt voor alle babbels, alle koffie/thee-pauzes, alle technische hulp, alle schouderklopjes, alle hilarische momenten, kortom bedankt voor alles! Ik wil jou nog heel veel succes wensen in je verdere leven (privé en professioneel) en dit is geen vaarwel he?!

**Vrienden en familie**, iedereen één voor één opnoemen zou mij nog eens tien pagina's kosten, maar ik wil elk van jullie bedanken voor alles wat jullie voor mij hebben gedaan! Alleen in een (h)echte vrienden- en familiekring kan iemand gelukkig en succesvol zijn!

**Mama, Papa**, jullie wil ik toch wel even persoonlijk bedanken, ook al weet ik dat jullie dat niet nodig vinden! Jullie dochters álle kansen geven en ze áltijd in álles 100% steunen, dat is voor jullie vanzelfsprekend! Toch wil ik van deze gelengheid gebruik maken om jullie daar oprecht voor te bedanken! Vanuit het diepste van mijn hart: dank je Mama en Papa, zonder jullie onvoorwaardelijke steun stond ik hier vandaag niet!

**Yannick**, al 14 jaar mijn zielsverwant… Ik kan niet in woorden vatten wat jij voor mij betekent! Jij hebt in de afgelopen vijf jaar van mijn doctoraat elke frustratie, elke ergernis moeten aanhoren, we hebben heel wat persoonlijke tegenslagen overwonnen, maar hier staan we dan, samen, sterker dan ooit en binnenkort niet met twee maar met drie, in ons eigen huisje, de toekomst lacht ons toe! Lieve schat, bedankt voor alles, IK HOU VAN JOU!

En als laatste, niet te vergeten, **mijn klein wondertje**! De afgelopen maanden was ik letterlijk nooit alleen (sorry voor alle stress momentjes)! Jij maakt mijn leven compleet kleine meid, mama houdt nu al zielsveel van jou!

*“ If you see someone without a smile, give them yours ”*